Memory encoding by cortical circuits and engrams

Raimundo Pinto De Matos, Mariana

2022

document version
Publisher's PDF, also known as Version of record

2004-2008 BsC degree in Biology at Faculdade de Ciências, Universidade do Porto.
2008-2009 master degree in Biology, at Faculdade de Ciências, Universidade do Porto. The thesis was produced at the Department of Experimental Biology, Faculdade de Medicina, Universidade do Porto.

2014-2019 PhD at Molecular and Cellular Neurobiology department, CNCR, Vrije Universiteit
2019-Present Services and Support Specialist at iSens Electrónica Lda

CNCR Amsterdam

MEMORY ENCODING BY CORTICAL CIRCUITS AND ENGRAMS MARIANA RAIMUNDO PINTO DE MATOS

MEMORY ENCODING BY CORTICAL CIRCUITS AND ENGRAMS

MARIANA RAIMUNDO PINTO DE MATOS

Memory encoding by cortical circuits and engrams

Mariana Raimundo Pinto de Matos

Para a minha Mãe

The work present in this thesis was performed at the Molecular and Cellular Neurobiology department, Center for Neurogenomics and Cognitive Research, Vrije Universiteit, Amsterdam

The research was funded by EU MSCA-ITN CognitionNet (FP7-PEOPLE-2013-ITN 607508) grant.

Printing by: Berci-impressão digital

VRIJE UNIVERSITEIT

MEMORY ENCODING BY CORTICAL CIRCUITS AND ENGRAMS

ACADEMISCH PROEFSCHRIFT

ter verkrijging van de graad Doctor of Philosophy aan
de Vrije Universiteit Amsterdam,
op gezag van de rector magnificus
prof.dr. C.M. van Praag,
in het openbaar te verdedigen
ten overstaan van de promotiecommissie
van de Faculteit der Bètawetenschappen
op donderdag 3 maart 2022 om 11.45 uur
in een bijeenkomst van de universiteit,
De Boelelaan 1105

door

Mariana Raimundo Pinto De Matos
geboren te Porto, Portugal

promotor:	prof.dr. A.B. Smit
copromotor:	dr. M.C. van den Oever
promotiecommissie:	prof. dr. T.J. de Vries prof.dr. M. Kindt dr. E. Koya dr. M.J.A.G. Henckens dr. M.M. Karnani

Contents

Chapter 1

General Introduction

1.1 Memory: the conundrum

A question that has been repeatedly put forward over centuries and from one generation to the next is: "Who are we?" Probably the best answer is: we are our memories, personal and cultural. As such, memory has always intrigued humankind and has been object of study dating as far back as Plato. Memory guides our future actions and with that it shapes our future self. We form memories of almost every experience, but most fade with time. However, in particular events with a strong emotional valence result in persistent memories and thereby shape actions for extended periods of time. After coming to the notion that the brain is home to our memories, the question arose where in the brain memories are formed and stored. This search is especially relevant if we consider how memories can overpower us. This is for instance the case in people with a substance use disorder or in patients that suffer from a post-traumatic stress disorder (PTSD). Both disorders are characterized by strong recurring memories that hinder the daily functioning of affected individuals.

1.2 Associative learning and animal models

Of particular relevance to the formation of persistent memories with a strong emotional valence is associative learning. Associative learning happens when two events occur closely related in time and subsequently help to predict each other. As a result of this type of learning, humans and animals can adapt their behavior to be prepared for similar future events. Moreover, more complex logic can be built and evolve from this type of learning. A well-known form of associative learning is Pavlovian conditioning (*1*). The definition of this type of learning is that (repeated) pairings of a neutral stimulus (e.g., a specific environment or context) with an aversive or rewarding stimulus will subsequently provoke a response when only the previously neutral stimulus is presented. For instance, when a mouse experiences a foot-shock (unconditioned stimulus (US)) in a specific context, the animal learns that this context (now a conditioned stimulus (CS)) signals a future unpleasant experience, as such changing the valence of the context from neutral to aversive in order to adapt behavior (*2*). According to Fanselow and Wassum (*3*), Pavlovian conditioning is "the process whereby experience with a conditional relationship between stimuli bestows these stimuli with the ability to promote adaptive behavior patterns that did not occur before the experience". The behavioral change (the conditioned response (CR)) to

the CS, depends on the type of US and can be used as a measurable read-out of acquisition of the learned relationship. To study aversive and appetitive associative learning, I made use of two mouse paradigms of Pavlovian conditioning, which I will focus on throughout the remainder of my introduction.

Contextual Fear Conditioning (CFC): In this form of conditioning, mice receive one or multiple foot-shocks (US) after a short period of exploring a specific environment (context) (*4, 5*) (see Fig. 1). Future exposure to the conditioning context (CS) elicits freezing behavior (CR), even in the absence of another foot-shock. Freezing is typically defined as the absence of all movement except respiration (*6*).

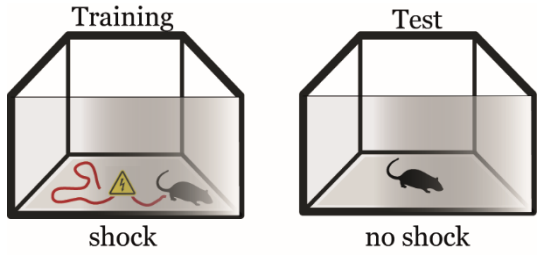

Figure 1. Contextual Fear Conditioning paradigm. On the conditioning day, mice are first allowed to explore a novel context inside a sound-proof cabin with white noise. After a predefined exploration time, mice receive one foot-shock or multiple foot-shocks (US) with a specific interval via the metal grid at the bottom of the chamber. After the last foot-shock, mice are allowed to explore the box again for a short period of time and are then returned to the home-cage. On test day, mice are re-exposed to the conditioning chamber (CS) (without delivery of foot-shock(s)) and freezing behavior is measured.

Animals freeze because fear conditioning activates a defense mechanism which aids to avoid an attack when they are encountered by predators. In evolutionary terms, freezing is effective because preys become more difficult to detect and predators often attack after sensing movement from their target (*2, 3*). Additionally, freezing behavior is accompanied by changes in heart rate, shallow and rapid breathing and decreased pain sensitivity (*3*). It should be noted, however, that when a shock is given immediately after placing a rodent in the conditioning context, no association is formed between these two stimuli and consequently no freezing is detected upon re-exposure to the context. This lack of conditioning is known as immediate-shock deficit (*7*). Thus, the animal requires a certain minimal amount of time to process

the context before it experiences a foot-shock to be able to use the context as a subsequent predictor for the aversive stimulus.

Conditioned Place Preference: The original example of Pavlovian conditioning concerned reward-related learning. Pavlov's dog learned to associate the sound of a bell with the delivery of food (*1*). In my thesis, I performed Conditioned place preference (CPP) using cocaine as a rewarding stimulus. In this paradigm, mice are initially allowed to freely explore a box consisting of two chambers with different visual and tactile cues that typically can be accessed via an intermediate corridor (see Fig. 2 below). This session (Pre-test) serves to determine the baseline preference of each animal for one of the chambers. Conditioning follows over consecutive days, during which the animal receives a saline injection and is then confined to one of the two chambers. In a subsequent session, the animal receives a rewarding substance (e.g., cocaine) and is allowed to explore the other chamber only. These sessions are typically repeated several times and the reward- and saline-paired compartment should be counterbalanced within a group. By doing so, animals associate an otherwise neutral context with rewarding effects, such that in the future the context reminds the animal of the reward and triggers a CR (*8*). This response can be measured as rodents tend to spend more time in the reward-associated compartment when they are again allowed to freely explore the saline- and reward-paired chamber (Post-test) (*8-10*).

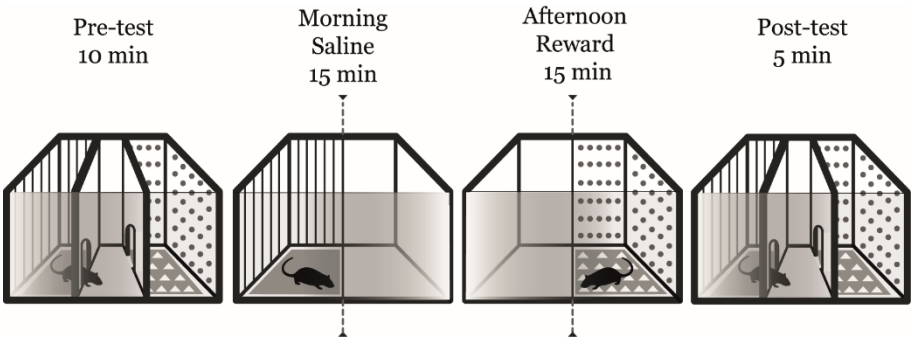

Figure 2. Conditioned Place Preference paradigm. Before conditioning, mice are first allowed to freely move between all chambers of the CPP apparatus (Pre-test). During conditioning, mice receive a saline injection and can then explore only one chamber of the CPP box (saline-paired side). During another session, mice receive a reward (e.g. cocaine injection) and are placed in the opposite chamber (reward-paired side). Depending on the reward and dose, these conditioning sessions are repeated a predefined number of times. During a CPP memory retrieval session (Post-test), mice can again explore all chambers and their memory for the reward-associated compartment is assessed by measuring the preference score, defined by the time spent in the reward-paired chamber minus the saline-paired chamber.

1.3 Stages of memory processing

Acquisition/Consolidation: During learning, neuronal activity increases in particular regions that support memory. However, to retrieve learned information in the following days or later, the acquired information has to be properly stored and transformed into long-term memory through a process called synaptic consolidation. This is a relatively fast process and occurs within 6 to 24 hours after learning (*11, 12*). It involves the growth of new dendritic spines, adaptation of existing spines and the strengthening of synapses (*13, 14*). This is only possible due to the activation of intracellular signaling cascades upon neuronal stimulation as a consequence of learning. Activation of transcription factors, such as CREB (*11, 15, 16*), regulates transcription of specific gene sets and thereby induces new protein synthesis, which underlies morphological changes at the synaptic level (*17*). Interference with either gene transcription or protein synthesis during the window of synaptic consolidation will disrupt long-term memory formation (*18*). It is due to the transformation of an initially labile to persistent form of long-term memory that the association between the CS and the US is stored (*14*). Synaptic consolidation is followed by a more gradual and slower process of systems consolidation, referring to reorganization of the brain-wide neuronal network that supports a given memory, over a period of days to weeks (*19*). I will elaborate on the process of systems consolidation in section 1.4 below. Collectively, the learning-induced physical changes that are required to store and retrieve a given memory are called an engram (*20, 21*).

Retrieval/Reconsolidation: The presentation of the CS reactivates the stored association and induces the expression of the CR. Under certain conditions, retrieval can drive the stored memory into a labile state again, allowing the insertion of new information and/or changes in the strength of the memory (*22-24*). This phenomenon of memory update is crucial for animals to adapt behavior based on new experiences, however stabilization and storage of this updated memory relies on a process called reconsolidation (*23*). Importantly, reconsolidation is not merely a recapitulation of the cellular and molecular consolidation processes observed after learning and several elements can affect the transition of a labile to new permanent state after retrieval, such as the age of the memory (*25, 26*), the length of the retrieval session (*27*) and the initial training intensity (*26*).

Extinction: Reduction of the CR can be obtained by prolonged/repeated exposure to the CS without delivery of the US (*28*). It was initially believed that extinction was the result of a reduction of the strength of the memory, due to unlearning of the original association. However, a CR can return in a time-dependent manner after extinction (spontaneous recovery) or upon brief re-exposure to a US (reinstatement) (*29*). The observation of a gradual reoccurrence of the CR after extinction learning (*1, 29*) led to a reformulation of the definition of extinction by adopting the idea that extinction involves a new learning process during which animals create a new association. After extinction learning, the CS no longer predicts the US, i.e., a CS-no US association is acquired. Notably, extinction is strongly linked to the original CS, meaning that associations of the same US with other CSs are not altered as a result of extinction learning in presence of the original CS only (*29, 30*).

1.4 Memory retention in the brain: from recent to remote

How is our brain capable of creating memories and to store these throughout a lifetime? The case of Henri Molaison, world-wide known as patient H.M. (*31*) provided important insight into the role of the medial temporal lobe (MTL) in memory acquisition and retention. H.M. had severe damage to his MTL due to the surgical removal of the hippocampal formation with the aim to diminish his epileptic seizures (*32*). This procedure produced anterograde amnesia, meaning that H.M. was not able to form new memories (*32*). So, if you happened to be his childhood friend he might remember you, but in case you met him yesterday, you would have to reintroduce yourself again today. This is a typical example of temporally graded retrograde amnesia, or in other words, the older the memory, the less severe the memory loss. Therefore H.M. could vividly recall memories from his childhood, but not events that happened the day before surgery. H.M. did not stand alone, as this same phenomenon was observed in other subjects, some of which suffered from even more severe amnesia due to damage to brain tissue beyond the MTL (*33, 34*). Moreover, brain insult encompassing the neocortex produces non-graded retrograde amnesia, which is observed as total loss of memories that were acquired before the insult (*34, 35*). Parallel studies in animals corroborated the evidence from human patients. Fear conditioned rats have poor memory expression when the hippocampus is lesioned 1 day after training, but show successful recall when the lesion is induced 28 days later (*36*). The introduction of optogenetics technology allowed

for more elegant intervention, as it enables temporally precise cell-type selective silencing/stimulation of neuronal activity in specific brain regions, in contrast to temporally imprecise lesioning or pharmacological manipulation of an entire area. *Goshen et al.* used optogenetics to demonstrate that prolonged inactivation of the hippocampus does not affect expression of a 28-days-old CFC memory, however, this effect was dependent on the duration of the optogenetic intervention, as retrieval was impaired when the inactivation was restricted to the duration of the recall test (*37*). Nonetheless, the findings obtained with such interventions in rodents are in line with the observations from human patients. This supports the theory that longer periods of hippocampal loss of function (mimicking lesions) may facilitate and engage compensatory circuits to drive remote memory expression and hippocampal-independent memory retrieval (*34, 38*). These findings show that memory is probably not statically stored in the brain, but rather evolves and the neuronal network involved changes over time. This process is called systems consolidation, enabling memory to transform into a more permanent and interference-resistant form (*17, 38, 39*).

As silencing the hippocampus spares remote memories under certain conditions, it is likely that other brain regions compensate for its loss. Memory maturation may rely on the replay of learning-associated neuronal firing in cortical nodes governed by the hippocampus. Activity patterns in the hippocampus detected during learning mimic those recorded during a subsequent phase of rest and sleep (*40, 41*) and this replay seems to coordinate parallel activity in cortical areas (*42*). It is believed that communication between the hippocampus and cortical areas supports the strengthening of cortical-cortical connections, slowly transforming these nodes in permanent memory repository sites (*17*). Based on experiments aimed at identifying the cortical nodes involved in systems consolidation, the prefrontal cortex emerged as an important hub (*37, 43, 44*). I will now first describe the anatomy of the prefrontal cortex and will then discuss its role in aversive and appetitive memory, including systems consolidation of these memories.

1.5 Anatomy of the prefrontal cortex

The rodent prefrontal cortex can be divided into the medial prefrontal cortex (mPFC) and orbitofrontal cortices (OFC). I will focus on the anatomy of the mPFC, as this region has been implicated in both

aversive and appetitive memories and has been the primary subject of the experiments in my thesis.

mPFC architecture and connectivity

Four main subareas can be distinguished within the mPFC of rodents: the medial precentral area (PrCm), the anterior cingulate cortex (ACC), the prelimbic cortex (PL) and the infralimbic cortex (IL) (*45*). Taking into account differences in connectivity and function, the mPFC is often less precisely separated into two components: the dorsal mPFC (dmPFC) comprising the PrCm, ACC and the dorsal area of the PL, and the ventral mPFC (vmPFC) constituting the ventral area of the PL, IL and dorsal peduncular cortex (DPC). For the remainder of this thesis, I will refer to the dmPFC and vmPFC whenever relevant, or otherwise use the term mPFC.

The laminar organization of the mPFC is crucial for the functions it serves. Notably, compared with other cortical regions, the rodent mPFC lacks an input layer IV (*46*) (see Fig. 3). Layers I, II and III receive input from limbic and cortical regions, such as the contralateral mPFC, the basolateral amygdala (BLA) and ventral hippocampus (HPC) (*47*). Moreover, these layers are also densely innervated by thalamic input and are responsible for a substantial amount of feed-forward inhibition in layers II and III (*48*). Layer V neurons of the mPFC are targeted by the mediodorsal thalamus (MD) and the ventromedial thalamus (VM), although these thalamic regions project predominantly to the superficial layers (*49*).

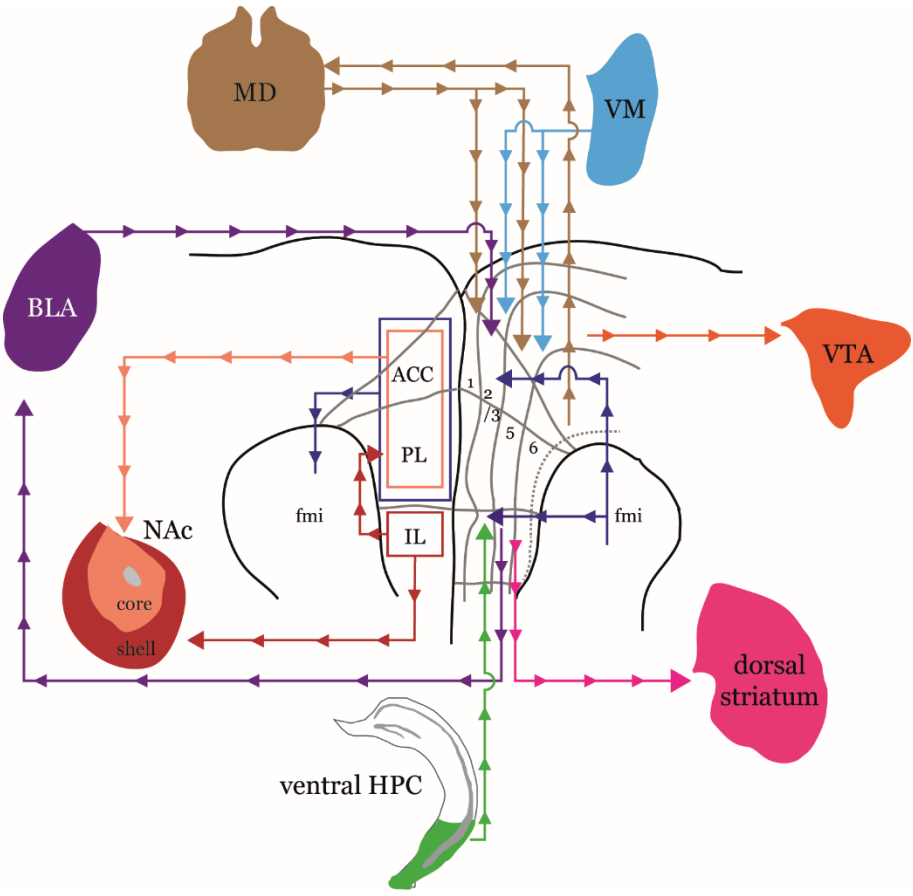

Figure 3. Key afferent and efferent connections of the mPFC. The different layers in the mPFC receive and send output to distinct brain areas. Moreover, differential organization of afferent and efferent connections also occurs along the dorsal-ventral axis of the mPFC. MD – mediodorsal thalamus (brown), VM – ventromedial thalamus (light blue), VTA – ventral tegmental area (dark orange), HPC – hippocampus (green), NAc – nucleus accumbens core (light orange) and shell (red), BLA – basolateral amygdala (purple), ACC – anterior cingulate area, PL – prelimbic cortex (dark blue arrows depict projection to the contralateral PL and infralimbic cortex (IL)), fmi – forceps minor of the corpus callosum.

The mPFC has efferent projections to cortical and subcortical areas and thereby regulates visceral, limbic and cognitive functions (*50, 51*). Neurons in layer V of the mPFC heavily target the ventral tegmental area and the dorsal striatum, whereas neurons in deep layer VI target the MD (*52*), among other regions. There seems to be a segregation between the dmPFC and vmPFC in terms of brain regions that they innervate, namely sensorimotor regions and limbic structures, respectively (*50, 53*). Moreover, the dmPFC innervates the nucleus accumbens (NAc) core and the vmPFC preferentially targets the NAc shell (*54, 55*), a dichotomy relevant for the role of the mPFC in addictive behavior (*56-58*). The BLA, implicated in aversive memory (*59-61*) and addictive behavior (*62*), receives strong projections from layer II, III and V dmPFC neurons. In turn, the BLA preferentially

targets neurons in dmPFC that project to BLA (*63*). This type of bi-directional communication is thought to be of utmost importance for integration of top-down cognitive control over the processing of emotional stimuli by the amygdala (*64*).

The dmPFC and vmPFC are also interconnected, as observed in tracing studies and more recently by employing optogenetics (*45, 65, 66*). Optic stimulation of vmPFC pyramidal neurons reduces firing of dmPFC neurons, indicating that the vmPFC is able to control excitatory output of the dmPFC (*66*). Moreover, disruption of neural oscillation within the mPFC can be observed after physical separation of the dmPFC and vmPFC (*67*). In a more recent study, infusion of retrobeads in the vmPFC resulted in labelling of layer II/III and more densely layer V/VI neurons of the dmPFC (*68*). The vast majority of dmPFC-to-vmPFC projecting neurons innervate neurons in layers V/VI of the vmPFC that exhibit strong projections to the amygdala (*68*). It is noteworthy that vmPFC-to-dmPFC projections are less abundant than dmPFC-to-vmPFC afferents (*68*). As mentioned, output targets of these two mPFC subareas differ, as well as their roles in aversive and appetitive memories (discussed below) (*69, 70*). Hence, dmPFC control over vmPFC output may have important consequences for regulation of behavioral responses, however, despite the anatomical elucidation of reciprocal connectivity between the vmPFC and dmPFC, the functional relevance has remained poorly understood.

GABAergic interneurons in the mPFC

Glutamatergic pyramidal neurons comprise 80 to 90% of all neurons in the mPFC and are responsible for the excitatory activity observed in this brain region, whereas the remaining 10-20% neurons are inhibitory interneurons that produce the neurotransmitter *gamma*-aminobutyric acid (GABA) (*71*). These main populations can be further classified depending on their morphology, physiological and molecular characteristics (*71, 72*). The three main inhibitory populations in the rodent cortex are fast-spiking parvalbumin (PV)-expressing neurons, the dendritic targeting somatostatin (SOM) interneurons and vasoactive intestinal peptide (VIP) positive interneurons (*73*). Both PV and SOM interneurons are responsible for inhibitory control over mPFC pyramidal neurons (*74*), whereas VIP interneurons are thought to function as a disinhibitory interface regulating both PV and SOM interneurons (*75*). As PV interneurons mainly target the soma of pyramidal cells, they are responsible for controlling the output of these neurons, whereas SOM interneurons act upstream and modulate the

level of excitatory input at the dendritic tree (*74, 76*). Optogenetic suppression of dmPFC PV interneurons in behaving mice revealed that a lack of phasic PV-mediated inhibition synchronizes activity of dmPFC pyramidal neurons, thereby increasing output of neurons projecting to the BLA, which evokes fear expression in the form of freezing behavior (*77*). Furthermore, optic stimulation of dmPFC PV interneurons accelerates extinction of reward seeking behavior (*76*). Even though PV interneurons appear implicated in controlling excitatory activity in cortical areas, they also have a more general role in synchronizing neuronal activity between regions. Fear learning induces spindle and ripple oscillations in the mPFC and hippocampus, respectively, and the synchronization of such spiking activity between the two brain regions is important for systems consolidation of contextual fear memory (*78*). The absence of hippocampal-prefrontal synchronization upon chemogenetically-suppressed PV activity leads to impairments in fear memory consolidation (*78*). Thus, even though interneurons form a small percentage of the total neuronal population in the mPFC, through modulation of the input that pyramidal neurons receive and control over their output, they function as critical components in the neuronal circuitry that regulates cognitive behavior.

1.6 The mPFC and memory

The mPFC enables top-down control over conditioned behavior elicited by either aversive or appetitive stimuli, integrating and processing information about events, contexts and discrete cues (*79*). Due to sometimes opposing roles in memory expression, the dmPFC and vmPFC have been regarded as a "go" and "stop" system, respectively (*45*), a view that has been debated in recent years and which I will discuss in the following sections.

Aversive fear memory

Although early studies on the role of the mPFC in the fear circuitry focused on auditory fear conditioning and extinction (*80, 81*), later reports confirmed a causal role for this brain area in contextual fear memory expression and extinction (*82, 83*). Global pharmacological inactivation of the dmPFC, induced by administration of a sodium channel blocker tetrodotoxin (TTX), during a test session revealed that activity in this brain region is necessary for expression of recent contextual fear memory (*82*). A similar result was observed when

animals received another sodium channel inhibitor, bupivacaine, bilaterally in the dmPFC before a retrieval test performed 1 day after conditioning (*84*). In contrast, TTX-induced inactivation of the dmPFC during CFC did not disrupt the formation of long-term fear memory, despite rats displaying lower freezing levels during the last portion of the conditioning session (*82*). This result is in stark contrast with the observation that infusion of a N-methyl-D-aspartate (NMDA) receptor subunit 2B antagonist in the ACC impaired formation of fear memory (*85*). Injection of anisomycin in the ACC immediately after CFC, which blocked protein synthesis during memory consolidation (*86*), also disrupted fear memory when animals were tested 1 day after conditioning (*85*). The cellular mechanisms necessary for the storage of a contextual fear memory, such as long-term potentiation (LTP - strengthening of synapses between two neurons) in the mPFC have also been investigated (*87*). The process of LTP, required for adequate learning and memory (*88*), is induced by tetanic stimulation and mediated via NMDA receptors (*89-91*). As observed in the ACC, activation of NMDA receptors containing NR2A and NR2B subunits is responsible for the occurrence of LTP and subsequent blockade using antagonists or genetic manipulations impairs the formation of contextual fear memory (*87*). Additionally, inhibition of the ACC by delivery of muscimol, a GABA-A receptor agonist, shortly before conditioning, prevents the formation of fear memory, as measured by reduced freezing levels on test days (*92*). The vmPFC has been implicated in extinction of fear memory (*83*). Inactivation of NMDA receptors in the vmPFC, by administration of ifenprodil, leads to impairments in the consolidation of extinction memory, as rats that received ifenprodil exhibited higher freezing levels when compared to controls 1 day after extinction learning (*83*). However, all test groups showed similar extinction learning curves and reached plateau around the same time. Moreover, animals that received muscimol before or after extinction learning had high freezing levels, comparable to the ifenprodil treated group, pointing to the requirement of neuronal activity in the vmPFC for adequate maintenance of extinction memory (*83*). Research on the role of the vmPFC in extinction of auditory fear memories showed similar findings, further supporting the necessity of NMDAR activation for consolidation of extinction memory (*93*). Inhibition of the vmPFC during non-reinforced re-exposure to a CS impairs fear extinction *learning* (*94*) and stimulation of the vmPFC during extinction learning facilitated extinction and promoted a decrease in freezing (*94*). Moreover, inhibition during extinction *recall* does not affect the suppression of extinguished freezing behavior (*95*),

pointing to a selective role of the vmPFC in the acquisition of extinction memory.

As discussed in section 1.4, the mPFC has been implicated in systems consolidation and expression of remote fear memory. It was found that time-dependent changes in retrieval-evoked neuronal activity in the prefrontal cortex develop in an opposite direction compared with the hippocampus. Whereas increased activity in the hippocampus correlates with recall of a 5-day-old memory, a higher degree of activity in mPFC is associated with recall of a 25-day-old memory (*96*). Furthermore, lesioning of the ACC at 28-30 days after fear or eye-blink conditioning disrupts memory expression, an effect that does not occur after hippocampal lesions (*97*). More recent findings from Goshen et al. (2011) also pinpoint to the specific involvement of the prefrontal cortex in remote memory, as optogenetic inhibition of the ACC impaired fear memory expression at 28 days, but not 24 h, after conditioning (*37*). An elegant study by Do-Monte et al. (2015) established that dmPFC-to-BLA projections are important for expression of recent auditory fear memory, but at later timepoints (7-28 days), the same CR is supported by dmPFC projections to the paraventricular nucleus of the thalamus (*98*). Whether the latter circuitry also plays a role in the expression of a contextual fear memory remains to be elucidated. As the mPFC acts as an integration hub for the processing of emotional and sensory information, it may control the expression of remote fear memory in a similar way the hippocampus does for recent fear memories, orchestrating the reactivation of the brain-wide memory network and thereby guiding behavior (*46, 51, 99, 100*).

Appetitive cocaine memory

Recurrent pairing of contextual cues with drugs of abuse drives associative learning between such cues and the rewarding effects upon intake of addictive substances. Drug-associated cues act as triggers for memory retrieval and initiation of reward seeking (the CR) during periods of abstinence (*101, 102*). This can be modeled in the laboratory using CPP induced by a plethora of drugs (Fig. 2). As I studied associative memory related to cocaine reward in my thesis, I will now primarily focus on the role of the mPFC in cocaine CPP.

The mPFC has been heavily implicated in the establishment and maintenance of addictive behavior in general and cocaine CPP in particular. Moreover, similar to fear conditioning, a differential role of the dorsal and ventral region of the mPFC has been observed in

addictive behavior. Pharmacological interventions revealed that the dmPFC drives conditioned cocaine seeking behavior, whereas the vmPFC can both inhibit and facilitate cocaine seeking (*58, 70*). The vmPFC can suppress conditioned cocaine seeking through the consolidation and expression of extinction memory (*56, 103*). With respect to cocaine CPP, lesioning of the different mPFC subareas, by local infusion of quinolinic acid before training, leads to distinct outcomes when preference for the cocaine context is assessed (*104*). While lesioning of the PL blocks acquisition of cocaine CPP, lesions of the ACC or IL have no effect on CPP (*104, 105*). However, lesioning of the entire mPFC mimics the results observed when only the PL is affected (*104*). Zavala and colleagues report no effect of quinolinic acid delivery into PL on initial expression of cocaine CPP, but cocaine-primed reinstatement of CPP is abolished in lesioned animals (*106*). Notably, the pre-conditioning PL lesion also did not affect extinction learning, since learning curves were similar between controls and lesioned rats (*106*). An elegant study in rats revealed that retrieval of cocaine CPP memory leads to an increase in the intrinsic excitability of PL neurons (*107*). After distinguishing between rats with a high or low CPP score, the authors observed enhanced excitability specifically in rats with a high CPP score, which is mediated by reduced spike amplitude attenuation over a train of action potentials. Pharmacological rescue of the spike amplitude attenuation impairs expression of cocaine CPP memory, as well as subsequent cocaine-primed reinstatement (*107*). A more recent study showed that retrieval of cocaine CPP memory induces neuronal activation in the mPFC (mainly PL), as measured by increased levels of pERK1/2 and Fos (*108*). However, inactivation of this area by chemogenetics did not reduce the amount of time spent in the cocaine-paired context (*108*). Strikingly, another study utilizing chemogenetics to suppress the activity of either pyramidal or GABAergic interneurons in the PL reports different findings (*109*). In this study, mice received CNO before each conditioning session to reduce the activity of PL pyramidal neurons or GABAergic neurons. Acquisition of cocaine CPP memory was only impaired upon suppression of PL pyramidal neurons. The same discrepancy between these neuronal subtypes was also observed when CNO was administered just before a CPP test, reinforcing the notion that activity of excitatory neurons in the PL is necessary for the acquisition and expression of cocaine CPP memory (*109*). In an attempt to investigate whether neuronal activation in the PL and IL during CPP expression occurs in a cell-type specific manner, Miller and Marshall sacrificed animals after a retrieval session performed 1 day

after conditioning and investigated the brains for differential activation of excitatory or inhibitory neurons (*110*). Retrieval of cocaine CPP memory was accompanied by enhanced neuronal activation in the PL, but not IL (*110*). Interestingly, in the PL, a higher percentage of GABAergic neurons and lower percentage of excitatory neurons was activated compared with control animals, and this was not observed in other brain regions (*110*). Thus, these conflicting reports warrant further investigation of the specific contribution of excitatory and inhibitory mPFC neurons in expression of cocaine CPP memory.

The dmPFC and vmPFC also have a time-dependent role in conditioned cocaine seeking behavior. After 30 days, but not 1 day, of abstinence, re-exposure to a cocaine-associated cue enhances neuronal activity in the dmPFC, but not the vmPFC (*111*). With respect to cocaine CPP, optogenetic stimulation of vmPFC pyramidal cells facilitates extinction of CPP memory, but only at a remote timepoint (21 days) after conditioning (*112*). Conversely, inhibiting pyramidal cells in this brain region 21 days after conditioning blocked extinction of the cocaine CPP, whereas optic inhibition during expression of a 1-day-old cocaine CPP memory decreases the amount of time spent in a cocaine-associated context (*112*). In line with extinction of fear memory, activation of vmPFC NMDA receptors containing GluN2B subunits supports extinction of cocaine CPP (*113*). Together, this indicates that, similar to aversive memory, the mPFC has a time-dependent role in expression of cocaine-associated memories and the predominant view suggests that the dmPFC and vmPFC function as a 'go' and 'stop' hub, respectively.

1.7 Memory encoding by neuronal ensembles

Accumulating evidence indicates that learned associations are not encoded by global or random neuronal activity in memory-relevant brain regions, but rather by the synchronized activity of sparsely distributed neurons, referred to as neuronal ensembles or engram cells (*114*). The theory that learned associations are encoded by sparse groups of neurons was first proposed by Donald. O. Hebb in 1949 (*20, 21*). The discovery of immediate early genes (IEGs) provided support for his theory. Expression of an IEG, such as Fos, is rapidly induced by strong neuronal activation and peaks within 1-2 hours after learning and memory retrieval (*115, 116*). As such, they can be used as a proxy for neuronal activation to identify the neurons that harbor the structural and physiological changes (*i.e.*, engram) supporting memory (*117, 118*). Indeed, the recent integration of IEG promoter-driven

tagging systems in transgenic animals with opto- or chemogenetics enabled the identification and manipulation of neuronal ensembles, proving that memory encoding and expression depends on activation of specific neuronal ensembles (*119, 120*).

Neuronal ensembles in the mPFC

Investigation of memory processing at the level of neuronal ensembles has provided unprecedented detailed insight into how aversive and appetitive memories are encoded in the brain. Animals that undergo CFC form neuronal ensembles in brain areas known to have a central role in fear memory, such as the amygdala, the hippocampus and the mPFC (*121*). Interestingly, neuronal ensembles in the dmPFC are activated by exposure to a context alone and by a context-shock association (*121*), whereas no difference in neuronal activity occurs in the vmPFC (*121*). Potentially, vmPFC neurons are recruited when conditions change, as is the case with extinction learning (*122*). With respect to appetitive memory, the vmPFC harbors neuronal ensembles supporting conditioned food seeking and extinction of this CR (*123*). While this partly contrasts with the mainstream theory of the functional dichotomy of the dmPFC and vmPFC, it may be explained by the refined manipulation of a neuronal ensemble as opposed to an entire brain region. A recent study by Ye et al. (2016) focused on disentangling neuronal ensembles in the mPFC representing different experiences (fear and cocaine memory) (*124*). They found non-overlapping ensembles in the mPFC coding for aversive and appetitive experiences, and optogenetic stimulation of these populations induces acute place avoidance and preference, respectively. Moreover, these two different neuronal ensembles in the mPFC exhibit different projection patterns; neurons coding for the aversive memory (foot-shock) heavily target the lateral habenula and neurons representing the appetitive experience (cocaine CPP) innervate the NAc. Although these studies have substantially increased our understanding of the cellular substrate of aversive and appetitive memories, little is known about the time-dependent involvement of mPFC neuronal ensembles in encoding and expression of conditioned behavior.

1.8 Aims and outline of this thesis

Memory consolidation and persistence depends on several critical steps at the brain-wide neuronal network, local micro-circuit and cellular level. The mPFC has been implicated as a key region that influences memory formation, expression and extinction. However, how expression and extinction of remote aversive and appetitive memories is regulated within local mPFC circuitry and at the level of neuronal ensembles has remained elusive.

Hence, in this thesis I aimed to determine the involvement of the mPFC circuitry in the temporal organization of aversive and appetitive memories. To achieve this my subgoals were to:

1. Design and functionally validate a new technique to persistently tag and manipulate neuronal ensembles in the mPFC.

2. Assess the role of mPFC neuronal ensembles in systems consolidation of fear memory.

3. Dissect the role of interaction of the vmPFC and dmPFC circuitry in extinction of cocaine memory.

In chapter 2, I provide an overview of studies that used optogenetics to dissect the role of the mPFC circuitry in various behavioral phenotypes.

In chapter 3, I describe the creation of a new viral vector system using the *Fos* promoter to drive an inducible Cre recombinase. I combined this system with chemogenetics to permanently label and manipulate neuronal ensembles.

In chapter 4, I used the viral vector tool described in chapter 3 in a CFC paradigm to investigate the time-dependent role of mPFC neuronal ensembles in systems consolidation of fear memory. Moreover, I investigated the role of CREB-mediated gene transcription in these ensembles and how learning intensity modulates the involvement of mPFC ensembles in fear memory expression.

In chapter 5, I dissected the mPFC neuronal circuitry supporting cocaine memory extinction. I explored the connectivity between the vmPFC and dmPFC and how these two brain regions interact during extinction of cocaine CPP. In addition, I investigated whether activity of PV interneurons is crucial for the acquisition of cocaine CPP extinction memory.

Finally, in chapter 6 I discuss the results of each chapter in light of existing literature and propose a model of the mPFC memory circuit at the level of neuronal ensembles and inter-regional connectivity.

Additionally, I propose complementary studies in order to address outstanding questions based on my experiments and provide future perspectives that may advance our understanding of the role of the mPFC circuit in remote memory retrieval and extinction.

Chapter 2

Optogenetic dissection of medial prefrontal cortex circuitry

Danai Riga[1#], Mariana R. Matos[1#], Annet Glas[1], August B. Smit[1], Sabine Spijker[1], Michel C. Van den Oever[1*]

[1]Dept. Molecular and Cellular Neurobiology, Center for Neurogenomics and Cognitive Research, Neuroscience Campus Amsterdam, VU University Amsterdam. The Netherlands

[#]these authors contributed equally

Frontiers in systems neuroscience, 2014, 9;8:230

Abstract

The medial prefrontal cortex (mPFC) is critically involved in numerous cognitive functions, including attention, inhibitory control, habit formation, working memory and long-term memory. Moreover, through its dense interconnectivity with subcortical regions (e.g., thalamus, striatum, amygdala and hippocampus), the mPFC is thought to exert top-down executive control over the processing of aversive and appetitive stimuli. Because the mPFC has been implicated in the processing of a wide range of cognitive and emotional stimuli, it is thought to function as a central hub in the brain circuitry mediating symptoms of psychiatric disorders. New optogenetics technology enables anatomical and functional dissection of mPFC circuitry with unprecedented spatial and temporal resolution. This provides important novel insights in the contribution of specific neuronal subpopulations and their connectivity to mPFC function in health and disease states. In this review, we present the current knowledge obtained with optogenetic methods concerning mPFC function and dysfunction and integrate this with findings from traditional intervention approaches used to investigate the mPFC circuitry in animal models of cognitive processing and psychiatric disorders.

Keywords – optogenetics, prefrontal cortex, cognition, depression, addiction, fear, memory

Introduction

Detailed insight into the connectivity and functionality of the nervous system is of pivotal importance for understanding how the brain functions in health and disease states. The mPFC is a brain region that has been implicated in a plethora of neurological and psychiatric disorders. However, for a long time, its anatomical complexity has hindered a thorough investigation of the contribution of different mPFC cell-types and their afferent and efferent projections, to the development and expression of behavior associated with neural dysfunction. Through its many connections with other cortical and subcortical areas (*125*), the mPFC may act as a control board, integrating information it receives from numerous input structures and converging updated information to output structures (*51*). Several human psychiatric conditions, including depression, schizophrenia and substance abuse, have been linked to altered mPFC function (*45, 70, 126*). This is supported by a substantial number of experimental animal studies in which lesions, pharmacological intervention and electrophysiological techniques were employed to determine whether the mPFC is involved in cognitive processes and symptoms of psychiatric disorders (as detailed below). However, accurate dissection of the complex organization of the mPFC requires intervention with high cell-specificity and temporal resolution at a subsecond timescale. In recent years, a rapidly growing number of studies have used optogenetic approaches to address this issue, which substantially enhanced our understanding of mPFC circuitry. We will first briefly introduce the technological background and possibilities of optogenetic tools and will then review currently available literature that used optogenetics to dissect the contribution of different mPFC cell-types, and their connections within the mPFC and with other brain regions, to cognition and psychiatric disorders.

Optogenetics technology

Optogenetics technology takes advantage of genetically encoded light-sensitive proteins, such as microbial opsins, that are introduced in intact living mammalian neurons, allowing manipulation of neuronal activity *in vitro* and *in vivo* (*127, 128*). The technique is characterized by the ability to modulate neuronal firing on a millisecond second timescale with great cell-type specificity in awake, freely moving animals (*129*). A widely used depolarizing opsin is Channelrhodopsin-2 (ChR2; and genetically modified variants), a cation channel that

induces action potential firing upon illumination with pulses of blue light (*130*). In contrast, the chloride pump Halorhodopsin (NpHR) or the proton pump Archaerhodopsin (Arch or ArchT) are often used to hyperpolarize neuronal membranes (*130*). An elaborate discussion on the use and relevance of different opsin variants and optogenetic tools would be beyond the scope of this review, but has been excellently reviewed by others (*131, 132*). In brief, cell-type specific expression of opsins can be achieved using gene-based targeting strategies (*131*). Transgenic animals and viral constructs carrying opsin genes under direct control of tissue specific promoter sequences enable the expression of opsins in genetically defined cell-types (see supplementary **Table S1** for an overview of optogenetic manipulations discussed in this review). Alternatively, cell selective expression can be achieved using mouse or rat Cre-recombinase (Cre) driver lines combined with Cre-dependent viral opsin vectors. With respect to excitatory pyramidal neurons that are present in the mPFC, the CaMKIIα or Thy1 promoter can be used express opsins in these cells (*112, 129*). As these are relatively strong promoters, they are suitable to drive the expression of an opsin gene placed downstream of the promoter. Promoter regions that are used to target GABAergic interneurons are generally relatively weak promoters, and therefore modulation of mPFC interneuron activity is typically achieved using transgenic mice in which a GABAergic cell-specific promoter drives the expression of Cre-recombinase (Cre) (*131*). For example, to manipulate fast-spiking GABAergic interneurons, parvalbumin (PV)::Cre mice are widely used (*76, 133*). When these transgenic animals receive a viral vector in which the opsin gene is inserted in a double floxed inversed open reading frame, Cre expressing cells will irreversibly invert the open reading frame to enable opsin expression driven by a strong ubiquitously active promoter (e.g. elongation factor 1α; EF1α promoter)(*131*).

For *in vivo* experiments, light can be delivered in the brain by a laser or LED device coupled to a thin optical fiber (~100-300 μm) that is implanted in the brain and aimed at opsin expressing cells (*134*). The type of opsin used and the depth of the tissue illuminated determine the wavelength and appropriate light source required. In addition to optic modulation of opsin expressing somata, projection-specific manipulation is feasible by illuminating opsin expressing efferent projections in an innervated target region (*131*). Other advantages include rapid reversibility and repeatability of photostimulation, integration with electrophysiological recordings and anatomical

tracing using fluorescent reporter proteins fused to opsins (*129*). Important limitations to consider are the toxicity of viral vectors and the potentially harmful heating of neurons during photostimulation. Albeit with few limitations, optogenetic approaches have an unprecedented capacity to selectively and robustly modulate mPFC neuronal activity in behavioral paradigms and acute slice preparations (*132*). As the vast majority of currently published optogenetic experiments were performed in mice and rats, we will primarily focus on the anatomy and functionality of the rodent mPFC circuitry.

Anatomy

Within the mPFC, four distinct areas have been defined along a dorsal to ventral axis, i.e., the medial precentral area (PrCm; also known as the second frontal area (Fr2)), the anterior cingulate cortex (ACC), the prelimbic cortex (PLC) and the infralimbic cortex (ILC) (*45*). In addition to this division, which is mainly based on cytoarchitectural differences, the mPFC is often divided into a dorsal component (dmPFC), encompassing the ACC and dorsal region of the PLC, and a ventral component (vmPFC), encompassing the ventral PLC, ILC and dorsal peduncular cortex (DPC), according to functional criteria and connectivity with other brain areas (*45*). For the purpose of this review, in the following sections we will focus mainly on anatomical evidence derived with optogenetic tools, and mention the precise subregion of the mPFC when this information is available, or otherwise refer to dmPFC and vmPFC.

Cytoarchitecture of the mPFC

The local mPFC network consists mainly of excitatory pyramidal cells (80-90% of the total population) and inhibitory GABAergic interneurons (10-20% of the total population), both of which can be further subdivided into different cell types based on morphological, physiological and molecular properties (*72, 135*). Well-studied GABAergic interneuron subtypes include the perisomatic targeting fast spiking parvalbumin (PV) interneurons, and the dendritic targeting somatostatin (SOM) interneurons. PV interneurons are of particular clinical interest, as their numbers are known to be decreased in schizophrenia patients (discussed below)(*136, 137*). Both interneuron types excise strong control over local circuitry, as they are able to synchronize the spiking activity of pyramidal cells generating neuronal

oscillations (*74*). Selective photostimulation of ChR2-expressing PV and SOM interneurons in the mPFC of mice has been shown to generate distinct circuit responses (*74*). PV neurons were found to control the outputs of principal pyramidal neurons, as they exerted fast, powerful and uniform inhibition on principal cell firing (*74, 76*). SOM neurons on the other hand modulated the input that principal pyramidal neurons received and the inhibitory effect of synchronous photostimulation of these neurons was weak, more variable and stretched over a longer time (*74*). Optogenetic approaches validated the critical contribution of GABAergic interneuron firing to gamma oscillations and emotional behavior (*48, 63, 64, 138*). Pyramidal neurons in layer V (see below) of the mPFC can be characterized as thick tufted, subcortically projecting cells and as thin-tufted, colossally projecting cells (*139*). Optogenetic modulation revealed that colossally projecting cells differentially innervate both subtypes and showed that PV interneurons preferentially inhibit subcortically projecting pyramidal neurons (*140*). Pyramidal cell subtypes can also be distinguished based on expression of the dopamine D1 or dopamine D2 receptor (D1-R and D2-R), of which D1-R neurons have been implicated in control over food intake by selective optogenetic activation of this population (*141*).

Layers and connectivity of the mPFC

The laminar organization of the rodent mPFC is slightly different from that of other cortical regions, which have a distinct input layer IV (*46*). The efferent projections of granular cortices to subcortical areas arise from the deep layers V and VI, and granular cortico-cortico connections are mainly made by neurons in the superficial layers II and III (*142*). The rodent mPFC however lacks the classical input layer IV (*46*). Furthermore, both deep and superficial mPFC layers receive long-range inputs from cortical and subcortical regions and project to other (limbic) structures (*50, 52, 53*).

The laminar pattern has important implications for signal processing in the mPFC. Afferent projections originating from limbic and cortical regions mainly target the superficial layers I and II/III (*143*). For long, technical constraints have hampered the mapping of functional connections, as mere overlap of a spine and axonal varicosity does not necessarily indicate a functional connection and paired recordings are unsuitable for exploring long-range connections (*144*). Furthermore, most long-range excitatory inputs are severed in acute slices, hindering measurements with electrical stimulation. Optogenetic activation of ChR2-expressing presynaptic terminals

showed that layer II PLC pyramidal neurons received functional inputs from the contralateral mPFC, midline thalamic nucleus (MTN), basolateral amygdala (BLA), and ventral hippocampus (HPC) (*47*). These input fibers synapsed at different dendritic locations, which were often poorly predicted by anatomy alone, and the connections showed bias for populations of spines of distinct volume (*47*). As spine volume has been suggested to correlate with the strength of excitatory postsynaptic current (EPSC) (*145*), this finely tuned anatomical and functional connectivity ideally positions the mPFC to integrate and relay information from preferential afferent sources. Both dmPFC and vmPFC are heavily interconnected with the thalamus (*52, 138*). Thalamocortical connections are vital for mediating processes of sensation, perception, and consciousness (*146, 147*). In addition to the thalamic input received by layer II neurons (*47*), thalamic neurons that synapse onto mPFC layer I neurons have also been identified with optogenetics (*48*). Photostimulation of thalamocortical projections originating from midline and paralaminar thalamic nuclei drove fast and robust synaptic responses in layer I late-spiking interneurons, which were more heavily excited than pyramidal cells (*48*). These interneurons were able to drive feed forward inhibition of layer II/III pyramidal cells (*48*). In contrast, pharmacological activation of layer I neocortical interneurons using cholinergic agonists did not induce feed-forward inhibition (*148*). Furthermore, synaptic responses of mPFC interneurons were sustained upon repetitive photostimulation of thalamocortical projections (*48*). These optogenetic findings suggest that thalamocortical projection neurons are able to drive transmission over relatively long periods of time (minutes), required for working memory function (discussed below).

The mPFC subregions are also reciprocally interconnected (*45*). Connectivity between ILC and PLC has been assessed by tracing methods and recently also by optogenetic tools (*65, 66*). Ji and Neugebauer demonstrated that photostimulation of ILC pyramidal cells reduced spontaneous and evoked activity in PLC pyramidal cells, probably mediated by feed forward inhibition (*66*). In contrast, both spontaneous and evoked activity in ChR2 expressing deep-layer ILC pyramidal neurons was increased upon optical activation of this neuronal population, without affecting ILC inhibitory neuron spiking behavior (*66*). As the ILC and PLC project differently over the brain and have differential roles in several processes, including habitual behavior, expression of conditioned-fear and addictive behavior (*65,*

69, 70, 149), this mechanism may allow the ILC to inhibit PLC output, while simultaneously activating its subcortical target regions.

The mPFC heavily projects to other cortical and subcortical brain regions, which enables it to exert control over visceral, automatic, limbic and cognitive functions (*50, 51*). Tracing studies have shown a dorsoventral shift along the mPFC from predominantly sensorimotor target regions of the dmPFC to limbic target regions of the vmPFC (*50, 53*). Glutamatergic projections of the mPFC to the nucleus accumbens (NAc) core and shell have been well described and validated by optogenetic approaches (*150, 151*). Interestingly, by microinjection of a Cre-dependent ChR2 AAV vector in Dlxi12b::Cre mice, Lee et al. provided evidence for the existence of mPFC GABAergic neurons that have long-range projections to the NAc (*152*). This indicates that not all GABAergic neurons residing in the mPFC are local interneurons. In addition, glutamatergic PLC projections to the BLA have been studied using optogenetics technology. This pathway is thought to be important for integrating higher cognitive processing with innate emotional responses (*64*), a process dysregulated in mood disorders (covered in greater detail below). Little and colleagues optogenetically targeted PLC layer II and identified two distinct pyramidal cell populations within this layer that either project to the contralateral mPFC or to the BLA (*63*). These PLC projection neurons were similar in anatomy and physiological properties, complicating examination of their circuit function. Photostimulation of contralateral mPFC or BLA ChR2-expressing presynaptic terminals paired with whole-cell recordings of mPFC or BLA projecting pyramidal neurons demonstrated that BLA to BLA-projecting PLC neurons exhibited the strongest synaptic connection. Enhanced synaptic transmission in this pathway was associated with increased spine density, larger spine volume and synaptic targeting. Moreover, BLA inputs targeted spines near the soma of PLC-BLA neurons, which were able to elicit stronger EPSCs than projections targeting the dendrite (*63*). PLC-BLA projections also target a fraction of GABAergic interneurons in the BLA, which in some cases evoked feed-forward inhibition of GABAergic transmission (*153*). This unique interconnectivity between the PLC and BLA may enable highly efficient bi-directional communication, which could be important for top-down control over responding to emotional stimuli.

These initial investigations demonstrate the unique possibilities of optogenetics to probe the mPFC circuitry at the level of individual cells, intra-mPFC connectivity and long-range afferent and

efferent projections. Photostimulation in acute slice preparations is a highly relevant method to anatomically dissect functional connections and to measure synaptic properties between different neuronal populations. However, to determine whether a specific connection is causally involved in a defined cognitive process, *in vivo* modulation of neural activity is required. In the following sections, we will discuss findings derived from optogenetic interventions in freely moving animals.

Cognition

Traditional manipulation techniques have implicated the mPFC in a diverse range of cognitive functions, of which memory performance, alertness, learning and memory and habitual behavior thus far have been addressed by optogenetics technology.

Working memory performance, alertness and temporal control.

Working memory is a complex brain process that refers to temporary storage of information (time scale of seconds to minutes) necessary for cognitive performance (*154*). The mPFC has been implicated in this process as it was found that reversible pharmacological inactivation of the PLC impaired working memory performance (*155*). Working memory function can be assessed using the trace fear-conditioning task, in which a conditioned stimulus is followed by an aversive unconditioned stimulus after a delay of several seconds. Prefrontal neurons are known to exhibit persistent firing during the delay (*156*), suggesting a role for the mPFC in maintaining a representation of the conditioned stimulus during the delay. However, causal evidence for necessity of mPFC neuronal activity bridging the delay has only recently been provided using optogenetic intervention. Gilmartin and colleagues expressed ArchT in PLC neurons (using a non-selective CAG promoter) to allow inhibition specifically during the delay phase of the trace fear-conditioning task (*157*). Indeed, photoinhibition during the delay impaired learning of an association between the conditioned and unconditioned stimulus, confirming that spiking of PLC neurons is required for working memory performance during trace fear-conditioning. A different task to measure working memory performance is the operant delayed alternation task, in which animals alternate lever presses with a predetermined delay to obtain a reward (*158*). Excitotoxic lesions and pharmacological inactivation of the

mPFC specifically impaired acquisition and expression of the delayed alternation task with long delays, indicating that mPFC activity is crucial when working memory demands are high (*159*). Lesions of the ventral striatum or dorsal hippocampus, areas that are heavily connected with mPFC, did not lead to reduced delayed alternation performance. Importantly, ChR2-mediated activation of PV interneurons in the PLC selectively during the delay also significantly impaired performance in this task (*159*). Together, these studies show that PLC activity is necessary for working memory performance and demonstrate that photoactivation of PV interneurons can mimic the effects of chronic lesion and pharmacological inactivation in a spatially and temporally precise manner.

Working memory function of the mPFC is modulated by several monoamine systems, including the noradrenalin and dopamine (DA) system (*160, 161*). During spatial working memory, extracellular noradrenaline levels increase in the mPFC and pharmacological stimulation of alpha-2A adrenoreceptors in the PLC enhanced working memory performance (*161, 162*). Using optogenetics, it was found that photoactivation of ChR2-expressing noradrenergic projections from the locus coeruleus evoked persistent firing, a cellular correlate of working memory, in PLC and ACC pyramidal neurons, which was mediated through activation of presynaptic alpha1 and postsynaptic alpha2 adrenoreceptors (*163*). Cortical noradrenaline has not only been implicated in working memory function, but is believed to correlate more generally with states of attention, wakefulness and arousal (*164*). Carter and colleagues used optogenetic intervention to precisely evoke noradrenalin transmission and to study its influence on alertness in mice (*165*). Illumination of NpHR-expressing locus coeruleus noradrenalin neurons reduced wakefulness during the animal's active period and caused a decrease of extracellular noradrenalin levels in the mPFC. In line with this, tonic and phasic photostimulation of ChR2-expressing locus coeruleus neurons produced immediate sleep-to-wake transitions. Interestingly, tonic activation increased general locomotor activity, whereas phasic activation had the opposite effect. Moreover, sustained high frequency (> 5 Hz) photoactivation of locus coeruleus neurons evoked a state of behavioral arrest. Carter and colleagues show that this latter effect may be induced by a depletion of mPFC noradrenalin stores, as prolonged photostimulation reduced extracellular noradrenalin levels in the mPFC, and behavioral arrests were attenuated by noradrenalin reuptake inhibitors (*165*). This elegant study shows that prefrontal

noradrenalin release is finely tuned to influence wakefulness, with even subtle differences having significant effects on sleep-to-wake transitions and arousal.

Working memory is generally considered to represent memory of two sensory stimuli that are separated by a delay. Time-tracking or memory of a defined time-interval at a timescale of seconds is thought to involve an internal clock system, in which the mPFC circuitry has also been implicated (*166*). In particular, DA transmission in the mPFC has been implicated in the timing of a defined interval using the fixed interval-timing task (*167*). In a recent study, D1 dopamine receptor (D1-R) transmission in the mPFC was shown to have a critical role in the temporal control of movement towards a goal (reward) during a defined time-interval (*168*). Pharmacological blockade of D1 dopamine receptors (D1-R), but not the D2 dopamine receptors (D2-R) in the ILC and PLC impaired temporal control over responding in the fixed interval-timing task. In support of the specific role of D1-Rs, NpHR-mediated optical inhibition of mPFC D1-R expressing neurons impaired fixed interval timing performance (*168*). Strikingly, ChR2-mediated stimulation of D1-R neurons during the last 10 s of a 20-s interval enhanced responding only at 20 s. Based on this evidence, the authors argue that the mPFC D1 system regulates temporal control of goal-directed behavior, rather than the encoding of passage of time.

Despite considerable advances in recent years, much remains to be learned about the neurobiological substrate of working memory and related functions by comparing mPFC optogenetic interventions in different tasks within the same animal. This is of relevance to, for example, assess the commonalities and differences in mPFC circuitry mechanisms that regulate interval timing and working memory performance. Finely tuned firing of mPFC D1 neurons mediates precise temporal control over goal directed responding, but whether (sustained) activity of this neuronal population is also required for optimal working memory performance remains to be studied (*157, 168*). Furthermore, although traditional manipulation approaches indicate that the mPFC cholinergic system has a pivotal role in working memory (*169*), within the mPFC, this neurotransmitter system has not been directly targeted yet by optogenetics technology.

Learning, memory and extinction

The mPFC is thought to exert cognitive control over conditioned responding to aversive and rewarding stimuli by integrating

information about experienced contexts and events (*79*). The fear-conditioning paradigm is a widely used animal model to study learning and memory function, as well as extinction of acquired fear memories (*170-172*). Specific roles for mPFC subareas have been established in the expression of conditioned fear memory, with dorsal regions mediating the encoding and expression of fear memory and ventral regions contributing to consolidation and expression of extinction memory (*58, 173*). These findings are supported by lesions, pharmacological inactivations and *in vivo* spike recordings (*80, 173, 174*). However, research into the temporal contribution of specific mPFC circuitry elements has only been initiated recently. Using optogenetics, Courtin and colleagues established that phasic inhibition of dmPFC PV interneurons underlies the expression of fear, as assessed by freezing behavior in the fear-conditioning paradigm (*77*). They first showed that activity of a specific subpopulation of GABAergic interneurons is inhibited during the presentation of a conditioned stimulus associated with a foot-shock. Next, this subpopulation was identified as PV interneurons, since ChR2- and ArchT-mediated optical modulation of PV neurons, respectively, attenuated or evoked expression of conditioned-fear. Remarkably, optical inhibition of these neurons also evoked freezing behavior before fear-conditioning and reinstated expression of fear after extinction training (*77*). They found that the PV neuron controlled fear response was mediated by resetting of theta phase oscillations in the mPFC and disinhibition of pyramidal cells projecting to the BLA, further supporting the role of the mPFC-BLA projection in emotional control. This study also identified a second population of inhibitory interneurons that showed increased activity during fear states. The authors speculate that this subpopulation may inhibit PV interneurons and receives input from brain regions (e.g. hippocampus, BLA) that drive the expression of fear (*77*), an interesting hypothesis that remains to be addressed by future research. Extinction of conditioned-fear is associated with decreased excitatory synaptic efficacy transmission of mPFC to BLA pyramidal cells, but did not affect output to GABAergic BLA interneurons and intercalated cells, as demonstrated using optogenetics (*175*). As a result, the excitation/inhibition (E/I) balance in this pathway is likely changed, favoring inhibition and resulting in suppression of the conditioned-fear response (*175*). These optogenetic studies confirm the role of the dmPFC in driving of fear responses and refine the temporal contribution of subpopulations of GABAergic interneurons in this behavior. An interesting study by Lee and colleagues showed that photoactivation of long-range GABAergic mPFC projections to the NAc

evoked real-time place avoidance (*152*), suggesting this novel pathway may also regulate responding to aversive stimuli.

Habitual behavior

Habits are defined as behavioral patterns that are insensitive to changes in outcome value. Habitual behavior is differentially regulated by mPFC subareas; whereas the PLC promotes flexibility, ILC activation inhibits flexibility and promotes behavioral rigidity (*149*). Previous studies demonstrated that lesion and pharmacological inactivation of the ILC induce a switch from fixed to flexible responding (*176*). The temporal control of ILC neurons to habitual behavior has been confirmed and refined by repetitive optogenetic modulation. Brief photoinhibition of ILC pyramidal cells blocked the formation and expression of habitual behavior, but the subsequent behavioral response depended on the timing of inhibition (*177, 178*). In these studies, habitual behavior was assessed by training rats to obtain a reward in a cued T-maze task. Following overtraining, rats became insensitive to devaluation of the reward. Animals continued goal-directed behavior when ILC pyramidal cells were optogenetically silenced during habit formation, but once the habit was fully expressed, photoinhibition evoked a new habitual pattern. Moreover, when photoinhibition was repeated during execution of the new habit, animals re-expressed the original habit (*177*). This immediate switching between habitual behaviors demonstrates that even semiautomatic behaviors are under cortical control while they are being performed. The ILC target region that mediates switching between habits has not been identified yet, but projections to the dorsolateral striatum are of particular interest, as a similar spike activity pattern was observed in both regions after a habit was established (*178*). Based on this evidence, the authors suggested that the development of habitual performance is determined by the balance of sensorimotor striatal activity and value-sensitive ILC activity. Interestingly, only the superficial ILC layers mimicked spiking activity in the dorsolateral striatum (*178*), stressing the need to apply layer- and pathway-specific optogenetic manipulations to study the habit circuitry in more detail.

Psychiatric disorders

Optogenetics has provided important new insights in mPFC function in the healthy brain, but has also been used to elucidate neural circuitry elements involved in disease-related phenotypes (*179*). In the following sections, we will discuss how optogenetic manipulations have validated, and in some cases updated current theories that aim to explain the contribution of the mPFC circuitry to various psychiatric disorders, including depression, schizophrenia and drug addiction.

Depression

Major Depressive Disorder (MDD) is one of the most prevalent psychiatric disorders, estimated to affect about 5% of the global population and therefore considered as a leading cause of disability worldwide (*180*). MDD diagnosis criteria include depressed mood and anhedonia (reduced ability to experience pleasure) that persist over time and affect every day-life experience (*181*). In addition, MDD diagnosis includes somatic effects, such as disturbances in food intake (weight loss or gain), in sleep (insomnia or hypersomnia), as well as in levels of psychomotor activity (agitation or retardation). Cognitive decline characterized by impairments in working memory and decision making, loss of concentration and attentional biases is also considered a key factor in perpetuation of the depressive state (*182*). The multifaceted phenotypic expressions that accompany depression are attributed to dysfunctional processes in multiple brain areas and circuitries, including the brain's reward, affective and executive control centers.

As the mPFC is considered a circuit hub that promotes higher-order cognitive functions and provides top-down control over automatic limbic system-associated processes (*182-184*), it is suggested to have critical role in affective and cognitive deficits associated with depression. In humans, depressive states are linked to disrupted frontal activity (hyper- or hypo-activation) and morphology, which are thought to contribute to working memory deficits, maladaptive regulation of emotions (anhedonia, negative affect), attentional biases and impaired decision making (*185-188*). Stress exposure, tightly associated with the onset and development of the depressive state, is considered detrimental for mPFC functioning. Proper mPFC performance is necessary for modulating stress-induced behavioral adaptations and for exerting control over stress-activated subcortical regions (*189-193*). In recent years, the clinical toolbox for treating depression has been expanded with deep brain stimulation

(DBS) of the PFC. These recent studies showed that chronic stimulation of the subgenual cingulate cortex (Cg25), the human equivalent of the rodent vmPFC (*194, 195*), reverses depression-induced cortical functional deficits and alleviates symptoms in treatment-resistant depressed patients (*196*). Subsequent reverse translational studies confirmed the involvement of the mPFC in antidepressant-like responses, as high-frequency electrical stimulation of the rat PLC alleviated behavioral despair modeled in the forced swim test (FST) (*197*), which correlates with motivational, active adaptation to challenging environments. Similarly, following chronic unpredictable mild stress, chronic vmPFC DBS reduced depression-associated anhedonia, as assessed by a sucrose preference test in rats and relieved from social avoidance in mice susceptible to chronic social defeat stress (*198, 199*). Taken together, over the years both clinical and preclinical research implicated the mPFC as a crucial mediator of depressive symptomatology (*200*), which triggered a quest for causality and a clarification of the exact contributions of mPFC subregions and their distinct afferent and efferent projections in the development of the disorder and antidepressant response.

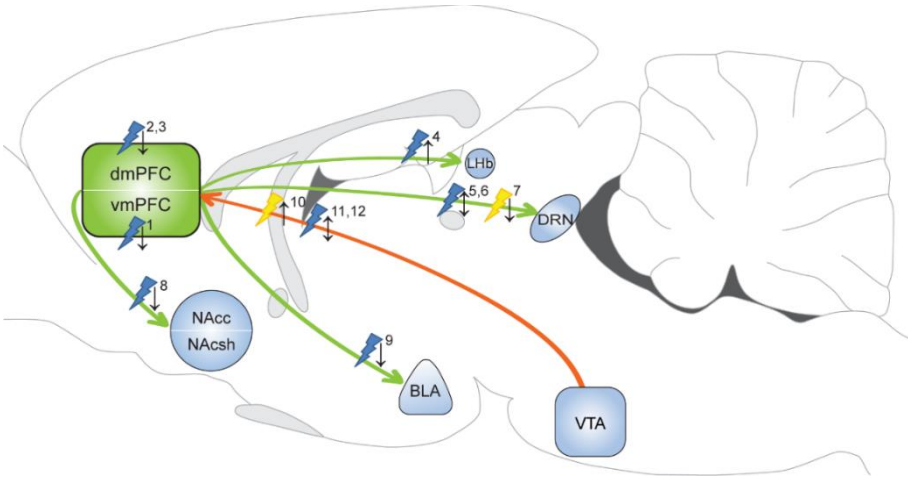

Figure 1. Optogenetic evidence for the involvement of the mPFC in depressive-like behavior and anxiety. Yellow flash: photoinhibition; blue flash: photoactivation ↑ = pro-depressive/anxiogenic effects; ↓ = antidepressant/anxiolytic effects. [1]Convington et al., 2010: photoactivation increased sucrose preference and restored social interaction in defeat-susceptible mice. [2]Kumar et al., 2013: photoactivation layer V pyramidal cells decreased immobility FST in naïve animals. [3]Kumar et al., 2013: photoactivation layer V pyramidal cells increased time in open arms EPM test in defeated animals. [4]Warden et al., 2012: photoactivation of mPFC-LHb projection promoted immobility FST in naïve animals. [5]Warden et al., 2012: photoactivation of mPFC-DRN projection decreased immobility FST in naïve animals. [6]Challis et al., 2014: photoactivation of vmPFC-DRN projection reduced social interaction in naïve animals. [7]Challis et al., 2014: photoinhibition of vmPFC-DRN projection prevented social withdrawal in

defeated animals. [8]Vialou et al., 2014: photoactivation of dmPFC-Nac projection prevented social withdrawal. [9]Vialou et al., 2014: photoactivation of dmPFC-BLA projection increased time in open armsEPM test. [10]Chaudhury et al., 2013: photoinhibition of VTA-mPFC DA projection reduced social interaction in sub-threshold defeat animals. [11]Friedman et al., 2014: photoactivation of VTA-mPFC DA projection restored social interaction in defeat-susceptible mice. [12]Gunaydin et al., 2014: photoactivation of VTA-mPFC DA projection evoked anxiety-like behavior and place avoidance in naïve mice. dmPFC: dorsal medial prefrontal cortex; vmPFC: ventral medial prefrontal cortex; NAcc: nucleus accumbens core; NAcsh: nucleus accumbens shell; LHb: lateral habenula; DRN: dorsal raphe nucleus; BLA: basolateral amygdala; VTA: ventral tegmental area.

The first optogenetic experiments that directly assessed the role of mPFC activity in depression-like behavior confirmed that activation of vmPFC neurons reverses depressive-like symptomatology in a depression-vulnerable population of mice (*201*) (**Fig. 1**). In this study, the authors used the chronic social defeat paradigm, a depression model with high face, predictive and construct validity (*202*) to distinguish mice on their resilience/vulnerability to social stress.

Photostimulation of the vmPFC was achieved using a herpes simplex virus (HSV) viral vector coding for ChR2 driven by the IE4/5 promoter, which targeted ChR2 to mPFC neurons in a non-selective manner (*201*). Specifically, the ILC and PLC of stress-susceptible mice were stimulated in a pattern similar to DBS parameters that previously alleviated depressive symptoms and mimicking cortical burst firing (*197*). Photostimulation fully restored social interaction scores and diminished anhedonia, as expressed in preference for drinking a sucrose solution over water, without altering anxiety levels or social memory performance (*201*). Notably, traditional mPFC manipulations have led to contradictory observations. For example, generic mPFC lesions led to the expression of depressive-like behavior, including learned helplessness (*203*), whereas transient pharmacological inactivation of the ILC resulted in an antidepressant response, as assessed by the FST (*204*). These opposing findings might originate from the different temporal resolution of the methodologies and/or the different (sub)regions examined, e.g., whole mPFC (*203*) versus vmPFC (*201*) or ILC (*204*). As optogenetic activation of the vmPFC by Covington et al. was not specific for a particular neuronal subtype, the direction of the net effect of stimulation at the circuit level remains unresolved. These data may reflect the variability of mPFC involvement seen in human studies, which support either reduced or

increased activity of distinct frontal areas in the expression of the depressive state.

In a subsequent study, Kumar and colleagues employed layer V pyramidal cell-specific photostimulation of the PLC to examine the contribution of this mPFC sub-region in depressive-like symptomatology (*205*). To this end, Thy1::Chr2 mice expressing ChR2 in pyramidal cells projecting to limbic structures, including the ventral tegmental area (VTA), BLA and NAc were used. Acute PLC stimulation in naïve animals induced a robust antidepressant-like response, as expressed in reduced immobility in the FST. Accordingly, in animals subjected to the chronic social defeat model, chronic optical stimulation of PLC pyramidal cells induced a long-lasting anxiolytic effect in the elevated plus maze (EPM) test, a classical test to assess anxiety. In addition to the behavioral effects of PLC stimulation, the authors reported synchronized oscillatory activity across PLC target limbic structures (VTA, BLA and NAc), providing evidence for downstream effects of PLC pyramidal cell modulation on subcortical regions responsible for affective and reward-related processing. Importantly, similar alterations in neuronal activity in this circuit has been observed in depressed patients (*206*) and might underlie the antidepressant-like effects of mPFC DBS in humans (*196*). Interestingly, in contrast to vmPFC activation, PLC pyramidal cell stimulation did not reverse the well characterized defeat-induced social avoidance phenotype (*205*). These discrepancies may be attributed to the different frequency stimulation parameters used or the different cell-types and mPFC layers targeted. Importantly, as the optic fiber in these experiments was targeted to ChR2+ somata in the mPFC, the exact projections that exerted the antidepressant-like effects remain to be determined by projection-specific targeting.

Warden and colleagues examined the role of mPFC efferents in depressive behavior, with a focus on projections to the dorsal raphe nucleus (DRN) and the lateral habenula (LHb) (*207*), regions that are heavily implicated in MDD (*208-211*). The mPFC-DRN projection is of particular interest, as the antidepressant effect of vmPFC DBS in rats is accompanied by structural and functional alterations in serotoninergic DRN neurons (*199*) and it is completely abolished following serotoninergic depletion in the DRN (*198*). In naïve animals, optogenetic activation of the mPFC-DRN excitatory projection through illumination of mPFC terminals in the DRN promoted behavioral activation in the FST (*207*). In contrast, photoactivation of mPFC terminals in the LHb induced immobility in the FST, whereas

illumination of vmPFC pyramidal cell bodies was without effect. More recently, the vmPFC-DRN pathway contribution to a depressive-like state was examined using the chronic social defeat paradigm (*212*). In naïve animals, repeated ChR2-mediated activation of vmPFC-DRN projections increased avoidance of a social target, pointing to a depressive-like phenotype. In line with this, Arch-mediated photoinhibition of the same pathway prevented the development of social withdrawal in animals subjected to social defeat (*212*). The authors provide evidence that vmPFC neurons mainly target GABAergic neurons in the DRN, which likely inhibit serotonergic neurons, explaining the pro-depressant effects they observed. However, their data is inconsistent with the anti-depressive, proactive effects that were found in the FST following stimulation of the vmPFC-DRN pathway (*207*). This suggests that the mPFC-DRN pathway may be differentially involved in regulating social interaction and behavioral despair, the two behavioral constructs these tests assess. Alternatively, the contrasting observations may be explained by a differential effect of acute (*207*) versus repeated post-defeat photoactivation of the vmPFC-DRN pathway (*212*) on expression of depressive-like behavior. Nonetheless, these experiments demonstrate the contributions of the mPFC to the adaptive capacity under physically (proactive vs. passive reactivity) or emotionally (affective decision-making) challenging conditions, which is severely disrupted in depression (*213-216*). Vialou and colleagues showed that PLC-NAc and PLC-BLA projections are differentially involved in depression susceptibility and anxiety-related behavior (*217*). They found that chronic social defeat stress up-regulated ΔFosB in the PLC, which was linked to increased cholecystokinin B (CCKB) receptor expression and the induction of a depression-susceptible phenotype in animals exposed to sub-threshold defeat stress (*217*). In support of this, local application of a CCK agonist (CCK-8) in the PLC promoted a susceptible phenotype and ChR2-mediated optical stimulation of PLC glutamatergic terminals in the NAc prevented CCK-8 administration-induced social deficits (*217*). CCK-8 infusion in the PLC also produced an anxiogenic effect in the EPM and this effect was reversed by photostimulation of the PLC-BLA, but not PLC-NAc, pathway. Taken together, these data highlight the importance of selectively manipulating specific mPFC projections to determine their role in top-down control of subcortical structures in depressive-like behavior and (mal)adaptive responsiveness to stressors (*64, 218, 219*).

In addition to the modulation of efferent projections, optogenetics has also been used to intervene with mPFC afferent DA projections (*220-222*). To selectively manipulate the VTA-mPFC DA projection, Chaudhury and colleagues microinjected a retrograde travelling pseudorabies virus coding for Cre in the mPFC and Cre-dependent ChR2 or NpHR vectors in the VTA. Photoinhibition of the VTA-mPFC pathway reduced social interaction in mice that underwent sub-threshold social defeat (*220*). Interestingly, they also found that the firing rate of VTA DA neurons that project to the mPFC was substantially reduced in susceptible mice that received social defeat stress. Together, this indicates that DA release in the mPFC may prevent the development of a depression susceptible phenotype. ChR2-mediated activation of the VTA-mPFC pathway did not affect the development of a susceptible phenotype following sub-threshold social defeat (*220*). However, repeated stimulation of ChR2-expressing VTA-mPFC neurons reversed social avoidance in a depression-susceptible population following chronic social defeat (*222*). Opposite effects have been observed of ChR2-mediated stimulation of the VTA-mPFC DA pathway in naïve mice, which showed no change in social interaction, but instead showed an increase in anxiety-like behavior and conditioned place aversion (*221*). Together, these studies demonstrate that the direction of behavioral effects depends on the behavioral state of an animal. In depression-prone animals, alterations in the activity of mPFC afferent DA projections are sufficient to enhance vulnerability to develop a depressed phenotype or to reverse depressive-like behavior.

Optogenetic control of the mPFC and connected brain regions has greatly advanced our understanding of the neurobiological underpinnings of depression (*223*). In particular, important steps have been made in the dissection of the contribution of specific mPFC efferent projections to specific behavioral components of the depressive symptomatology, such as social, anxiety and reward-related behaviors. Interestingly, these studies have also revealed resilience mechanisms, including anatomical (VTA-mPFC DA projection) and molecular (CCK) pathways, which could prove of great use in the battle against this debilitating disorder. In the future, profiling of gene and protein expression changes in the mPFC upon optogenetic stimulation could provide insight in molecular mechanisms underlying susceptibility and resilience to depressive behavior and may open new avenues for medical intervention (*218*).

Despite these advances that have been made possible by optogenetic tools, several clinically relevant issues have not been addressed yet. As depression is characterized by individual-based phenotypic expression, with versatile symptomatology, single-construct assessment of depressive-like behavior and anxiety using relatively simplistic behavioral assays (FST, EPM, sucrose preference) may restrict the translational value of these findings (*224*), arguing for the development and use of models with enhanced validity to study a depressed state. Importantly, cortical manipulations that affect social interaction in animals do not necessarily reflect a depressive-like phenotype, but may be indicative of mechanisms supporting social behavior in general. As such, identified mPFC circuits might also have a role in other psychiatric conditions that are characterized by social impairments, e.g., autism-spectrum disorders, anxiety disorders and schizophrenia (see below; (*64, 225*). In addition, depending on the behavioral read-out (e.g., sociability or anhedonia), optogenetic intervention can have a differential effect (*226*), further complicating interpretation of the role of specific circuitry elements in a complex behavioral state. Finally, perturbation of the circuitries mediating depression-induced cognitive decline, which is a critical vulnerability factor for the perseverance of the disorder, has remained an unexplored area regarding optogenetic manipulations, but holds high promise for elucidation of novel targets that can be used for treatment of this prevalent psychiatric disorder.

Schizophrenia

Schizophrenia is characterized by highly heterogeneous cognitive (working memory, attention), positive (delusions, hallucinations) and negative (flat affect, anhedonia) symptoms, as well as disorganized speech and abnormal motor behavior (*181*). Current pharmacotherapy addresses only a small fraction of symptoms, with the majority of treatments being limited in controlling psychosis-related deficits and unable to attend to the primary cause of disability, i.e., cognitive decline (*227, 228*). As the pathogenesis of schizophrenia remains unclear and likely involves a complex neural circuitry, optogenetic dissection of the underlying neural substrates and neuroadaptations will be instrumental for understanding this severe and currently incurable mental disorder (*228, 229*).

Many of the cognitive deficits accompanying schizophrenia, such as impaired working and episodic memory and impaired affective control and reward evaluation, have been traced back to dysregulated PFC function, resulting in altered connectivity with subcortical areas,

such as the amygdala, striatum and the hippocampus (*227, 230, 231*). Several theories exist concerning mPFC alterations that cause schizophrenia symptoms, including altered dopaminergic modulation, a change in E/I balance and abnormal oscillatory activity in the gamma frequency range (*230, 232*). Optogenetic approaches have begun to address the merits of these theories by providing causal insight in the underlying mechanisms of the heterogeneous symptoms of schizophrenia, in particular the cognitive dysfunction and aberrant information processing associated with this disorder (*233, 234*).

A dual role of dopamine has been hypothesized to contribute to the development of schizophrenia. In particular, it is thought that increased DA transmission in the mesolimbic system and parallel DA hypoactivity in the mPFC account for the expression of schizophrenic symptoms (*228, 235*). Additionally, imbalanced activation of cortical D1-Rs and D2-Rs, which have opposing effects on neuronal excitability (*236*), is considered crucial for impaired information processing and the manifestation of both positive and negative symptoms in schizophrenia (*235, 237, 238*). The involvement of D2-Rs is supported by the fact that all antipsychotics that are being used to treat positive symptoms of schizophrenia, block D2-R function (*228*). Furthermore, prefrontal D2-Rs have a critical role in cognitive processes that are disrupted in schizophrenia, including working memory and sensorimotor gating, as determined with mutant mice and pharmacological interventions (*237-239*). Optogenetic modulation of D2-R expressing neurons in the mPFC provided new insight in the functionality of D2-Rs and their potential contribution to schizophrenia symptoms. Intra-mPFC infusion of a Cre-dependent ChR2 vector in D2-R::Cre mice enabled robust expression of ChR2 in a subpopulation of layer V pyramidal cells projecting to the thalamus (*240*). Acute slice recordings demonstrated that, at baseline, the D2-R agonist quinpirole had minimal effect on current injections in D2-R neurons, however, a significant after-depolarisation occurred when quinpirole application was closely preceded by optogenetic activation of contralateral D2-R-expressing mPFC projection neurons, generating voltage fluctuations and spiking for hundreds of milliseconds (*240*). Given the specificity of D2-R expression in cortico-thalamic projecting layer V neurons, D2-R-mediated after-depolarization might enhance outputs to subcortical structures. Under pathological conditions, such as D2-R overrepresentation seen in schizophrenia (*241*), this sustained signal amplification might enhance the level of noise in the mPFC, thereby distorting relay of information

to subcortical areas and potentially enhancing susceptibility to psychosis. As the level of noise within the mPFC is thought to be increased in schizophrenic patients (discussed below), diminishing the D2-R-mediated after-depolarisation might be a neurophysiological basis for the beneficial effect of antipsychotics on schizophrenia symptoms. Further research using *in vivo* models will have to verify whether D2-R induced after-depolarisation is involved in the cognitive dysfunction observed in schizophrenia.

The E/I balance theory poses that an elevation in the ratio of cortical E/I, mediated either via hyperexcitability of pyramidal cells or hypoactivity of inhibitory interneurons, underlies the behavioral and cognitive symptoms of schizophrenia, including social dysfunction (*232, 233*). Network and behavioral effects of an altered E/I balance in the mPFC has been addressed using the stable step function opsin (SSFO), a ChR2 mutant with significantly reduced deactivation time (~30 min) (*64, 242*) upon excitation with a single pulse of blue light, thereby reducing the threshold for action potential firing in SSFO-expressing neurons. Brief photoactivation of SSFO-expressing mPFC pyramidal neurons increased the E/I balance, impaired information processing at the cellular level and increased rhythmic high-frequency activity, resembling clinical indications of schizophrenia (*242*) (see section below). At a behavioral level, these manipulations were sufficient to completely abolish social interaction and reversibly impaired acquisition of conditioned-fear memory. Enhanced E/I balance in the primary visual cortex did not alter social behavior, which alludes to specificity of the mPFC in mediating these behavioral deficits. Interestingly, depolarization of SSFO-expressing mPFC GABAergic PV neurons did not affect social interaction and conditioned-fear (*242*), despite the fact that it robustly reduced spiking and synaptic activity. However, social deficits observed after photoactivation of SSFO-expressing pyramidal cells were partially rescued by co-activation of ChR2-expressing PV neurons (*242*). As discussed earlier, inhibition of mPFC PV neurons can result in severe working memory deficits (*159*), further stressing the importance of a properly balanced cortical excitatory tone. Notably, an elevated E/I balance within the mPFC is also thought to contribute to social dysfunction associated with autism spectrum disorders (*242*), hence, these findings may point to a pathophysiological mechanism that mediates general impairments in social behavior. Although the use of SSFOs aids in explaining the consequence of a distorted mPFC E/I balance at a cellular level and on social interaction, altered E/I balance

in schizophrenia and autism is likely the result of an aberrant neurodevelopmental mechanism. Hence, in patients, E/I balance is elevated for a time-period that is far beyond the deactivation time-scale of currently available SSFOs. The relatively "acute" effects of a change in E/I balance in developmentally normal animals should therefore be interpreted with caution. That being said, optogenetic manipulations using SSFOs have for the first time demonstrated robust differential effects of an alteration in mPFC E/I balance on network activity and behavior. Furthermore, SSFOs can be used to assess whether E/I balance is perturbed in other psychiatric diseases, including autism, depression and addiction, potentially unifying the etiology of these disorders (*243*).

A third avenue that aims to explain the cognitive deficits of schizophrenia patients involves gamma rhythms, 30–80 Hz neuronal oscillations that play a pivotal function in synchronizing neuronal activity within and between areas, which is known to be required for working memory, perception and attention (*137, 233*), and is likely important for many other brain functions. In schizophrenia patients, abnormal gamma oscillations have been consistently observed, and they correlate with changes in working memory and cognitive control (*244, 245*). When PV neuron function is impaired, suboptimal inhibitory drive leads to desynchronization, contributing to altered gamma rhythm and presumably to working memory impairments associated with schizophrenia (*137*). In accordance with this notion, local GABA synthesis and reuptake are consistently reduced in the PFC of schizophrenia patients and this change is specifically mediated by PV neurons, implying aberrant functionality of this particular interneuron population (*137*). Similarly, reduced PV immunoreactivity in the PFC of schizophrenic patients has been reported (*136*). Optogenetic studies validated the critical importance of cortical PV interneurons in driving gamma oscillations (*133, 246*). Sohal and colleagues showed that photostimulation of ChR2-expressing PFC pyramidal cells elicited gamma oscillations *in vivo*, however, simultaneous NpHR-mediated inhibition of PV+ interneurons specifically suppressed gamma power, suggesting that pyramidal cells stimulation activated downstream PV neurons. Importantly, when subjecting pyramidal neurons to gamma-frequency input, microcircuit signal transmission was improved by reducing circuit noise and amplifying circuit signals, including signals to local interneurons (*133*). PV interneuron-driven gamma-mediated neuronal synchrony dependents on NMDA receptor activation, as targeted NMDA receptor

deletion in PV neurons impaired optogenetic induction of gamma oscillations and resulted in selective cognitive decline, resembling schizophrenic deficits (*247*). Together, selective optogenetic modulation of PV interneuron activity confirmed that this neuronal subtype drives gamma oscillations, which sequentially promotes fast and targeted information processing; a "sharpening" of cortical response to sensory inputs (*233*). Changes in oscillation synchrony are also thought to underlie other psychiatric conditions, including bipolar disorder and autism, as well as epilepsy (*206, 248*). Thus, efforts aimed at further elucidation of circuit and molecular adaptations that contribute to aberrant generation of neuronal oscillations are of utmost importance.

Taken together, the first optogenetic manipulations of the mPFC circuitry have at least partially validated existing theories that aim to explain neuropathological mechanisms underlying schizophrenia. Enhanced excitatory drive, potentially as a result of D2-R overexpression, resulting in desynchronized neuronal transmission and impaired cortical information processing contributes to symptoms associated with this disorder. Given the multifaceted and complex nature of schizophrenia, it will likely be impossible to mimic the full phenotypic spectrum in an animal model. Although optogenetic manipulations in the rodent brain are invaluable for providing new directions into this field of research, the translational value of the observed mechanisms remains a challenge that needs to be addressed in the future.

Addiction

Addicted individuals display a behavioral repertoire restricted to repeated cycles of drug seeking, consumption and recovery from drug use despite often severe negative consequences (*249*). Drug addiction is the endpoint of a series of transitions from initial, hedonic drug use to habitual and ultimately compulsive drug use, which coincides with long-lasting adaptations in neural circuits (*250, 251*). High relapse rates are a major problem in treatment of addiction, as addicted individuals remain highly susceptible to relapse even after long periods (months to years) of abstinence (*252*). This persistent vulnerability is thought to be maintained by strong and persistent associative memories of drug effects and environmental cues (*253*). The brain circuitry that supports addiction is complex, but ample evidence indicates that the mPFC has a significant role in the development and

persistence of addictive behavior (*254*). More specifically, the mPFC has been implicated in the attribution of salience to rewarding stimuli, compulsive drug taking, the expression of drug-associated memories and relapse to drug seeking (*70, 255, 256*). Optogenetic approaches confirmed the important function of the mPFC in animal models of addictive behavior and provided interesting new insights in the temporal contribution of mPFC subregions and projections to the NAc to compulsive drug taking and drug seeking behavior.

Evidence from neuroimaging studies suggests that hypofunction of the mPFC contributes to a loss of control over limiting intake in human addicts (*257*). This hypothesis was recently addressed using optogenetics in rats that continued to self-administer cocaine despite the pairing of cocaine reward with delivery of a noxious stimulus (foot-shock). Chen et al. showed that long-term cocaine self-administration reduced PLC neuron excitability, with the most robust effect in aversion-resistant rats (*258*). Restoring PLC pyramidal function by optogenetic stimulation alleviated cocaine intake in aversion-resistant rats (**Fig. 2A**). In contrast, when PLC neurons were optogenetically silenced, non-resistant rats engaged in cocaine self-administration paired with a foot-shock. This study indicates that when cocaine use is paired with an adverse consequence, hypoactivity of PLC pyramidal cells contributes to a loss of inhibitory control over compulsive cocaine intake.

Pharmacological interventions in animal models of conditioned drug seeking indicate that the dmPFC and vmPFC differentially contribute to the expression of this specific behavior (*58, 70*). Whereas dmPFC activity is thought to drive drug seeking responses, the vmPFC either promotes or inhibits drug seeking responses depending on the type of drug that was previously administered and the implementation of extinction sessions before a drug-seeking test (*56, 259-263*).

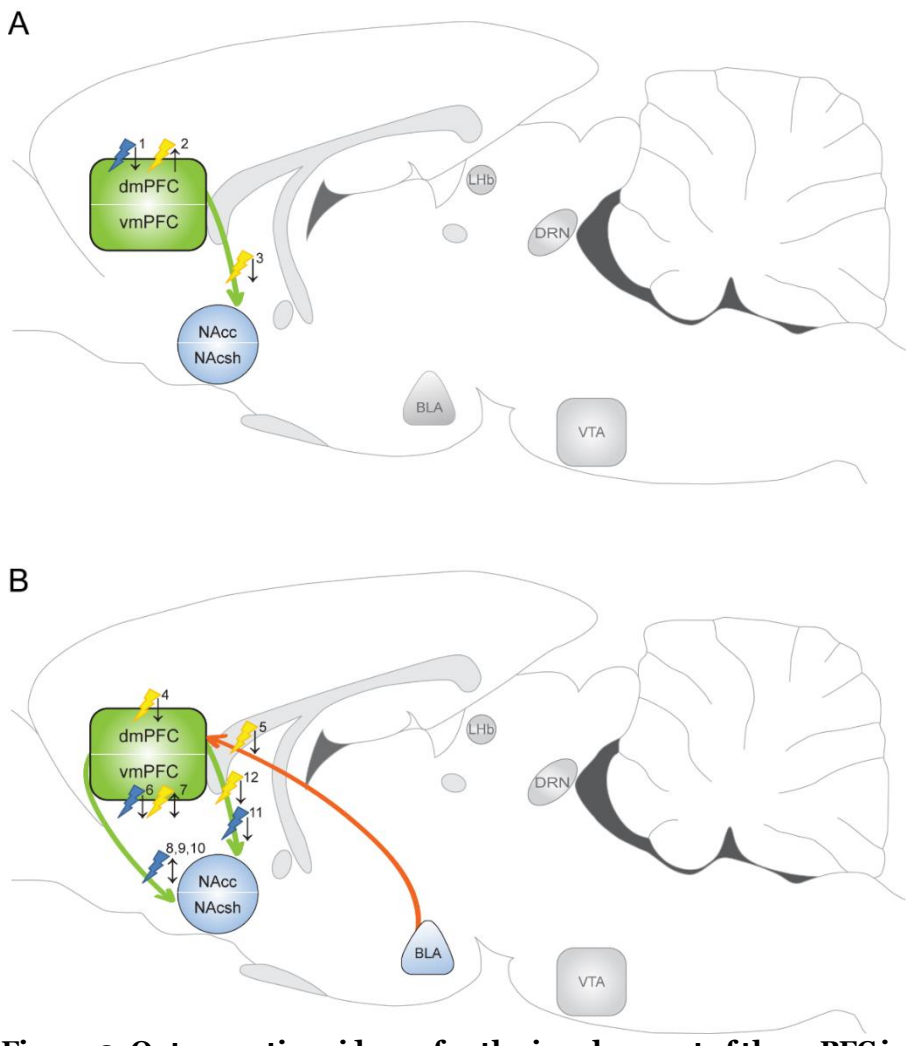

Figure 2: Optogenetic evidence for the involvement of the mPFC in addictive behavior. Yellow flash: photoinhibition; blue flash: photoactivation. ↑ = enhanced drug taking / seeking; ↓ = reduced drug taking/seeking. Optogenetic manipulations indicate that the circuitry that regulates drug taking (when the drug is available) differs from the circuitry that mediates drug seeking (in absence of the drug). **A** Manipulation of drug *taking*. [1]Chen et al, 2013: Photoactivation PLC diminished compulsive cocaine taking in aversion resistant rats. [2]Chen et al, 2013; Martin-Garcia et al., 2014: Photoinhibition PLC evoked compulsive cocaine taking in aversion sensitive rats and resumption of cocaine intake in rats with history of high-frequency self-administration. [3]Seif et al, 2013: Photoinhibition of dmPFC-NAcc projection reduced alcohol intake paired with aversive stimulus. **B** Manipulation of drug *seeking*. [4]Stefanik et al, 2013; Martin-Garcia et al, 2014: Photoinhibition dmPFC attenuated cocaine seeking. [5]Stefanik and Kalivas, 2013: Photoinhibition of BLA-dmPFC projection reduced reinstatement of cocaine seeking. [6]Van den Oever, 2013: Photoactivation vmPFC facilitated extinction of remote, but not recent, cocaine memory. [7]Van den Oever, 2013: Photoinhibition vmPFC impaired recall of recent cocaine memory, but prevented extinction of remote cocaine memory. [8]Ma et al, 2014: Photoactivation (1Hz) evoked LTD in vmPFC-NAcsh projection reversed cocaine-induced synaptic adaptation and enhanced subsequent cocaine seeking. [9]Pascoli et al, 2012: Photoactivation (1Hz) of vmPFC-NAcsh projection reversed cocaine-induced synaptic adaptation and locomotor

sensitization. [10]Pascoli et al, 2014: Photoactivation (13Hz) of vmPFC-NAcsh projection reversed cocaine-induced synaptic adaptation and abolished cocaine seeking. [11]Ma et al., 2014: Photoactivation (1Hz) evoked LTD in dmPFC-NAcc projection reversed cocaine-induced synaptic adaptation and decreased subsequent cocaine seeking. [12]Stefanik et al, 2013: Photoinhibition of PLC-NAc core projection attenuated cocaine-primed reinstatement of cocaine seeking.

In fact, several lines of evidence suggest that the ILC mediates the consolidation and expression of extinction memory (*56, 103*), and as such, inhibition of this region after extinction learning evokes expression of the original cocaine seeking response. Optogenetic manipulation of the vmPFC extended these findings by showing that vmPFC pyramidal cells indeed contribute to expression and extinction of conditioned cocaine seeking, but in a time-dependent manner (*112*) (**Fig. 2B**). ChR2-mediated activation of vmPFC pyramidal cells facilitated extinction of a cocaine conditioned place preference (CPP) memory only when photostimulation was applied 3 weeks after, but not 1 day after conditioning. In line with this observation, NpHR-mediated inhibition of these neurons blocked extinction of CPP memory 3 weeks after conditioning. Surprisingly, photoinhibition selectively attenuated expression of a 1-day-old cocaine memory. Together, optogenetic manipulation of pyramidal cells pointed to a temporal reorganization of the circuitry that controls expression of cocaine-associated memories and a differential role of the vmPFC in regulation of conditioned cocaine seeking over time.

Optogenetic studies confirmed that PLC activity is required for reinstatement of cocaine seeking in extinguished animals. Similar to pharmacological inactivation, photoinhibition of PLC neurons (using a non-selective promoter) reduced cocaine-primed reinstatement of cocaine seeking (*264*). In addition, the same group demonstrated that the BLA-PLC pathway is critically involved in reinstatement of cocaine seeking by optical inhibition of BLA presynaptic terminals in the PLC (*265*). Optogenetic inhibition of dmPFC pyramidal neurons also attenuated stress-induced reinstatement of palatable food seeking in rats (*266*), suggesting that different modalities activate dmPFC circuitry to evoke reinstatement of reward seeking. In addition, this shows that PLC activity drives reinstatement of cocaine and natural reward seeking, whereas increased activity of the same neurons suppresses compulsive cocaine taking (*258*). The opposing function the PLC may depend on the presence or absence of cocaine in operant

tests. This is supported by the observation that photoinhibition of PLC pyramidal cells enhanced cocaine self-administration and attenuated reinstatement of cocaine seeking in rats that were subjected to a high-frequency cocaine intake schedule (*267*). GABAergic interneurons have not been manipulated yet in addiction models, but the role PV interneurons in natural reward (sucrose) learning and extinction was recently examined. ChR2-mediated activation of PLC PV interneurons did not affect acquisition of sucrose reward self-administration, but accelerated extinction of reward seeking by inhibiting PL network activity (*76*). Whether PLC PV activity also affects extinction of drug seeking remains a topic for future research.

By integrating input from sources such as the BLA, VTA and HPC and conveying excitatory output to the NAc, the mPFC is thought to exert control over the motor circuitry to regulate responding to drugs and drug-associated stimuli (*268*). Dorsal regions of the mPFC mainly project to the dorsolateral striatum and NAc core, whereas ventral regions predominantly target the dorsomedial striatum and NAc shell (*269*). Pharmacological disconnection experiments have indeed implicated the dmPFC-NAc core and vmPFC-NAc shell pathway in drug- and cue-induced cocaine and heroin seeking (*56, 270-272*), but with this method the effects on indirect pathways cannot be ruled out. Photoinhibiton of PLC presynaptic terminals in the NAc core attenuated cocaine-primed reinstatement of cocaine seeking (*264*), confirming that a monosynaptic glutamatergic projection from PLC to NAc core has a critically role in this behavioral response. Optogenetic evidence for the involvement of the mPFC-NAc shell pathway was provided by a optic modulation of ILC terminals in NAc brain slices obtained from animals that were exposed to cocaine (*150*). This revealed that presynaptic input of mPFC terminals in the NAc shell was strengthened after both short- (1 day) and long-term (45 days) abstinence from non-contingent and contingent exposure to cocaine, but only after contingent exposure this strengthening significantly increased over time. The presynaptic enhancement was caused by an increase in glutamate release probability, rather than increased quantal size of glutamatergic release or the number of active release sites (*150*). Interestingly, cocaine exposure did not affect presynaptic transmission in the BLA-NAc shell projection (*150*), suggesting that input from the mPFC is favoured over BLA input after cocaine administration. In an elegant study by Ma et al., it was shown that cocaine self-administration induced silent synapses in the mPFC-NAc pathway (*273*). Interestingly, silent synapses in the ILC-NAc shell

pathway matured by recruiting GluA2-lacking AMPA-Rs (observed at day 45 of abstinence), whereas silent synapses in the PLC-NAc core pathway recruited GluA2-containing AMPA-Rs. AMPA-Rs lacking the GluA2 subunit are calcium permeable, have greater channel conductance, exhibit faster channel deactivation kinetics and thereby contribute to rapid synaptic signaling, homeostatic synaptic scaling and specialized forms of short- and long-term plasticity (for excellent review see (*274*)). Optogenetically evoked long-term depression (1Hz for 10 min) reintroduced silent synapses in both pathways, but this either enhanced (ILC-NAc shell) or reduced (PLC-NAc core) subsequent cocaine seeking (*273*), further supporting differential roles of the dmPFC and vmPFC in this behavior.

The principal cell population in the NAc consists of GABAergic medium spiny neurons (MSNs) that can be subdivided in a D1-R and D2-R expressing population, together comprising ~90-95% of all NAc neurons (*275*). Selective expression of ChR2 in each NAc MSN population showed that activation of D1-R neurons enhanced cocaine reward learning in the CPP paradigm, whereas activation of D2-R neurons had the opposite effect (*276*). Photostimulation of mPFC terminals in the NAc core specifically induced ΔFosB expression in D1-R neurons, whereas in the NAc shell, ΔFosB expression was induced in both D1-R and D2-R subtypes (*277*). This suggests that the distribution of mPFC terminals onto NAc neurons differs for the shell and core (Lobo et al 2013). However, this will require validation by whole-cell recordings. The functional relevance of mPFC to NAc D1-R MSNs projections was demonstrated by Pascoli et al., who showed that low frequency (1 Hz) photostimulation of the ILC-NAc shell pathway reversed non-contingent cocaine-induced synaptic potentiation in D1-R neurons and locomotor sensitization (*278*). More recently, the same group used optogenetics to reveal the presence of GluA2-lacking AMPA-Rs in the ILC-NAc D1-R MSN projection 1 month after cocaine self-administration (*279*). Photostimulation of this pathway at 13 Hz, but not 1 Hz, reversed synaptic adaptations after cocaine self-administration and abolished cue-induced cocaine seeking. The authors speculated that a 13-Hz stimulation was required for this effect because this evokes mGluR-mediated long-term depression, an efficient mechanism to remove synaptic GluA2-lacking AMPA-Rs (*280*). However, this finding contradicts with the observation by Ma and colleagues ((*273*); discussed above). Differences in circuit specificity (optogenetic modulation of projections to D1-R neurons *vs.* projections to all NAc shell MSN neurons) and in the cocaine self-

administration regimen may explain the opposing effects observed in these studies.

In addition to being involved in relapse to drug seeking, the mPFC-NAc pathway has been implicated in compulsive aversion-resistant alcohol consumption. Photoinhibition of the dmPFC-NAc core projection reduced alcohol intake paired with aversive stimuli of different sensory modalities and different methods of intake (*281*). Alcohol intake was unaffected by photoinhibition when it was not paired with an adverse consequence, suggesting that this pathway predominates in orchestrating the aversion-resistant, compulsive aspects of alcoholism, in which intake is often accompanied by conflict or challenge (*282*). However, these results contradict with the finding that photoinhibition of the PLC enhances aversion-resistant cocaine intake (*258*), suggesting that the PLC might differentially regulate compulsive alcohol and cocaine intake.

The involvement of the mPFC-NAc pathway in acquisition of reward and drug self-administration has also been explored with optogenetic approaches. Stuber and colleagues. found that optical activation of the mPFC-NAc shell projection (20 Hz) did not support the acquisition of operant self-stimulation behavior (active responses triggered light pulses delivered to presynaptic mPFC terminals in the NAc), despite the fact that optical activation of the mPFC projection elicited excitatory postsynaptic currents in the NAc (*283*). A subsequent study demonstrated that animals acquire optical self-stimulation of the mPFC-NAc shell pathway when the frequency of stimulation is increased to 30 Hz (*151*). Hence, the glutamatergic projection from the mPFC to NAc may only evoke spiking of MSNs and reinforce behavior with strong activation of the mPFC or when DA levels in the NAc are elevated in parallel. The exact stimulation site within the mPFC may be of critical importance to achieve this effect, considering that the ILC is thought to have a stronger projection to the NAc shell than the PLC (*269*). As in the above-mentioned studies ChR2 expression was not specifically targeted to the PLC or ILC, it remains to be determined whether a difference exists in the potency of both pathways to evoke spiking in NAc shell MSNs and to reinforce reward seeking behavior.

In line with traditional intervention techniques, optogenetic manipulations of the mPFC circuity in rodent addiction models have validated the critical involvement of this region in regulating drug taking and drug seeking behavior and further support a functional segregation along the dorsal-ventral axis of the mPFC. Moreover,

pathway specific modulation has provided new insights in the role of BLA-PLC and mPFC-NAc projections. In particular, optic stimulation of PLC and ILC axonal terminals in acute brain slices preparations of the NAc core and shell demonstrated cocaine-induced pathway-specific neuroadaptations that could be reversed using defined photoactivation frequencies (*273, 278, 279*). This may provide opportunities for DBS-mediated reversal of drug-induced neuroadaptations in addicts. However, as electrical stimulation affects neuronal activity in a non-selective manner, translational efficacy to DBS remains to be approached with caution and requires further studies.

Concluding remarks

The relatively recent application of optogenetic technology to neuroscience research has deepened insight into function of various types of circuitry in the brain, and already contributed substantially to our understanding of the mPFC circuitry in health and disease conditions. Optogenetic manipulations enable causal system-level research on diverse cognitive and neuropathological behaviors in freely moving animals and allow integration of *in vivo* and *ex vivo* electrophysiological recordings, which was not feasible with traditional intervention methods. However, over decades, the extensive body of research involving lesion, pharmacological and electrophysiological methods has provided crucial knowledge on the involvement of the mPFC in diverse cognitive processes. Integration of data obtained with these traditional intervention methods and optogenetic modulations will continue to be invaluable for our understanding of mPFC circuitry and for creating computational models of mPFC function.

A major breakthrough in dissection of neuronal circuitries that has been enabled by optogenetics technology is the direct manipulation of neuronal projections within and between brain regions. With respect to the mPFC circuitry, this has led to a better understanding of intra-mPFC connectivity, the role of afferent and efferent mPFC projections in cognitive processes and mental disorders, and even to the discovery of a new GABAergic cell population with long-range projections to the NAc (*152*). Moreover, due to the excellent compatibility of optogenetics and *ex vivo* brain slice physiology, differential cocaine-induced neuroadaptations in PLC and ILC projections to the NAc have been elucidated (*273*), demonstrating the feasibility of dissection of mPFC subregion-specific mechanisms using optogenetics.

Although great progress has been made, several factors have received little attention and, in some cases, require technical improvements to be properly addressed in future experiments. With respect to the GABAergic interneuron population in the mPFC, opsin expression has thus far been primarily targeted to PV interneurons, leaving the role of many other GABAergic cell-types (e.g. SOM+, calretinin+ cells, etc.) unaddressed. As transgenic mouse and rat Cre-driver lines become increasingly available, this opens new avenues to investigate the role of other mPFC subpopulations in cognitive performance and psychiatric disorders. Importantly, previous optogenetic studies have pointed to the existence of subpopulations within the GABAergic and pyramidal cell population that may only be distinguished based on their differential activity during defined behavioral states (*63, 77*). For instance, PV interneurons have been linked to working memory performance (*159*), expression of fear responses (*77*), maintaining a proper E/I balance (*74, 242*), and synchronization of gamma oscillations (*133, 284*). Optogenetic tagging of neurons that show increased activity during a particular behavioral task will be a crucial next step to dissect the causal involvement of these specific neuronal ensembles in expression of behavioral performance (*285*). Opsin expression driven by the promoter of the immediate early gene *c-fos,* a widely used marker of neuronal activity, in hippocampal neurons that were active during fear-conditioning demonstrates that this is an attainable goal (*286*). Interpretation of optogenetic data is often hindered by non-specific targeting of opsins to mPFC subregions. As it becomes increasingly clear that dorsal and ventral regions of the mPFC have different and sometimes even opposing functions (*45, 70*), stereotactic delivery of opsin vectors to these defined subregions is of high relevance. Furthermore, technical advances that enable targeting of opsins to specific layers within the mPFC would be of great value given the complex layer- and subregion-defined neuronal connectivity of mPFC neurons (*50, 125, 269*).

Currently, many FDA approved pharmaceutical agents target G-protein coupled receptors in the brain (*287*). Thus, improving insight in the temporal role of these receptors to specific behavioral states will be instrumental for treatment of psychiatric disorders with novel, more-selective pharmacotherapy. Design of opsins that consist of a chimaera of an opsin fused to the intracellular domain of a G-protein coupled receptor (optoXR), enables interrogation of the causal involvement of G-protein coupled signaling cascades with high spatiotemporal resolution (*288*). Thus far, optoXRs have not been used

to study the contribution of specific signaling cascades to mPFC circuitry function, but would be extremely useful for explaining the role of altered G-protein signaling observed in psychiatric diseases (*289, 290*). In addition, new developments in the field of chemogenetic technology (e.g., DREADD: Designer Receptors Exclusively Activated by Designer Drugs) will further contribute to the dissection of mPFC circuitry and the identification of drugable targets (*291*).

The use of optogenetics in humans for treatment of neurological disorders has been extensively discussed (*205, 229, 234*), however, clinical application of optogenetics technology is, to our knowledge, currently not feasible. Extending optogenetic methods to species beyond rodents has only been stably, safely and efficiently applied in the rhesus macaque, a non-human primate (*292-297*). Further studies and clinical trials will be required to safely express and photostimulate opsins in the human brain. Hence, in spite of high promise for clinical treatment, at present, optogenetics should primarily be regarded as a powerful toolbox to functionally dissect neural circuits in animal models of disease-related symptoms and to discover and refine targets for pharmaceutical and DBS treatment.

Acknowledgements

MRM is funded by EU MSCA-ITN CognitionNet (FP7-PEOPLE-2013-ITN 607508). ABS, SS are funded partly by a grant awarded to NeuroBasic Pharmaphenomics consortium. DR is partly funded by a NCA proof-of-concept fund (SS). MCvdO is funded by a ZonMw VENI grant (916.12.034) and Hersenstichting Nederland grant (KS 2012(1)-162).

Chapter 3

Viral-TRAP: inducible permanent tagging of Fos-expressing neurons using a dual virus approach

Mariana R. Matos[1], Robbert Zalm[2], Lineke Ouwerkerk[1], Yvonne Gouwenberg[1], Titia Gebuis[1], August B. Smit[1], Michel C. van den Oever[1]

[1]Department of Molecular and Cellular Neurobiology, Center for Neurogenomics and Cognitive Research, Amsterdam Neuroscience, Vrije Universiteit Amsterdam, 1081HV Amsterdam, The Netherlands.
[2]Department of Functional Genomics, Center for Neurogenomics and Cognitive Research, Amsterdam Neuroscience, Vrije Universiteit Amsterdam, 1081HV Amsterdam, The Netherlands

Abstract

Neuronal ensembles are considered to function as a physical substrate for learning-induced changes that underlie memory storage and retrieval. These ensembles can be identified by neuronal activity-induced expression of immediate early genes (IEGs), such as *Fos*. The recent generation of transgenic mouse lines in which an IEG promoter is used to drive the expression of a transgene (e.g., reporter, opsin or DREADD) has facilitated the identification and manipulation of neuronal ensembles and confirmed their causal involvement in memory expression. Moreover, TRAP (Targeted Recombination in Activated Populations) transgenic mouse lines enable permanent expression of transgenes, which facilitates the investigation of neuronal ensembles over prolonged periods of time. To overcome limitations of transgenic approaches, we developed viral-TRAP, consisting of a mixture of AAV-Fos::CreER^{T2} and a Cre-dependent Adeno-Associated Virus. We first demonstrate *in vitro* that viral-TRAP enables expression of a fluorescent reporter in a 4-hydroxytamoxifen (4TM)-dependent manner and then *in vivo* that this is also regulated in an experience-dependent manner. We conclude that behaviorally-activated neuronal populations can be effectively and permanently tagged using viral-TRAP, enabling the long-term analysis of neuronal ensembles and their contribution to learned behavior in wild-type animals.

Introduction

Sparsely distributed neurons that are activated during learning and expression of conditioned behavior, so-called neuronal ensembles, are thought to function as a substrate for the storage of learned information. The elucidation of immediate early genes (IEGs), such as *Arc* or *Fos*, whose expression levels correlate with patterns of neuronal activity (*298-301*), facilitated the identification of neurons that are involved in memory expression. *Fos* is one of the most studied IEGs and known to have an mRNA and protein expression peak at approximately 60 min and 90-120 min, respectively, after neuronal activation. In behavioral paradigms used to study learning and memory, Fos-expressing neuronal ensembles have been detected in numerous brain areas, including the hippocampus, amygdala, striatum and prefrontal cortex (*44, 96, 302-307*).

To proof that IEG-expressing neuronal ensembles are indeed responsible for memory expression, it is necessary to show that these neurons are reactivated upon memory recall and sufficient and/or necessary for the expression of what was learnt. However, the transient mRNA and protein expression of *Fos* and other IEGs provides a relatively short time-window to investigate brain patterns of neuronal activity (*117, 302*). To extend the window of analysis, transgenic mouse lines have been generated in which an IEG promoter region drives expression of a transgene under conditions known to induce neuronal activation (*301, 308-310*). For instance, the *Fos*::LacZ rat allows identification of Fos-expressing neuronal ensembles over several hours and inactivation of these neurons by treatment of animals with the pro-drug DaunO2, which is converted by β-galactosidase into the toxic compound Daunorubicin (*311*). Furthermore, the *Fos::*tTA mouse, also known as the TetTag mouse, makes use of the *Fos* promoter to induce the expression of a transgene in a doxycycline (Dox)-regulated manner (*301*), enabling the tagging of activated neuronal ensembles during an experimenter-defined time-window (*286, 312*). With these transgenic approaches, it was found that learning-activated neurons are reactivated during subsequent memory retrieval, and importantly, that these neurons are also sufficient and required for memory expression (*286, 311, 312*). Due to the transient expression of a molecular tag in *Fos*::LacZ, *Fos*::tTA, or e.g., *Fos*::GFP and *Arc*::dVenus (*309, 313*) mice, other mouse lines have been developed that use an IEG promoter to drive expression of Cre recombinase (Cre), enabling permanent expression of a transgene. When Cre is fused to a mutated ligand-binding estrogen receptor domain (ER^{T2}), as in *Fos*::$CreER^{T2}$ or

Arc::CreER^{T2} mice (*310, 314, 315*), recombination becomes inducible by administration of tamoxifen or its derivative 4-hydroxytamoxifen (4TM) in neurons in which the IEG promoter is activated. Therefore, this tagging method is also called targeted recombination in active populations (TRAP) (*310*). As these mice can be crossed with Cre-reporter lines to irreversibly and permanently express a molecular marker in activated neurons (*124, 316-319*), this enabled the investigation of the long-lasting involvement of neuronal ensembles in memory storage and retrieval.

To surpass limitations of transgenic approaches, such as relatively high non-specific background tagging (i.e., leakiness) (*310*), inability of cross-species application and additional breeding costs, we aimed to develop a virus-based tagging method that allows the analysis of neuronal ensembles over prolonged periods of time. Here, we describe the development and characterization of viral-TRAP. We first confirmed 4TM-dependent control over transgene expression *in vitro* and then validated the *in vivo* tagging of neurons that are activated by a behavioral experience.

Results

Generation of a Fos::CreER^{T2} Adeno-Associated Virus (AAV) vector

To generate a CreER^{T2} construct that is under control of the *Fos* promoter, we utilized a pre-existing AAV-Fos::tTA plasmid, in which the sequence of the *Fos* promoter precedes the coding sequence of tetracycline transactivator (tTA) (*301*). This plasmid served as the backbone to receive the CreER^{T2} coding sequence from pRetroQ-CreER^{T2}. CreER^{T2} was first amplified by PCR and the AAV-Fos::tTA plasmid was linearized by digestion with EcoR1 and Not1. We then used One-Step Sequence- and ligation-independent cloning (SLIC; (*320*)) to create pAAV-Fos::CreER^{T2}. The final construct, pAAV-Fos::CreER^{T2} (Fig. 1a) enables *Fos* promoter-driven expression of CreER^{T2}, which can induce the irreversible recombination of a Cre-dependent transgene upon binding of 4TM (Fig. 1b).

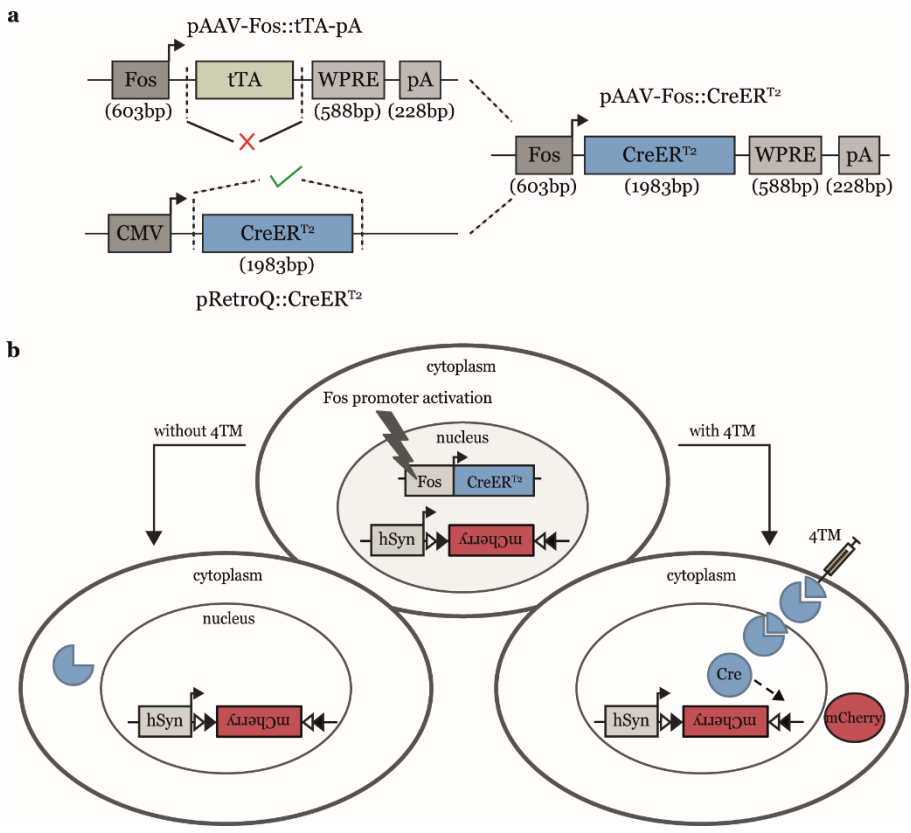

Figure 1. Generation of pAAV-Fos::CreER^{T2}. a. The tTA coding sequence was excised from pAAV-Fos::tTA-pA. The resulting plasmid was then used to insert CreER^{T2} obtained from pRetroQ-CreER^{T2} by PCR and SLIC. **b.** Schematic representation of viral-TRAP-mediated expression of a molecular tag. In this example, the combination of the TRAP vector (AAV5-Fos::CreER^{T2}) and Cre-dependent mCherry vector (AAV5-hSyn::DIO-mCherry; DIO = Double-floxed Inverse Open reading frame) will allow the 4TM-controlled permanent expression of mCherry in activated neurons. Activation of the *Fos* promoter will induce the expression of CreER^{T2}, but due to the ER^{T2} domain, Cre will remain in the cytoplasm (left). When 4-hydroxytamoxifen (4TM) binds to CreER^{T2}, Cre is translocated to the nucleus (right) where it enables the recombination of the Cre-dependent vector and then expression of mCherry is constitutively driven by the human *Synapsin* (hSyn) promoter.

In vitro validation of TRAP-mediated reporter expression

Before generating viral particles of pAAV-Fos::CreER^{T2} for injection into a mouse brain, we studied whether this TRAP construct is functional *in vitro* and controlled by 4TM. For this, we transfected HEK293T cells with a combination of pAAV-Fos::CreER^{T2} and a Cre-dependent pAAV-EF1a::DIO-mCherry reporter vector (Fig. 2). Additionally, cells were transfected with pTRCGW-CMV::EGFP (*321, 322*) to induce constitutive EGFP expression for assessment of transfection efficiency. At 6 h after transfection, 0, 1 or 2 µM 4TM was

added to the culture medium. As the *Fos* promoter is activated in HEK293T cells under basal conditions in a substantial fraction of HEK293T cells (unpublished observation), we did not apply additional stimulation to trigger expression of the mCherry reporter. We determined whether Cre-induced recombination had occurred by examining mCherry expression 2 days after transfection. As expected, we did not observe mCherry$^+$ cells without addition of 4TM to the medium (Fig. 2a, b), whereas in the presence of 1 and 2 µM 4TM we could detect mCherry expression in HEK293T cells (Fig. 2c-f). The density of mCherry$^+$ cells appeared to be higher after 2 µM (Fig. 2f) compared with 1 µM 4TM (Fig. 2d), but we did not quantify this. Importantly, in all conditions we observed EGFP$^+$ cells, indicating that the lack of mCherry expression in cells without 4TM treatment was not due to a deficiency in the transfection procedure. Hence, this demonstrates that the Fos::CreER^{T2} construct is functional *in vitro* and that the expression of the Cre-dependent gene is controlled by the presence of 4TM.

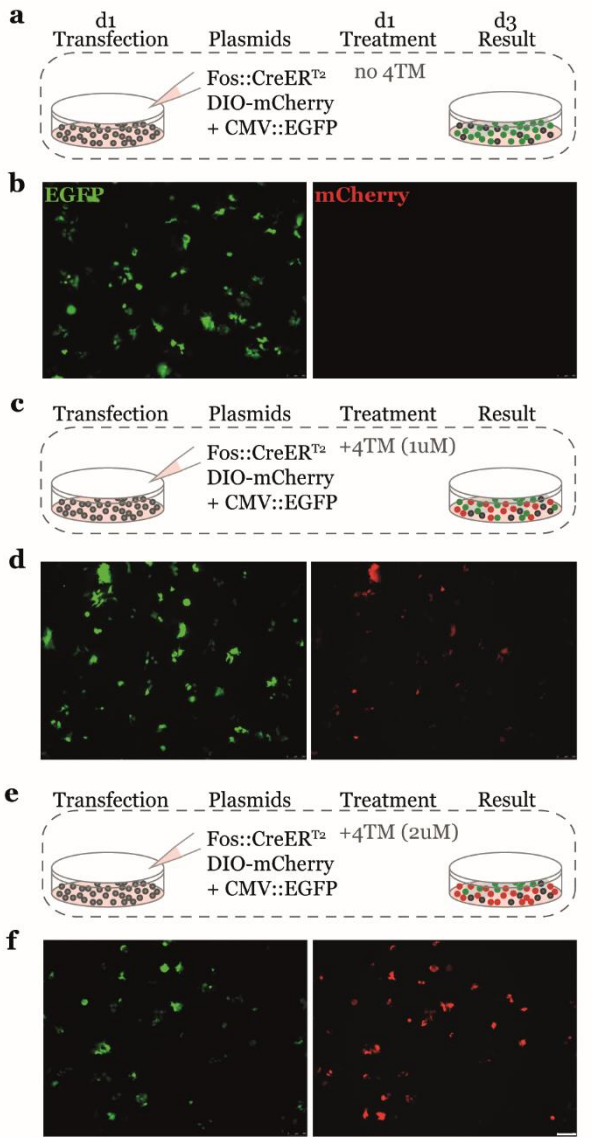

Figure 2. *In vitro* validation of TRAP-mediated reporter expression. After plating HEK293T cells, all conditions were transfected on day 1 with pTRCGW-CMV::EGFP to determine cell transfection efficiency, and with pAAV-Fos::CreER^{T2} and pAAV-EF1a::DIO-mCherry to assess 4TM-controlled reporter expression. At 6 h after transfection, cells were cultured in medium without or with 4-hydroxytamoxifen (4TM) and on day 3 images were taken. **a.** In absence of 4TM, mCherry is not expressed. **b.** mCherry expression in the presence of 1 µM 4TM. **c**. mCherry expression in the presence of 2 µM 4TM. Scale bar = 100 µM.

In vivo validation and optimization of viral-TRAP

As our main goal was to create a new virus-based method that allows the expression of a stable molecular tag in behaviorally activated neurons, we next tested the viral-TRAP system *in vivo* using a contextual fear conditioning (CFC) paradigm. We hypothesized that non-specific tagging of neurons (i.e., leakiness) would depend on the injected titer of AAV5-Fos::CreER^{T2}. To address this point, we produced 3 mixtures of AAV5-Fos::CreER^{T2} and Cre-dependent AAV5-

hSyn::DIO-hM3Dq-mCherry with a ratio of 1:100, 1:500, 1:1000, meaning that AAV5-Fos::CreER^{T2} was injected at final titer of 1.2 X 10^{11}, 2.4 X 10^{10} or 1.2 X 10^{10} gc/mL, respectively, and AAV5-hSyn::DIO-hM3Dq-mCherry at a titer of 5 X 10^{12} gc/mL. Notably, AAV5-Fos::CreER^{T2} was first diluted in sterile phosphate buffered saline, such that the injected volume of each mixture (0.5 µl per hemisphere) was the same for all conditions. These virus mixtures were injected bilaterally into the dorsal medial prefrontal cortex (dmPFC) of wild-type C57Bl/6J mice (Fig. 3a). On the tag day, mice remained in their home-cage (HC) in the absence or presence of 25 mg/kg 4TM treatment or underwent CFC and received 4TM (*124, 310*) 2 h after conditioning (Fig. 3b). On day 4 after CFC, all mice were sacrificed and brain sections generated for visualization of hM3Dq-mCherry^{+} cells in the mPFC (Fig. 3c-d). We observed robust differences in hM3Dq-mCherry expression between virus mixtures and groups (Fig. 3d). Although viral-TRAP induced tagging of cells activated by CFC with all mixtures, the condition with the highest AAV5-Fos::CreER^{T2} titer (ratio 1:100) also showed a high amount of hM3Dq-mCherry^{+} cells in both HC groups, thus reflecting non-specific tagging of neurons. With the 1:500 and 1:1000 mixture, hM3Dq-mCherry expression was substantially reduced overall and we observed a clear difference between CFC and HC groups (Fig 3d).

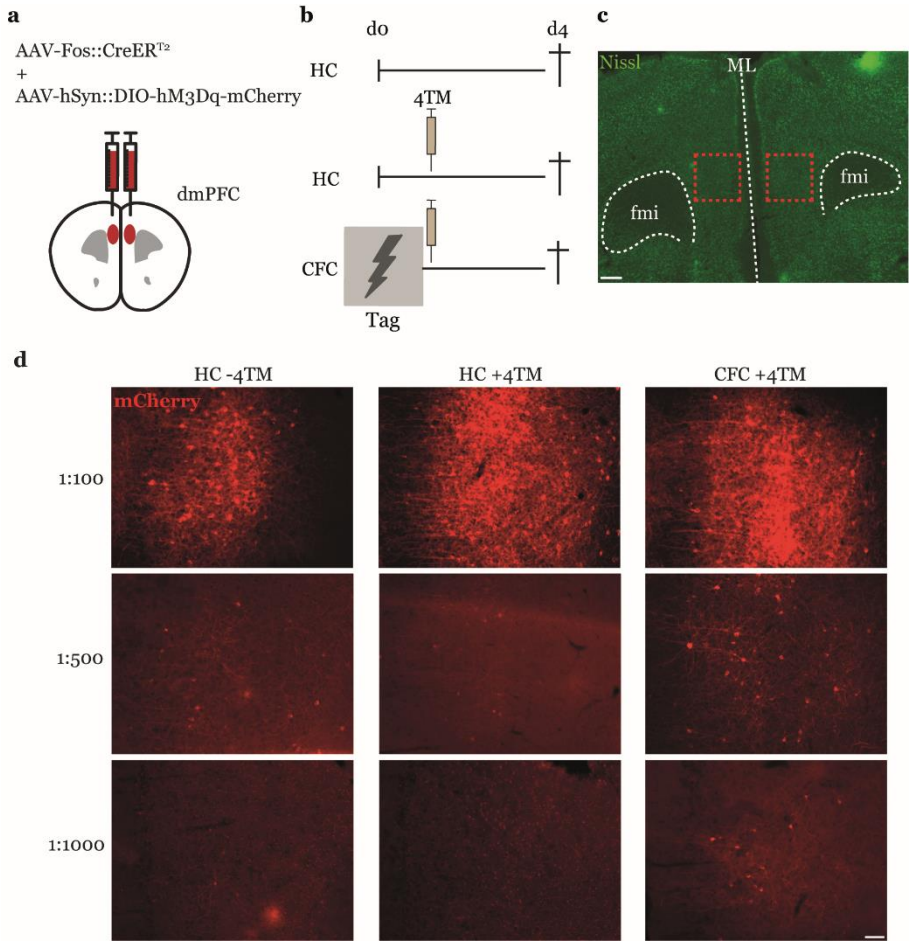

Figure 3. ***In vivo*** **validation and optimization of viral-TRAP. a.** Mixtures of AAV5-Fos::CreER^{T2} and Cre-dependent AAV5-hSyn::DIO-hM3Dq-mCherry (ratios: 1:100, 1:500, 1:1000, respectively) were injected bilaterally into the dmPFC of wild-type mice. **b.** Experimental design of groups used to qualitatively assess the neuronal activity and 4TM-dependent tagging with viral-TRAP. Home-cage without and with 4TM treatment (HC -4TM, n = 2 mice; HC +4TM, n = 2 mice), Contextual fear conditioning with 4TM treatment (CFC +4TM, n = 2 mice). The CFC group received 4TM 2h after training on day 0 and mice were sacrificed 4 days later. **c** Image of the mPFC stained with Nissl. The red boxes indicate the dmPFC area that was imaged for assessment of mCherry^{+} neurons. ML = Midline. fmi = forceps minor of the corpus callosum. Scale bar = 250 µM. **d** Representative pictures of hM3Dq-mCherry expression in the dmPFC of each group. ML = Midline. fmi = forceps minor of the corpus callosum. Scale bar = 75µM.

More mCherry^{+} cells were present after CFC in mice that received the 1:500 mixture compared with the 1:1000 mixture. Although the latter condition showed negligible hM3Dq-mCherry expression in HC groups, we think that the number of CFC-tagged neurons with the 1:1000 mixture might reflect an underrepresentation of the percentage of neurons that were activated during CFC. Thus, viral-TRAP allows expression of a Cre-dependent transgene, but optimization of the

amount of injected AAV-Fos::CreER^{T2} particles (depending on the titer of the virus) is required to minimize leakiness.

Quantification of *in vivo* tagged dmPFC neurons using viral-TRAP

We next quantified the percentage of tagged dmPFC neurons using a viral-TRAP mixture ratio of 1:500. For this, AAV5-Fos::CreER^{T2} and AAV5-hSyn::DIO-hM3Dq-mCherry (*323*) were injected bilaterally in the dmPFC of an independent and bigger cohort of C57Bl/6J mice (Fig. 4a). We used the same experimental timeline and included the same groups as described for the *in vivo* titration experiment (Fig. 4b). We quantified hM3Dq-mCherry^{+} neurons as a percentage of the total neuronal population (Nissl^{+}) in the mPFC (Fig. 4c-d). One-way ANOVA revealed a difference between groups ($F(2,15) = 32.79$, $p < 0.0001$). Post-hoc Bonferroni analyses confirmed that CFC mice exhibited a higher percentage of hM3Dq-mCherry^{+} neurons (6.9 ± 0.7%) compared with mice in the HC group that received 4TM (2.2 ± 0.3%; $p < 0.0001$) and with the home-cage group that did not receive 4TM (1.4 ± 0.2%; $p < 0.0001$). This indicates that using this mixture (1:500), and in particular this titer of the AAV5-Fos::CreER^{T2} virus, viral-TRAP enables neuronal-activity and 4TM-dependent tagging of mPFC neurons with limited non-specific background tagging (Fig. 4d).

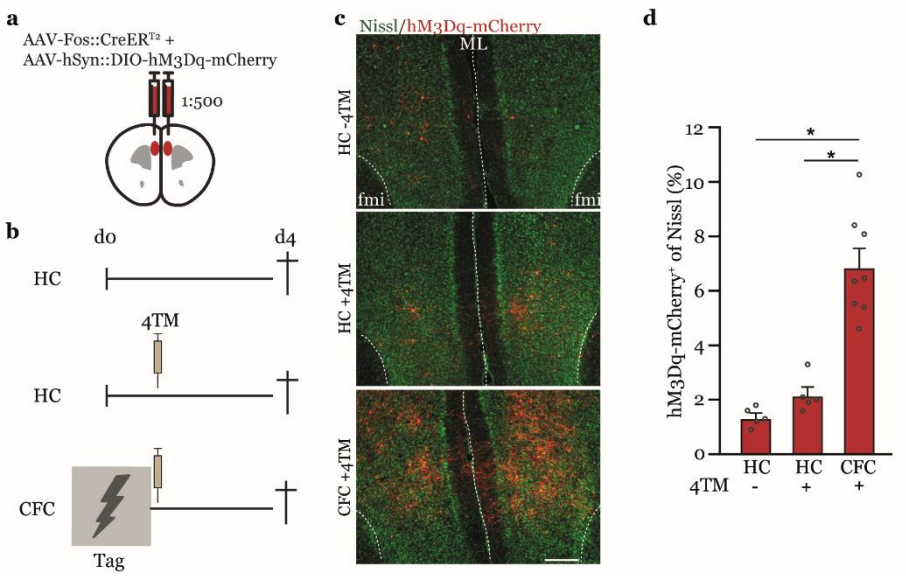

Figure 4. Quantification of *in vivo* tagged mPFC neurons using viral-TRAP. **a.** A mixture of AAV-Fos::CreER^{T2} and Cre-dependent AAV-hSyn::DIO-hM3Dq-mCherry at a ratio of 1:500 was injected bilaterally into the dmPFC of wild-type mice. **b.** Experimental design of groups used to quantitively assess the neuronal activity and 4TM-dependent tagging with viral-TRAP. Home-cage without and with 4TM treatment (HC -4TM, n = 5; HC +4TM, n = 5), Contextual fear conditioning with 4TM treatment (CFC

+4TM, n = 8). The CFC group received 4TM 2 h after training on day 0 and mice were sacrificed 4 days later. **c.** Representative pictures of hM3Dq-mCherry (red) expression in the dorsal mPFC of each group. fmi = forceps minor of the corpus callosum. ML = midline. Scale bar = 250μM. **d.** Percentage of hM3Dq-mCherry$^+$ neurons in the dmPFC. Post-hoc Bonferroni test: CFC *vs.* HC -4TM, $*p < 0.0001$, CFC *vs.* HC +4TM, $*p < 0.0001$. Bar graph shows mean + s.e.m.

Incorporation of GABAergic neurons in the CFC-tagged mPFC population

As a final step, we characterized the contribution of GABAergic neurons to the tagged dmPFC populations in the aforementioned groups. To asses this, we first verified whether the percentage of GAD67 (Glutamic acid decarboxylase 67) expressing cells in the mPFC did not differ between groups (Fig. 5a, b). On average, GAD67$^+$ neurons represented approximately 7% of Nissl$^+$ cells in the dmPFC and we did not observe differences between groups (One-way ANOVA: $F(2,14) = 1.366$, $p = 0.294$). Next, we quantified the percentage of neurons that expressed GAD67 within the hM3Dq-mCherry$^-$ versus hM3Dq-mCherry$^+$ population of each group (Fig. 5a, c). Two-way repeated measures ANOVA revealed a significant population effect: $F(1,14) = 32.54$, $*p < 0.0001$. A post-hoc Bonferroni test confirmed that GAD67$^+$ neurons were overrepresented in the hM3Dq-mCherry$^+$ population in the experimental groups that received 4TM treatment (HC +4TM mCherry$^-$ *vs.* mCherry$^+$ $p < 0.01$; CFC +4TM mCherry$^-$ *vs.* mCherry$^+$ $p < 0.01$), whereas the populations did not significantly differ within the HC -4TM group. The percentage of GAD67$^+$ neurons within the hM3Dq-mCherry$^+$ populations of the CFC +4TM (16 ± 1.8%) and HC +4TM (18.3 ± 2.4%) was very similar. Hence, compared with the total neuronal population, we found that GABAergic neurons constituted ~16% of the tagged dmPFC ensembles and this was not influenced by the type and degree of behavioral stimulation that mice experienced.

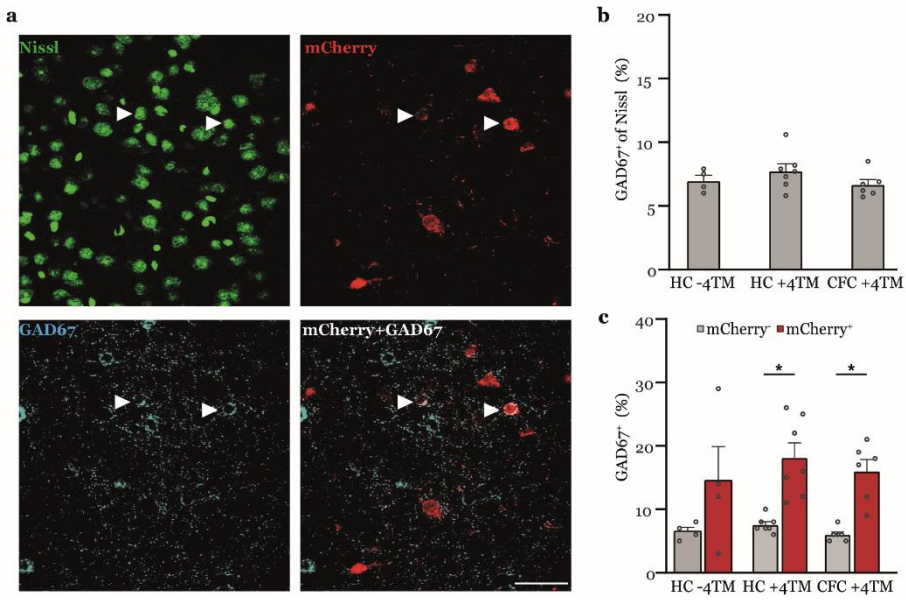

Figure 5. Incorporation of GABAergic neurons in tagged dmPFC populations. a Representative picture of neuronal nuclei (Nissl^{+}), tagged neurons (mCherry^{+}) and GABAergic interneurons (GAD67^{+}) in the dmPFC. White arrowheads highlight neurons that co-express GAD67 and mCherry. Scale bar = 50 µM. **b** Percentage of GAD67^{+} interneurons in the dmPFC (HC -4TM, n = 4; HC +4TM, n = 7; CFC +4TM, n = 6). One-way ANOVA: $F(2,14)=1.366$, p = 0.294. Bar graph shows mean + s.e.m. **c** Percentage of GAD67^{+} interneurons in hM3Dq-mCherry^{-} (Nissl^{+}) and hM3Dq-mCherry^{+} tagged neuronal population, (HC -4TM, n = 4; HC +4TM, n = 7; CFC +4TM, n = 6). Two-way repeated measures ANOVA revealed a significant Population effect: $F(1,14)=32.54$, $^{*}p<0.0001$. Post-hoc Bonferroni test: HC +4TM mCherry^{-} *vs.* mCherry^{+} $^{*}p<0.01$; CFC +4TM mCherry^{-} *vs.* mCherry^{+} $^{*}p<0.01$. Bar graph shows mean + s.e.m.

Discussion

We developed and characterized viral-TRAP, a new non-transgenic method to express a permanent molecular tag in activated neurons. We confirmed that viral-TRAP enables the expression of a Cre-dependent reporter in *Fos*-expressing cells, both *in vitro* and *in vivo,* and that this is tightly controlled by the presence of 4TM. Furthermore, we found that leakiness of this system could be reduced by adjustment of the injected titer of AAV-Fos::CreER^{T2} particles, as demonstrated by a reduction in mCherry^{+} mPFC neurons under conditions with limited neuronal activation (i.e., when animals remain in their home cage) and in the absence of 4TM treatment. By doing so, we found a virus mixture ratio of the AAV-Fos::CreER^{T2} and Cre-dependent vector (1:500, respectively) that enabled neuronal activity- and 4TM-controlled permanent tagging of Fos-expressing dmPFC neurons.

Implementing a technique to identify and manipulate a neuronal ensemble activated by a specific behavioral experience is crucial to determine the causal involvement of these neurons in memory storage and retrieval. In addition, it can be used to analyze the cellular and molecular changes that support memory processing by comparison of tagged neurons with their non-activated counterparts. Although existing tools, such as *Fos*::tTA and TRAP transgenic mouse lines, were already available for this purpose, we aimed to develop a new virus-based tool to overcome limitations of the use of transgenic mice. The principal mechanism of viral-TRAP is based on pre-existing transgenic TRAP mouse lines (*310, 315*), however, there are several important differences between these approaches. First, viral-TRAP allows optimization of the amount of viral particles that are injected in a given brain region. Given the leakiness of the original TRAP mouse line in several brain regions (*310*), it will be possible to reduce background tagging in these areas using viral-TRAP. Of note, when we used a high titer (1.2 X 10^{11} gc/mL) of AAV5-Fos::CreER^{T2}, we also observed considerable leakiness with viral-TRAP. We speculate that when a high number of AAV particles enters a cell (i.e., multiple copies of the Fos::CreER^{T2} construct), basal levels of activation of the *Fos* promoter may lead to an accumulation of CreER^{T2} in the cytoplasm and translocation of Cre to the nucleus in absence of 4TM. Hence, the degree of dilution of AAV5-Fos::CreER^{T2} in the viral-TRAP mixture should be adjusted based on the titer of the virus batch. A second advantage of viral-TRAP compared with TRAP transgenic mice is that it can be applied to wild-type mice and to other species for which the availability of transgenic lines is limited, such as rats. It also

circumvents the need to breed and genotype transgenic animals and the costs associated with this. Finally, the AAV-Fos::CreER^{T2} vector can be easily modified (e.g., change of IEG promoter) and rapidly validated *in vitro* and then *in vivo* for efficiency.

Fos::tTA mice have been extensively used to tag activated neurons and have provided evidence concerning the role of neuronal ensembles in fear memory expression (*286, 312*). However, they cannot be used to answer questions about the role of neuronal ensembles in memory maturation over prolonged periods of time (> 2 weeks) due to the transient expression of transgenes in these mice. Viral-TRAP can overcome this by inducing a permanent molecular tag in activated neurons. Similar to TRAP transgenic mice, *Fos*::tTA mice also suffer from considerable leakiness (*286, 301*), which viral-TRAP can circumvent. The fact that the *Fos*::tTA system is controlled by Dox poses another limitation associated with these mice. Dox has to be removed from the food or drinking water of mice at least 24-48 h before a tag session and blockade of neuronal tagging after the session relies on the intake of Dox via food or water (*300*). As such, the time-window to tag activated neurons is substantially longer and variable than with the TRAP system (approximately 6 h when 4TM is used) (*124, 314*). On the other hand, it is known that 4TM and tamoxifen can have aversive side-effects, in particular at high concentrations (*324, 325*). In addition to binding to CreER^{T2}, these compounds have affinity for endogenous estrogen receptors, which may explain side-effects. Therefore, it is important to use a low dose of 4TM or tamoxifen in *in vivo* studies. Previous reports using TRAP transgenic mice used a dose of 50-150 mg/kg 4TM to activate the TRAP system and did not report side-effects (*310, 314*). Thus, the dose of 25 mg/kg 4TM that we used in our experiments can be considered relatively low and safe, although we did not examine the occurrence of potential side-effects on behavior and health of the mice.

Even though we addressed limitations of previous tagging methods with the development of viral-TRAP, it is relevant to acknowledge that we also observed some leakiness with the 1:500 ratio in the virus mixture in the absence of 4TM. We found that 1.4 ± 0.2% of mPFC neurons were tagged when animals remained in their home-cage without 4TM treatment. When viral-TRAP is used to tag neurons that are activated by a behavioral experience, these non-specifically tagged neurons will be included. Consequently, this fraction of cells will also be activated/suppressed upon manipulation and can confound the interpretation of behavioral effects and for instance the role of a neuronal ensemble in memory acquisition/expression. Therefore,

adequate control groups should always be included to rule out potential non-specific effects. This could, for instance, be a group in which a similar-sized, but task irrelevant, ensemble in the same brain region is tagged and manipulated. For investigations into the cellular and molecular properties of neurons ensembles, we recommend to use a virus mixture with a ratio of 1:1000, as with that mixture we did not observe tagged mPFC neurons in the absence of 4TM treatment.

Interestingly, we found that GABAergic neurons are overrepresented in the tagged mPFC population, independent of whether mice remained in their home cage or underwent CFC. In the total neuronal population, we detected ~7% GAD67$^+$ neurons, whereas within the tagged population this was more than twofold higher (~16%). It remains to be elucidated which GABAergic interneuron subtypes are included in the tagged GAD67$^+$ population and stresses the importance to further characterize the tagged neurons. In particular, because different interneuron subtypes have distinct roles within neuronal networks and accumulating evidence implicates parvalbumin-, somatostatin-, cholecystokinin- and vasoactive intestinal polypeptide-expressing GABAergic interneurons in memory encoding and retrieval (*75, 76*).

Taken together, we created and characterized a new virus-based method that efficiently tags Fos-expressing neurons in a 4TM-dependent manner. Importantly, it enables the visualization, manipulation and characterization of neuronal ensembles over a prolonged period of time. In addition to the Cre-dependent mCherry and hM3Dq-mCherry viruses used in this study, any other Cre-dependent virus or Cre-dependent transgenic mouse or rat line can be combined with the TRAP vector. Hence, viral-TRAP is a versatile tool that can be used in wild-type and transgenic animals of different species, thereby facilitating research into neuronal ensembles that support the acquisition and expression of learned behaviors.

Materials and Methods

Animals

Wild-type C57BL/6J male mice that were 2 to 3 months old at the start of experiments were individually housed on a 12 h light/dark cycle with constant access to food and water. Behavior was studied during the light phase. Experiments were performed in accordance with ethical regulations for animal testing and approved by The Netherlands central committee for animal experiments (CCD) and the animal ethical care committee (IvD/DEC) of the Vrije Universiteit Amsterdam.

Constructs

The pAAV-Fos::CreER^{T2} plasmid was generated by replacing the coding sequence of tTA from pAAV-Fos::tTA-pA (gift from William Wisden, Addgene plasmid #66794) with the coding sequence of CreER^{T2} from pRetroQ-Cre-ER^{T2} (gift from Richard Youle, Addgene plasmid #59701). CreER^{T2} was first amplified by PCR using TCGATTCTAGAATTACCATGTCCAATTTACTGACCGTACACC and GTTAAAGCTTGCGGCCTCAAGCTGTGGCAGGGAAACCCTC oligonucleotides. Next, pAAV-Fos-tTA-pA was digested with restriction enzymes EcoRI and NotI (New England Biolabs) to remove tTA and then replaced by CreER^{T2} using SLIC (*320*). HEK293 cells were transfected with pAAV-EF1a::DIO-mCherry (gift from Brian Roth, Addgene plasmid #50462) and pTRCGW-EGFP (gift from Joost Verhaagen, NIN, The Netherlands). The pAAV-hSyn::DIO-hM3D(Gq)-mCherry (Brian Roth Lab, Addgene plasmid #44361) plasmid was packaged as serotype AAV5 for *in vivo* experiments.

HEK293T cell experiments

On the day before transfection glass coverslips were placed on a 24-well culture plate and coated with Poly-L-Lysine (PLL, 100mg/L H_2O) for 15 minutes at 37°C, after which PLL was removed and coverslips were washed with H_2O. A total of ~30000 HEK293T cells were plated per well and cultured in DMEM/10%FBS/P/S (Gibco 31966021). Cells were transfected with a total of 160 ng DNA/well using Polyethylenimine in PBS (PEI, Polysciences; ratio PEI/DNA 5:1). Cells were transfected with pTRCGW::CMV-EGFP, pAAV-EF1a::DIO-mCherry and pAAV-Fos::CreER^{T2} (53 ng DNA/plasmid, DNA stock at 1µg/µL); Each experimental condition was performed in 2 non-consecutive wells in the same culture plate and in triplicate. Transfection medium was removed 6h after the start and cells were cultured in medium supplemented with 0, 1 or 2 µM of 4TM (4-

hydroxytamoxifen, H6278 Sigma-Aldrich) dissolved in 100% ethanol (stock: 2 mg 4TM in 1 mL 100% ethanol). The day after transfection cells were checked for EGFP and mCherry expression. Two days after transfection cells were fixed with cold 4% Paraformaldehyde (PFA) in PBS pH 7.4 for 20 minutes at room temperature (RT) and then washed with PBS pH 7.4. Cells were imaged for further analysis using a widefield fluorescence microscope (Leica Microsystems, DiM8).

AAV vectors and stereotactic micro-injections

pAAV-Fos::CreER^{T2} (titer 1.2 X 10^{13}) and Cre-dependent pAAV-hSyn::DIO-hM3Dq-mCherry (titer 5.0 X 10^{12} gc/mL) were packaged as serotype 5 virus (AAV5). For stereotactic micro-injections, mice received 0.05 mg/kg Temgesic (RB Pharmaceuticals, UK) and were then anesthetized with isofluorane and placed in a stereotactic frame. For local analgesia, mice received Lidocaine (2%, Sigma-Aldrich Chemie N.V, The Netherlands) topically to the skull. Virus mixtures of AAV5-Fos::CreER^{T2} and Cre-dependent AAV5-hSyn::DIO-hM3Dq-mCherry (ratio 1:100, 1:500, 1:1000; AAV-Fos::CreER^{T2} was injected at final titer of 1.2 X 10^{11}, 2.4 X 10^{10} and 1.2 X 10^{10} gc/mL, respectively) were bilaterally injected in the dorsal mPFC (+1.8 mm AP; ±0.45 mm ML; -2.1 mm DV, relative do Bregma) via microinjection glass needles. Each brain hemisphere received 0.5 µL of the viral mixture at a flow rate of 0.1 µL per minute. An additional 5 minutes after viral delivery were given to allow viral diffusion, before removing the glass needle. At the end of the surgery, the animals were returned to their home-cage where they remained for an additional 3 weeks before the start of experiments.

Contextual Fear Conditioning (CFC)

Before the start of CFC, each mouse was handled for three consecutive days. CFC was performed 48 h after the last handling session, as described previously (*326, 327*). The conditioning chamber was made of Plexiglass with a stainless-steel grid floor and placed in a sound-proof cabinet. White noise (68 dB; Ugo Basil, Italy) was present during conditioning sessions. The chamber was cleaned between each trial with 70% ethanol. Mice explored the conditioning context for 120 s before presentation of a foot-shock (0.7 mA, 2 s). Each trial ended 30 s after the foot-shock and then mice were returned to their home-cage. Freezing behavior was analyzed by video tracking using Ethovision XT (Noldus, The Netherlands).

4-hydroxytamoxifen (4TM)

4TM (H6278, Sigma-Aldrich Chemie N.V, The Netherlands) was injected intraperitoneal (*i.p.*) in an aqueous formulation (*124*). 4TM was dissolved in DMSO (100%, D8418 Sigma-Aldrich N.V, The Netherlands) (15 mg 4TM in 300µL DMSO). The stock solution was then diluted in a mixture of saline and 2% Tween80 (P1754, Sigma-Aldrich N.V, The Netherlands) and finally in the same volume of saline (no addition of other components). The final solution thus contained 2.5 mg of 4TM in 5% DMSO and 1% Tween80 Saline. Each mouse received 25 mg/kg (*i.p.*) of 4TM 2 h after the conditioning session (see experimental design explained in figures).

Immunohistochemistry

Mice were transcardially perfused with ice-cold PBS pH 7.4, followed by 4% Paraformaldehyde (PFA) prepared in PBS pH 7.4. Then, brains were removed and post-fixed overnight in 4 % PFA at 4°C. The tissue was transferred to 30% sucrose in PBS with 0.02% NaN_3. Once this step was completed, sections of 35 µM were generated using a cryostat and kept in PBS with 0.02% NaN_3 until further use. Sections were washed in PBS to remove NaN_3 and then incubated with blocking solution containing 5% normal goat serum (NGS), 2.5% bovine serum albumin and 0.25% Triton X-100 in PBS at room temperature (RT, 22°C) for 1 h. Then, the sections were incubated overnight at 4°C in blocking solution supplemented with rat anti-GAD67 (1:1000, Merck, USA). Brain sections were washed with PBS and incubated with secondary antibody and NeuroTraceTM 500/525 (1:400, ThermoFisher, USA) for fluorescent Nissl stain in blocking solution for 2 h at RT (*112*). Last, sections were again washed in PBS and mounted using 0.2% gelatin in PBS. Cover slipping was performed using polyvinyl alcohol mounting medium with DABCO (10981, Sigma-Aldrich N.V, The Netherlands). For qualitative assessment of hM3Dq-mCherry$^+$ neurons, images were obtained using a widefield fluorescence microscope (Leica Microsystems, DiM8). For the quantitative analysis, 6 z-stacks per animal were generated using a confocal microscope (Zeiss, LSM510), while the experimenter was blind for the treatment groups. ImageJ Software was used to extract the regions of interest (ROIs) of the cells stained with green Nissl (Gaussian filter, Li threshold, watershed). Only ROIs with a predefined range size (80-2000 square units; to exclude glial cells and non-specific staining) and circularity (0.5 to 1.0) were included for further analysis. As one cell could be present in 2-3 images of a z-stack, we developed a MATLAB (MathWorks) script to group the ROIs that

belonged to the same Nissl-stained cell and recalculated the total number of Nissl$^+$ cells present in each z-stack. The GAD67$^+$ and hM3Dq-mCherry$^+$ tagged cells were counted manually and the experimenter was blind to the treatment conditions.

Statistical analysis

The statistical details, including the number of animals, are described in the figure legends. Mice with viral displacement (in total: hM3Dq-mCherry n = 1) were excluded from this study. All graphs show means + s.e.m. Prism 9 (GraphPad) and SPSS (IBM) software were used for the statistical analysis. For quantification of the percentage of tagged neurons and GAD67$^+$, we performed a One-way ANOVA followed by Post-hoc Bonferroni test when applicable. For within group comparisons of the distribution of GAD67$^+$ neurons, we applied a two-factor Repeated measures ANOVA and Post-hoc Bonferroni test. Significance was set at $p < 0.05$.

Chapter 4

Memory strength gates the involvement of a CREB-dependent cortical fear engram in remote memory

Mariana R. Matos[1], Esther Visser[1], Ioannis Kramvis[1], Rolinka J. van der Loo[1], Titia Gebuis[1], Robbert Zalm[2], Priyanka Rao-Ruiz[1], Huibert D. Mansvelder[3], August B. Smit[1] and Michel C. van den Oever[1,*].

[1]Department of Molecular and Cellular Neurobiology, Center for Neurogenomics and Cognitive Research, Amsterdam Neuroscience, Vrije Universiteit Amsterdam, 1081 HV, Amsterdam, The Netherlands

[2]Department of Functional Genomics, Center for Neurogenomics and Cognitive Research, Amsterdam Neuroscience, Vrije Universiteit Amsterdam, 1081 HV, Amsterdam, The Netherlands

[3]Department of Integrative Neurophysiology, Center for Neurogenomics and Cognitive Research, Amsterdam Neuroscience, Vrije Universiteit Amsterdam, 1081 HV, Amsterdam, The Netherlands

Nature communications, 2019, 10:2315

Abstract

Encoding and retrieval of contextual memories is initially mediated by sparsely activated neurons, so-called engram cells, in the hippocampus. Subsequent memory persistence is thought to depend on network-wide changes involving progressive contribution of cortical regions, a process referred to as systems consolidation. Using a viral-based TRAP (Targeted Recombination in Activated Populations) approach, we studied whether consolidation of contextual fear memory by neurons in the medial prefrontal cortex (mPFC) is modulated by memory strength and CREB function. We demonstrate that activity of a small subset of mPFC neurons is sufficient and necessary for remote memory expression, but their involvement depends on the strength of conditioning. Furthermore, selective disruption of CREB function in mPFC engram cells after mild conditioning impairs remote memory expression. Together, our data demonstrate that memory consolidation by mPFC engram cells requires CREB-mediated transcription, with the functionality of this network hub being gated by memory strength.

Introduction

In recent years, great progress has been made in understanding the neurobiological substrate, or engram, of a recently acquired (< 1-week-old) memory. For instance, initial formation and expression of conditioned-fear memory is mediated by coordinated activity of small subsets of neurons, referred to as neuronal ensembles (*285*) or engram cells (*328*), in hippocampal circuitry and the amygdala (*119, 286, 315, 329*). Persistence of memory is thought to depend on systems consolidation, a time-dependent process through which a given memory is gradually consolidated in cortical networks (*17, 330*). This concept is supported by the observation that retrieval of contextual fear memory initially does not depend on activity in cortical areas, including the mPFC, however cortical activity is required for memory retrieval at remote time-points (*37, 44, 331*). Despite these findings, the molecular and cellular mechanisms that support the consolidation of remote (≥ month-old) memories and the influence of memory strength on the engagement of cortical neuronal ensembles in remote memory expression are poorly understood. This is mainly because of technical limitations to selectively manipulate subsets of neurons several weeks after they are activated by a specific experience.

Memory consolidation initially depends on de novo RNA and protein synthesis (*332*), critical for changes in structural plasticity and synaptic strength between neurons in an engram network (*333*). It is well-established that the transcription factor CREB (cAMP-responsive element binding protein) has a crucial role in regulating gene expression that underlies formation of long-term memory (*334*), as determined by systemic knock-out or global knock-down of CREB function (*335-337*). More recently, it was shown that modulation of CREB function in small subsets of neurons prior to learning affects the probability that these cells will be incorporated in a memory engram (*338, 339*), suggesting that differences in CREB levels at the time of learning determine which neurons will become engram cells (*340*). However, whether CREB function in cortical engram cells is required after learning to support systems consolidation of memory has never been demonstrated.

Here, we investigated (1) whether the mPFC harbors engram cells supporting remote contextual fear memory; (2) whether involvement of mPFC neurons is modulated by the strength of conditioning; and (3) whether CREB function in these neurons is required for memory persistence. To test this, we developed a dual-virus variant of TRAP (*310*). This allowed us to express a lasting

molecular tag (e.g. Designer Receptor Exclusively Activated by Designer Drugs (DREADD)(*341*) or mCREB (a repressor of CREB function)) in activated neurons of wild-type mice. Using this system, we found that engram cells in the mPFC are already defined during learning, but their functional contribution to memory expression requires CREB-mediated transcription and depends on memory strength.

Results

Fear conditioning evokes neuronal activation in the mPFC

We first assessed whether neurons in the dorsal mPFC region (comprising the prelimbic cortex (PL) and anterior cingulate cortex (ACC)) were activated during CFC (using a single foot-shock = unconditioned stimulus (US)) or exposure to the CFC context in absence of a foot-shock (Ctx). Mice that remained in their home-cage were used as controls (HC; Fig. 1a). An activated neuron was defined by the expression of the immediate early gene *Fos* (Fos expression is rapidly and transiently induced by neuronal activity(*342*); Fig. 1b). Compared with HC controls (1.7 ± 0.1%; mean ± SEM Fos^+ neurons), the percentage of Fos^+ neurons was significantly enhanced in Ctx (7.3 ± 0.1%) and CFC (8.5 ± 0.4%) groups (Fig. 1c). A minor, but significant, difference was found between Ctx and CFC mice. Hence, sparse neuronal activity is induced in the mPFC by CFC, as well as by mere exposure to a novel context. Therefore, we next investigated the functional relevance of CFC-activated mPFC ensembles.

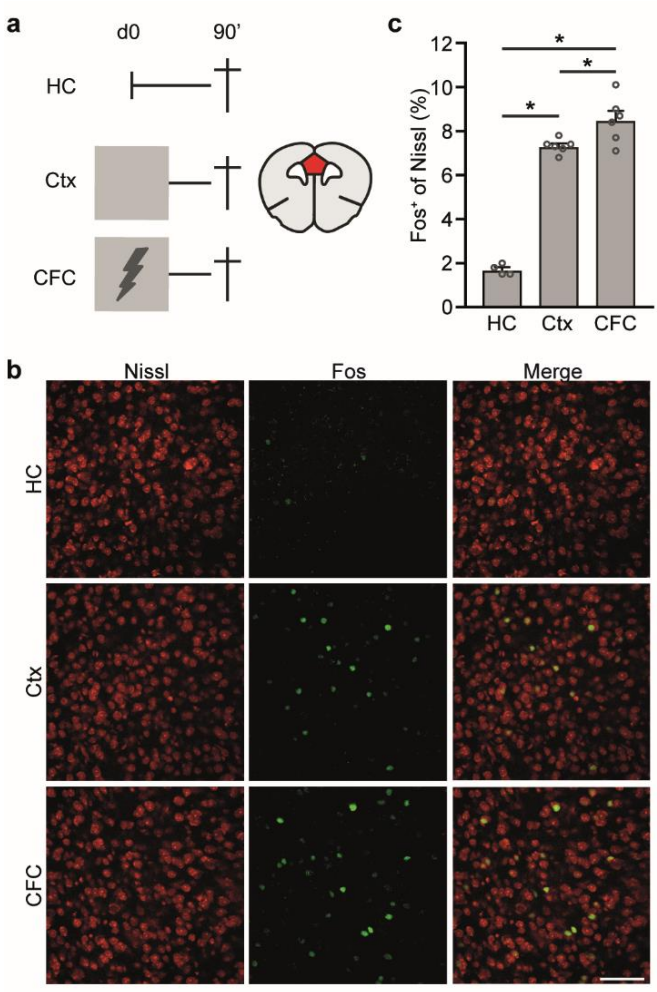

Figure 1. CFC enhanced neuronal activity in the mPFC. a Left: experimental design of groups used to assess Fos expression. Home-cage (HC; n = 4), Context exposure only (Ctx; n = 6), Contextual fear conditioning (CFC; n = 6). Lightning bold indicates foot-shock (1US). Right: illustration of a coronal brain section indicating the mPFC region (red) where Fos$^+$ neurons were analyzed. **b** Representative examples of Fos$^+$ cells (green) in all groups. **c** Percentage of Fos$^+$ cells in each group. One-way ANOVA $F_{(2,13)} = 126.3$, $p < 0.0001$. Post-hoc Bonferroni test: HC *vs.* Ctx $^*p < 0.0001$, HC *vs.* CFC $^*p < 0.0001$, Ctx *vs.* CFC $^*p = 0.032$. Scale bar = 50 µm. Bar graph shows mean + s.e.m.. Source data are provided as a Source Data file.

Viral-TRAP enables molecular tagging of activated neurons

To enable chemogenetic manipulation of CFC-activated mPFC neurons during retrieval of a recent (< 1-week-old) and remote (1-month-old) fear memory, we developed an inducible dual-virus system based on TRAP(*310*). This method comprised an Adeno-Associated Virus (AAV) coding for inducible Cre recombinase under the control of the *Fos* promoter (AAV-Fos::CreER^{T2}) and a second Cre-dependent AAV, e.g., containing the coding sequence of hM4Di (inhibitory Gi-DREADD(*343*)) in an inverse open reading frame and flanked by Cre

recognition sites. With this method, CreER^{T2}-mediated hM4Di expression is coupled to the *Fos* promoter and controlled by systemic injection of 4-hydroxytamoxifen (4TM(*124, 310*); Fig. 2a).

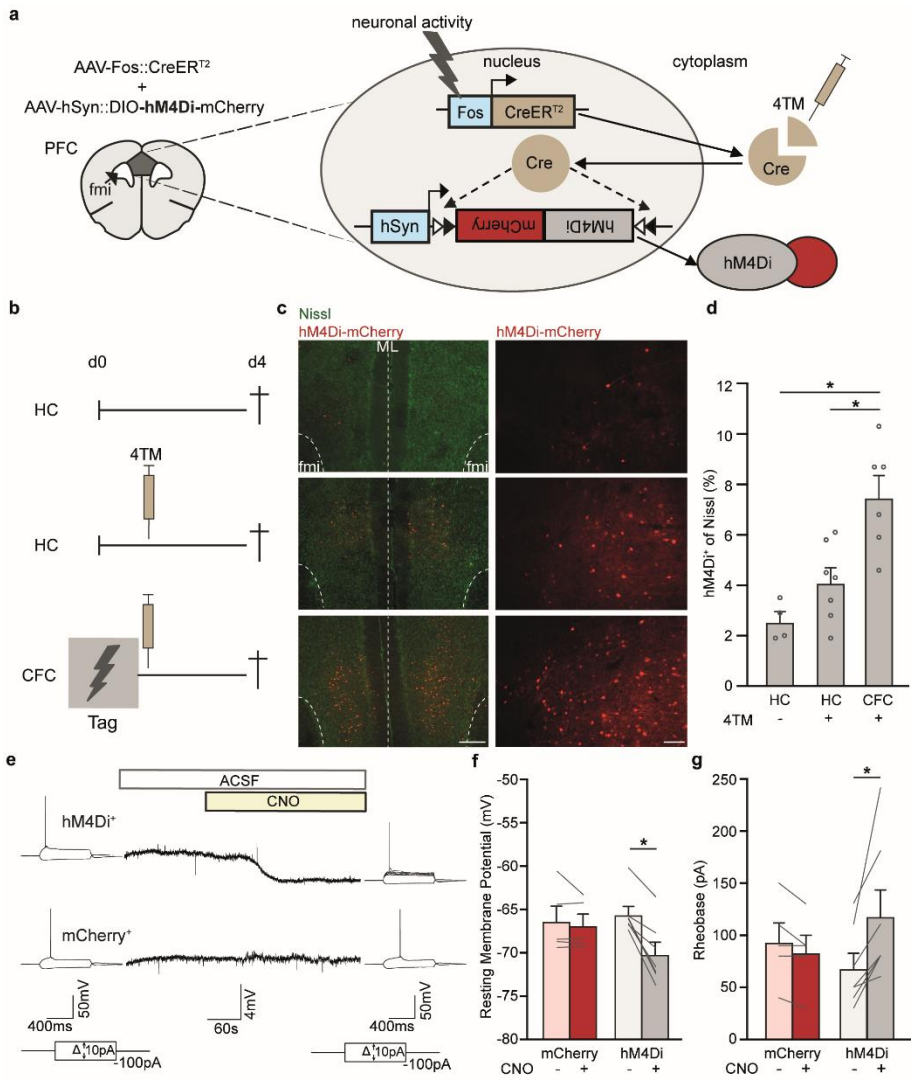

Figure 2. Viral-TRAP enables inducible activity-dependent tagging of mPFC neurons. **a** Schematic representation of the viral-TRAP method. A mixture of AAV-Fos::CreER^{T2} and Cre-dependent AAV (e.g., AAV-hSyn::DIO-hM4Di-mCherry) is bilaterally infused into the mPFC. The *Fos* promoter is activated by neuronal activity, resulting in CreER^{T2} expression. Systemic injection of 4-hydroxytamoxifen (4TM) allows translocation of CreER^{T2} into the nucleus enabling irreversible recombination of the Cre-dependent vector and expression of hM4Di-mCherry driven by the human *Synapsin* (hSyn) promoter. fmi = forceps minor of the corpus callosum. **b** Experimental design of groups used to validate viral-TRAP. Home-cage (HC) -4TM (n = 4), HC +4TM (n = 7), Contextual fear conditioning (CFC) +4TM (n = 6). 4TM was injected systemically 2 h after CFC on day 0 and all groups were sacrificed 4 days later. **c** Expression of hM4Di-mCherry in mPFC. fmi = forceps minor of the corpus callosum. ML = midline. Left: scale bar = 250 µm; Right: scale bar = 100 µm. **d** Percentage of hM4Di-mCherry$^+$ cells in mPFC. One-way ANOVA: $F_{(2,14)}$=12.3, p = 0.001; post-hoc Bonferroni test: CFC *vs.*

HC -4TM, p = 0.001, CFC *vs.* HC +4TM, *p = 0.007.. **e** Patch-clamp recordings of hM4Di$^+$ and mCherry$^+$ (control) cells before and after CNO application. ACSF = artificial cerebrospinal fluid. **f** Resting membrane potential changes for mCherry$^+$ (n = 5) and hM4Di$^+$ (n = 7) neurons. Wilcoxon signed rank test, hM4Di$^+$: Z = -2.37, *p = 0.018; mCherry$^+$: Z = -0.41, p = 0.69. **g** Rheobase changes for mCherry$^+$ (n = 5) and hM4Di$^+$ (n = 7) neurons. Wilcoxon signed rank test, hM4DI$^+$: Z = -2.38 *p = 0.018; mCherry$^+$: Z = -1.63, p = 0.10. All bar graphs show means + s.e.m. Source data are provided as a Source Data file.

Mice received an AAV mixture of Fos::CreER^{T2} and Cre-dependent hM4Di fused to mCherry (fluorescent reporter) in the dorsal mPFC and remained in their home-cage or underwent CFC followed by 4TM treatment (Fig. 2b). CFC +4TM induced hM4Di-mCherry expression in 7.5 ± 0.9% (mean ± SEM) of mPFC neurons (Fig. 2c-d; Supplementary Fig. 1), similar to the percentage of Fos$^+$ cells induced by CFC (Fig. 1c). Home-cage control mice without (HC -4TM) and with (HC +4TM) 4TM treatment showed significantly less hM4Di-expressing (hM4Di$^+$) neurons (2.5 ± 0.4% and 4.1 ± 0.6%, respectively), confirming that this technique enabled activity-dependent tagging of mPFC neurons. In addition to a difference in the number of tagged cells, the fluorescence intensity of hM4Di$^+$ cells seemed higher in 4TM treated groups (Fig. 2c). Next, we assessed functionality of hM4Di expression by patch-clamp recordings in acute brain slices 4-7 days after CFC.

Clozapine N-oxide (CNO) reduced the resting membrane potential and increased the depolarization threshold (rheobase) in hM4Di$^+$ neurons, but not in neurons that expressed mCherry alone (Fig. 2e-g). This indicates that CNO reduced excitability of hM4Di$^+$ mPFC neurons, enabling suppression of their activity.

CFC-tagged mPFC neurons are required for remote memory

To determine whether mPFC neurons activated during CFC are involved in recent and remote fear memory expression, we re-exposed mice to the conditioning context at day 4 or 30 after training while suppressing CFC-tagged hM4Di$^+$ neurons (Fig. 3a, c). Independent groups of mice were used to avoid potentially confounding effects of repeated testing (e.g., extinction) and the possibility of lasting effects of CNO treatment. CNO-induced suppression of CFC-tagged neurons on day 4 (recent memory) did not affect freezing compared with control

mice (Fig. 3b). In contrast, at day 30 after training (remote memory), suppression of CFC-tagged mPFC neurons reduced freezing behavior (Fig. 3d). We next examined whether the lack of effect of CNO on recent memory expression could be explained by a difference in the size of the subset of manipulated neurons. To assess this, mice were sacrificed 24 h after the last test. Quantification of the number of hM4Di$^+$ cells in the recent and remote groups revealed no difference (5.7 ± 0.2% and 6.9 ± 0.8%, respectively; Fig. 3e). This, together with the observation that CNO was able to reduce the excitability of hM4Di$^+$ neurons within the first week after CFC (Fig. 2e-g), indicates that potential differences in hM4Di expression likely did not contribute to the differential effect of CNO on recent and remote memory expression. Next, we assessed whether the effect on remote memory could be specifically attributed to CFC-tagged mPFC neurons. To this end, we first exposed mice to a neutral context (context B) and treated animals with 4TM to express hM4Di in mPFC neurons activated by this context (Fig. 3f). Three days later, mice received CFC training in context A and then underwent a remote memory test in context A (day 30 after tagging) in the presence of CNO treatment. Suppression of context B-tagged neurons did not affect freezing in context A (Fig. 3g). Importantly, context B tagged a similar percentage of mPFC neurons (5.9 ± 0.4%) as CFC (compare Fig. 3e and h), indicating that suppression of a different similar-sized subset of mPFC neurons did not affect expression of remote fear memory. Thus, remote, but not recent, memory depended on the activity of mPFC ensembles activated by a single pairing of the CFC context with an aversive stimulus and allocation of fear memory to these specific neurons already occurred during conditioning.

We next determined whether involvement of mPFC neurons in remote memory generalized to stronger fear conditioning. For this, mice received three foot-shocks (3US) during CFC and were treated with 4TM to express hM4Di-mCherry in activated mPFC neurons (Fig. 3i). In contrast with 1US CFC, chemogenetic suppression of tagged mPFC neurons after 3US CFC had no effect on expression of remote fear memory (Fig. 3j), despite the observation that a similar percentage of mPFC neurons was tagged (Fig. 3k). Given this difference, we investigated whether 1 and 3US CFC evoked differential neuronal activity (Fos expression) in several regions that are known to have a crucial role in contextual fear memory and systems consolidation. Neuronal activity did not differ in the mPFC (PL), posterior ACC and hippocampal subregions (dentate gyrus and CA3), but 3US CFC activated more cells in the basolateral amygdala (BLA) and Reunions

thalamic nucleus (Re; Supplementary Fig. 2), in line with the established involvement of these latter regions in remote fear memory when mice are conditioned using multiple foot-shocks (*331, 344, 345*).

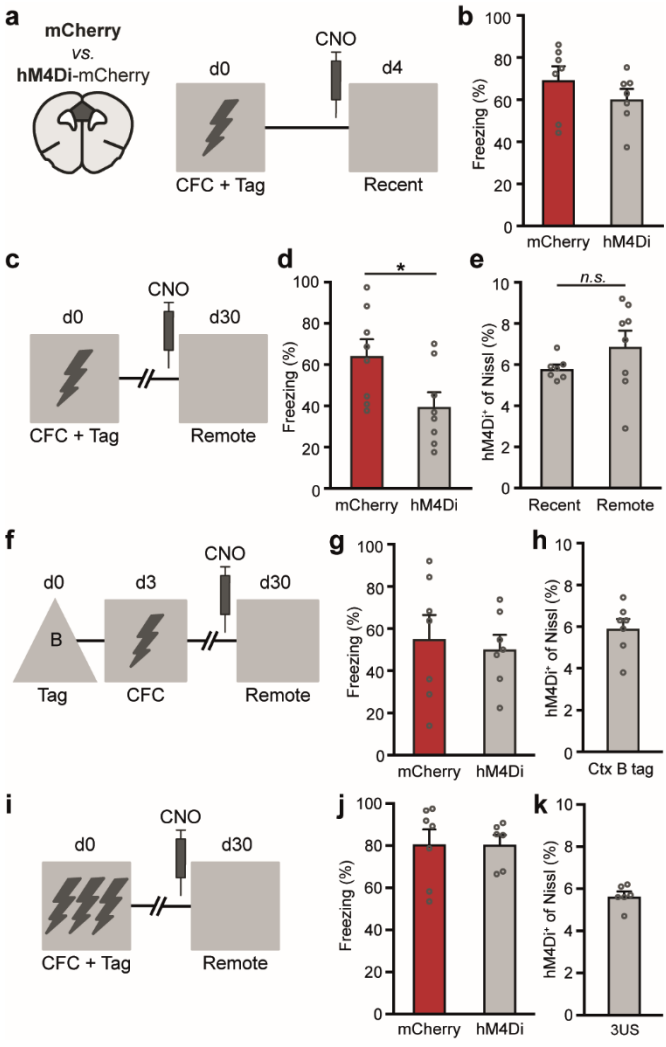

Figure 3. CFC-tagged mPFC neurons are selectively involved in remote memory expression. **a** Experimental design. mPFC neurons activated during CFC were tagged with hM4Di-mCherry or mCherry. Both groups received CNO before a recent memory test on day 4. **b** CNO did not affect freezing levels on day 4. Unpaired *t*-test: t_{12}=1.169, p = 0.265, mCherry (n = 7), hM4Di (n = 7). **c** Experimental design. Groups received CNO before a remote memory test on day 30. **d** CNO reduced freezing of the hM4Di group compared with mCherry on day 30. Unpaired *t*-test: t_{14} = 2.36, *p = 0.033, n = 8 per group. **e** Percentage of hM4Di$^+$ neurons in recent and remote groups. Unpaired *t*-test: t_{13} = 1.413, p = 0.18. *n.s.* = not significant. **f** Experimental design. mPFC neurons activated by context B were tagged with hM4Di-mCherry or mCherry. Mice receive CNO before a remote memory test in the CFC context. **g** CNO did not affect freezing in the CFC context. Unpaired *t*-test: t_{12} = 0.381, p = 0.71, mCherry (n = 7), hM4Di (n = 7). **h** Percentage of hM4Di-mCherry$^+$ neurons tagged by context B exposure. **i** mPFC neurons activated during 3US CFC were tagged with hM4Di-mCherry or mCherry. **j** CNO did not affect freezing on day 30. Unpaired *t*-test: t_{11} = 0.016, p = 0.988,

mCherry (n = 7), hM4Di (n = 6). **k** Percentage of hM4Di$^+$ neurons tagged during 3US CFC. All bar graphs show means + s.e.m. Source data are provided as a Source Data file.

Stimulation of CFC-tagged neurons evokes memory expression

Although mPFC ensembles were not necessary for recent memory expression, we next determined whether chemogenetic stimulation of these neurons is sufficient to evoke fear memory expression at recent and remote time-points after 1US CFC. To test this, mice received AAV-Fos::CreER^{T2} combined with a Cre-dependent AAV encoding hM3Dq (activating Gq-DREADD(*346*)) fused to mCherry. Using this virus mixture, we again observed inducible neuronal activity-dependent tagging of mPFC neurons. Next, mice that underwent CFC followed by 4TM treatment were exposed to a neutral context (B) on day 3 and 4 after training and we assessed freezing behavior after vehicle and CNO treatment, respectively (Fig. 4a). In the same mice, we repeated this treatment protocol at day 30 and 31 in a different neutral context (context C). As expected, animals showed minimal freezing in context B and C after vehicle treatment, but CNO enhanced freezing at both time-points (Fig. 4b). Repeated measures ANOVA revealed a significant effect of treatment only, confirming that CNO induced memory expression at both time-points. To verify that CNO increased activity of hM3Dq$^+$ neurons, mice received either vehicle or CNO in their home-cage and were perfused 120 min later to examine colocalization of hM3Dq-mCherry and cells expressing endogenous Fos protein (Fig. 4c, d). Indeed, CNO induced Fos in hM3Dq$^+$ neurons (27 ± 1.3%), whereas very few Fos$^+$ neurons colocalized with hM3Dq$^+$ cells (0.6 ± 0.9%) after vehicle treatment (Fig. 4e). Notably, CNO did not enhance freezing in mice that expressed hM3Dq in mPFC neurons that were activated by exposure to the conditioning context only (in the absence of a foot-shock) or mCherry alone in CFC-tagged mPFC neurons (Supplementary Fig. 3). This indicates that enhanced freezing of the CFC-tagged hM3Dq group was not caused by non-specific effects of CNO, stimulation of a random ensemble in the mPFC, nor by potential formation of an aversive association with the neutral context after vehicle treatment. Taken together, this shows that chemogenetic stimulation of CFC-tagged mPFC neurons was sufficient to induce memory expression at both recent and remote time-points after CFC.

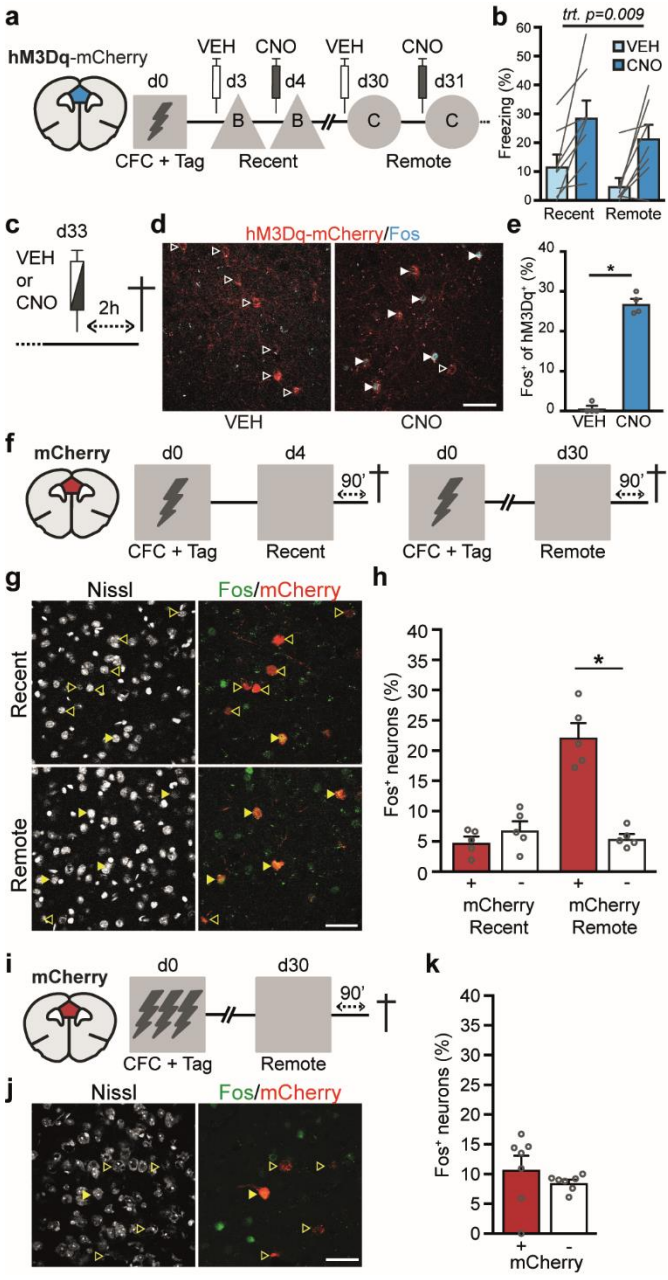

Figure 4. Stimulation and reactivation of CFC-tagged mPFC neurons. **a** Experimental design. mPFC neurons activated during CFC were tagged with hM3Dq-mCherry. Freezing levels were assessed after vehicle (VEH) and CNO treatment in context B (recent) and C (remote). **b** CNO-enhanced freezing at recent and remote time-points. Repeated measures ANOVA, treatment: $F_{(1,7)} = 13.1$, $p = 0.009$ (n = 8 mice). **c** On day 33, mice received VEH or CNO, remained in their home-cage and were perfused 2 h later. **d** hM3Dq-mCherry and Fos expression in mPFC after VEH or CNO treatment. White outlined arrowheads indicate hM3Dq-mCherry$^+$/Fos$^-$ cells; white filled arrowheads indicate hM3Dq-mcherry$^+$/Fos$^+$ cells. **e** Percentage of hM3Dq-mcherry$^+$ cells that express Fos after VEH or CNO. Mann-Whitney $U = 0$, $p = 0.017$ (n = 4 per treatment). **f** Experimental design. mPFC neurons were tagged with mCherry after CFC and re-exposed to the conditioning context 4 or 30 days later. **g** Example of colocalization of mCherry$^+$ and Fos$^+$ cells in the mPFC. Yellow outlined arrowheads indicate mCherry$^+$/Fos$^-$ cells;

yellow filled arrowheads indicate mCherry$^+$/Fos$^+$ cells. **h** Percentage of Fos$^+$ cells within the mCherry$^+$ and mCherry$^-$ populations. Two-way repeated measures ANOVA revealed a significant Time-point x Population interaction: $F_{(1,8)} = 93.601$, $p < 0.001$. Post-hoc Bonferroni test: Remote mCherry$^+$ *vs.* mCherry$^-$ *$p < 0.0001$; Recent mCherry$^+$ *vs.* Remote mCherry$^+$ $p < 0.0001$; Recent mCherry$^-$ *vs.* Remote mCherry$^+$ $p < 0.0001$; n = 5 per group. **i** mPFC neurons were tagged with mCherry after 3US CFC and re-exposed to the conditioning context 30 days later. **j** Example of colocalization of mCherry$^+$ and Fos$^+$ cells in the mPFC. Yellow outlined arrowheads indicate mCherry$^+$/Fos$^-$ cells; yellow filled arrowheads indicate mCherry$^+$/Fos$^+$ cells. **k** Percentage of Fos$^+$ cells within the mCherry$^+$ and mCherry$^-$ populations. Paired *t*-test: $t_6 = 1.186$, $p = 0.281$ (n = 7 mice). All bar graphs show means + s.e.m. Scale bars = 50 μm. Source data are provided as a Source Data file.

CFC-tagged neurons are reactivated during remote retrieval.

Although activity of mPFC neurons tagged after 1US CFC was required for remote memory expression only (Fig. 3a-d), chemogenetic stimulation of these cells was sufficient to evoke memory expression already at a recent time-point after CFC. This indicates that mPFC neurons can support recent fear memory. Therefore, we hypothesized that they may not causally contribute to recent memory retrieval, because they are not reactivated upon re-exposure to the conditioning context at this early stage. To study this, we expressed mCherry in neurons that were activated during CFC and then mice were re-exposed to the conditioning context either 4 or 30 days later (Fig. 4f). Ninety minutes after the memory test mice were sacrificed to study expression of Fos (induced by the test) in the mCherry$^+$ and mCherry$^-$ cell population (Fig. 4g). After recent retrieval, the percentage of Fos$^+$ neurons within the mCherry$^+$ and mCherry$^-$ population did not differ, indicating that reactivation of CFC-activated neurons occurred by chance at this time-point. In contrast, mCherry$^+$ neurons showed enhanced reactivation during retrieval of remote fear memory (Fig. 4h). Furthermore, we hypothesized that the lack of effect of chemogenetic suppression of tagged mPFC neurons after 3US CFC was due to reduced involvement of these cells in remote memory retrieval. Indeed, in mice that underwent 3US CFC, we found that CFC-tagged mPFC neurons were not reactivated above chance level during remote memory retrieval (Fig. 4i-k). Hence, this confirms that CFC-activated mPFC neurons were preferentially reactivated during remote, but not recent memory retrieval, and only following 1US conditioning.

Stimulation of remote memory-tagged neurons evokes freezing

CFC-activated neurons were not reactivated during recent retrieval, but this did not exclude the possibility that neurons activated during recent retrieval can also mediate expression of fear memory. To functionally investigate this, we determined whether chemogenetic stimulation of mPFC neurons tagged by recent and remote memory retrieval tests could subsequently evoke memory expression in a neutral context (Fig. 5a and c, respectively). After 1US CFC, mPFC neurons were tagged by re-exposing mice to the CFC context (no shock) on day 3 or 30 after training. CNO-induced stimulation of mPFC neurons tagged with hM3Dq during recent retrieval did not enhance freezing in a neutral context on day 6 and 31 after training (Fig. 5b). In contrast, chemogenetic stimulation of mPFC neurons tagged during remote retrieval (day 30) enhanced freezing on day 34 compared with the vehicle session on day 33 (Fig. 5d). Thus, in contrast to remote memory, mPFC neurons activated during recent memory retrieval likely do not encode conditioned-fear memory. Remarkably, a similar percentage of mPFC neurons was tagged after CFC and recent retrieval (6.9 ± 0.7% and 6.5 ± 0.9%, respectively; Supplementary Fig. 4), but less neurons were tagged after remote retrieval (3.6 ± 0.2%). Thus, despite the observation that during recent retrieval more mPFC neurons were tagged, these cells were not sufficient to enhance freezing behavior, whereas a smaller neuronal subset tagged during remote retrieval was sufficient to at least partially recover memory expression.

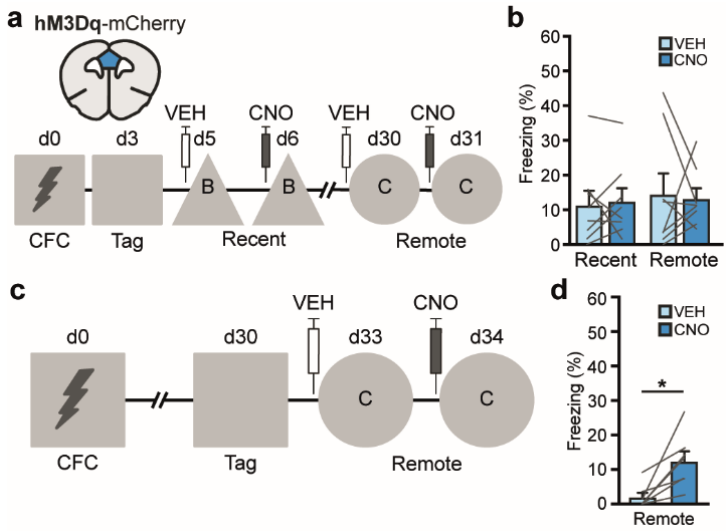

Figure 5. Stimulation of retrieval-tagged mPFC neurons. a Experimental design. mPFC neurons were tagged with hM3Dq-mCherry after recent retrieval in the CFC context and freezing was subsequently assessed in context B and C after VEH and CNO treatment. **b** Repeated measures ANOVA did not reveal differences in freezing levels between VEH and CNO sessions at both time-points (treatment: $F_{(1,7)}$ = 0.169, p = 0.69; n = 8 mice). **c** Experimental design. mPFC neurons were tagged with hM3Dq-mCherry after remote retrieval in the CFC context and freezing was subsequently assessed in context C. **d** CNO induced freezing compared with VEH. Paired t-test, t_6 = 3.56, *p = 0.012 (n = 7 mice). All bar graphs show means + s.e.m. Source data are provided as a Source Data file.

Remote memory depends on CREB function in CFC-tagged neurons

Lastly, we hypothesized that CREB signaling in mPFC neurons activated during 1US CFC is necessary for systems consolidation and memory persistence. To test this, we generated a Cre-dependent AAV encoding mutant CREB^{S133A} (AAV-hSyn::DIO-EGFP-mCREB), a well-established repressor of CREB-mediated gene transcription (*337, 347*). We first confirmed on day 4 after CFC that expression of mCREB was induced in mPFC neurons and controlled by 4TM (Fig. 6a, b). Notably, we found that mCREB expression was already detectable 24 h after CFC (Supplementary Fig. 5). Next, mCREB or mCherry was expressed in mPFC neurons activated during CFC and fear memory was assessed 4 or 30 days later (Fig. 6c). Expression of mCREB in CFC-tagged mPFC neurons did not alter freezing behavior during a recent memory test (Fig. 6d), but impaired freezing during the remote test (Fig. 6e). Generalization of contextual memory was not induced by mCREB as both groups showed similar low levels of freezing in a neutral context (Supplementary Fig. 6). CFC evoked mCREB expression in 6.8 ± 0.4% of mPFC neurons (Supplementary Fig. 6c), similar to with what we

observed 24 h after CFC (Supplementary Fig. 5) and with hM4Di (Fig. 2) and hM3Dq (Fig. 4, Chapter 3). As *Fos* transcription is regulated by phosphorylation of CREB at ser133 (*348*), we hypothesized that mCREB-expressing mPFC neurons should not show Fos induction after a remote memory test. Indeed, we found a complete segregation of mCREB^{+} and Fos^{+} cells after a remote test (Supplementary Fig. 7). Hence, disruption of CREB function in mPFC neurons activated during CFC induced a time-dependent impairment in conditioned freezing.

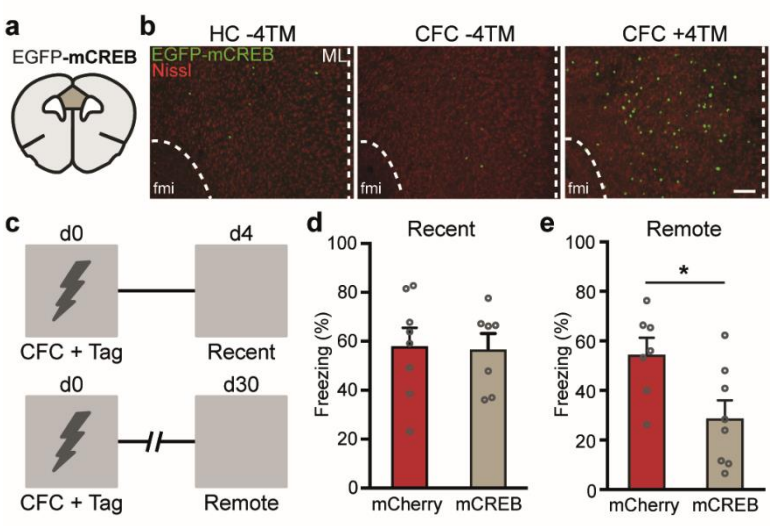

Figure 6. Disruption of CREB function in mPFC engram cells impairs remote fear memory. a Mice received AAV-Fos::CreER^{T2} combined with AAV-hSyn::DIO-EGFP-mCREB into the mPFC. **b** Representative expression of EGFP-mCREB in mPFC in mice that remained in their home-cage (HC -4TM) and mice that underwent CFC without and with 4TM treatment. Mice were sacrificed 4 days later. Scale bar = 100 µm. fmi = forceps minor of the corpus callosum. ML = midline. **c** Experimental design. mPFC neurons activated during CFC were tagged with EGFP-mCREB and memory was assessed on day 4 and 30 in the conditioning context. **d** On day 4, freezing did not differ between mCREB and control mice. Unpaired *t*-test: t_{13} = 0.159, p = 0.876. mCherry (n = 8), mCREB (n = 7). **e** Freezing was significantly reduced in the mCREB mice compared with control mice. Unpaired *t*-test: t_{13} = 2.669, *p = 0.019. mCherry (n = 7), mCREB (n = 8). All bar graphs show means + s.e.m. Source data are provided as a Source Data file.

Discussion

Using a viral-TRAP based approach, we demonstrate that contextual fear memory induced by a single US exposure is allocated to neuronal ensembles in the mPFC during memory encoding and that the activity of these specific neurons is subsequently necessary and sufficient for memory expression one month later. Chemogenetic suppression of a different similar sized "neutral" subset of neurons in the mPFC did not affect remote fear memory, confirming the selectivity of our tag approach and the memory-encoding specificity of activated neuronal ensembles in the mPFC. Strikingly, we found that mPFC ensembles were not involved in remote memory expression after strong (3US) fear conditioning.

Mounting evidence supports the involvement of learning-activated neuronal ensembles in subsequent memory expression (*119, 286, 315, 329*). For ensembles in the mPFC, this causality appears to be modulated by memory strength. It remains to be determined why mPFC ensembles do not contribute to the expression of a stronger fear memory, but our data is in line with a lack of effect of global prelimbic cortex inactivation on expression of a month-old fear memory when animals are conditioned with multiple foot-shocks (*44, 344*). Furthermore, we found that, compared with mild conditioning, strong conditioning induced more activated neurons in the BLA and Re, but not in the mPFC. A strong fear memory may therefore involve a relative increase in the contribution of the BLA and Re to systems consolidation. In support of this, the BLA mediates integration of foot-shock and contextual information (*121, 349*) and the Re has been implicated as a critical network hub in remote fear memory when mice received multiple foot-shocks during CFC (*344, 350*). We compared Fos expression after mild and strong CFC in a number of regions that have previously been implicated in the processing of contextual fear memory. This, however, does not exclude the possibility that neuronal activity in other regions than those we examined is enhanced during strong CFC and that additional regions are engaged in consolidation and retrieval of a strong fear memory (*350*). Therefore, we speculate that a strong fearful experience results in recruitment of a more extensive neuronal circuit, with the Re and BLA acting as critical hubs in this engram network. As a result of this broader circuit, the involvement of the mPFC ensemble that is activated during conditioning may be diminished, potentially reflecting a loss of top-down control by the mPFC after a severely aversive experience (*351*). In line with this reasoning, it was recently suggested that the mPFC is

engaged in the processing of conditioned fear when the threat level is low, but not when it the threat is high (*352*). Thus, our study indicates that the strength of an aversive learning experience affects the composition of ensembles that together form a persistent memory engram. Future research should provide insight in the circuitry that gates the recruitment of mPFC neurons that are activated during CFC in expression of remote fear memory.

Our observation that fear-encoding mPFC neurons after mild CFC were not reactivated during recent retrieval of contextual fear memory is in agreement with a recent study (*331*). However, this correlative evidence did not address the possibility that neurons activated during recent retrieval can also mediate conditioned freezing behavior. By tagging mPFC neurons that were activated during memory retrieval, we demonstrate that chemogenetic stimulation of neurons activated during remote retrieval can partially recover memory expression, whereas this is not true for neurons activated during recent retrieval. Together, this indicates that fear-encoding cells in the mPFC are not yet involved in memory retrieval evoked by the conditioning context at recent time-points after learning. Hence, the mPFC engram circuit may initially persist in a dormant state. Why mPFC engram cells are not required for recent memory retrieval remains currently unknown, but they may not be involved yet, because a network of engram cells in other brain regions controls memory expression at this stage. This early network is potentially dominated by the hippocampus, as hippocampal engram cells are critical for recall within the first week(s) after memory acquisition (*315, 329, 331*). Furthermore, systems consolidation by engram cells in cortical regions, such as the mPFC, is thought to require interaction between hippocampus and cortical modules (*78, 353*) and strengthening of connectivity between engram cells in different cortical regions in the first days to weeks after learning (*17*). These time-dependent processes may engage cortical engram cells to progressively contribute to memory expression.

Neuronal ensembles activated during mild CFC were preferentially reactivated during remote memory expression. Interestingly, we found that only a subset of the learning-activated neurons were reactivated, in line with previous reports (*315, 331, 354*). This could indicate refinement or contraction of the engram size over time (*355*). Alternatively, the partial reactivation of learning-activated cells might be explained by an overestimation of the number of neurons involved in encoding of the memory or by the possibility that memory

retrieval only requires reactivation of a subset of the engram population. The latter is in line with our observation that the size of the engram population tagged by remote memory retrieval was smaller than the population tagged by CFC, despite that CFC and remote retrieval activated a similar percentage of neurons in the mPFC (Supplementary Fig. 8). Potentially, expression of a molecular tag using viral-TRAP is only detectable when activation of the Fos promoter exceeds a certain threshold, which may have occurred only in the subset of engram cells that was reactivated during remote retrieval.

Although the precise molecular mechanisms that contribute to maturation of cortical networks supporting fear memory are yet unknown, to our knowledge, we provide the first evidence that CREB signaling in cortical engram cells is crucial for consolidation and subsequent remote memory expression. Our CREB intervention differs from previous studies in important aspects. Firstly, we disrupted CREB function selectively in cortical neurons that were activated during learning, instead of systemically (*335*), forebrain-wide (*337*) or non-discriminatively in the majority of neurons of a defined brain region (*336*). Secondly, previous reports show that manipulation of CREB function in a subset of neurons prior to fear learning affects the probability that these neurons will participate in encoding of an aversive or appetitive memory (*120, 338, 339*). In contrast, here the CREB repressor was induced after learning, and therefore endogenous selection defined the neurons that encoded the fear memory. The CREB-dependent changes in gene expression that support systems consolidation by engram cells in the mPFC remain to be determined, but they likely involve genes supporting synaptic and structural plasticity processes, as reported for other brain regions (*356-359*).

To conclude, we demonstrate that upon a mild fearful experience the fear memory is allocated to cortical neurons already during learning and is thus not gradually transferred from the hippocampus to the neocortex after the experience. Together, our data provide crucial insight into the spatiotemporal principles of memory consolidation in cortical networks and reveal that the strength of an aversive learning experience determines whether neuronal ensembles in the mPFC will function as an important network hub in expression of remote memory following a time- and CREB-dependent maturation process.

Methods

Animals

Male wild-type C57BL/6J mice aged 2-3 months at the start of experiments were individually housed on a 12 h light/dark cycle with food and water available *ad libitum*. Behavioral experiments were performed during the light phase and mice were randomly assigned to experimental groups. We have complied with all relevant ethical regulations for animal testing and research. All experimental procedures were approved by The Netherlands central committee for animal experiments (CCD) and the animal ethical care committee (DEC) of the Vrije Universiteit Amsterdam.

Constructs

The pAAV-Fos::CreER^{T2} plasmid was generated by replacing the coding sequence of tTA in pAAV-cFos-tTA-pA (gift from William Wisden, Addgene plasmid #66794) with the coding sequence of CreER^{T2} from pRetroQ-Cre-ERT2 (gift from Richard Youle, Addgene plasmid #59701) using SLiCE(*360*). Similarly, we used SliCE to replacing the coding sequence of mCherry in pAAV-hSyn-DIO-mCherry (gift from Brian Roth, Addgene plasmid #50459) with the sequence of EGFP-mCREB in pAAV-mCREB (gift from Eric Nestler, Addgene plasmid #68551) to produce pAAV-hSyn::DIO-EGFP-mCREB.

AAV vectors and stereotactic micro-injections.

AAV-Fos::CreER^{T2} (titer: 1.2 X 10^{13}) and Cre-dependent AAVs AAV-hSyn::DIO-hM3Dq-mCherry, AAV-hSyn::DIO-hM4Di-mCherry, AAV-hSyn::DIO-mCherry (titers: 5.0-6.0 X 10^{12}) and AAV-hSyn::DIO-EGFP-mCREB (titer: 3.0 X 10^{12}) were packaged as serotype 5 virus. For stereotactic micro-injections in the mPFC(*112*), mice first received 0.1 mg per kg Temgesic (RB Pharmaceuticals, UK) and were then anesthetized with isoflurane and mounted in a stereotactic frame. Lidocaine (2%, Sigma-Aldrich Chemie N.V, The Netherlands) was topically applied to the skull to provide local analgesia. A virus mixture of AAV5-Fos::CreER^{T2} and Cre-dependent AAV (ratio 1:500; AAV-Fos-CreER^{T2} was injected at a final titer of 2.4 X 10^{10}) was bilaterally injected in the mPFC (+1.8 mm AP; ±0.45 mm ML; -2.1 mm DV; relative to Bregma) using microinjection glass needles. Each hemisphere received 0.5 µL of the virus mixture at a flow rate of 0.1 µL per min followed by an additional 5 min to allow diffusion of the virus.

Animals remained in their home-cage for 3 weeks until the start of behavioral experiments.

Contextual Fear Conditioning (CFC)

Mice were first handled for three consecutive days. After an interval of 48 h, mice underwent CFC(*326, 327*). Conditioning was performed in a Plexiglas chamber with a stainless-steel grid floor inside a soundproof cabinet with continuous white noise (68 dB; Ugo Basil, Italy). The CFC context was cleaned with 70% ethanol between each trial. Mice were allowed to explore the CFC context for 120 s prior to the onset of a foot-shock (0.7 mA, 2 s). For 3US conditioning, mice received three foot-shocks (0.7 mA, 2s) with an interval of 60 seconds. All mice were returned to their home-cage 30 seconds after the last foot-shock. Context control groups were allowed to explore the CFC box for 150 s in absence of a foot-shock. Neutral context B (triangular shape, white plastic walls and floor) and C (round shape, white plastic walls and floor) differed in shape and texture and were cleaned with 2% acetic acid. Sessions in context B and C were performed by a different experimenter. During memory tests in context A, B or C, mice were allowed to explore the context for 2 min. Freezing behavior was analyzed by video tracking using Ethovision XT (Noldus, The Netherlands). Freezing bouts were defined as a lack of movement except respiration for at least 1.5 s.

4-hydroxytamoxifen (4TM) treatment

4TM (H6278, Sigma-Aldrich Chemie N.V, The Netherlands) was injected in an aqueous solution(*124*). First, 15 mg of 4TM was dissolved in 300 µL of DMSO (D8418, Sigma-Aldrich Chemie N.V, The Netherlands). The DMSO stock solution was then diluted in 2850 µl saline containing 2% Tween80 (P1754, Sigma-Aldrich Chemie N.V, The Netherlands) and once more in the same volume of saline. The final solution contained 2.5 mg per ml 4TM, 5% DMSO and 1% Tween80 in saline. Animals received 4TM (25 mg per kg, i.p.) 2 h after a “tag session” (see experimental design in figures).

Chemogenetic intervention

Clozapine N-oxide (CNO; BML-NS105, Enzo LifeSciences, Brussels) was dissolved in sterile saline. For hM4Di or hMD3q experiments, mice received 5 or 2 mg per kg (i.p.) CNO, respectively, 30 min before a test session.

Immunohistochemistry

Mice were transcardially perfused using ice-cold PBS pH 7.4, followed by ice-cold 4% paraformaldehyde (PFA) in PBS pH 7.4. Brains were removed, post-fixed overnight in 4% PFA solution and then immersed in 30% sucrose in PBS with 0.02% NaN_3. Brains were then sliced in 35 µm coronal sections using a cryostat and stored in PBS with 0.02% NaN_3 at 4°C until further use. Immunohistochemical stainings were performed using standard procedures (*112*), using the following antibodies: rabbit anti-Fos (1:500, sc52, Santa Cruz, USA), rabbit anti-RFP (1:1000, Rockland, USA) and NeuroTrace™ 500/525 Green Fluorescent Nissl Stain or NeuroTrace™ 530/615 Red Fluorescent Nissl Stain (1:400, ThermoFisher, USA). Sections were first rinsed in PBS and then incubated with blocking solution containing 5% normal goat serum, 2.5% bovine serum albumin and 0.25% Triton X in PBS at room temperature for 1 h. Primary antibodies were diluted in blocking solution and sections were incubated with primary antibody solution at 4° C overnight. Then, sections were rinsed in PBS and incubated with secondary antibodies dissolved in PBS for 2 h at room temperature. NeuroTrace™ for Nissl staining was added to the secondary antibody solution. Finally, sections were rinsed in PBS and mounted using 0.2% gelatin dissolved in PBS. Qualitative expression pictures were generated using a widefield fluorescence microscope (Leica Microsystems, DMi8). For quantification experiments, 6-8 z-stacks per animal were generated using a confocal microscope (Zeiss, LSM510) with the experimenter blinded to the treatment conditions. ImageJ software was used to extract the regions of interest (ROIs) of the cells stained with Nissl (Gaussian filter, Li threshold, watershed). Only ROIs within a predefined range for size (80-2000 square units; to exclude glial cells and non-specific staining) and circularity (0.5 to 1.0) were included. To account for the fact that (parts of the) cells were often present in 2 or 3 images of a z-stack, MATLAB (Mathworks) was used to group the ROIs that belonged to the same Nissl cell and then to count the total number of $Nissl^+$ cells in a z-stack. Cells expressing hM4Di-mCherry, hM3Dq-mCherry, EGFP-mCREB, mCherry or Fos were counted manually.

Electrophysiological recordings

Mice were swiftly decapitated and brains were extracted in ice-cold partial sucrose solution (70 mM NaCl, 2.5mM KCl, 1.25 mM NaH_2PO_4*H20, 5 mM $MgSO_4$*$7H_2O$, 1 mM $CaCl_2$*$2H_2O$, 70 mM Sucrose, 25 mM D-Glucose, 25 mM $NaHCO_3$, 1 mM Na-Ascorbate, 3 mM Na-Pyruvate, 7.4 pH, 300 mOsm) continuously gassed with

carbogen mixture (95% O_2, 5% CO_2). Acute 300 µm coronal slices containing the mPFC were generated using a vibrating microtome while the brain was submerged in carbogenated ice-cold partial sucrose solution. Slices were transferred in holding ACSF (125 mM NaCl, 3 mM KCl, 1.25 mM NaH_2PO_4* H_2O, 2 mM $MgCl_2$*$6H_2O$, 1.3 mM $CaCl_2$*$2H_2O$, 25mM D-Glucose, 25 mM $NaHCO_3$, 25 mM D-Glucose, 25 mM $NaHCO_3$, 1 mM Na-Ascorbate, 3 mM Na-Pyruvate, 7.4 pH, 300 mOsm), and left to recover at room temperature for at least 1 hour before recording. Subsequently, slices were transferred to a submerged recording chamber, and left to equilibrate for 10 min under continuous perfusion of 2 mL per min of carbogenated running ACSF (= holding ACSF with no Na-Ascorbate or Na Pyruvate and only 1 mM $MgCl_2$*$6H_2O$) supplemented with 10 µM CNQX. The mPFC was identified under visual guidance from differential interference contrast microscopy, and cells expressing either hM4Di-mCherry or mCherry were identified using a mercury-vapor lamp combined with an appropriate fluorescent filter. Whole cell recordings were conducted using borosilicate glass pipettes (2.5-5.5 MΩ) containing K-Gluconate based intracellular (70 mM K-Gluconate, 148 mM KCl, 10 mM Hepes, 4 mM Mg-ATP, 4 mM K2-phosphocreatinine, 0.4 mM GTP, at 280-290 mOsm, 7.2-7.3 pH). Upon establishing a stable giga seal, a step profile was generated from the patched cell, by injecting incrementally increasing current ranging from -100 pA to +300 pA at steps of 10 pA, for 750 ms. Baseline rheobase was assessed by injecting incrementally increasing current ranging from 0pA up to +400 pA at steps of 20 pA, for 2000 ms. Subsequently, running ACSF containing 50 µm CNO was perfused in, at a rate of approximately 2 mL per min, for at least 5 minutes, and the ramp and step profile protocols were performed once more. Recordings were acquired with pClamp software (Molecular Devices), using a Multiclamp 700B amplifier (Molecular Devices), sampled at 20 kHz low-pass filtered at 6 kHz, and digitized with an Axon Digidata 1440A (Molecular Devices).

Statistical analyses

Statistical details are presented in the figure legends. Number of animals and number of cells are shown as n. Mice with virus misplacements (in total: hM4Di-mCherry = 6; hM3Dq-mCherry = 5; mCherry = 5; EGFP-mCREB = 1) were excluded from analysis. All graphs show means + s.e.m. SPSS software (IBM) was used for statistical analysis of all data. Comparisons between and within groups were made using two-tailed unpaired or paired Student's *t*-test, respectively. When the data was not modeled by a normal distribution,

it was subjected to non-parametric Mann Whitney U test for between group comparisons and Wilcoxon signed rank test for within group comparisons. In case of comparisons that involved more than two groups, analyses were performed by One-way ANOVA followed by post-hoc Bonferroni test. In case of more than two within group comparisons, a Repeated measures ANOVA was used. Significance was set at $p < 0.05$.

Supplementary Information

Figures and legends

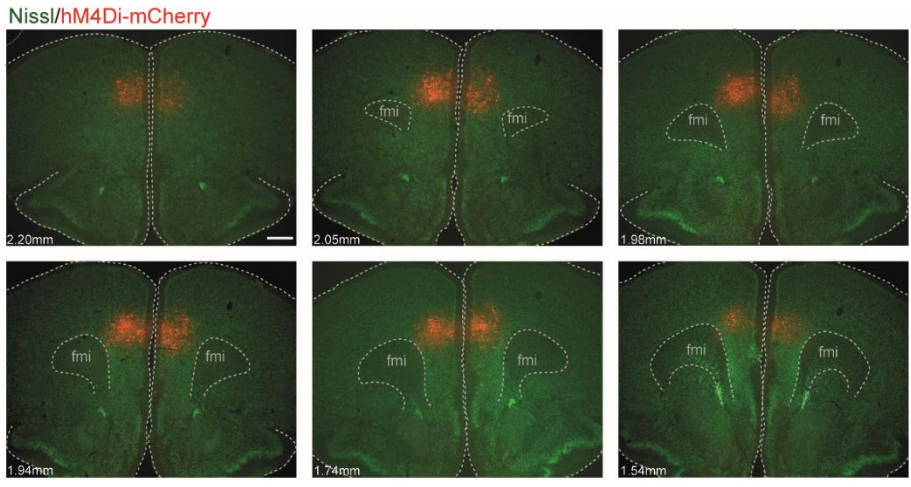

Supplementary Figure 1. Representative example of hM4Di-mCherry expression in the mPFC after CFC and 4TM treatment. A mixture of AAV-Fos::CreER^{T2} and AAV-hSyn::DIO-hM4Di-mCherry was injected into the dorsal region of the mPFC. Tagged neurons expressing hM4Di-mCherry (red) were observed along the entire rostro-caudal axis of the dorsal mPFC. In the bottom right of each image, coordinates relative to Bregma are shown based on the Paxinos and Watson mouse brain atlas. Scale bar = 500 μm. fmi = forceps minor of the corpus callosum.

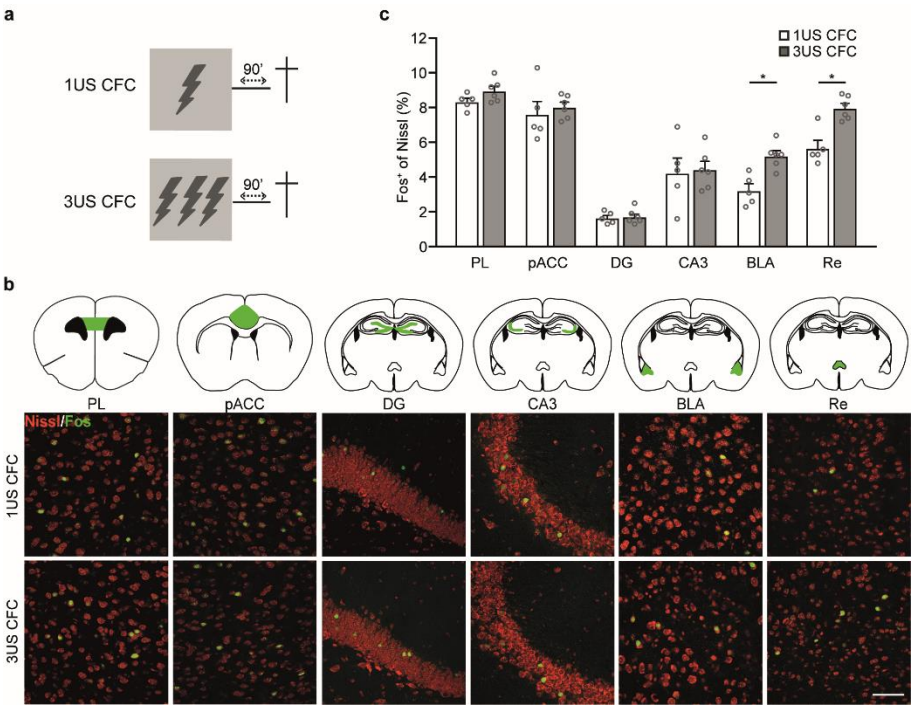

Supplementary Figure 2. Fos expression after 1US and 3US CFC. **a** Left: experimental design. 1US CFC (n = 5 mice); 3US CFC (n = 6 mice). **b** Top: illustration of a coronal brain section indicating the region (green) where Fos$^+$ neurons were analyzed. Bottom: representative examples of Nissl$^+$ (red) and Fos$^+$ cells (green). Scale bar = 50 µm. **c** Percentage of Fos$^+$ cells in each region. Unpaired *t*-test: BLA $t_9 = 4.164$, $^*p = 0.0024$; Re $t_9 = 4.526$, $^*p = 0.0014$. All bar graphs show means + s.e.m. Source data are provided as a Source Data file.

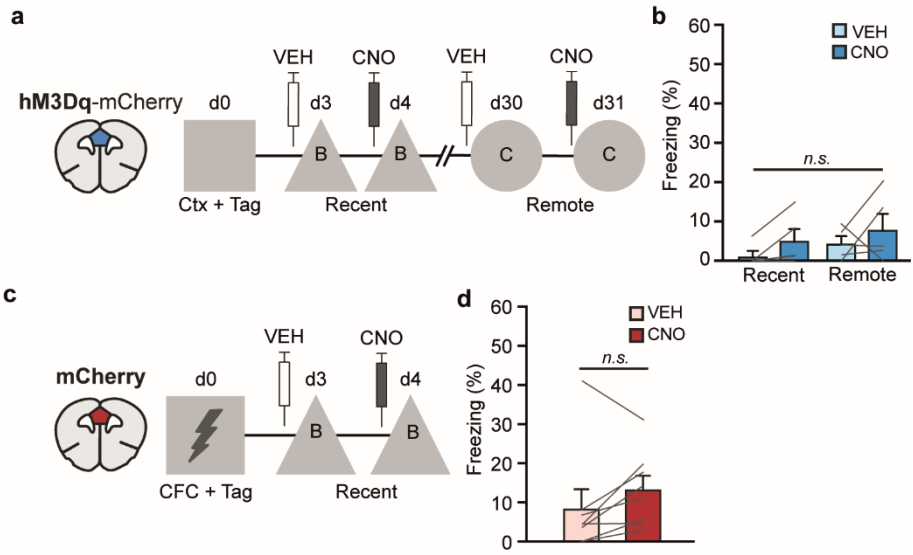

Supplementary Figure 3. Stimulation of mPFC neurons in control mice did not enhance freezing. **a** Experimental design. On d0, neurons activated during exploration of a neutral context in the absence of a foot-shock were tagged with hM3Dq-mCherry. Changes in freezing levels were assessed during vehicle (VEH) or CNO sessions in either context B (recent) or Context C (remote). **b** No changes were observed after CNO administration when compared to VEH at both time points. Repeated measures ANOVA: $F_{(1,4)}$ =

2.117, $p = 0.184$ (n = 5 mice). Note that not all individual data points are visible as several animals did not show freezing behavior. **c** Neurons activated during CFC were tagged with mCherry. Freezing levels were assessed after VEH and CNO treatment in context B. **d** CNO did not enhance freezing compared with VEH. Paired *t*-test, $t_7 = 1.786$, $p = 0.117$ (n = 8 mice). Bar graphs show mean + s.e.m. Source data are provided as a Source Data file.

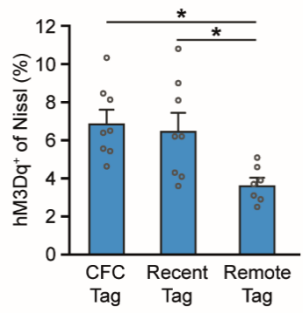

Supplementary Figure 4. Number of hM3Dq⁺ neurons in CFC- and retrieval-tagged experimental groups. 'CFC Tag' reflects the group presented in Fig. 4a, b (n = 8 mice). 'Recent Tag' reflects the group presented in Fig. 5a, b (n = 8 mice). 'Remote Tag' reflects the group presented in Fig. 5c, d (n = 7 mice). One-way ANOVA $F_{(2,20)} = 5.95$, $p = 0.009$. Post-hoc Bonferroni test: CFC tag *vs.* Remote tag $^*p = 0.014$; Recent tag *vs.* Remote tag $^*p = 0.033$. Bar graph shows means + s.e.m. Source data are provided as a Source Data file.

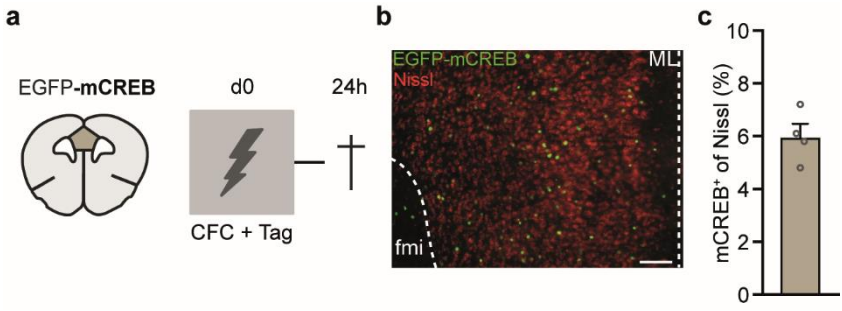

Supplementary Figure 5. EGFP-mCREB was detectable 24 h after CFC. **a** Neurons activated during CFC were tagged with EGFP-mCREB and mice were perfused 24 h later. **b** Representative image of EGFP-mCREB⁺ neurons in mPFC. Scale bar = 100 µm. fmi = forceps minor of the corpus callosum. ML = midline. **c** Percentage of mCREB⁺ neurons 24 h after CFC (n = 4 mice). Bar graph shows mean + s.e.m. Source data are provided as a Source Data file.

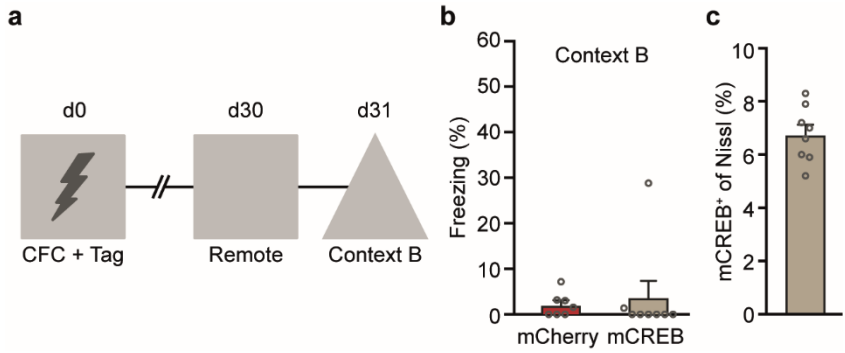

Supplementary Figure 6. EGFP-mCREB expression in CFC-tagged neurons did not induce expression of generalized fear. **a** Experimental outline. mPFC neurons activated during CFC were tagged with EGFP-mCREB and remote memory was first assessed on day 30 in the CFC context (see Figure 6) and subsequently on day 31 in a neutral context B. **b** Both groups showed similar, very low levels of freezing in context B. Mann-Whitney U test: U = 19, p = 0.276. **c** Percentage of CFC-tagged mPFC neurons expressing EGFP-mCREB. Bar graphs show mean + s.e.m. Source data are provided as a Source Data file.

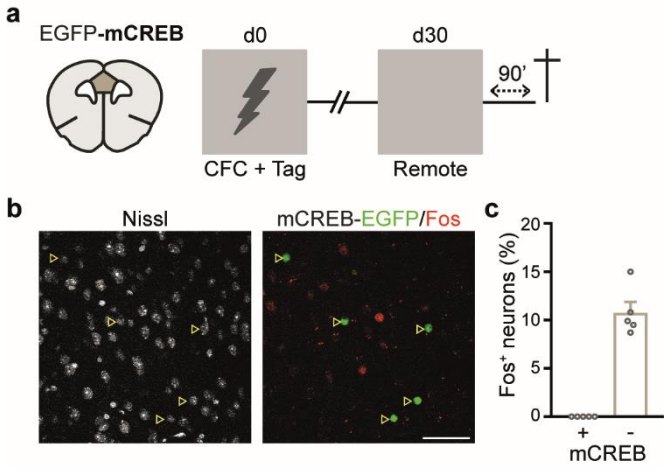

Supplementary Figure 7. Remote memory retrieval did not induce Fos expression in mCREB$^+$ neurons. **a** Experimental design. Neurons activated during CFC were tagged with EGFP-mCREB and mice were subsequently perfused after a re-exposure to the conditioning context on day 30 after training. **b** Example of mCREB$^+$ and Fos$^+$ cells within the total population of mPFC neurons (Nissl$^+$). Yellow outlined arrowheads indicate mCREB$^+$/Fos$^-$ cells. **c** Percentage of Fos$^+$ cells within the mCREB$^+$ and mCREB$^-$ population. Bar graph shows mean + s.e.m. Source data are provided as a Source Data file.

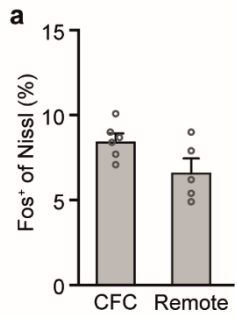

Supplementary Figure 8. The percentage of Fos$^+$ neurons did not significantly differ after CFC and remote memory retrieval. Fos expression was analyzed in mice that were perfused after 1US CFC or after re-exposure to the conditioning context at day 30 following 1US CFC. Data of the CFC group was copied from Figure 1c. Data of the remote group was derived from the reactivation experiment shown in Figure 4f-h. *n.s.* = not significant. Bar graph shows mean + s.e.m. Source data are provided as a Source Data file.

Acknowledgements

The authors thank Yvonne Gouwenberg for AAV packaging and Lizz Fellinger, Lineke Ouwerkerk, Flora Nelissen and Ioannis Koutlas for assistance with immunohistochemical stainings and imaging. This study was funded by EU MSCA-ITN CognitionNet (FP7-PEOPLE-2013-ITN 607508) to M.R.M., ZonMw VENI grant (916.12.034) to M.C.v.d.O. and VIDI grant (016.168.313) to E.V. and M.C.v.d.O., Amsterdam Neuroscience PoC grant (8-PoC-CIA-2017) to M.C.v.d.O., NWO Veni grant (016.171.033) to P.R-R., and a ZonMw TOP grant (91215030).

Author contributions

Conceptualization, M.R.M., P.R-R., A.B.S., M.C.v.d.O.; Methodology, M.R.M., R.Z., M.C.v.d.O.; Software, T.G.; Formal analysis, M.R.M., I.K., M.C.v.d.O.; Investigation, M.R.M., E.V., I.K., R.J.v.d.L; Resources, H.D.M.; Writing – original draft, M.R.M., P.R-R., A.B.S., M.C.v.d.O.; Supervision, A.B.S., M.C.v.d.O.; Funding acquisition, P.R-R., A.B.S., M.C.v.d.O.

Chapter 5

Extinction of cocaine memory depends on a feed-forward inhibition circuit within the medial prefrontal cortex

Esther Visser[1,#], Mariana R. Matos[1,#], Miodrag Mitrić[1,#], Ioannis Kramvis[1], Rolinka J. van der Loo[1], Huibert D. Mansvelder[2], August B. Smit[1] and Michel C. van den Oever[1]

[1]Department of Molecular and Cellular Neurobiology, Center for Neurogenomics and Cognitive Research, Amsterdam Neuroscience, Vrije Universiteit Amsterdam, 1081 HV, The Netherlands
[2]Department of Integrated Neurophysiology, Center for Neurogenomics and Cognitive Research, Amsterdam Neuroscience, Vrije Universiteit Amsterdam, 1081 HV, The Netherlands
[#]These authors contributed equally

Biological Psychiatry, provisionally accepted

Abstract

Cocaine-associated environments (*i.e.,* contexts) evoke persistent memories of cocaine reward and thereby contribute to the maintenance of addictive behavior in cocaine users. From a therapeutic perspective, enhancing inhibitory control over cocaine seeking is of pivotal importance, but requires a more detailed understanding of the neural circuitry that can suppress context-evoked cocaine memories, *e.g.,* through extinction learning. The ventral and dorsal medial prefrontal cortex (vmPFC and dmPFC) are thought to bidirectionally regulate conditioned cocaine seeking through their projections to other brain regions. However, whether these mPFC subregions interact to enable adaptive responding to cocaine-associated contextual stimuli has remained elusive.

We used antero- and retrograde tracing combined with chemogenetic intervention to examine the role of vmPFC-to-dmPFC projections in extinction of cocaine memory in mice. In addition, electrophysiological recordings and optogenetics were used to determine whether Parvalbumin-expressing inhibitory interneurons (PV-INs) and pyramidal neurons (PNs) in the dmPFC are innervated by vmPFC projections.

We found that vmPFC-to-dmPFC projecting neurons are activated during unreinforced re-exposure to a cocaine-associated context and selective suppression of these cells impairs extinction learning. PV-INs in the dmPFC receive stronger monosynaptic excitatory input from vmPFC projections than PNs, consequently resulting in disynaptic inhibition of PNs. In line with this, we show that chemogenetic suppression of dmPFC PV-INs impairs extinction learning.

Our data reveal that vmPFC projections mediate suppression of context-evoked cocaine memory through recruitment of feed-forward inhibition in the dmPFC, thereby providing a novel neuronal substrate that promotes extinction-induced inhibitory control.

Introduction

Persistently recurring memories of cocaine reward interfere with the ability of chronic cocaine users to abstain from cocaine intake. It is well-established that locations where cocaine is repeatedly used (*e.g.* drug houses or clubs) become strongly associated with the rewarding effects of cocaine and re-exposure to these cocaine contexts during prolonged periods of abstinence triggers retrieval of cocaine memory and thereby promotes relapse (*361*). The salience of cocaine-associated contextual cues can be reduced by prolonged cue exposure in absence of cocaine reward, a process called extinction learning (*58*). However, cue exposure therapies have been largely unsuccessful in treatment of substance use disorders (*362*). Therefore, it is crucial to elucidate the neuronal circuitry that promotes suppression of behavioral responding to cocaine-contextual cues, with the ultimate goal to facilitate the design of therapeutic interventions that can strengthen inhibitory control over cocaine seeking behavior.

The medial prefrontal cortex (mPFC) has been implicated in cue-induced craving in humans (*257*) and cocaine seeking in animal models (*70*). Specifically, the dorsal mPFC (dmPFC) is thought to drive conditioned cocaine seeking via projections to the nucleus accumbens (NAc) core (*363, 364*). The ventral mPFC (vmPFC) has a more complex role, as it is able to promote cocaine seeking (*260, 365*), as well as inhibit conditioned responses after extinction learning (*56, 112, 365*). Projections of the vmPFC to the NAc shell mediate the effect of extinction-induced inhibitory control (*365, 366*). Thus, both the dmPFC and vmPFC have a critical role in conditioned cocaine seeking, but have thus far been considered to function as separate hubs in parallel circuits that regulate this behavior. Recent studies point to reciprocal connectivity between the vmPFC and the dmPFC (*50, 67, 68, 122*). However, how this intrinsic mPFC connectivity contributes to adaptive responding to cocaine-associated stimuli has remained poorly understood.

To this end, we anatomically and physiologically dissected vmPFC-to-dmPFC projections and investigated whether this circuit modulates extinction of responding to a cocaine-associated context. We found that vmPFC projections innervate Parvalbumin-expressing interneurons (PV-INs) in the dmPFC, resulting in disynaptic inhibition of dmPFC pyramidal neurons (PNs). Furthermore, vmPFC-to-dmPFC neurons were preferentially activated during unreinforced re-exposure to a cocaine-associated context and selective suppression of vmPFC-to-dmPFC projecting neurons or direct suppression of dmPFC PV-INs

impaired extinction of context-evoked cocaine memory, confirming the critical contribution of this circuit to extinction learning.

Results

Identification of vmPFC-to-dmPFC projecting neurons

We previously found that non-selective optogenetic stimulation or inhibition of vmPFC pyramidal neurons (PNs) facilitates or impairs, respectively, extinction of cocaine memory three weeks after conditioning (*112*). We now aimed to identify the neuronal target of vmPFC PN projections that promote extinction learning. To anatomically trace projections of vmPFC PNs, we unilaterally expressed *CaMKIIα* promoter-driven Channelrhodopsin (ChR2) fused to Enhanced Yellow Fluorescent Protein (EYFP) in the vmPFC of mice and observed EYFP$^+$ axonal fibers in the ipsi- and contralateral dmPFC (Figure 1a). Layer 5/6 of the dmPFC exhibited the highest density of EYFP$^+$ fibers. We then applied retrograde viral tracing by injecting retroAAV-*hSyn*::Cre in the dmPFC and Cre-dependent AAV-*hSyn*::DIO-mCherry in the contralateral vmPFC. This revealed a population of vmPFC-to-dmPFC projecting neurons (Figure 1b). Axonal fibers of were observed in the corpus collosum, indicating that they ran via the ipsilateral forceps minor of the corpus collosum (fmi) through the corpus collosum and then back through the contralateral fmi to terminate in the dmPFC (Figure 1c). The vmPFC heavily innervates the NAc shell (*112*) and projections to this region have been implicated in extinction of cocaine seeking (*365, 366*). Therefore, we questioned whether vmPFC neurons that project to the dmPFC have collateral projections to the NAc shell. Whereas dense mCherry$^+$ axonal fibers were observed in the dmPFC after retrograde labelling, very sparse mCherry$^+$ fibers were observed in the NAc shell (Figure 1d), suggesting that vmPFC neurons that project to the dmPFC and NAc shell overlap to a small extend only. To confirm this, we retrogradely labeled vmPFC neurons by injection of Cholera Toxin B (CTB)-488 or CTB-555 in the NAc shell and dmPFC, respectively (Figure 1e). We examined colocalization in the contralateral vmPFC to exclude the possibility that neurons in the ipsilateral vmPFC were labeled as a result of CTB injection in the adjacent dmPFC and/or NAc shell. Of the vmPFC-to-dmPFC projecting neurons (CTB-555$^+$), 9.96 ± 4.8% (mean ± s.e.m.) was also CTB-488$^+$ (Figure 1f). Inversely, only 5.54 ± 2.1% of the vmPFC-to-NAc shell projecting neurons (CTB-488$^+$) was CTB-555$^+$. Hence, vmPFC neurons that project to the dmPFC and NAc shell represent largely distinct populations.

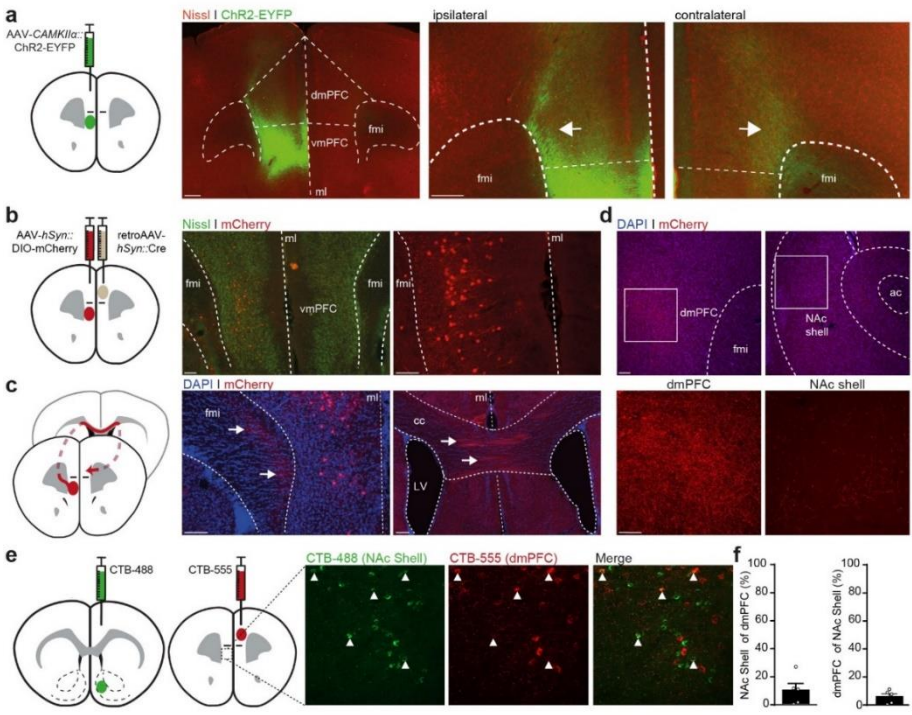

Figure 1. Identification of vmPFC-to-dmPFC projecting neurons. a AAV-*CaMKII*α::ChR2-EYFP was injected into vmPFC. EYFP$^+$ vmPFC terminals were present in the ipsi- and contralateral dmPFC. Scalebar: 250 µm. **b** After retroAAV-*hSyn*::Cre injection into the dmPFC and Cre-dependent AAV-*hSyn*::DIO-mCherry into the contralateral vmPFC, retrogradely labelled mCherry$^+$ cells were observed in the vmPFC. Scalebars: 100 µm. **c** Trajectory of retrogradely labelled contralateral projections (mCherry$^+$). Axonal fibers (arrows) were present in the forceps minor (fmi; right top panel) and the corpus callosum (cc; right bottom panel). ml = midline, LV = lateral ventricle. Scalebars: 100 µm. **d** Example of mCherry$^+$ axonal fibers of vmPFC neurons in the dmPFC and NAc shell. Boxed areas (top) indicate region imaged at higher magnification (bottom). Contralateral retrograde labeling n = 3; Bilateral retrograde labeling n = 3. ac: anterior commissure. Scalebar top: 100 µm; bottom: 50 µm. **e** CTB-488 was injected into NAc shell and CTB-555 in the dmPFC (n = 5 mice). CTB-488$^+$ and CTB-555$^+$ neurons were observed and quantified in the vmPFC. Arrowheads indicate colocalization. Scalebar: 50 µm. **f** Colocalization of NAc shell-projecting neurons within the dmPFC-projecting population (left) and vice versa (right). All graphs show mean ± s.e.m.. CTB-488, cholera toxin subunit B conjugated with Alexa Fluor 488; CTB-555, CTB conjugated with Alexa Fluor 555; dmPFC, dorsal medial prefrontal cortex; vmPFC, ventral medial PFC; NAc, nucleus accumbens.

vmPFC-to-dmPFC projecting neurons mediate extinction of cocaine memory

We next assessed whether vmPFC-to-dmPFC projecting cells are activated upon re-exposure to a cocaine-associated context. Mice were conditioned to associate one of two distinct contexts with cocaine reward and after three weeks of forced abstinence, they showed a strong preference to explore the previously cocaine-paired context over the neutral (saline-paired) context (Figure 2a). Unreinforced re-exposure to the cocaine and neutral context on the day before the test reduced preference for the cocaine context (Figure 2a) (*112*), pointing to successful extinction learning. Next, independent groups underwent conditioning and were re-exposed to the cocaine-associated context in the presence (no extinction) or absence (extinction) of cocaine reinforcement (Figure 2b). Ninety minutes later, animals were sacrificed to examine colocalization of the neuronal activity marker Fos and retrogradely labelled mCherry$^+$ vmPFC-to-dmPFC projecting neurons (Figure 2c). Both groups showed a similar percentage of Fos$^+$ and mCherry$^+$ neurons in the vmPFC, but mCherry and Fos preferentially colocalized in mice that did not receive cocaine before the last session (Figure 2d), suggesting that the vmPFC-to-dmPFC projecting neuronal population is activated during extinction learning. Additionally, we found that Fos colocalized more with vmPFC-to-dmPFC projecting neurons after unreinforced exposure to the cocaine context compared with a novel context (Figure S1).

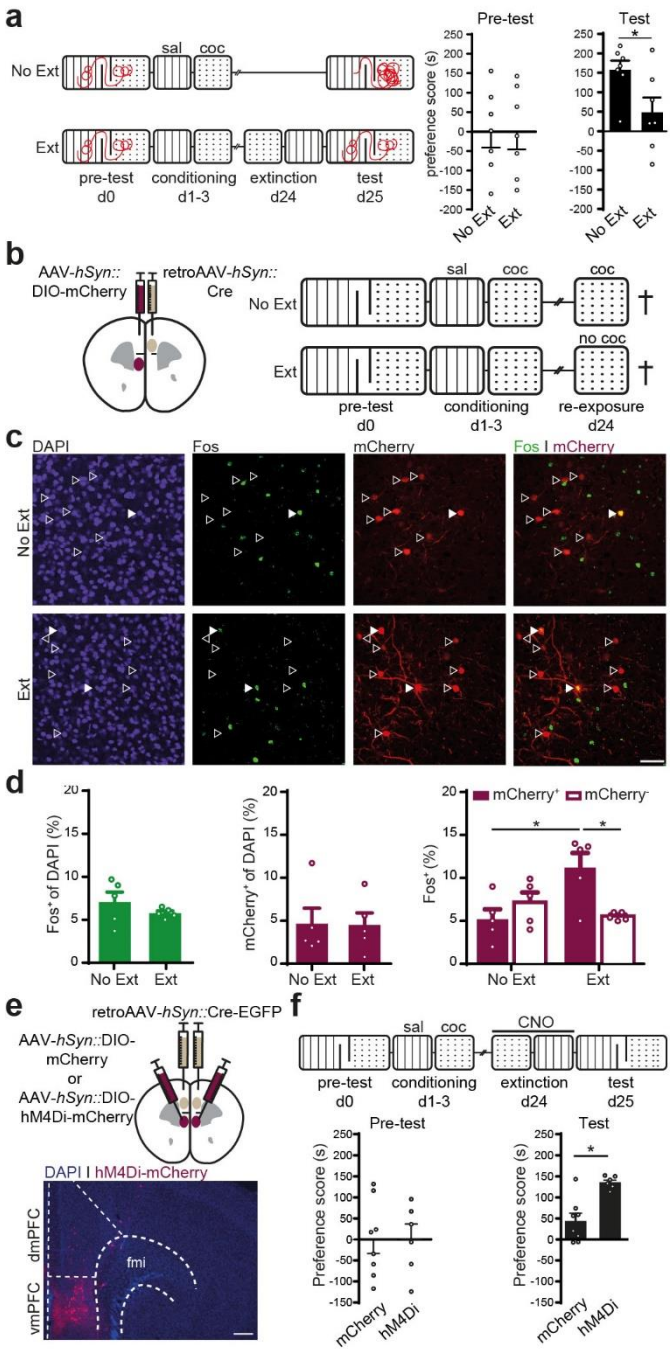

Figure 2. vmPFC-to-dmPFC projecting neurons mediate extinction of cocaine memory. a Experimental design of the conditioning paradigm. sal = saline, coc = cocaine. Red lines depict fictional trajectories of mice during tests. On day 24, animals remained in their home cage (No Ext; n = 7) or underwent extinction training (Ext; n = 7) through unreinforced re-exposure to the saline and cocaine context. On day 25, preference for the cocaine context was reduced in the Ext compared to the No Ext group (t_{12} = 2.417, P = 0.033). **b** Mice with retrogradely labelled vmPFC-to-dmPFC projecting neurons underwent conditioning. On day 24, animals were re-exposed to the cocaine context for 15 min in the presence (No Ext; n = 5) or absence (Ext; n = 5) of cocaine reinforcement. **c** Representative images of DAPI, Fos and mCherry expression in the vmPFC. Scalebar: 50 µm. **d** Percentage of Fos$^+$ and mCherry$^+$ neurons did not differ between groups. In the Ext. group, Fos colocalized more with the mCherry$^+$ than mCherry$^-$ population (Population x Group interaction $F_{1,8}$ = 8.86, *P = 0.018; post-hoc Fos$^+$/mCherry$^+$ No Ext *vs.* Ext t_{16} = 3.58, *P = 0.005; post-hoc Fos$^+$/mCherry$^+$ *vs.* Fos$^+$/mCherry$^-$ Ext

group $t_8 = 3.12$, $^*P = 0.028$). **e** Top: hM4Di-mCherry ($n = 6$) or mCherry ($n = 8$) was bilaterally expressed in vmPFC-to-dmPFC projecting neurons. Bottom: representative example of hM4Di-mCherry expression in vmPFC. **f** Top: experimental design. Mice received CNO before extinction training. Test: preference for the cocaine context was higher in hM4Di-mCherry mice than controls (U = 44, $^*P = 0.008$). All graphs show mean ± s.e.m.

To determine whether this projection is necessary for extinction learning, we retrogradely expressed the inhibitory DREADD hM4Di fused to mCherry or mCherry alone (control) in vmPFC-to-dmPFC projecting neurons (Figure 2e). One day after chemogenetic suppression during extinction training, preference for the cocaine context was diminished in control mice, whereas hM4Di mice still showed a robust preference to explore the cocaine context (Figure 2f). Hence, vmPFC-to-dmPFC projecting neurons are activated upon unreinforced re-exposure to a cocaine-associated context, and accordingly, are required for extinction learning.

vmPFC projections evoke strong monosynaptic excitation of dmPFC PV-INs and disynaptic inhibition of PNs

Global optogenetic stimulation of the vmPFC reduces firing of dmPFC PNs (*66*), suggesting that vmPFC PNs may target local GABAergic interneurons. Furthermore, dmPFC PV-INs facilitate extinction of natural reward seeking (*367*) and conditioned fear (*77*). We found that PV-INs comprise the majority (~66%) of GABAergic neurons in the dmPFC and are most abundant in dmPFC layers 5/6 (Figure S2), where we also observed the highest density of vmPFC axons (see Figure 1a). Based on this, we determined whether vmPFC projections inhibit dmPFC PNs via innervation of PV-INs in this region. Expression of ChR2-EYFP in vmPFC PNs revealed $EYFP^+$ puncta on somata and dendrites of PV-INs in the dmPFC (Figure 3a). To determine whether these puncta reflect functional synapses and to compare the strength of innervation of dmPFC PV-INs and PNs, we used *PV::Cre* mice to label dmPFC PV-INs with mCherry and expressed ChR2-EYFP in vmPFC PNs (Figure 3b). PNs and PV-INs were distinguished based on mCherry expression and electrophysiological profiles (Figure S3a-i). Upon optic stimulation of $ChR2^+$ vmPFC terminals, we measured evoked excitatory and inhibitory postsynaptic currents (eEPSCs and eIPSCs, respectively) in dmPFC PV-INs and PNs using whole-cell electrophysiological recordings (Figure 3c, 3d and S3j). Evoked

excitatory drive was strongest onto dmPFC PV-INs (Figure 3E and S3K), whereas evoked inhibitory drive was strongest onto dmPFC PNs (Figure 3f and S3l). In neurons exhibiting both excitatory and inhibitory responses (12/15 PNs; 8/9 PV-INs), the eEPSC/eIPSC (E/I) ratio robustly favored excitation of dmPFC PV-INs (Figure 3g and S3m). The latency to onset of eEPSCs was shorter than of eIPSCs in PNs and PV-INs (Figure 3h and S3n), suggestive of monosynaptic excitation and disynaptic inhibition. In support of this, application of the AMPA/kainate receptor antagonist CNQX abolished both eEPSCs and eIPSCs (Figure 3i and 3j), whereas $GABA_A$ receptor blockade by Gabazine only affected eIPSCs (Figure 3k), demonstrating that glutamate release initiated both evoked responses. Gabazine applied together with CNQX and the NMDA receptor antagonist D-AP5 prevented the residual eEPSC (Figure 3k). In line with this, both responses were also abolished by tetrodotoxin (TTX; Figure S3o and S3p) and co-application of the potassium channel blocker 4-aminopyridine (4-AP (*175*)) recovered the eEPSCs only (Figure S3q), further confirming the monosynaptic and disynaptic nature of the excitatory and inhibitory response, respectively.

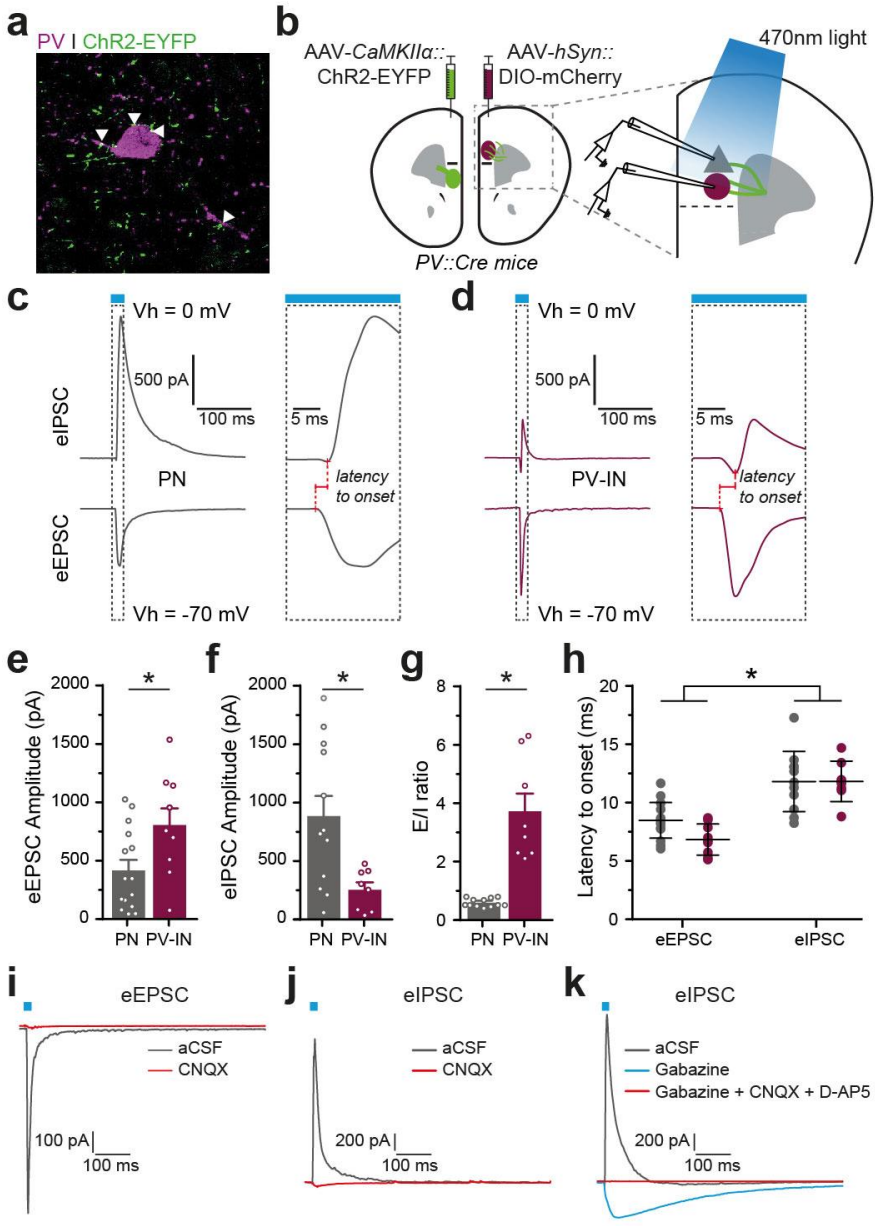

Figure 3. vmPFC projections evoke strong monosynaptic excitation of dmPFC PV-INs and disynaptic inhibition of PNs. a After AAV-*CaMKIIα*::ChR2-EYFP injection into the vmPFC, ChR2-EYFP$^+$ puncta (arrowheads) were detected on PV$^+$ cells in the dmPFC. **b** Experimental design. ChR2-EYFP was expressed in vmPFC PNs and mCherry in PV-INs in the dmPFC. Whole-cell recordings were obtained from dmPFC PNs and PV-INs upon optic stimulation of ChR2$^+$ terminals. **c,d** Representative eIPSC (top) and eEPSC (bottom) traces in PNs (C) and PV-INs (D) in response to a blue light pulse (20 ms, blue line). The initial downward peak in the eIPSC trace of PV-IN represents a residual excitatory current at Vh 0 mV. Vh = holding potential. **e** eEPSC amplitude was higher in PV-INs than PNs (t_{22} = 2.38, P = 0.026; PN N/n = 15/6, PV-IN N/n = 9/6). **f** eIPSC amplitude was higher in PNs than PV-INs ($t_{13.49}$ = 3.34, *P = 0.005; PN N/n = 12/6, PV-IN N/n = 8/6). **g** eEPSC/eIPSC ratio was higher in PV-INs than PNs ($t_{7.06}$ = 5.11; *P = 0.001; PN N/n = 12/6, PV-IN N/n = 8/6). **h** Latency to onset was lower for eEPSCs than eIPSCs in both cell-types ($F_{1,39}$ = 50.93, *P < 0.001). **I,j** PN recording demonstrating that CNQX (10 μM) abolished eEPSCs (i) and eIPSCs

(j) upon optic stimulation (20 ms pulse, blue line) of vmPFC terminals. **k** Application of Gabazine (10 μM) abolished eIPSCs and co-application of CNQX (10 μM) and D-AP5 (10 μM) blocked the residual eEPSC at a holding potential of 0 mV. All graphs show mean ± s.e.m.. eEPSC, evoked excitatory postsynaptic current; eIPSC, evoked inhibitory PSC. PV-IN, parvalbumin-expresing interneurons; PN, pyramidal neuron.

dmPFC PV-INs mediate feed-forward inhibition and extinction of cocaine memory

To determine whether the disynaptic inhibitory response in PNs is evoked by excitation of PV-INs, we expressed hM4Di-mCherry in dmPFC PV-INs and ChR2-EYFP in vmPFC PNs (Figure 4). PN responses to optic stimulation of ChR2$^+$ vmPFC terminals were recorded before and after CNO-mediated suppression of PV-INs (Figure 4b-c). CNO did not alter the EPSC amplitude (Figure 4d), but reduced the eIPSC amplitude in dmPFC PNs (Figure 4e). Consequently, the E/I ratio shifted towards less inhibition (Figure 4f), confirming that disynaptic inhibition of dmPFC PNs is at least partially mediated by excitation of PV-INs. CNO similarly suppressed disynaptic inhibition of PV-INs (Figure S4). Finally, we determined whether activity of dmPFC PV-INs is necessary to extinguish preference to explore a cocaine-associated context. In *PV::Cre* mice, hM4Di-mCherry or mCherry alone (control) was expressed in the majority of dmPFC PV-INs (Figure 4g-i). Following chemogenetic suppression of PV-INs during extinction training, hM4Di animals showed stronger preference for the cocaine context than control mice (Figure 4j), confirming that extinction learning requires activity of these neurons

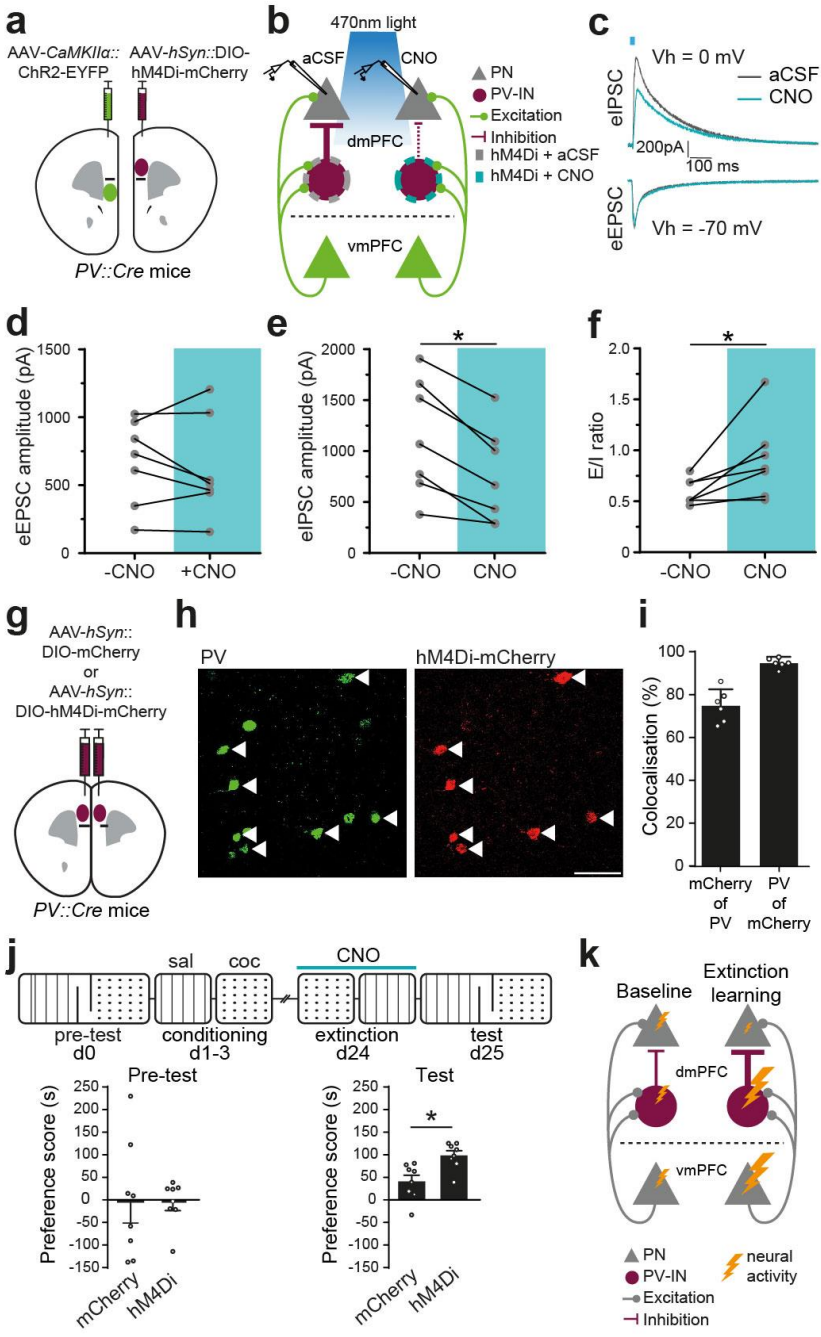

Figure 4. dmPFC PV-INs mediate feed-forward inhibition and extinction of cocaine memory. a In *PV::Cre* mice, ChR2-EYFP was expressed in vmPFC PNs and hM4Di-mCherry in dmPFC PV-INs. **B** Experimental design and hypothetical effect of chemogenetic suppression of PV-INs on vmPFC-mediated inhibition of PNs. **c** Representative traces at baseline (black) or after CNO application (turquoise) in PNs. **d** eEPSC amplitude of PNs was unaltered by CNO application ($t_6 = 0.67$, $P = 0.53$; $N/n = 7/4$). **e** eIPSC amplitude of PNs was decreased by CNO ($t_6 = 5.69$, $^*P = 0.001$; $N/n = 7/4$). **f** E/I ratio in PNs was increased by CNO ($t_6 = 2.75$, $^*P = 0.033$; $N/n = 7/4$). **g** Using *PV::Cre* mice, mCherry or hM4Di-mCherry was bilaterally expressed in dmPFC PV-INs. **h** Example of PV (left) and mCherry (right) expression. White arrows indicate colocalisation of PV and mCherry ($n = 6$). Scalebar: 50 µm. **i** 74.7 ± 3.2% of PV^+ cells expressed mCherry and 94.7 ± 1.0% of $mCherry^+$ cells were PV^+. **j** Mice (hM4Di $n = 8$; mCherry $n = 8$)

underwent cocaine conditioning (sal = saline, coc = cocaine) and received CNO before extinction training. During the test, hM4Di animals showed higher preference for the cocaine context than control mice (t_{14} = 3.33, $^{*}P$ = 0.005). **k** Model of vmPFC-to-dmPFC circuit. Unreinforced re-exposure to a cocaine-associated context triggers activation of vmPFC-to-dmPFC projecting neurons, which strongly excite dmPFC PV-INs, resulting in feed-forward inhibition of PNs. All graphs show mean ± s.e.m.

Discussion

Our data reveal that extinction of context-evoked cocaine memory depends on activation of an intrinsic mPFC circuit (Figure 4k). We show that vmPFC projections innervate the dmPFC and vmPFC-to-dmPFC projecting neurons are activated upon unreinforced re-exposure to a cocaine-associated context. In line with this, chemogenetic suppression of vmPFC-to-dmPFC projecting neurons prevented extinction of context-evoked cocaine memory. In the dmPFC, PV-INs receive strong monosynaptic excitatory input from vmPFC terminals and subsequently inhibit PNs, typical for feed-forward inhibition (*175*). Similar to manipulation of vmPFC-to-dmPFC neurons, chemogenetic suppression of dmPFC PV-INs impaired extinction of context-evoked cocaine reward memory. Hence, under extinction conditions, vmPFC projections recruit feed-forward GABAergic inhibition in the dmPFC to attenuate conditioned responding to a cocaine-associated context.

Whereas previous models propose that the dmPFC and vmPFC exert control over conditioned cocaine seeking via divergent projections to other brain regions (*58, 70, 365, 366*), we now demonstrate that direct connectivity between the vmPFC and dmPFC provides critical adaptive control over responding to cocaine-associated contextual cues. Our findings do not rule out the involvement of vmPFC projections to other regions, such as the NAc shell (*365, 366*), but reveal an additional mechanism for extinction-induced behavioral inhibition. Of relevance is that we found that vmPFC-to-dmPFC projections are required for acquisition of extinction, whereas vmPFC-to-NAc shell connectivity exerts inhibitory control over cocaine seeking after extinction learning (*365, 366*), but not during a first extinction session (*56*). Global manipulation of vmPFC function, however, affects both the acquisition and expression of extinguished cocaine seeking (*103*). As we found that the vmPFC-to-dmPFC projecting neuronal population has little overlap with the

vmPFC-to-NAC shell projecting neurons and sends only sparse collateral projections to the NAc shell, this suggests that extinction learning requires vmPFC projections to the dmPFC, whereas vmPFC projections to the NAc shell control the retention of extinguished cocaine seeking.

Recruitment of feed-forward GABAergic inhibition in the dmPFC during extinction learning may result in global suppression of PN firing and a reduction of output from this region. However, we think that the cortical network effect might be more nuanced. This is based on the observation that neurons within the prelimbic cortex fire during the initiation of reward seeking and under extinction conditions, both in a context-dependent manner (*57*). Therefore, distinct neuronal ensembles within the dmPFC may drive and inhibit cocaine conditioned responses, similar to what has been reported for the vmPFC (*365*). Whether PV-INs in the dmPFC suppress dmPFC neurons that drive expression of cocaine memory and/or facilitate the recruitment of dmPFC neurons that mediates extinction-induced behavioral inhibition is an important topic for future research.

We implicate the vmPFC-to-dmPFC feed-forward inhibition circuit in extinction of cocaine conditioned behavior, but this network may be involved in extinction learning in general. To our knowledge, the monosynaptic innervation of dmPFC PV-INs by vmPFC projections has not been previously reported, but independent studies have shown that silencing of vmPFC-to-dmPFC projections or PV-INs mediates extinction of conditioned fear (*77, 122*). Furthermore, excitatory projections in the opposite direction, from dmPFC to vmPFC, also mediate extinction of conditioned fear (*68*). Together with our findings, this indicates that a reciprocal intrinsic mPFC circuit serves to provide important adaptive control over conditioned behavior, in particular when an originally learned association (context→reinforcer) does not match with the conditions during re-exposure to the same context and an alternative association (*e.g.,* context→no reinforcer) is learned.

To conclude, we discovered that monosynaptic interaction between the vmPFC and dmPFC mediates extinction of cocaine reward memory through activation of dmPFC PV-INs. This sheds new light on the architecture of the neuronal circuit that enables adaptive responding to cocaine-contextual cues and may provide a new therapeutic target for strengthening of behavioral inhibition upon context-evoked retrieval of cocaine memories.

Methods and Materials

Animals

Male wild-type C57BL/6J and transgenic *PV::Cre* mice (The Jackson Laboratory, stock number 017320, maintained on a C57BL/6J background) aged 6-8 weeks at the start of experiments were individually housed. Mice were kept on a 12-h light/dark cycle with regular laboratory chow food and water available *ad libitum*. Behavioral experiments were conducted during the animals' light phase. All experimental procedures were approved by the Central Committee for Animal experiments (Centrale Commissie Dierproeven) of The Netherlands and the Animal Ethical care Committee (Instantie voor Dierenwelzijn) of the Vrije Universiteit Amsterdam.

AAV vectors and stereotactic micro-injections

AAV-*CaMKIIα*::ChR2(H134R)-EYFP (titer: 4.0 X 10^{12}), AAV-*hSyn*::DIO-mCherry and AAV-*hSyn*::DIO-hM4Di-mCherry (titers: 5.0-6.0 X 10^{12}) were packaged as serotype 2/5. For retrograde tracing, we used retroAAV2-*hSyn*::EGFP-iCre (titer: 2 X 10^{12}; v146, Zürich Viral Vector Facility, Switzerland) and retroAAV2-*hSyn-1::*Cre (titer: 1.3 X 10^{12}; Janelia Research Campus, USA (*368*)). For stereotaxic micro-injection of AAVs, mice received 0.05 mg/kg Temgesic (RB Pharmaceuticals, UK) 30 min before the start of surgery, were then anesthetized with isoflurane and mounted onto a stereotactic frame. Lidocaine (2%, Sigma-Aldrich Chemie N.V., The Netherlands) was topically applied to the skull before incision to provide local analgesia. Microinjection glass needles were used to infuse virus in the dmPFC (+1.8 mm AP; +0.45 mm ML; -2.1 mm DV; relative to Bregma) or vmPFC (+1.9 mm AP; -0.5 mm ML; -3.0 mm DV; relative to Bregma; unless otherwise indicated) at a flow rate of 0.1 µL/min followed by an additional 5 min to allow diffusion, followed by stepwise retraction of the needle. For visualization of vmPFC-to-dmPFC projecting neurons, retroAAV-*hSyn*::EGFP-iCre (0.4 µL) was unilaterally injected in the dmPFC and AAV-*hSyn*::DIO-mCherry (0.4 µL) in the contralateral vmPFC. For chemogenetic suppression of vmPFC-to-dmPFC projecting neurons, retroAAV-*hSyn*::EGFP-iCre (0.3 µL/hemisphere) was bilaterally injected in the dmPFC and Cre-dependent AAV-*hSyn*::DIO-hM4Di-mCherry virus (0.3 µL/hemisphere) bilaterally injected in the vmPFC (ML-DV angle 25°; +1.9 mm AP; ±1.37 mm ML; -3.0 mm DV; relative to Bregma). For chemogenetic suppression of PV-INs, *PV::Cre* mice received AAV-*hSyn*::DIO-hM4Di-mCherry or AAV-*hSyn*::DIO-mCherry bilaterally in the dmPFC (0.5 µL/hemisphere). For electrophysiology recordings, *PV::Cre* mice received AAV-

CaMKIIα::ChR2(H134R)-EYFP into the vmPFC (0.4 µL/unilateral) and AAV-*hSyn*::DIO-hM4Di-mCherry or AAV-*hSyn*::DIO-mCherry into the contralateral dmPFC (0.5 µL/unilateral). Analgesia was provided 24 and 48 h after surgery (Carprofen, 5 mg/kg). Animals remained in their home-cage for 3 weeks until the start of behavioral experiments or for at least 5 weeks until electrophysiological recordings were performed. Mice with virus misplacements were excluded from analysis (n = 1 CTB tracing Figure 1F, n = 1 Ext group and n = 1 No Ext group Figure 2B-D, n = 2 hM4Di-mCherry group Figure 2E-F)

CTB tracing

CTB conjugated to Alexa 555 or Alexa 488 (ThermoFisher) was dissolved in sterile PBS (0.33 or 1% w/v; as no differences were observed between the two concentrations, animals were pooled) and injected into the dmPFC (+1.8 mm AP; +0.45 mm ML; -2.1 mm DV) and NAc shell (+1.25 mm AP; +0.6 mm ML; -4.7 mm DV). One week later, animals were sacrificed by transcardial perfusion.

Cocaine conditioned place preference

The conditioning apparatus consisted of two main compartments that differed in tactile and visual cues, connected by a small center compartment (*112*). On day 0, baseline preference for the main compartments was assessed by allowing animals to freely explore all compartments (pre-test; 10 min). The cocaine-paired and saline-paired compartment were counterbalanced within all groups, such that on average the groups did not have a baseline preference for one the two main compartments, thereby allowing an unbiased procedure. Conditioning sessions (15 min) were conducted twice daily over 3 consecutive days. For this, mice received saline (i.p.; morning) or cocaine (15 mg/kg in saline; i.p.; afternoon) prior to being confined to one of the main compartments. After 3 weeks of forced abstinence in the home-cage, animals were subjected to extinction training and/or a post-conditioning test (post-test). For extinction training, mice were re-exposed to the cocaine- and saline-paired compartment (15 min) in the absence of cocaine or saline treatment. In a post-test, we determined preference scores by allowing animals to freely explore all compartments for 5 min (to avoid within session extinction) under drug-free conditions. Time spent in each compartment was measured using a video camera and Ethovision video-tracking software (Noldus, The Netherlands). A preference score for each animal was calculated

as: time spent in cocaine-paired compartment minus saline-paired compartment.

Chemogenetic intervention

Clozapine N-oxide (CNO; HB6149 HelloBio, United Kingdom) was dissolved in sterile saline. Mice received an injection of 5 mg/kg (i.p.) CNO 30 min before a test session.

Immunohistochemistry

Mice were transcardially perfused using ice-cold PBS pH 7.4, followed by ice-cold 4% paraformaldehyde (PFA) in PBS pH 7.4. Brains were removed, post-fixed overnight in 4% PFA solution and then immersed in 30% sucrose in PBS with 0.02% NaN_3. Brains were then sliced in 35 µm coronal sections using a cryostat and stored in PBS with 0.02% NaN_3 at 4°C until further use. Immunohistochemical stainings were performed using standard procedures (*112*), using the following antibodies: rabbit anti-Fos (1:500, sc52, Santa Cruz, USA), mouse anti-PV (1:1000, MAB1572, Millipore, USA), mouse anti-GAD67 (1:1000, MAB5406, Millipore, USA) and NeuroTrace™ 500/525 Green Fluorescent Nissl Stain or 4',6-diamidino-2-phenylindole (DAPI, Vectashield). For quantification experiments, 4-6 z-stacks per animal were generated using a confocal microscope (Zeiss LSM510 or Nikon Ti) with the experimenter blinded to the treatment conditions. ImageJ software was used to extract the ROIs of the cells stained with Nissl or DAPI (Gaussian filter, Li threshold). Only ROIs within a predefined range for size (70-2000 square units; to exclude glial cells and non-specific staining) and circularity (0.5 to 1.0) were included. As cells were frequently present in 2 or 3 subsequent images of a z-stack, MATLAB (MathWorks) was used to group the ROIs that belonged to the same Nissl or DAPI cell, and then to count the total number of $Nissl^+$ or $DAPI^+$ cells in a stack. Cells expressing hM4Di-mCherry, mCherry, PV, GAD67, Fos or CTB-488/555 were counted manually.

Electrophysiological recordings

Mice were swiftly decapitated and brains were extracted in carbogenated (95% O_2, 5% CO_2) ice-cold partial sucrose solution containing (in mM): 70 NaCl, 2.5 KCl, 1.25 $NaH_2PO_4*H_20$, 5 $MgSO_4*7H_2O$, 1 $CaCl_2*2H_2O$, 70 Sucrose, 25 D-Glucose, 25 $NaHCO_3$, 1 Na-Ascorbate, 3 Na-Pyruvate (~300 mOsm/kg, pH 7.4). The brains were trimmed and glued onto the stage of a vibrating microtome (Microm). Coronal slices (thickness 300 µm) containing the mPFC were cut in the carbogenated ice-cold partial sucrose solution. Slices

were transferred into continuously carbogenated holding artificial cerebrospinal fluid (aCSF) containing (in mM): 125 NaCl, 3 KCl, 1.25 $NaH_2PO_4*H_2O$, 2 $MgCl_2*6H_2O$, 1.3 $CaCl_2*2H_2O$, 25 D-Glucose, 25 $NaHCO_3$, 25 D-Glucose, 25 $NaHCO_3$, 1 Na-Ascorbate, 3 Na-Pyruvate (~300 mOsm/kg, pH 7.4), where they were left to recover at room temperature for at least 1 hour before recording. Subsequently, slices were transferred to a submerged recording chamber of an upright microscope (BX51WI, Olympus) and left to equilibrate for 10 min under continuous perfusion (2 mL/min) with carbogenated running aCSF (holding aCSF without Na-Ascorbate or Na-Pyruvate and only 1 mM $MgCl_2*6H_2O$) heated to 31-33°C. The dmPFC was imaged using differential interference contrast microscopy and pyramidal neurons were identified based on their shape, large apical dendrites and typical action potential discharge pattern (*369*) (Figure S3). ChR2-EYFP positive fibers and PV-INs expressing hM4Di-mCherry or mCherry were identified in the dmPFC using a mercury-vapor lamp combined with a fluorescent filter. When possible, PNs were chosen in the close vicinity of a recorded PV-IN to control for potential differences in density of ChR2-EYFP$^+$ fibers. Whole-cell recordings were conducted using borosilicate glass pipettes (2.5-5.5 MΩ) pulled on a horizontal puller (P-87, Sutter Instruments Co). Recordings were acquired with pClamp software (Molecular Devices), using a Multiclamp 700B amplifier (Molecular Devices), sampled at 20 kHz, low-pass filtered at 6 kHz, and digitized with an Axon Digidata 1440A (Molecular Devices). Membrane and action potential (AP) discharge properties were investigated in current-clamp mode using K-gluconate based intracellular solution containing (in mM): 70 K-Gluconate, 148 KCl, 10 Hepes, 4 Mg-ATP, 4 K2-phosphocreatinine, 0.4 GTP, osmolarity 280-290 mOsm/kg, pH adjusted to 7.2-7.3 with KOH. To analyze passive membrane properties and characteristics of AP firing, depolarizing current steps (750 ms) with an increment of 25 pA were applied every 3 s ranging from -100 pA to 500 pA. Input resistance was calculated from the linear fit of the voltage-current response to hyperpolarizing current injection steps from -100 pA to 0 pA. Membrane time constant was obtained by a double exponential fit of the voltage response to a −50 pA current injection. AP threshold voltage was defined as the point where the depolarization speed first exceeded 10 mV/ms. AP amplitude and afterhyperpolarization (AHP) were determined relative to the AP threshold. Minimal inter-spike interval (ISI) was calculated including all the sweeps where APs were detected. Evoked excitatory postsynaptic currents (eEPSCs) and evoked inhibitory postsynaptic currents (eIPSCs) were recorded using Cs-gluconate-based

intracellular solution containing (in mM): 130 Cs-Gluconate, 8 NaCl, 10 Hepes, 0.3 EGTA, 4 Mg-ATP, 10 K2-phosphocreatinine, 0.3 GTP, 3 QX134-Cl, osmolarity 280-290 mOsm/kg, pH adjusted to 7.2-7.3 with CsOH. In experiments in Figure S3J-N a K-Gluconate based intracellular solution was used. Cells were recorded in an area of the dmPFC where ChR2-EYFP positive fibers were identified. Slices were illuminated by pulses of blue light (470 nm, 20 ms, 0.1 Hz) controlled by an electro-mechanical shutter. Duration of photostimulation was controlled using the patch-clamp digitizer. eEPSCs and eIPSCs were recorded at a holding potential of -70 mV and 0 mV, respectively. In the experiment using K-Gluconate intracellular solution, eIPSCs were recorded at -30 mV. In order to avoid the influence of insufficient or absent ChR2 expression in our recordings, only cells that showed a clear and stable excitatory or inhibitory response to photostimulation were included in the analysis. A minimum of ten traces were obtained at each holding potential and response amplitudes and latencies to onset averaged per cell. Latency to onset was measured as a time interval between the start of photostimulation and the onset of eEPSC or eIPSC. Excitatory-inhibitory (E/I) ratio was calculated by dividing the amplitude of eEPSC by the amplitude of eIPSC recorded within the same neuron. Running aCSF containing pharmacological reagents was perfused at a rate of approximately 2 mL/min, for at least 5 minutes before repeating the measurement of evoked responses. CNO (50 μM, HelloBio, UK) was used for chemogenetic inhibition. 6-cyano-7-nitroquinoxaline-2,3-dione (CNQX, 10 μM, HelloBio, UK) and DL-2-Amino-5-phosphonopentanoic acid (DL-AP5, 50 μM, HelloBio, UK) were used to block AMPA and NMDA receptors, respectively. Gabazine (10 μM, HelloBio, UK) was used to block $GABA_A$ receptors. For confirmation of a monosynaptic vmPFC-dmPFC excitatory connection (Figure S3) tetrodotoxin (TTX, 1 μM, Abcam, UK) was used to block Na^+ gating channels, and 4-aminopyridine (4-AP, 100 μM, Sigma-Aldrich, NL) to block K^+ channel-mediated shunting of the light-evoked response. Custom written MATLAB (Mathworks, Natick, MA) scripts were used to analyze passive membrane properties and AP discharge. Evoked currents were quantified using Clampfit software (Molecular Devices).

Quantification and Statistical analysis

Statistical details are presented in the figure legends. Number of animals is shown as *n* and number of cells as *N*. All graphs show means ± s.e.m. SPSS software (version 25, IBM) and GraphPad (Prism) were used for statistical analysis. Comparisons between groups were made

using two-tailed unpaired *t*-tests or in case of paired data, a two-tailed paired *t*-test. When the data was not modeled by a normal distribution, analysis was subjected to non-parametric Mann-Whitney U test for between group comparisons and Wilcoxon signed rank test for within-subject comparisons. To investigate differences in activation of labelled cells between groups (Group x Population ($Fos^+/mCherry^-$ *vs.* $Fos^+/mCherry^+$)), a repeated measures ANOVA was conducted, followed by post-hoc Bonferroni tests. Significance was set at $p < 0.05$.

Supplemental Information

Extinction of cocaine memory depends on a feed-forward inhibition circuit within the medial prefrontal cortex

Figure S1 – vmPFC-to-dmPFC projecting neurons are activated during extinction learning.
Figure S2 – Distribution of PV-INs in the dmPFC and proportion of the total GABAergic population.
Figure S3 – Electrophysiological profiles of recorded dmPFC PNs and PV-INs and their differential responses following stimulation of vmPFC terminals.
Figure S4 – Chemogenetic suppression of PV-INs reduces disynaptic inhibition of PV-INs in dmPFC.

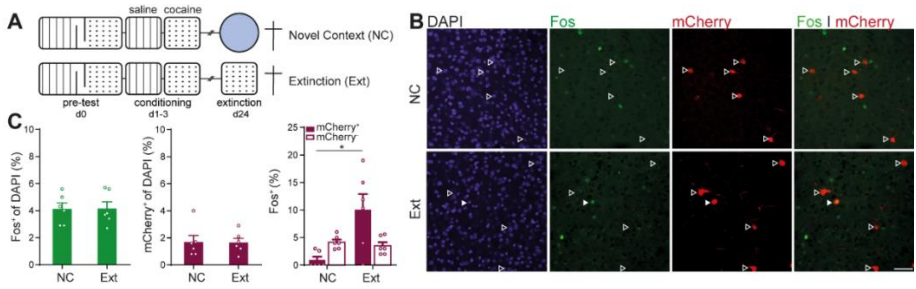

Figure S1. vmPFC-to-dmPFC projecting neurons are activated during extinction learning. A Mice received retroAAV-*hSyn::*Cre in the dmPFC and AAV-*hSyn::*DIO-mCherry in the vmPFC and underwent cocaine CPP training. Three weeks later, animals were exposed to a novel context (NC) or re-exposed to the cocaine-associated context in absence of cocaine reward (Extinction). **B** Representative images of DAPI, Fos and mCherry expression in the vmPFC. **C** Quantification of the percentage of Fos$^+$ and mCherry$^+$ neurons and colocalisation. Percentages of Fos$^+$ and mCherry$^+$ cells were similar in both groups, but the percentage of Fos$^+$/mCherry$^+$ neurons was higher in the extinction group than the novel context group (U = 4.0, P = 0.022). All graphs show mean ± s.e.m.

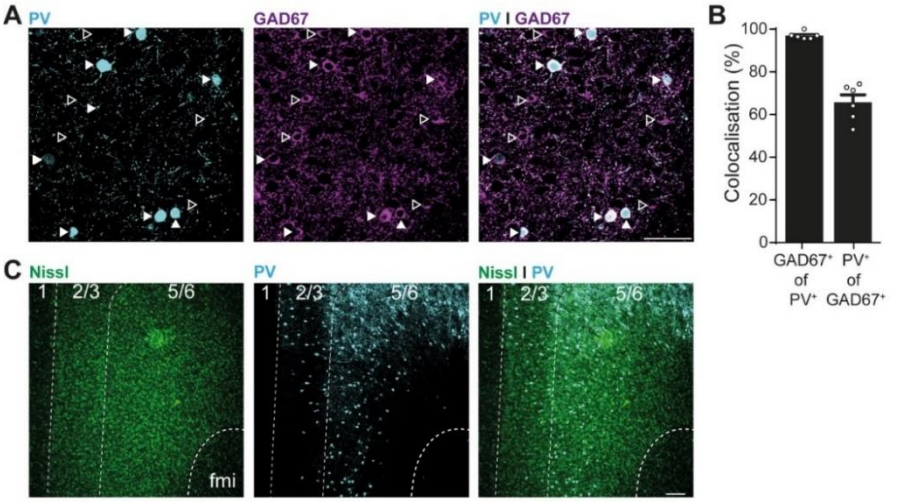

Figure S2. Distribution of PV-INs in the dmPFC and proportion of the total GABAergic population. A Example of PV and GAD67 immunostaining in dmPFC. Outlined arrowheads: PV$^-$/GAD67$^+$ cells. Filled arrowheads: PV$^+$/GAD67$^+$ cells. **B** Quantification of colocalization of PV$^+$ and GAD67$^+$ cells. Approximately all PV$^+$ cells express GAD67 (96.8 ± 0.7%), as expected, and the vast majority of GAD67$^+$ neurons express PV$^+$ (65.8 ± 3.5%). Graph shows mean ± s.e.m. **C** PV-IN density was highest in in the deep layers (mainly layer 5) compared with the superficial layers (layer 1-3) of the dmPFC. Scalebar = 100 µm. Fmi = forceps minor of the corpus callosum.

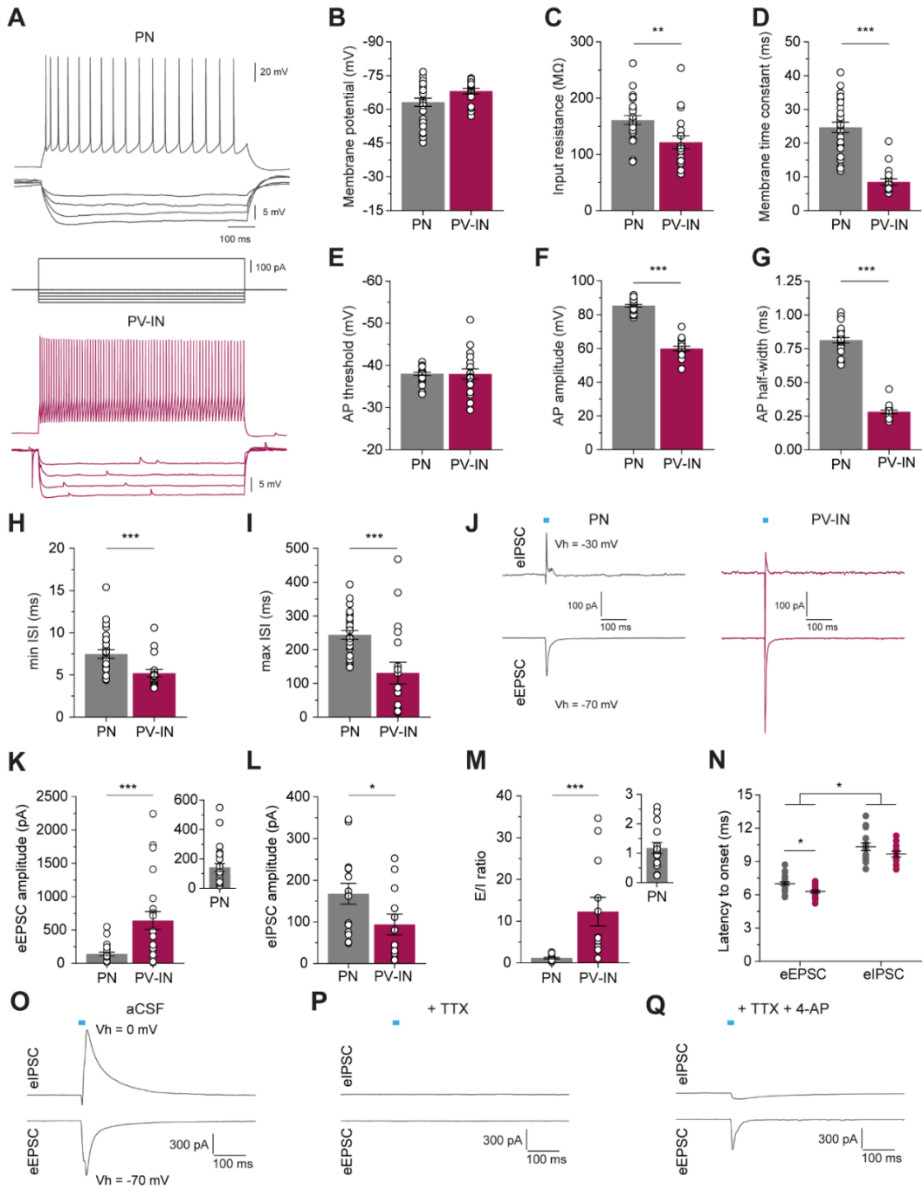

Figure S3. Electrophysiological profiles of recorded dmPFC PNs and PV-INs and their differential responses following stimulation of vmPFC terminals. A Representative electrophysiological profile of a PN (top) and PV-IN (bottom) in response to corresponding current steps. **B** Resting membrane potential did not differ between both cell-types (U = 161, P = 0.083). **C** PV-INs demonstrated a lower input resistance compared to PNs (U = 111, $^{**}P$ = 0.003). **D** Membrane time constant was lower in PV-INs (t_{42} = 19.93, $^{***}P < 0.001$). **E** AP threshold was similar in PNs and PV-INs (t_{42} = 0.0525, P = 0.958). **F** Action potential (AP) amplitude was higher in PNs than in PV-INs (t_{42} = 18.25, $^{***}P < 0.001$). **G** AP half-width was lower in PVs (U = 0, $^{***}P < 0.001$). **H** Minimum inter-spike interval (ISI) was lower in PV-INs than in PNs (U = 94, $^{***}P < 0.001$). **I** Maximum inter-spike interval (ISI) was lower in PV-INs than in PNs (U = 92, $^{***}P$ = 0.005). Graphs show mean ± s.e.m. (PN N/n = 26/9; PV-IN N/n = 18/7). **J** Representative eEPSC and eIPSC traces recorded with a K-Gluconate-based intracellular solution in PNs and PV-INs. The initial downward peak in the eIPSC trace represents a residual excitatory current at Vh -30 mV. Out of all cells that showed an eEPSC, 58% of PNs and 55% of PV-INs showed an eIPSC (eEPSC PN N/n = 26/9, eEPSC PV-IN N/n = 22/7, eIPSC PN N/n = 15/9, eIPSC PV-IN N/n =

12/7). Note that both percentages are lower than observed with a Cs-based intracellular solution due to reduced amplification of inhibitory responses with the K-Gluconate-based intracellular solution (see also Fig. 2c, e). Vh, holding potential. **K** eEPSC amplitude was higher in PV-INs than PNs (U = 112, ***P < 0.001; PN N = 26; PV N = 19). Inset displays PN eEPSC amplitude at reduced scale. **L** eIPSC amplitude was higher in PNs than PV-INs (t_{25} = 2.064, *P = 0.049). **M** E/I ratio is higher for PV-INs than PNs (U = 7, ***P < 0.001; PN N/n = 15/9, PV-IN N/n = 12/7). Inset displays PN E/I ratio at reduced scale. **N** Latency to onset of eEPSCs was lower than eIPSCs ($F_{1,71}$ = 258.2, P < 0.001; post-hoc eEPSC PN *vs.* eEPSC PV-IN t_{71} = 4.097, P = 0.025). **O-P** eEPSCs and eIPSCs (O) in response to optic stimulation (20 ms pulse; blue line) were abolished by application of TTX (1 µM; P). Vh = holding potential. **Q** Combined application of TTX and 4-AP (100 µM) abolished eIPSCs and partially recovered eEPSCs. All graphs show mean ± s.e.m.

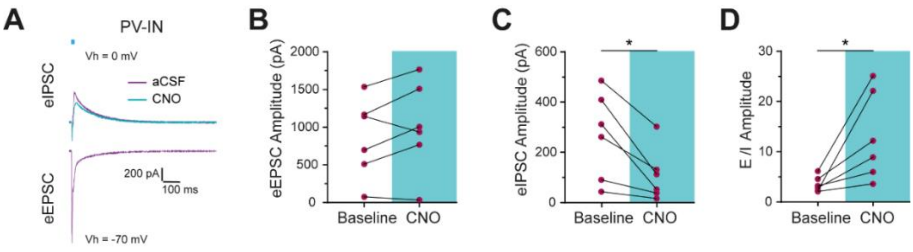

Figure S4. Chemogenetic suppression of PV-INs reduces disynaptic inhibition of PV-INs in the dmPFC. A Representative trace in PV-INs in absence (purple) and presence of CNO (turquoise) upon optic stimulation (blue line; 20 ms pulse) of ChR2-expressing vmPFC terminals. **B** eEPSC amplitude of PV-INs was unchanged by CNO (t_5 = 1.64, P = 0.16; N/n = 6/4). **C** eIPSC amplitude of PV-INs was decreased by CNO (t_5 = 3.56, *P = 0.016; N/n = 6/4). **D** E/I ratio in PV-INs was increased by CNO (t_5 = 2.89, *P = 0.034; N/n = 6/4).

Acknowledgements

The authors want to thank Yvonne Gouwenberg for AAV packaging, Joost Hoetjes for genotyping, Hans Lodder for technical support with electrophysiological recordings, Alexandra Nicolson and Petra de Bruijn for help with immunohistochemical stainings, and Taco J. de Vries for valuable input on the manuscript. This study was funded by an NWO VIDI grant (016.168.313) to M.C.v.d.O, E.V. and M.M.

Author Contributions - Conceptualization: E.V., M.R.M, M.M., I.K., A.B.S., M.C.v.d.O.; Methodology: E.V., M.R.M, M.M., I.K., H.D.M., M.C.v.d.O.; Formal analysis: E.V., M.R.M, M.M., I.K.; Investigation: E.V., M.R.M, M.M., I.K., R.J.v.d.L., M.C.v.d.O.; Resources: H.D.M.; Writing: E.V., M.R.M., M.M., A.B.S., M.C.v.d.O.; Supervision: A.B.S., M.C.v.d.O.; Funding acquisition: A.B.S., M.C.v.d.O.

Chapter 6

General Discussion

General Discussion

1. Summary of main findings

In my thesis I embraced the task of studying the role of the medial prefrontal cortex (mPFC) in memory processing at the level of neuronal ensembles and circuitry. More specifically, I dissected the temporal evolution of mPFC neuronal ensembles encoding an aversive memory and investigated mPFC circuitry and its contribution to extinction of an appetitive memory.

A large part of the work described here was made possible by the development of viral-TRAP, a viral vector system allowing conditional gene expression *in vivo*, presented in **Chapter 3**. In **Chapter 4**, I focused on addressing systems consolidation of memory at the level of cortical neuronal ensembles through application of the viral-TRAP method. I found that neuronal ensembles in the mPFC are defined at the time of fear learning and require time-dependent maturation to support remote memory expression. Additionally, I present results implicating the transcription factor CREB in systems consolidation of an aversive fear memory and demonstrating that involvement of the mPFC ensemble in remote memory is regulated by the intensity of conditioning. In **Chapter 5**, I reveal a vmPFC-to-dmPFC projection in extinction of an appetitive cocaine memory. These long-range projecting vmPFC neurons are activated during extinction of a cocaine conditioned place preference (CPP) memory and preferentially target parvalbumin (PV) interneurons in the dmPFC, evoking an increase in inhibition of neighboring pyramidal neurons.

Here, I will discuss my main findings in comparison with previous work in the field and suggest future directions to answer unresolved questions that arose from interrogating the data in my experimental chapters.

2. Permanent tagging of activated neurons

As part of my thesis, I aimed to resolve memory encoding and consolidation in the mPFC at the level of neuronal ensembles and for this we developed a new tool to express a permanent molecular tag in neurons that are activated during learning. These sparsely distributed cells can be identified by the expression of the immediate early gene (IEG) *Fos* upon neuronal activation. The transient nature of IEG expression (*370*), however, hinders the prolonged temporal tracking of memory encoding neuronal ensembles. In particular, the design of transgenic TRAP mice, expressing a tamoxifen-inducible Cre

recombinase (CreER^{T2}) under the control of an IEG promoter region, helped to overcome this limitation (*310, 315*). I deliberately aimed to develop a virus-based variant of TRAP to circumvent undesired characteristics observed in TRAP mice (*310*). Firstly, in the original knock-in TRAP mouse line (TRAP1), the CreER^{T2} sequence was inserted in the *Fos* locus, which resulted in disruption of endogenous Fos expression from one allele. As a consequence, Fos expression is reduced in some brain areas of this mouse (*310*). As viral-TRAP does not integrate in the mouse genome, endogenous Fos expression remains intact. Secondly, the use of AAV particles to deliver a *Fos* promoter-driven inducible CreER^{T2} allows adjustment of the viral titer and thereby the copy number of the Fos::CreER^{T2} transgene in infected neurons. Thereby, the basal level of CreER^{T2} in neurons can be reduced, such that tagging reflects the size of a Fos^{+} neuronal ensemble induced by a behavioral experience. Indeed, we found that the size of the contextual fear conditioning (CFC)-tagged mPFC population (~7% of mPFC neurons) was similar to the endogenous Fos^{+} ensemble (~8% of mPFC neurons) evoked by CFC (see Chapter 4). However, it is important to note that the CFC-tagged ensemble included ~1-2% of non-specifically-tagged mPFC neurons, meaning that we captured approximately 75% of CFC-induced Fos^{+} neurons. Thirdly, the *Fos* promoter in our viral-TRAP method can be replaced by a different IEG promoter when relevant. However, analysis of several IEGs in cortical areas revealed that most *Fos*$^{+}$ neurons co-express other IEGs, such as *Arc* and *Nr4a1* (*124, 371, 372*). In order to improve the tagging of activated neurons, IEG promoter sequences are also the target of modifications, such as the E-SARE promoter, potentially leading to stronger expression of transgenes with less leakiness (*373*). Although I did not directly compare the *Fos* promoter with modified synthetic IEG promoters, this might be a means to further reduce the nonspecific background tagging which I observed after CFC (see Chapter 3 and 4). Off note, crossing Fos::CreER^{T2} or Arc::CreER^{T2} mice with a Cre-dependent reporter line offers the advantage to examine brain-wide tagging of activated neurons (*124, 314, 374*), which is not feasible with viral-TRAP. When TRAP mice are combined with CLARITY (*124*) or iDISCO^{+} (*314*) connectivity between neuronal ensembles can be investigated that are distributed throughout the brain.

The CFC-activated neuronal ensemble that we tagged with viral-TRAP was comprised of glutamatergic pyramidal cells and GABAergic interneurons (see Chapter 3). Interestingly, GABAergic neurons were even overrepresented in the tagged ensemble. Interneurons have been implicated in a myriad of memory processes,

ranging from regulation of an ensemble size by PV^+ (*375*) and Somatostatin (SST^+) interneurons (*376*), to encoding of fear memory by SST^+ cells (*377*) and recruitment into an extinction ensemble (*378*). Therefore, it would be relevant to specifically tag activated interneurons and to assess their contribution to memory processing in future studies (*379*). This might be achieved through an interplay between Cre and Flp recombinase. By adapting the viral-TRAP construct to a Cre-dependent Fos::$FlpER^{T2}$ (e.g., AAV-Fos::DIO-FlpERT2) and injecting it in a Cre mouse line (e.g., PV::Cre or SST::Cre) together with a Flp-dependent virus, this will restrict expression of the transgene to, for instance, activated PV^+ or SST^+ interneurons.

We used the new viral-TRAP method to investigate mPFC neuronal ensembles in aversive (Chapter 4) as well as appetitive (alcohol reward) (*380*) memory and thereby provided valuable insight into their role in memory processing and persistency. The use of viral-TRAP also abolishes the need to investigate memory neuronal ensembles using transgenic animals and can be applied in different species, thereby bridging the gap between studies of neuronal ensembles in different species (e.g., mice vs. rats). Rats are often used in more cognitively demanding behavioral tasks, but the availability of rat transgenic lines is limited. Therefore, application of viral-TRAP in rats may yield important information regarding the role of neuronal ensembles in higher-order cognitive functions.

3. Systems consolidation and mPFC neuronal ensembles

A widely accepted traditional model of systems consolidation of memory assumes that new memories are formed in the hippocampus (HPC) and then is slowly transferred to cortical areas (*34*), after which they can be retrieved independent of the HPC. Based on this, the gradual transformation process is crucial for memory to persist and thought to be driven by synchronized activity of hippocampal and cortical neurons (*17, 43, 96*). A central cortical hub in this process is the mPFC, whose activity and plasticity are necessary for proper memory expression long after training (*85, 96, 381*). However, the question whether this brain area also functions as a memory storage site remained unanswered. We addressed this by identifying a neuronal ensemble in the mPFC that supports remote memory expression. Using viral-TRAP, we demonstrated that a contextual fear memory is allocated to neuronal ensembles in the mPFC already at the time of learning. These specific neurons are necessary for remote, but not recent, memory expression. Although systems consolidation is

likely still ongoing during the first days after conditioning, chemogenetic stimulation of the learning-tagged mPFC ensemble is sufficient to evoke recent memory expression. This observation is in line with reports of others (*314, 331*), despite the use of different tagging and intervention methods. Interestingly, remote auditory fear memory recall through stimulation of tagged mPFC neurons is impaired after interference with memory allocation to mPFC neurons during conditioning (*314*). Together, these findings demonstrate that mPFC neurons required for remote memory expression are already defined during learning, and are not gradually recruited into the memory engram during systems consolidation, as is postulated by the standard theory of systems consolidation.

Several studies do not support the standard theory of systems consolidation and this resulted in the formulation of the multiple trace theory (MTT) (*382-384*). This theory assumes that interaction between HPC and cortical neurons is required for the retrieval of detail-rich memories at both recent and remote timepoints after learning, and that encoding and consolidation occurs in hippocampal and cortical networks simultaneously within days (*382*). In support of this, temporally precise inhibition of the CA1 region of the hippocampus during retrieval impaired both recent and remote memory (*37*). Although I did not study the effect of suppression of HPC ensembles, the data in chapter 4 does not support MTT, as the mPFC ensemble was not involved in recent memory expression under natural conditions. To address gaps of the MTT theory (*385*), Yonelinas et al. (2019) proposed a contextual binding (CB) theory for episodic memories (*386*). CB assumes that the hippocampus is crucial for the binding of item and context related information. Whereas MTT does not include predictions about the role of sleep and memory interference, CB takes these factors into account and in particular how they could explain forgetting. Similar to MTT, CB assumes that episodic memory always depends on the HPC, whereas the neocortex is important for less detailed or decontextualized memories after repeated epochs of retrieval. According to CB, memory dependency on hippocampal or cortical activity seems to be the outcome of a fine balance between the amount of detail encoded and the recurrent re-encoding that takes place in both networks upon repeated memory reactivation. The latter might render the memory more dependent on cortical nodes, but at the cost of loss of contextualization for remote memories (*386*). Notably, the continuous involvement of the HPC in CB does not rule out that other brain areas cannot become more involved over time. In that respect, the data presented in Chapter 4 fits

within the CB framework, however, our data indicates that the learning-activated mPFC ensemble is already critically involved when the contextual memory is retrieved for the first time at one month after CFC. Strikingly, suppression of the mPFC ensemble that was tagged after strong (3US) CFC did not impair remote memory expression (Chapter 4). I speculate, based on the CB theory, that strong CFC induces the formation of a more detailed memory that relies longer on the HPC and less on cortical areas, despite the passage of time. I will discuss other potential explanations for the memory strength-dependent engagement of learning-activated mPFC neurons in section 4 below.

Neocortical memory maturation is driven by coordinated replay of encoded information between the hippocampus and cortical nodes during consolidation (*387*). Inhibition of hippocampal CA3 output during consolidation leads to remote memory impairments as a result of reduced ripple events in CA1 neurons (*388*). Furthermore, learning-induced changes in spine density on mPFC engram cells are prevented by post-learning ablation of output from dentate gyrus (DG) neurons encoding a CFC memory (*331*). It would be interesting to determine whether artificial recapitulation of patterns of hippocampal learning-induced activity accelerates the maturation process of mPFC ensemble neurons. If this would be technically feasible, memory expression might depend earlier on cortical ensemble activity than the actual time normally required for systems consolidation.

We reported that recall of a mild contextual fear memory reactivates 22% of neurons of the CFC-tagged population (Chapter 4). Potentially, this is the consequence of contraction of the learning-activated ensemble (*370*), which has been detected in different brain areas (*301, 338, 389, 390*). Thus, the initial pool of activated neurons tagged using viral-TRAP may represent an overestimation of the actual number of neurons that will eventually store and retrieve the memory. A study using two-photon imaging in transgenic Fos::GFP mice presented evidence supporting this hypothesis (*391*). Fos^+ neurons were identified based on expression of GFP after conditioned food seeking and were tracked over multiple sessions. Interestingly, from the total population of GFP^+ neurons detected during the first day of conditioning only 23% were reactivated during a recall session, similar to our findings. Furthermore, we found that the size of the mPFC ensemble that was tagged during remote, but not recent, memory recall was smaller (~4% of the total population) than the CFC-tagged ensemble (7% of the total population), further pointing to a reduction in ensemble size over time. We also have to consider that our CFC-

tagged neuronal ensemble includes non-specifically tagged neurons, which consequently reduces the percentage of the reactivated fraction. Assuming that all learning-induced Fos$^+$ neurons represent a memory-encoding ensemble, it remains to be determined why the brain would recruit a bigger starter population than required for retrieval. I speculate that maintaining a constant pool of ready-to-be-activated neurons assures the success of memory allocation and thereby prevents information loss that could ultimately affect survival of an organism.

4. Contribution of the mPFC to aversive memory circuits

Previous studies revealed a post-learning time-dependent shift in the neuronal circuitry supporting auditory fear memory expression (*98*) and this was also observed for the circuitry supporting contextual fear memory (*331*), as discussed above. Conditioned fear circuitry involves the amygdala, HPC and mPFC (*392*), among other regions. The emotional component of fear memory requires activity in the basolateral amygdala (BLA) (*393, 394*), which in turn activates neurons in the Central Amygdala (CeA), driving fear memory expression. The BLA also sends projections to neurons in the mPFC that contribute to fear responses (*395*). Moreover, communication between the BLA and mPFC is bidirectional, since mPFC neurons send excitatory projections to the BLA (*396*), thereby changing the activity of BLA neurons that either drive or suppress fear (*397*), crucial for the regulation of fear responses (*82*). The HPC is thought to be essential for encoding of contextual and spatial stimuli (*398*). The HPC projects to both the amygdala and the mPFC (*397, 399, 400*), although direct projections from the dorsal HPC to the mPFC are relatively sparse (*401*). In addition to direct HPC projections to the BLA, the HPC is able to control activity in this region via mPFC neurons that project to the BLA (*402*). Interestingly, with respect to contextual fear, Kitamura *et al.* demonstrated that neurons in the BLA and the medial entorhinal cortex (MEC) regulate the formation of a fear-encoding neuronal ensemble in the mPFC. Furthermore, they found that expression of remote fear memory relies on the MEC-BLA-mPFC pathway and does not require the DG ensemble that controls recent memory expression. Interestingly, the BLA is engaged at all times, thus at recent and remote time-points after conditioning (*331*). Future studies should focus on characterizing the axonal projections of the tagged mPFC population to the BLA as well as afferents from the HPC and BLA. Doing so will provide important insight in the temporal shift in the circuitry supporting fear memory expression.

A remarkable finding in Chapter 4 is the lack of effect of inhibition of the mPFC ensemble that was activated during strong CFC on remote memory expression. As yet, the mechanism underlying this observation is unknown, but I suggest three possible explanations. Firstly, inhibition via chemogenetics may not be sufficient to completely silence the activity of the mPFC ensemble. This is particularly relevant for our comparison of mild (1 foot-shock) and strong (3 foot-shock) CFC conditioning, as strong CFC produces higher freezing levels during memory retrieval and this may be supported by increased ensemble activity that (partially) overrules activation of the DREADD. Secondly, a recent study (pre-print) reports different behavioral effects of chemogenetic and optogenetic manipulation on expression of fear memory (*403*), suggesting that slower chemogenetic intervention can be masked by compensatory activity in other brain areas. In line with this, the duration of optogenetic manipulation of neuronal activity also influences the potential to recruit other brain regions (*37*). However, in our study, chemogenetic suppression of the mPFC ensemble was performed in the same manner after mild and strong CFC, making this explanation less likely. Thirdly, our differential effect on mild and strong fear memory expression can be the result of recruitment of different neuronal circuits. In Chapter 4, I report an increase in Fos^+ neurons in the BLA and Nucleus Reuniens of the midline thalamus (Re) in mice subjected to strong CFC compared to mild CFC. Both brain areas represent critical hubs in the brain-wide network that controls systems consolidation of fear memory (*404*). Notably, the Re receives projections from the mPFC and in turn sends projections to the mPFC (*405*) and HPC, preferentially the CA1 area (*406*). As Re neurons play a role in contextual fear learning and extinction (*407, 408*) and seem crucial for coordinating cortico-hippocampal slow-wave activity (*409*), this region is thought to function as a relay station between the HPC and mPFC in the regulation of memory expression. I speculate that in the case of strong fear memories, BLA and Re neurons are robustly activated and that this can overrule the top-down control of the mPFC over fear memory expression (Fig. 1). Tracing studies and targeted manipulations of projections within the HPC-BLA-Re-mPFC circuit might reveal a change in the circuitry supporting remote memory expression as a result of memory strength. It is noteworthy that our results are in contrast with a different study in mice that used strong fear conditioning (*331*). Kitamura *et al.* showed that optogenetic inhibition of an mPFC ensemble that was tagged after CFC using three foot-shock impaired remote memory expression (*331*). However, whereas they

examined remote memory retrieval at day 12 after CFC, we inhibited the mPFC ensemble at day 30 after training. Hence, the mPFC ensemble might have a time limited role in memory expression after strong CFC.

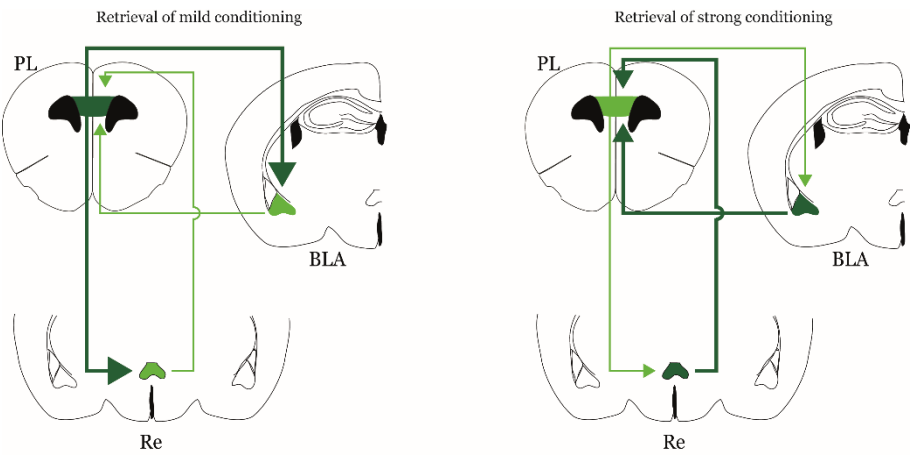

Figure 1. Aversive memory strength affects engagement of ensembles in a remote engram circuit. Remote contextual fear memory expression after mild conditioning depends on a circuitry involving the mPFC and BLA, and possibly the Re. Strong conditioning leads to more activated neurons in the BLA and Re and now remote memory expression does not require reactivation of the mPFC ensemble. Based on this, I speculate that a strong remote fear memory depends on a Re-BLA circuit without top-down control by the mPFC. Whether the strength of connectivity between these regions changes as a result of the intensity of conditioning is an important topic for future research.

5. Contribution of the mPFC to appetitive memory circuits

Unraveling the mechanisms that the brain uses for modifying previously learned associations is as important as identifying the mechanisms that underlie initial learning. Extinction memory is believed to be the result of the learning of a new association and competes with expression of an original memory (*410-412*). In my thesis, I studied the role of the internal mPFC circuitry in extinction of a cocaine contextual memory and report that interaction between the ventral and dorsal mPFC (vmPFC and dmPFC) is critical for the acquisition of extinction memory. These results challenge the assignment of a stop and go function, respectively, to these subregions (*413*). This is further challenged by *in vivo* electrophysiological recordings of neurons in the dorsal and ventral areas of the mPFC during drug self-administration, extinction and re-instatement, which

revealed different neuronal response profiles within the same region at these different phases (*57, 111*). More recently, a pharmacological inhibition study showed that silencing of both dmPFC and vmPFC impaired the expression of a previously learned discrimination task to obtain sucrose reward (*414*). Interaction between both areas of the mPFC is also crucial for acquisition of an alternation task (*122*). Whereas dmPFC projections to the vmPFC are required for initial learning of this task, vmPFC to dmPFC connectivity supported learning of an alternative response (*122*). Finally, dmPFC-to-vmPFC projecting neurons mediate extinction of auditory fear memory (*68*). Thus, the sometimes-conflicting results derived from manipulations of the dmPFC or the vmPFC in expression of learned behavior might be explained by the rather crude separation of the mPFC in a dorsal and ventral subregion with a stop and go function, respectively (*106, 259, 260, 415*). Together with the aforementioned findings, the absence of a clear boundary between the two brain areas, complex cellular composition of the mPFC and a gradient of afferent and efferent projections along the dorsal-ventral axis, suggest that this binary functional division based on anatomy is probably too simplistic.

In Chapter 5, I show that vmPFC projections target dmPFC PV^+ interneurons to mediate control over dmPFC pyramidal neurons and thereby promote extinction of cocaine CPP. This is in line with the observation that direct optogenetic stimulation of dmPFC PV^+ interneurons facilitates extinction of sucrose seeking (*367*). It remains to be determined whether other types of interneurons are recruited by the vmPFC to fulfill a similar or distinct role. It was previously shown that vmPFC GABAergic NPY^+ neurons exert inhibition over dmPFC pyramidal neurons (*416*). Neurogliaform and bipolar NPY^+ cells are located in layers 5 and 6 of the vmPFC, similar to PV^+ interneurons. However, compared with PV neurons, NPY^+ neurons are much sparser (*416*). Our findings differ in important aspects with the ones reported in the latter study. First, vmPFC NPY^+ neurons directly inhibit dmPFC pyramidal neurons, which differs from feed-forward inhibition. Second, NPY^+ neurons innervate dmPFC pyramidal neurons located in layer 2, whereas we found that dmPFC PV interneurons inhibit pyramidal cells distributed over layers 3-6. Third, we examined vmPFC-induced excitatory currents in PV^+ interneurons in the contralateral dmPFC (for technical reasons), whereas Saffari et al. studied NPY^+ neuron-mediated inhibition of pyramidal neurons in the ipsilateral dmPFC. Thus, it is yet unknown whether vmPFC projections innervate ipsilateral dmPFC PV^+ interneurons to inhibit local pyramidal neurons and whether vmPFC NPY^+ neurons inhibit

contralateral dmPFC pyramidal cells. Despite these differences, it is relevant to verify whether vmPFC NPY$^+$ cells complement the role of dmPFC PV neurons and thereby strengthen inhibitory control of the vmPFC over the dmPFC.

It is also worthwhile to investigate the role of other GABAergic interneurons, such as the Vasoactive-intestinal Peptide (VIP$^+$) and SST$^+$ interneurons, in appetitive memory formation and extinction learning. Together with PV$^+$ interneurons, SST$^+$ cells constitute the vast majority of GABAergic interneurons (*417*). The use of different fluorescent markers in the same transgenic mouse allows the simultaneous identification of SST$^+$ and PV$^+$ cells and to dissect the microcircuit between these two interneuron populations (*377*). In the dmPFC, PV$^+$ interneurons directly inhibit pyramidal neurons, in accordance with our own data, whereas SST$^+$ interneurons disinhibit the activity of pyramidal cells via strong suppression of PV$^+$ interneuron activity (*377*). As such, SST$^+$ interneurons do not only influence local pyramidal neurons, but indirectly activate distant brain regions that receive input from the dmPFC (*377*). It was also found that repeated morphine exposure alters the dendritic morphology and excitability of mPFC SST$^+$ interneurons, resulting in augmented inhibition of local PV$^+$ cells, which in turn disinhibits pyramidal neuron activity (*418, 419*). This morphine-induced plasticity is required for acquisition of CPP (*419*). Whether the same mechanism applies to cocaine CPP remains to be determined. VIP$^+$ interneurons constitute a smaller fraction (~15%) of the GABAergic interneuron population compared to PV$^+$ and SST$^+$ neurons, but may play a crucial role in mPFC circuits due to their ability to inhibit both PV$^+$ and SST$^+$ cells (*75*). In the mPFC, VIP$^+$ interneurons are located in superficial (*73*), placing them in an ideal position to indirectly modulate long-range input onto dendritic tufts. Taken together, my data provides valuable insight into role of PV$^+$ interneurons in extinction of cocaine memory, but investigations into the role of the different GABAergic interneuron populations during distinct stages of appetitive memory processing remains an important topic for future investigation.

The mPFC sends dense projections to the nucleus accumbens (NAc) (*112, 366, 420, 421*). Whereas the dmPFC targets the NAc core (*65, 422*), the vmPFC preferentially projects to the NAc shell (*65*). Interestingly, we found that vmPFC-to-dmPFC projecting neurons and vmPFC-to-NAc shell projecting neurons form distinct neuronal populations in the vmPFC. This is of relevance, because vmPFC projections to the NAc shell are critical for expression of extinguished

cocaine seeking (*366*). The vmPFC receives excitatory input from the ventral HPC (*50*). Recently, it was found that ventral HPC inputs recruit feed-forward inhibition in the vmPFC through activation of PV interneurons and chemogenetic inactivation of this projection impairs reinstatement of extinguished fear memory (*402*). Notably, vmPFC pyramidal neurons that project to the BLA receive feed-forward inhibition upon activation of the ventral HPC-to-vmPFC projection. Hence, in the vmPFC, feed-forward inhibition mediates recovery of an extinguished aversive memory, but whether the same circuit is involved in reinstatement of appetitive reward memory is yet unknown. Future studies should focus on and compare the different efferent and afferent mPFC projections in order to carefully dissect the neuronal circuitry supporting extinction of appetitive and aversive memories.

6. Conditioning versus extinction ensembles in the mPFC

In this thesis, I investigated an aversive memory at the level of neuronal ensembles and extinction of an appetitive memory at the level of long-range and local circuitry. Therefore, it remains to be determined whether the same circuitry and ensemble mechanisms are involved in both types of memory. I revealed a novel internal mPFC circuit that controls extinction learning, but it is yet unknown how this circuit regulates extinction at the neuronal ensemble level. Moreover, it remains to be determined whether mPFC neurons that are activated during appetitive learning undergo a process of time-dependent maturation and memory strength-dependent engagement in remote memory expression, similarly to what I have described for a fearful experience. Ultimately, one should also address whether the intrinsic mPFC extinction circuitry described here is also involved in the extinction of fear. Support for extrapolation is based on observations that substance abuse and trauma-related memories share, to a certain extent, the same neuronal circuitry involving the mPFC (*124*). In humans, this might be partly explained by a high incidence of comorbidity of substance abuse in patients suffering from traumatic memories (*423*). In animal models, expression, extinction and renewal/reinstatement of drug-seeking and fear memory seem to be similarly affected by mPFC manipulations (*58, 69, 261, 424, 425*). I hypothesize that co-existence of appetitive and aversive memories in the mPFC relies on the establishment of intermingled, but distinct, neuronal ensembles. Indeed, tools that allow the visualization and manipulation of sparsely distributed activated neurons have challenged the widely held view that the vmPFC merely mediates

extinction of drug conditioned behavior, whereas the dmPFC is necessary for promoting drug seeking behavior (*413*). Electrophysiological recordings of neurons in the dmPFC and vmPFC indicate that both regions encompass neurons that respond to reward seeking and extinction (*57*). Recently, distinct neuronal ensembles mediating food or cocaine seeking and extinction of these behaviors were identified within the vmPFC (*123, 365*). Furthermore, different vmPFC ensembles regulate responding to cues that signal to promote or suppress sucrose seeking (*426*). In contrast, another study reports that neuronal ensembles that mediate extinction of alcohol- and sucrose-associated cues largely overlap in the vmPFC (*427*). With respect to dmPFC ensembles encoding appetitive memories, we used viral-TRAP in an operant alcohol self-administration paradigm (not included in this thesis) and found that the same neuronal ensemble in the mPFC that is activated during cue-paired alcohol self-administration is subsequently required for cue-induced alcohol seeking one month later (*380*). Notably, this mechanism did not generalize to sucrose self-administration, suggesting that alcohol-cue and sucrose-cue encoding ensembles do not overlap in the dmPFC (*380*). Interestingly, Ye et al. (2016) demonstrated that the dmPFC can harbor neuronal ensembles that promote appetitive and aversive conditioned behavior and that these populations have differential projection patterns (*124*). Whereas an mPFC ensemble encoding a positive (cocaine) valence has more dense projections to the NAc, an mPFC ensemble encoding a negative (foot-shock) valence more densely innervates the lateral habenula. A similar stop and go dichotomy for the vmPFC and dmPFC has previously been suggested to regulate expression and extinction of aversive memory (*58*), but whether ensembles that promote and suppress aversive memory exist within the same mPFC subregion has not yet been investigated. A recent study described the concurrent existence of neuronal ensembles in the DG encoding a fear and extinction memory (*428*), suggesting that this may also apply to the mPFC. To add another layer of complexity, Sun *et al.* discovered that a fear memory engram can be comprised of distinct neuronal ensembles in the DG that can be identified based on the expression of different IEGs (e.g., *Fos* and *NPAS4*). Interestingly, stimulation of these ensembles results in the expression of opposite behaviors, i.e., fear generalization versus fear discrimination (*429*). Although regulation of these behavioral outcomes is particularly relevant for the pattern separation function of the DG, it is important to investigate whether distinct IEG-expressing ensembles can also be identified in the mPFC.

The allocation and reactivation of memory-encoding neurons is likely controlled via the activity of local GABAergic interneurons. My data in Chapter 5 points to a local mPFC circuitry that drives the shift between expression of conditioned cocaine behavior and inhibition of this response through activation of dmPFC PV$^+$ interneurons during extinction learning. In line with this, increased Fos expression has been observed in GABAergic neurons compared with pyramidal neurons in the dmPFC after (nonreinforced) expression of cocaine CPP (*110*), suggesting that extinction learning occurred in these animals. Although we did not study the formation of a cocaine CPP and extinction ensemble, I speculate that the emergence and suppression/activation of both ensembles is controlled by PV$^+$ GABAergic interneurons in the dmPFC and that this may also apply to aversive memories. Extinction learning might recruit dmPFC PV interneurons to drive a shift in neuronal ensemble activation and thereby facilitate the formation of an 'extinction ensemble', ultimately suppressing conditioned behavior (see Fig. 2). Analysis of Fos-expressing dmPFC neurons using 2-photon imaging in mice supports my hypothesis (*378*). Brebner et al. (2020) showed that extinction of conditioned food seeking recruits a stable subset of interneurons, while at the same time the likelihood of reactivation of pyramidal cells that were activated during the first extinction session decreased as extinction learning progressed (*378*). Hence, alterations in activation of subsets of GABAergic interneurons may result in a switch in ensembles that are activated during initial conditioning and those activated under extinction conditions.

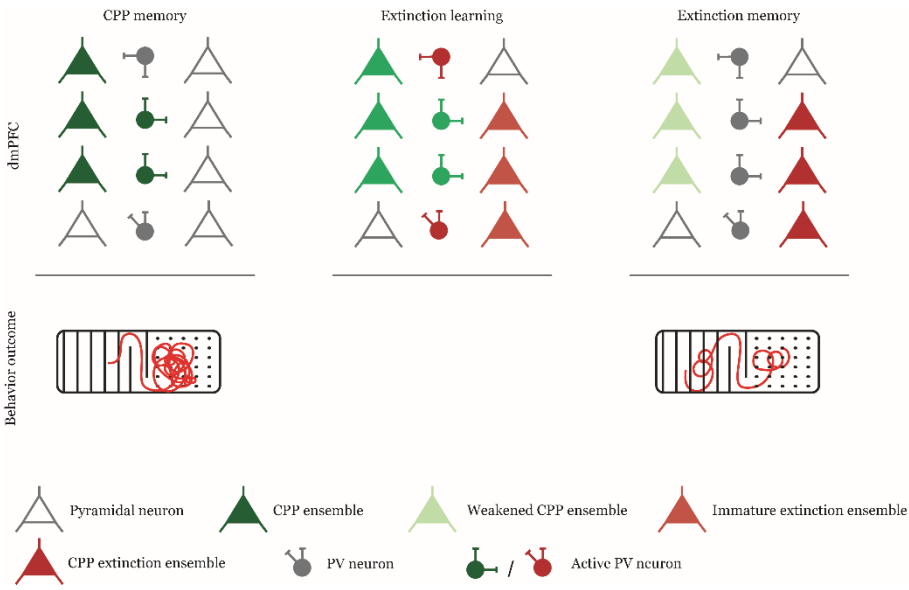

Figure 2. Hypothetical model of local mPFC circuitry supporting cocaine CPP and extinction memory. I hypothesize that similar to fear

memory, CPP memory expression is supported by the activity of a dmPFC neuronal ensemble. During extinction learning, vmPFC-to-dmPFC projecting neurons preferentially excite PV^+ interneurons (in red) in dmPFC that consequently may inhibit the activity of PNs in the CPP memory ensemble. At the same time, this may facilitate the emergence of an extinction ensemble (red pyramidal neurons) through disinhibition of another subset of dmPFC PNs. Next, recall of extinction memory potentially relies on the reactivation of the newly formed extinction ensemble.

7. Investigating ensembles and circuitry at the physiological and molecular level

Clinical success in treatment of pathological drug or fear memories will benefit from improved in-depth knowledge of the involved neuronal circuitry and in particular the identification of ensemble-specific physiological and molecular mechanisms that underlie the formation and persistence of an aversive or appetitive memory, as well as extinction memory. Therefore, I will now focus on several important findings regarding changes in the properties of ensemble neurons in the mPFC. Electrophysiological recordings of neuronal ensembles have been performed in the mPFC in Fos::GFP rats that learned food self-administration (*430*). Whitaker et al. first confirmed that ablation of the Fos-expressing dmPFC neurons impaired food seeking during a recall session (*430*). Next, they found that Fos^+ neurons were characterized by increased intrinsic excitability induced by operant learning, whereas Fos^- counterparts showed an opposite trend. This bidirectional modulation occurred as a consequence of learning, as it was not detected during the initial operant sessions (*430*). Contrary to these observations, Brebner et al. (2020) found that dmPFC pyramidal neurons that are activated (Fos^+) during a first Pavlovian food seeking session show increased excitability compared with non-activated mPFC neurons and this difference is no longer present after a final training session (*391*). Furthermore, prolonging the increase in excitability of Fos-expressing neurons by chemogenetic stimulation impairs the development of reliable cue-paired food seeking. Hence, their data suggests that an initial enhancement of excitability is important to form a stable ensemble, but then dissipation of excitability changes is necessary to maintain the learned behavior. The contradicting findings of the above-mentioned studies may be explained by different types of learning in the paradigms that were used (operant: action-outcome vs. Pavlovian: stimulus-response) and requires further investigation.

Generation of new synapses or strengthening of pre-existing ones between neurons activated during conditioning is believed to be crucial for memory formation, storage and retrieval (*21, 381, 431, 432*). Indeed, CFC resulted in a gradual increase in dendritic spine density on mPFC ensemble neurons and inhibiting this structural change impaired remote fear memory expression (*331*). As ensemble neurons are sparsely distributed, it is challenging to resolve connectivity changes between ensemble neurons. New technologies, like eGRASP, allow the selective visualization of synapses between ensemble neurons and to correlate this with changes in synaptic strength induced by learning (*433*). This technique has not yet been used to study mPFC ensembles, but has provided important insight into synaptic changes between hippocampal ensemble neurons after CFC. Interestingly, Choi et al. (2018) found that spine density and spine head diameter is selectively enhanced between CA3 and CA1 ensemble neurons and this depends on the intensity of CFC. Importantly, they show that these structural changes correlate with increased synaptic strength between ensemble neurons, whereas the size of the neuronal ensemble is unaffected by memory strength (*433*). Taken together, focusing on altered intrinsic excitability of ensemble neurons and synaptic connectivity between neuronal ensembles within and across different brain regions will help to disentangle the neuronal circuitry that functions as the substrate for memory storage.

Transcriptome and proteome analyses of neurons that are activated during initial conditioning or extinction will help to identify novel molecular targets for treatment of memory disorders. Formation of long-term memories relies on new gene transcription and protein synthesis, which is crucial for the synaptic and structural changes induced by learning (*434, 435*). Several studies indicate that CREB family transcription factors are responsible for regulating gene expression underlying memory consolidation in different species (*334, 335*). For instance, transgenic mice expressing a brain-wide dominant-negative mutant form of CREB (mCREB), which disrupts CREB-mediated gene transcription, exhibit long-term memory impairments (*18*). To my knowledge, we are the first to demonstrate that CREB function in neuronal ensembles is crucial for systems consolidation and thus for memory persistence (see Chapter 4). My results are in line with a recent study to which I contributed and that analyzed the transcriptome of activated DG neurons after CFC (*436*). CFC-activated DG neurons showed upregulation of a CREB-dependent transcriptional network 24 h after conditioning. Selective expression of mCREB in the DG neuronal ensemble resulted in impaired memory

expression 3 days after conditioning (*436*). Hence, generation of a transcriptome profile of activated DG neurons pointed to the involvement of CREB in memory consolidation and identified additional novel targets that may be critically involved in the encoding of long-term memories.

By combining viral-TRAP, or another tagging method, with Fluorescence-activated cell sorting or translating ribosome affinity purification (*437*), a detailed molecular profile of memory formation and persistence can be generated at the level of neuronal ensembles. For instance, Chen *et al.* used TRAP2 mice to analyze the gene expression profile of ensemble and non-ensemble neurons in the mPFC that were tagged during a recall test two weeks after fear conditioning (*438*). This revealed an increase in expression of genes involved in membrane fusion and vesicle release in ensemble neurons, suggestive of a strengthening of presynaptic function. In line with this, Dillingham *et al.* also found an enhancement in the expression of genes coding for proteins that regulate presynaptic vesicle release in mPFC ensemble neurons 30 days after CFC (*439*). Interestingly, they detected a time-dependent increase in the density of axon terminals of mPFC ensemble neurons in the basolateral amygdala (*439*), thereby corroborating the changes in gene expression. Ye et al. (2016) combined CLARITY for brain-wide circuitry mapping with RNA-sequencing of neurons activated by distinct experiences (cocaine reward vs. aversive shock) (*124*). In addition to the identification of distinct mPFC neuronal ensembles encoding these experiences, they observed a different transcriptional program in the neuronal populations that encode a positive and negative valence. Taken together, this highlights the relevance to dissect the molecular properties of identified neuronal ensembles and shows that learning-induced changes in the properties of ensemble neurons can differ between different forms of associative learning. Unfortunately, much less is known about physiological and molecular mechanisms that support formation of extinction memories, in particular at the level of neuronal ensembles, making this an important topic for future research. Investigating neuronal ensembles at the molecular level will ultimately help to identify functional changes evoked by normal (adaptive) and maladaptive learning and therefore has potential to reveal targets that can be used for treatment of memory disorders (e.g., persistent pathological memories or amnesia).

8. Future directions

The data in this thesis reinforces the concept that the mPFC functions as a critical cortical node in different types of memories by harboring distinct memory ensembles. With the acquisition of more detailed knowledge, we will be able to more accurately map local and inter-regional circuits encoding specific memories. In addition to the investigation of ensembles and circuits at a synaptic and molecular level, as discussed above, I suggest to dissect memory circuits in the future by addressing the following questions:

- Does expression of a strong remote fear memory depend on a Re-BLA circuit and loss of top-down control by the mPFC? Related to this, does the strength of connectivity within this circuit change according to the intensity of conditioning and does this affect connectivity with a fear-encoding neuronal ensemble in the mPFC? I speculate that stronger connectivity between different circuit nodes might drive behavior response with reduced mPFC activity. I also propose that the nature of connectivity between the Re/BLA and mPFC might shift to inhibition of mPFC ensemble neurons.

- Is expression or suppression of aversive/appetitive memory mediated by a switch in activity of the original memory-encoding ensemble to a potential extinction memory-encoding ensemble in the dmPFC? Related to this, is this switch mediated by distinct subsets of PV^+ interneurons, of which the 'extinction subset of PV neurons' is targeted by vmPFC projections? I hypothesize that during extinction learning a new subset of PV interneurons is responsible for the inhibition of encoding ensemble PV interneurons and pyramidal neurons that in turn facilitates the emergence of a new ensemble that encodes the new memory, that is the CS no longer predicts the US. Post-extinction memory expression relies on the activity of the new dmPFC ensemble.

- What is the role of the different GABAergic interneuron subtypes in the shaping and reactivation of aversive/appetitive memory and extinction memory ensembles? I speculate that SOM and VIP interneurons might regulate the activity of PV interneurons. In the same way I propose the existence of PV that are part of the original memory ensemble and another subset of PV that form the extinction ensemble, I hypothesize that SOM and VIP interneurons behave similarly.

- What are the molecular mechanisms in memory-encoding ensembles that support memory storage and retrieval? Related to this, do these mechanisms differ between aversive and appetitive memories, and between original memories and extinction memories? I believe that a molecular signature can be found for every phase of memory consolidation and expression. The different patterns can help the understanding on why extinction memories are less permanent or how to facilitate the extinction phase.

The combination of these different approaches will each contribute detailed insight into the neuronal architecture, activity patterns, connectivity and molecular properties of memory circuits, thereby providing crucial information for the decoding of the fundamental principles of memory processing in the brain.

References

1. I. P. Pavlov, *Condtioned Reflexes, an investigation of the psychological activity of the cerebral cortex*. (Oxford University Press, New York, 1927).
2. R. C. Bolles, M. S. Fanselow, A perceptual-defensive-recuperative model of fear and pain. *Behav Brain Sci*, 291-301 (1980).
3. M. S. Fanselow, K. M. Wassum, The Origins and Organization of Vertebrate Pavlovian Conditioning. *Cold Spring Harb Perspect Biol* **8**, a021717 (2015).
4. S. G. Anagnostaras *et al.*, Automated assessment of pavlovian conditioned freezing and shock reactivity in mice using the video freeze system. *Front Behav Neurosci* **4**, (2010).
5. M. S. Fanselow, R. C. Bolles, Naloxone and shock-elicited freezing in the rat. *J Comp Physiol Psychol* **93**, 736-744 (1979).
6. M. Bouton, R. Bolles. (Anim Learn Behav, 1980), vol. 8, pp. 429-434.
7. J. Landeira-Fernandez, J. P. DeCola, J. J. Kim, M. S. Fanselow, Immediate shock deficit in fear conditioning: effects of shock manipulations. *Behav Neurosci* **120**, 873-879 (2006).
8. M. T. Bardo, R. A. Bevins, Conditioned place preference: what does it add to our preclinical understanding of drug reward? *Psychopharmacology (Berl)* **153**, 31-43 (2000).
9. T. M. Tzschentke, Measuring reward with the conditioned place preference paradigm: a comprehensive review of drug effects, recent progress and new issues. *Prog Neurobiol* **56**, 613-672 (1998).
10. M. A. Aguilar, M. Rodriguez-Arias, J. Minarro, Neurobiological mechanisms of the reinstatement of drug-conditioned place preference. *Brain Res Rev* **59**, 253-277 (2009).
11. C. M. Alberini, Transcription factors in long-term memory and synaptic plasticity. *Physiol Rev* **89**, 121-145 (2009).
12. E. R. Kandel, The molecular biology of memory storage: a dialog between genes and synapses. *Biosci Rep* **21**, 565-611 (2001).
13. Y. Dudai, The neurobiology of consolidations, or, how stable is the engram? *Annu Rev Psychol* **55**, 51-86 (2004).
14. K. Nader, Memory traces unbound. *Trends Neurosci* **26**, 65-72 (2003).
15. A. J. Silva, J. H. Kogan, P. W. Frankland, S. Kida, CREB and memory. *Annu Rev Neurosci* **21**, 127-148 (1998).
16. E. R. Kandel, The molecular biology of memory: cAMP, PKA, CRE, CREB-1, CREB-2, and CPEB. *Mol Brain* **5**, 14 (2012).
17. P. W. Frankland, B. Bontempi, The organization of recent and remote memories. *Nat Rev Neurosci* **6**, 119-130 (2005).
18. S. Kida *et al.*, CREB required for the stability of new and reactivated fear memories. *Nat Neurosci* **5**, 348-355 (2002).
19. K. Nader, G. E. Schafe, J. E. LeDoux, The labile nature of consolidation theory. *Nat Rev Neurosci* **1**, 216-219 (2000).
20. R. Semon, *The mneme*. (G. Allen and Unwin, 1921), pp. 304.
21. D. O. Hebb, *The organization of Behavior: a Neuropsychological Theory*. (Wiley, 1949).
22. A. Ben-Yakov, Y. Dudai, M. R. Mayford, Memory Retrieval in Mice and Men. *Cold Spring Harb Perspect Biol* **7**, (2015).
23. K. Nader, Reconsolidation and the Dynamic Nature of Memory. *Cold Spring Harb Perspect Biol* **7**, a021782 (2015).
24. N. C. Tronson, J. R. Taylor, Molecular mechanisms of memory reconsolidation. *Nat Rev Neurosci* **8**, 262-275 (2007).
25. M. H. Milekic, C. M. Alberini, Temporally graded requirement for protein synthesis following memory reactivation. *Neuron* **36**, 521-525 (2002).

26. A. Suzuki *et al.*, Memory reconsolidation and extinction have distinct temporal and biochemical signatures. *J Neurosci* **24**, 4787-4795 (2004).
27. M. E. Pedreira, H. Maldonado, Protein synthesis subserves reconsolidation or extinction depending on reminder duration. *Neuron* **38**, 863-869 (2003).
28. K. M. Myers, M. Davis, Mechanisms of fear extinction. *Mol Psychiatry* **12**, 120-150 (2007).
29. M. E. Bouton, Context, time, and memory retrieval in the interference paradigms of Pavlovian learning. *Psychol Bull* **114**, 80-99 (1993).
30. W. Y. Chan, H. T. Leung, R. F. Westbrook, G. P. McNally, Effects of recent exposure to a conditioned stimulus on extinction of Pavlovian fear conditioning. *Learn Mem* **17**, 512-521 (2010).
31. S. Corkin, What's new with the amnesic patient H.M.? *Nat Rev Neurosci* **3**, 153-160 (2002).
32. W. B. SCOVILLE, B. MILNER, Loss of recent memory after bilateral hippocampal lesions. *J Neurol Neurosurg Psychiatry* **20**, 11-21 (1957).
33. N. L. Rempel-Clower, S. M. Zola, L. R. Squire, D. G. Amaral, Three cases of enduring memory impairment after bilateral damage limited to the hippocampal formation. *J Neurosci* **16**, 5233-5255 (1996).
34. L. R. Squire, P. Alvarez, Retrograde amnesia and memory consolidation: a neurobiological perspective. *Curr Opin Neurobiol* **5**, 169-177 (1995).
35. N. Kapur, Focal retrograde amnesia in neurological disease: a critical review. *Cortex* **29**, 217-234 (1993).
36. J. J. Kim, M. S. Fanselow, Modality-specific retrograde amnesia of fear. *Science* **256**, 675-677 (1992).
37. I. Goshen *et al.*, Dynamics of retrieval strategies for remote memories. *Cell* **147**, 678-689 (2011).
38. J. L. McClelland, B. L. McNaughton, R. C. O'Reilly, Why there are complementary learning systems in the hippocampus and neocortex: insights from the successes and failures of connectionist models of learning and memory. *Psychol Rev* **102**, 419-457 (1995).
39. B. J. Wiltgen, K. Z. Tanaka, Systems consolidation and the content of memory. *Neurobiol Learn Mem* **106**, 365-371 (2013).
40. K. Louie, M. A. Wilson, Temporally structured replay of awake hippocampal ensemble activity during rapid eye movement sleep. *Neuron* **29**, 145-156 (2001).
41. M. A. Wilson, B. L. McNaughton, Reactivation of hippocampal ensemble memories during sleep. *Science* **265**, 676-679 (1994).
42. A. G. Siapas, M. A. Wilson, Coordinated interactions between hippocampal ripples and cortical spindles during slow-wave sleep. *Neuron* **21**, 1123-1128 (1998).
43. T. Maviel, T. P. Durkin, F. Menzaghi, B. Bontempi, Sites of neocortical reorganization critical for remote spatial memory. *Science* **305**, 96-99 (2004).
44. P. W. Frankland, B. Bontempi, L. E. Talton, L. Kaczmarek, A. J. Silva, The involvement of the anterior cingulate cortex in remote contextual fear memory. *Science* **304**, 881-883 (2004).
45. C. A. Heidbreder, H. J. Groenewegen, The medial prefrontal cortex in the rat: evidence for a dorso-ventral distinction based upon functional and anatomical characteristics. *Neurosci Biobehav Rev* **27**, 555-579 (2003).
46. H. B. Uylings, H. J. Groenewegen, B. Kolb, Do rats have a prefrontal cortex? *Behav Brain Res* **146**, 3-17 (2003).

47. J. P. Little, A. G. Carter, Subcellular synaptic connectivity of layer 2 pyramidal neurons in the medial prefrontal cortex. *J Neurosci* **32**, 12808-12819 (2012).
48. S. J. Cruikshank *et al.*, Thalamic control of layer 1 circuits in prefrontal cortex. *J Neurosci* **32**, 17813-17823 (2012).
49. D. P. Collins, P. G. Anastasiades, J. J. Marlin, A. G. Carter, Reciprocal Circuits Linking the Prefrontal Cortex with Dorsal and Ventral Thalamic Nuclei. *Neuron* **98**, 366-379.e364 (2018).
50. W. B. Hoover, R. P. Vertes, Anatomical analysis of afferent projections to the medial prefrontal cortex in the rat. *Brain Struct Funct* **212**, 149-179 (2007).
51. E. K. Miller, J. D. Cohen, An integrative theory of prefrontal cortex function. *Annu Rev Neurosci* **24**, 167-202 (2001).
52. P. L. Gabbott, T. A. Warner, P. R. Jays, P. Salway, S. J. Busby, Prefrontal cortex in the rat: projections to subcortical autonomic, motor, and limbic centers. *J Comp Neurol* **492**, 145-177 (2005).
53. S. R. Sesack, A. Y. Deutch, R. H. Roth, B. S. Bunney, Topographical organization of the efferent projections of the medial prefrontal cortex in the rat: an anterograde tract-tracing study with Phaseolus vulgaris leucoagglutinin. *J Comp Neurol* **290**, 213-242 (1989).
54. D. Ongür, J. L. Price, The organization of networks within the orbital and medial prefrontal cortex of rats, monkeys and humans. *Cereb Cortex* **10**, 206-219 (2000).
55. N. Gorelova, C. R. Yang, The course of neural projection from the prefrontal cortex to the nucleus accumbens in the rat. *Neuroscience* **76**, 689-706 (1997).
56. J. Peters, R. T. LaLumiere, P. W. Kalivas, Infralimbic prefrontal cortex is responsible for inhibiting cocaine seeking in extinguished rats. *J Neurosci* **28**, 6046-6053 (2008).
57. D. E. Moorman, G. Aston-Jones, Prefrontal neurons encode context-based response execution and inhibition in reward seeking and extinction. *Proc Natl Acad Sci U S A* **112**, 9472-9477 (2015).
58. J. Peters, P. W. Kalivas, G. J. Quirk, Extinction circuits for fear and addiction overlap in prefrontal cortex. *Learn Mem* **16**, 279-288 (2009).
59. J. P. Johansen, C. K. Cain, L. E. Ostroff, J. E. LeDoux, Molecular mechanisms of fear learning and memory. *Cell* **147**, 509-524 (2011).
60. R. G. Phillips, J. E. LeDoux, Differential contribution of amygdala and hippocampus to cued and contextual fear conditioning. *Behav Neurosci* **106**, 274-285 (1992).
61. R. Marek, C. Strobel, T. W. Bredy, P. Sah, The amygdala and medial prefrontal cortex: partners in the fear circuit. *J Physiol* **591**, 2381-2391 (2013).
62. J. Peters, J. Vallone, K. Laurendi, P. W. Kalivas, Opposing roles for the ventral prefrontal cortex and the basolateral amygdala on the spontaneous recovery of cocaine-seeking in rats. *Psychopharmacology (Berl)* **197**, 319-326 (2008).
63. J. P. Little, A. G. Carter, Synaptic mechanisms underlying strong reciprocal connectivity between the medial prefrontal cortex and basolateral amygdala. *J Neurosci* **33**, 15333-15342 (2013).
64. O. Yizhar, Optogenetic insights into social behavior function. *Biol Psychiatry* **71**, 1075-1080 (2012).
65. R. P. Vertes, Differential projections of the infralimbic and prelimbic cortex in the rat. *Synapse* **51**, 32-58 (2004).
66. G. Ji, V. Neugebauer, Modulation of medial prefrontal cortical activity using in vivo recordings and optogenetics. *Mol Brain* **5**, 36 (2012).

67. K. I. van Aerde, T. S. Heistek, H. D. Mansvelder, Prelimbic and infralimbic prefrontal cortex interact during fast network oscillations. *PLoS One* **3**, e2725 (2008).
68. R. Marek, L. Xu, R. K. P. Sullivan, P. Sah, Excitatory connections between the prelimbic and infralimbic medial prefrontal cortex show a role for the prelimbic cortex in fear extinction. *Nat Neurosci* **21**, 654-658 (2018).
69. D. Sierra-Mercado, N. Padilla-Coreano, G. J. Quirk, Dissociable roles of prelimbic and infralimbic cortices, ventral hippocampus, and basolateral amygdala in the expression and extinction of conditioned fear. *Neuropsychopharmacology* **36**, 529-538 (2011).
70. M. C. Van den Oever, S. Spijker, A. B. Smit, T. J. De Vries, Prefrontal cortex plasticity mechanisms in drug seeking and relapse. *Neurosci Biobehav Rev* **35**, 276-284 (2010).
71. G. A. Ascoli *et al.*, Petilla terminology: nomenclature of features of GABAergic interneurons of the cerebral cortex. *Nat Rev Neurosci* **9**, 557-568 (2008).
72. J. DeFelipe *et al.*, New insights into the classification and nomenclature of cortical GABAergic interneurons. *Nat Rev Neurosci* **14**, 202-216 (2013).
73. X. Xu, K. D. Roby, E. M. Callaway, Immunochemical characterization of inhibitory mouse cortical neurons: Three chemically distinct classes of inhibitory cells. *J Comp Neurol* **518**, 389-404 (2010).
74. D. Kvitsiani *et al.*, Distinct behavioural and network correlates of two interneuron types in prefrontal cortex. *Nature* **498**, 363-366 (2013).
75. H. J. Pi *et al.*, Cortical interneurons that specialize in disinhibitory control. *Nature* **503**, 521-524 (2013).
76. D. R. Sparta *et al.*, Activation of prefrontal cortical parvalbumin interneurons facilitates extinction of reward-seeking behavior. *J Neurosci* **34**, 3699-3705 (2014).
77. J. Courtin *et al.*, Prefrontal parvalbumin interneurons shape neuronal activity to drive fear expression. *Nature* **505**, 92-96 (2014).
78. F. Xia *et al.*, Parvalbumin-positive interneurons mediate neocortical-hippocampal interactions that are necessary for memory consolidation. *Elife* **6**, (2017).
79. D. R. Euston, A. J. Gruber, B. L. McNaughton, The role of medial prefrontal cortex in memory and decision making. *Neuron* **76**, 1057-1070 (2012).
80. M. A. Morgan, J. E. LeDoux, Differential contribution of dorsal and ventral medial prefrontal cortex to the acquisition and extinction of conditioned fear in rats. *Behav Neurosci* **109**, 681-688 (1995).
81. M. A. Morgan, L. M. Romanski, J. E. LeDoux, Extinction of emotional learning: contribution of medial prefrontal cortex. *Neurosci Lett* **163**, 109-113 (1993).
82. K. A. Corcoran, G. J. Quirk, Activity in prelimbic cortex is necessary for the expression of learned, but not innate, fears. *J Neurosci* **27**, 840-844 (2007).
83. V. Laurent, R. F. Westbrook, Distinct contributions of the basolateral amygdala and the medial prefrontal cortex to learning and relearning extinction of context conditioned fear. *Learn Mem* **15**, 657-666 (2008).
84. C. W. Stevenson, Role of amygdala-prefrontal cortex circuitry in regulating the expression of contextual fear memory. *Neurobiol Learn Mem* **96**, 315-323 (2011).
85. E. Einarsson, K. Nader, Involvement of the anterior cingulate cortex in formation, consolidation, and reconsolidation of recent and remote contextual fear memory. *Learn Mem* **19**, 449-452 (2012).

86. K. Nader, O. Hardt, A single standard for memory: the case for reconsolidation. *Nat Rev Neurosci* **10**, 224-234 (2009).
87. M. G. Zhao *et al.*, Roles of NMDA NR2B subtype receptor in prefrontal long-term potentiation and contextual fear memory. *Neuron* **47**, 859-872 (2005).
88. A. J. Silva *et al.*, Impaired learning in mice with abnormal short-lived plasticity. *Curr Biol* **6**, 1509-1518 (1996).
89. R. C. Malenka, R. A. Nicoll, NMDA-receptor-dependent synaptic plasticity: multiple forms and mechanisms. *Trends Neurosci* **16**, 521-527 (1993).
90. G. Köhr *et al.*, Intracellular domains of NMDA receptor subtypes are determinants for long-term potentiation induction. *J Neurosci* **23**, 10791-10799 (2003).
91. M. F. Bear, A. Kirkwood, Neocortical long-term potentiation. *Curr Opin Neurobiol* **3**, 197-202 (1993).
92. J. Tang *et al.*, Pavlovian fear memory induced by activation in the anterior cingulate cortex. *Mol Pain* **1**, 6 (2005).
93. A. Burgos-Robles, I. Vidal-Gonzalez, E. Santini, G. J. Quirk, Consolidation of fear extinction requires NMDA receptor-dependent bursting in the ventromedial prefrontal cortex. *Neuron* **53**, 871-880 (2007).
94. O. Bukalo *et al.*, Prefrontal inputs to the amygdala instruct fear extinction memory formation. *Sci Adv* **1**, (2015).
95. F. H. Do-Monte, G. Manzano-Nieves, K. Quinones-Laracuente, L. Ramos-Medina, G. J. Quirk, Revisiting the role of infralimbic cortex in fear extinction with optogenetics. *J Neurosci* **35**, 3607-3615 (2015).
96. B. Bontempi, C. Laurent-Demir, C. Destrade, R. Jaffard, Time-dependent reorganization of brain circuitry underlying long-term memory storage. *Nature* **400**, 671-675 (1999).
97. K. Takehara, S. Kawahara, Y. Kirino, Time-dependent reorganization of the brain components underlying memory retention in trace eyeblink conditioning. *J Neurosci* **23**, 9897-9905 (2003).
98. F. H. Do-Monte, K. Quinones-Laracuente, G. J. Quirk, A temporal shift in the circuits mediating retrieval of fear memory. *Nature* **519**, 460-463 (2015).
99. R. Miller, Neural assemblies and laminar interactions in the cerebral cortex. *Biol Cybern* **75**, 253-261 (1996).
100. H. Tomita, M. Ohbayashi, K. Nakahara, I. Hasegawa, Y. Miyashita, Top-down signal from prefrontal cortex in executive control of memory retrieval. *Nature* **401**, 699-703 (1999).
101. A. R. Childress, A. T. McLellan, R. Ehrman, C. P. O'Brien, Classically conditioned responses in opioid and cocaine dependence: a role in relapse? *NIDA Res Monogr* **84**, 25-43 (1988).
102. A. R. Childress *et al.*, Limbic activation during cue-induced cocaine craving. *Am J Psychiatry* **156**, 11-18 (1999).
103. R. T. LaLumiere, K. E. Niehoff, P. W. Kalivas, The infralimbic cortex regulates the consolidation of extinction after cocaine self-administration. *Learn Mem* **17**, 168-175 (2010).
104. T. M. Tzschentke, W. J. Schmidt, Functional heterogeneity of the rat medial prefrontal cortex: effects of discrete subarea-specific lesions on drug-induced conditioned place preference and behavioural sensitization. *Eur J Neurosci* **11**, 4099-4109 (1999).
105. W. L. Isaac, A. J. Nonneman, J. Neisewander, T. Landers, M. T. Bardo, Prefrontal cortex lesions differentially disrupt cocaine-reinforced conditioned place preference but not conditioned taste aversion. *Behav Neurosci* **103**, 345-355 (1989).
106. A. R. Zavala, S. M. Weber, H. J. Rice, A. T. Alleweireldt, J. L. Neisewander, Role of the prelimbic subregion of the medial prefrontal cortex in acquisition, extinction, and reinstatement

of cocaine-conditioned place preference. *Brain Res* **990**, 157-164 (2003).
107. J. M. Otis *et al.*, Prefrontal Neuronal Excitability Maintains Cocaine-Associated Memory During Retrieval. *Front Behav Neurosci* **12**, 119 (2018).
108. Y. Zhou *et al.*, The Projection From Ventral CA1, Not Prefrontal Cortex, to Nucleus Accumbens Core Mediates Recent Memory Retrieval of Cocaine-Conditioned Place Preference. *Front Behav Neurosci* **14**, 558074 (2020).
109. T. Zhang *et al.*, Glutamatergic neurons in the medial prefrontal cortex mediate the formation and retrieval of cocaine-associated memories in mice. *Addict Biol* **25**, e12723 (2020).
110. C. A. Miller, J. F. Marshall, Altered prelimbic cortex output during cue-elicited drug seeking. *J Neurosci* **24**, 6889-6897 (2004).
111. E. A. West, M. P. Saddoris, E. C. Kerfoot, R. M. Carelli, Prelimbic and infralimbic cortical regions differentially encode cocaine-associated stimuli and cocaine-seeking before and following abstinence. *Eur J Neurosci* **39**, 1891-1902 (2014).
112. M. C. Van den Oever *et al.*, Ventromedial prefrontal cortex pyramidal cells have a temporal dynamic role in recall and extinction of cocaine-associated memory. *J Neurosci* **33**, 18225-18233 (2013).
113. J. M. Otis, M. K. Fitzgerald, D. Mueller, Infralimbic BDNF/TrkB enhancement of GluN2B currents facilitates extinction of a cocaine-conditioned place preference. *J Neurosci* **34**, 6057-6064 (2014).
114. F. C. Cruz *et al.*, New technologies for examining the role of neuronal ensembles in drug addiction and fear. *Nat Rev Neurosci* **14**, 743-754 (2013).
115. A. Lanahan, P. Worley, Immediate-early genes and synaptic function. *Neurobiol Learn Mem* **70**, 37-43 (1998).
116. J. I. Morgan, T. Curran, Stimulus-transcription coupling in the nervous system: involvement of the inducible proto-oncogenes fos and jun. *Annu Rev Neurosci* **14**, 421-451 (1991).
117. J. I. Morgan, D. R. Cohen, J. L. Hempstead, T. Curran, Mapping patterns of c-fos expression in the central nervous system after seizure. *Science* **237**, 192-197 (1987).
118. G. L. Lyford *et al.*, Arc, a growth factor and activity-regulated gene, encodes a novel cytoskeleton-associated protein that is enriched in neuronal dendrites. *Neuron* **14**, 433-445 (1995).
119. J. H. Han *et al.*, Selective erasure of a fear memory. *Science* **323**, 1492-1496 (2009).
120. H. L. Hsiang *et al.*, Manipulating a "cocaine engram" in mice. *J Neurosci* **34**, 14115-14127 (2014).
121. M. Zelikowsky, S. Hersman, M. K. Chawla, C. A. Barnes, M. S. Fanselow, Neuronal ensembles in amygdala, hippocampus, and prefrontal cortex track differential components of contextual fear. *J Neurosci* **34**, 8462-8466 (2014).
122. A. Mukherjee, P. Caroni, Infralimbic cortex is required for learning alternatives to prelimbic promoted associations through reciprocal connectivity. *Nature communications* **9**, 2727 (2018).
123. B. L. Warren *et al.*, Distinct Fos-Expressing Neuronal Ensembles in the Ventromedial Prefrontal Cortex Mediate Food Reward and Extinction Memories. *J Neurosci* **36**, 6691-6703 (2016).
124. L. Ye *et al.*, Wiring and Molecular Features of Prefrontal Ensembles Representing Distinct Experiences. *Cell* **165**, 1776-1788 (2016).
125. H. J. Groenewegen, C. I. Wright, H. B. Uylings, The anatomical relationships of the prefrontal cortex with limbic structures and the basal ganglia. *J Psychopharmacol* **11**, 99-106 (1997).

126. T. M. Tzschentke, Pharmacology and behavioral pharmacology of the mesocortical dopamine system. *Prog Neurobiol* **63**, 241-320 (2001).
127. E. S. Boyden, F. Zhang, E. Bamberg, G. Nagel, K. Deisseroth, Millisecond-timescale, genetically targeted optical control of neural activity. *Nat Neurosci* **8**, 1263-1268 (2005).
128. K. Deisseroth, Controlling the brain with light. *Sci Am* **303**, 48-55 (2010).
129. V. Gradinaru *et al.*, Targeting and readout strategies for fast optical neural control in vitro and in vivo. *J Neurosci* **27**, 14231-14238 (2007).
130. J. Mattis *et al.*, Principles for applying optogenetic tools derived from direct comparative analysis of microbial opsins. *Nat Methods* **9**, 159-172 (2012).
131. F. Zhang *et al.*, Optogenetic interrogation of neural circuits: technology for probing mammalian brain structures. *Nat Protoc* **5**, 439-456 (2010).
132. O. Yizhar, L. E. Fenno, T. J. Davidson, M. Mogri, K. Deisseroth, Optogenetics in neural systems. *Neuron* **71**, 9-34 (2011).
133. V. S. Sohal, F. Zhang, O. Yizhar, K. Deisseroth, Parvalbumin neurons and gamma rhythms enhance cortical circuit performance. *Nature* **459**, 698-702 (2009).
134. D. R. Sparta *et al.*, Construction of implantable optical fibers for long-term optogenetic manipulation of neural circuits. *Nat Protoc* **7**, 12-23 (2012).
135. G. A. Ascoli *et al.*, Petilla terminology: nomenclature of features of GABAergic interneurons of the cerebral cortex. *Nat Rev Neurosci* **9**, 557-568 (2008).
136. C. L. Beasley, G. P. Reynolds, Parvalbumin-immunoreactive neurons are reduced in the prefrontal cortex of schizophrenics. *Schizophrenia research* **24**, 349-355 (1997).
137. D. A. Lewis, T. Hashimoto, D. W. Volk, Cortical inhibitory neurons and schizophrenia. *Nat Rev Neurosci* **6**, 312-324 (2005).
138. R. P. Vertes, Interactions among the medial prefrontal cortex, hippocampus and midline thalamus in emotional and cognitive processing in the rat. *Neuroscience* **142**, 1-20 (2006).
139. N. Dembrow, D. Johnston, Subcircuit-specific neuromodulation in the prefrontal cortex. *Front Neural Circuits* **8**, 54 (2014).
140. A. T. Lee *et al.*, Pyramidal neurons in prefrontal cortex receive subtype-specific forms of excitation and inhibition. *Neuron* **81**, 61-68 (2014).
141. B. B. Land *et al.*, Medial prefrontal D1 dopamine neurons control food intake. *Nat Neurosci* **17**, 248-253 (2014).
142. R. J. Douglas, K. A. Martin, Neuronal circuits of the neocortex. *Annu Rev Neurosci* **27**, 419-451 (2004).
143. L. M. Romanski *et al.*, Dual streams of auditory afferents target multiple domains in the primate prefrontal cortex. *Nat Neurosci* **2**, 1131-1136 (1999).
144. L. Petreanu, D. Huber, A. Sobczyk, K. Svoboda, Channelrhodopsin-2-assisted circuit mapping of long-range callosal projections. *Nat Neurosci* **10**, 663-668 (2007).
145. Y. Humeau *et al.*, Dendritic spine heterogeneity determines afferent-specific Hebbian plasticity in the amygdala. *Neuron* **45**, 119-131 (2005).
146. H. J. Alitto, W. M. Usrey, Corticothalamic feedback and sensory processing. *Curr Opin Neurobiol* **13**, 440-445 (2003).
147. E. R. John, The neurophysics of consciousness. *Brain Res Brain Res Rev* **39**, 1-28 (2002).
148. E. Christophe *et al.*, Two types of nicotinic receptors mediate an excitation of neocortical layer I interneurons. *J Neurophysiol* **88**, 1318-1327 (2002).

149. S. Killcross, E. Coutureau, Coordination of actions and habits in the medial prefrontal cortex of rats. *Cereb Cortex* **13**, 400-408 (2003).
150. A. Suska, B. R. Lee, Y. H. Huang, Y. Dong, O. M. Schluter, Selective presynaptic enhancement of the prefrontal cortex to nucleus accumbens pathway by cocaine. *Proc Natl Acad Sci U S A* **110**, 713-718 (2013).
151. J. P. Britt *et al.*, Synaptic and behavioral profile of multiple glutamatergic inputs to the nucleus accumbens. *Neuron* **76**, 790-803 (2012).
152. A. T. Lee, D. Vogt, J. L. Rubenstein, V. S. Sohal, A class of GABAergic neurons in the prefrontal cortex sends long-range projections to the nucleus accumbens and elicits acute avoidance behavior. *J Neurosci* **34**, 11519-11525 (2014).
153. C. Hubner, D. Bosch, A. Gall, A. Luthi, I. Ehrlich, Ex vivo dissection of optogenetically activated mPFC and hippocampal inputs to neurons in the basolateral amygdala: implications for fear and emotional memory. *Frontiers in behavioral neuroscience* **8**, 64 (2014).
154. A. Baddeley, Working memory. *Science* **255**, 556-559 (1992).
155. M. R. Gilmartin, F. J. Helmstetter, Trace and contextual fear conditioning require neural activity and NMDA receptor-dependent transmission in the medial prefrontal cortex. *Learn Mem* **17**, 289-296 (2010).
156. M. R. Gilmartin, M. D. McEchron, Single neurons in the medial prefrontal cortex of the rat exhibit tonic and phasic coding during trace fear conditioning. *Behav Neurosci* **119**, 1496-1510 (2005).
157. M. R. Gilmartin, H. Miyawaki, F. J. Helmstetter, K. Diba, Prefrontal activity links nonoverlapping events in memory. *J Neurosci* **33**, 10910-10914 (2013).
158. S. B. Dunnett, F. Nathwani, P. J. Brasted, Medial prefrontal and neostriatal lesions disrupt performance in an operant delayed alternation task in rats. *Behav Brain Res* **106**, 13-28 (1999).
159. M. A. Rossi *et al.*, Prefrontal cortical mechanisms underlying delayed alternation in mice. *J Neurophysiol* **108**, 1211-1222 (2012).
160. T. W. Robbins, A. C. Roberts, Differential regulation of fronto-executive function by the monoamines and acetylcholine. *Cereb Cortex* **17 Suppl 1**, i151-160 (2007).
161. Z. L. Rossetti, S. Carboni, Noradrenaline and dopamine elevations in the rat prefrontal cortex in spatial working memory. *J Neurosci* **25**, 2322-2329 (2005).
162. B. P. Ramos, D. Stark, L. Verduzco, C. H. van Dyck, A. F. Arnsten, Alpha2A-adrenoceptor stimulation improves prefrontal cortical regulation of behavior through inhibition of cAMP signaling in aging animals. *Learn Mem* **13**, 770-776 (2006).
163. Z. Zhang, S. Cordeiro Matos, S. Jego, A. Adamantidis, P. Seguela, Norepinephrine drives persistent activity in prefrontal cortex via synergistic alpha1 and alpha2 adrenoceptors. *PLoS One* **8**, e66122 (2013).
164. C. W. Berridge, Noradrenergic modulation of arousal. *Brain Res Rev* **58**, 1-17 (2008).
165. M. E. Carter *et al.*, Tuning arousal with optogenetic modulation of locus coeruleus neurons. *Nat Neurosci* **13**, 1526-1533 (2010).
166. J. Kim, J. W. Ghim, J. H. Lee, M. W. Jung, Neural correlates of interval timing in rodent prefrontal cortex. *J Neurosci* **33**, 13834-13847 (2013).
167. M. R. Drew, S. Fairhurst, C. Malapani, J. C. Horvitz, P. D. Balsam, Effects of dopamine antagonists on the timing of two intervals. *Pharmacol Biochem Behav* **75**, 9-15 (2003).

168. N. S. Narayanan, B. B. Land, J. E. Solder, K. Deisseroth, R. J. DiLeone, Prefrontal D1 dopamine signaling is required for temporal control. *Proc Natl Acad Sci U S A* **109**, 20726-20731 (2012).
169. Y. Chudasama, J. W. Dalley, F. Nathwani, P. Bouger, T. W. Robbins, Cholinergic modulation of visual attention and working memory: dissociable effects of basal forebrain 192-IgG-saporin lesions and intraprefrontal infusions of scopolamine. *Learn Mem* **11**, 78-86 (2004).
170. S. Maren, K. L. Phan, I. Liberzon, The contextual brain: implications for fear conditioning, extinction and psychopathology. *Nat Rev Neurosci* **14**, 417-428 (2013).
171. M. R. Milad, G. J. Quirk, Fear extinction as a model for translational neuroscience: ten years of progress. *Annu Rev Psychol* **63**, 129-151 (2012).
172. J. E. LeDoux, Emotion circuits in the brain. *Annu Rev Neurosci* **23**, 155-184 (2000).
173. J. Courtin, T. C. Bienvenu, E. O. Einarsson, C. Herry, Medial prefrontal cortex neuronal circuits in fear behavior. *Neuroscience* **240**, 219-242 (2013).
174. M. R. Milad, G. J. Quirk, Neurons in medial prefrontal cortex signal memory for fear extinction. *Nature* **420**, 70-74 (2002).
175. J. H. Cho, K. Deisseroth, V. Y. Bolshakov, Synaptic encoding of fear extinction in mPFC-amygdala circuits. *Neuron* **80**, 1491-1507 (2013).
176. E. Coutureau, S. Killcross, Inactivation of the infralimbic prefrontal cortex reinstates goal-directed responding in overtrained rats. *Behav Brain Res* **146**, 167-174 (2003).
177. K. S. Smith, A. Virkud, K. Deisseroth, A. M. Graybiel, Reversible online control of habitual behavior by optogenetic perturbation of medial prefrontal cortex. *Proc Natl Acad Sci U S A* **109**, 18932-18937 (2012).
178. K. S. Smith, A. M. Graybiel, A dual operator view of habitual behavior reflecting cortical and striatal dynamics. *Neuron* **79**, 361-374 (2013).
179. E. E. Steinberg, D. J. Christoffel, K. Deisseroth, R. C. Malenka, Illuminating circuitry relevant to psychiatric disorders with optogenetics. *Curr Opin Neurobiol* **30C**, 9-16 (2014).
180. World Health Organization. (2012), vol. 2014.
181. American Psychiatric Association, *Diagnostic and statistical manual of mental disorders*. (American Psychiatric Publishing, Arlington, VA, ed. 5th, 2013).
182. J. W. Murrough, B. Iacoviello, A. Neumeister, D. S. Charney, D. V. Iosifescu, Cognitive dysfunction in depression: neurocircuitry and new therapeutic strategies. *Neurobiol Learn Mem* **96**, 553-563 (2011).
183. M. T. Treadway, D. H. Zald, Reconsidering anhedonia in depression: lessons from translational neuroscience. *Neurosci Biobehav Rev* **35**, 537-555 (2011).
184. L. Clark, S. R. Chamberlain, B. J. Sahakian, Neurocognitive mechanisms in depression: implications for treatment. *Annu Rev Neurosci* **32**, 57-74 (2009).
185. S. M. Southwick, M. Vythilingam, D. S. Charney, The psychobiology of depression and resilience to stress: implications for prevention and treatment. *Annu Rev Clin Psychol* **1**, 255-291 (2005).
186. C. G. Beevers, P. Clasen, E. Stice, D. Schnyer, Depression symptoms and cognitive control of emotion cues: a functional magnetic resonance imaging study. *Neuroscience* **167**, 97-103 (2010).
187. S. G. Disner, C. G. Beevers, E. A. Haigh, A. T. Beck, Neural mechanisms of the cognitive model of depression. *Nat Rev Neurosci* **12**, 467-477 (2011).

188. C. L. Fales *et al.*, Altered emotional interference processing in affective and cognitive-control brain circuitry in major depression. *Biol Psychiatry* **63**, 377-384 (2008).
189. J. Amat *et al.*, Medial prefrontal cortex determines how stressor controllability affects behavior and dorsal raphe nucleus. *Nat Neurosci* **8**, 365-371 (2005).
190. B. Czeh *et al.*, Chronic social stress inhibits cell proliferation in the adult medial prefrontal cortex: hemispheric asymmetry and reversal by fluoxetine treatment. *Neuropsychopharmacology* **32**, 1490-1503 (2007).
191. A. F. Arnsten, Stress signalling pathways that impair prefrontal cortex structure and function. *Nat Rev Neurosci* **10**, 410-422 (2009).
192. E. Dias-Ferreira *et al.*, Chronic stress causes frontostriatal reorganization and affects decision-making. *Science* **325**, 621-625 (2009).
193. M. T. Treadway, J. W. Buckholtz, D. H. Zald, Perceived stress predicts altered reward and loss feedback processing in medial prefrontal cortex. *Front Hum Neurosci* **7**, 180 (2013).
194. C. Hamani *et al.*, Antidepressant-like effects of medial prefrontal cortex deep brain stimulation in rats. *Biol Psychiatry* **67**, 117-124 (2010).
195. C. H. Chang, M. C. Chen, M. H. Qiu, J. Lu, Ventromedial prefrontal cortex regulates depressive-like behavior and rapid eye movement sleep in the rat. *Neuropharmacology* **86C**, 125-132 (2014).
196. H. S. Mayberg *et al.*, Deep brain stimulation for treatment-resistant depression. *Neuron* **45**, 651-660 (2005).
197. C. Hamani, M. Diwan, S. Isabella, A. M. Lozano, J. N. Nobrega, Effects of different stimulation parameters on the antidepressant-like response of medial prefrontal cortex deep brain stimulation in rats. *J Psychiatr Res* **44**, 683-687 (2010).
198. C. Hamani *et al.*, Deep brain stimulation reverses anhedonic-like behavior in a chronic model of depression: role of serotonin and brain derived neurotrophic factor. *Biol Psychiatry* **71**, 30-35 (2012).
199. A. Veerakumar *et al.*, Antidepressant-like effects of cortical deep brain stimulation coincide with pro-neuroplastic adaptations of serotonin systems. *Biol Psychiatry* **76**, 203-212 (2014).
200. M. Koenigs, J. Grafman, The functional neuroanatomy of depression: distinct roles for ventromedial and dorsolateral prefrontal cortex. *Behav Brain Res* **201**, 239-243 (2009).
201. H. E. Covington, 3rd *et al.*, Antidepressant effect of optogenetic stimulation of the medial prefrontal cortex. *J Neurosci* **30**, 16082-16090 (2010).
202. E. J. Nestler, S. E. Hyman, Animal models of neuropsychiatric disorders. *Nat Neurosci* **13**, 1161-1169 (2010).
203. J. Klein *et al.*, Lesion of the medial prefrontal cortex and the subthalamic nucleus selectively affect depression-like behavior in rats. *Behav Brain Res* **213**, 73-81 (2010).
204. D. A. Slattery, I. D. Neumann, J. F. Cryan, Transient inactivation of the infralimbic cortex induces antidepressant-like effects in the rat. *J Psychopharmacol* **25**, 1295-1303 (2011).
205. S. Kumar *et al.*, Cortical control of affective networks. *J Neurosci* **33**, 1116-1129 (2013).
206. Y. I. Sheline, J. L. Price, Z. Yan, M. A. Mintun, Resting-state functional MRI in depression unmasks increased connectivity between networks via the dorsal nexus. *Proc Natl Acad Sci U S A* **107**, 11020-11025 (2010).
207. M. R. Warden *et al.*, A prefrontal cortex-brainstem neuronal projection that controls response to behavioural challenge. *Nature* **492**, 428-432 (2012).

208. A. Sartorius *et al.*, Remission of major depression under deep brain stimulation of the lateral habenula in a therapy-refractory patient. *Biol Psychiatry* **67**, e9-e11 (2010).
209. P. Willner, J. Scheel-Kruger, C. Belzung, The neurobiology of depression and antidepressant action. *Neurosci Biobehav Rev* **37**, 2331-2371 (2013).
210. P. R. Albert, F. Vahid-Ansari, C. Luckhart, Serotonin-prefrontal cortical circuitry in anxiety and depression phenotypes: pivotal role of pre- and post-synaptic 5-HT1A receptor expression. *Frontiers in behavioral neuroscience* **8**, 199 (2014).
211. I. Mahar, F. R. Bambico, N. Mechawar, J. N. Nobrega, Stress, serotonin, and hippocampal neurogenesis in relation to depression and antidepressant effects. *Neurosci Biobehav Rev* **38**, 173-192 (2014).
212. C. Challis, S. G. Beck, O. Berton, Optogenetic modulation of descending prefrontocortical inputs to the dorsal raphe bidirectionally bias socioaffective choices after social defeat. *Frontiers in behavioral neuroscience* **8**, 43 (2014).
213. I. H. Gotlib, J. Joormann, K. L. Minor, J. Hallmayer, HPA axis reactivity: a mechanism underlying the associations among 5-HTTLPR, stress, and depression. *Biol Psychiatry* **63**, 847-851 (2008).
214. B. Derntl *et al.*, Neural correlates of social approach and withdrawal in patients with major depression. *Soc Neurosci* **6**, 482-501 (2011).
215. I. Volman, K. Roelofs, S. Koch, L. Verhagen, I. Toni, Anterior prefrontal cortex inhibition impairs control over social emotional actions. *Curr Biol* **21**, 1766-1770 (2011).
216. T. Cruwys, S. A. Haslam, G. A. Dingle, C. Haslam, J. Jetten, Depression and Social Identity: An Integrative Review. *Pers Soc Psychol Rev* **18**, 215-238 (2014).
217. V. Vialou *et al.*, Prefrontal cortical circuit for depression- and anxiety-related behaviors mediated by cholecystokinin: role of DeltaFosB. *J Neurosci* **34**, 3878-3887 (2014).
218. M. K. Lobo, E. J. Nestler, H. E. Covington, 3rd, Potential utility of optogenetics in the study of depression. *Biol Psychiatry* **71**, 1068-1074 (2012).
219. A. Shenhav, M. M. Botvinick, Motivated action: new light on prefrontal-neuromodulatory circuits. *Curr Biol* **23**, R161-163 (2013).
220. D. Chaudhury *et al.*, Rapid regulation of depression-related behaviours by control of midbrain dopamine neurons. *Nature* **493**, 532-536 (2013).
221. L. A. Gunaydin *et al.*, Natural neural projection dynamics underlying social behavior. *Cell* **157**, 1535-1551 (2014).
222. A. K. Friedman *et al.*, Enhancing depression mechanisms in midbrain dopamine neurons achieves homeostatic resilience. *Science* **344**, 313-319 (2014).
223. S. Lammel, K. M. Tye, M. R. Warden, Progress in understanding mood disorders: optogenetic dissection of neural circuits. *Genes Brain Behav* **13**, 38-51 (2014).
224. C. Belzung, M. Turiault, G. Griebel, Optogenetics to study the circuits of fear- and depression-like behaviors: a critical analysis. *Pharmacol Biochem Behav* **122**, 144-157 (2014).
225. S. A. Allsop, C. M. Vander Weele, R. Wichmann, K. M. Tye, Optogenetic insights on the relationship between anxiety-related behaviors and social deficits. *Frontiers in behavioral neuroscience* **8**, 241 (2014).
226. P. R. Albert, Light up your life: optogenetics for depression? *J Psychiatry Neurosci* **39**, 3-5 (2014).
227. C. A. Ross, R. L. Margolis, S. A. Reading, M. Pletnikov, J. T. Coyle, Neurobiology of schizophrenia. *Neuron* **52**, 139-153 (2006).

228. K. K. Cho, V. S. Sohal, Optogenetic approaches for investigating neural pathways implicated in schizophrenia and related disorders. *Hum Mol Genet* **23**, R64-R68 (2014).
229. A. Peled, Optogenetic neuronal control in schizophrenia. *Med Hypotheses* **76**, 914-921 (2011).
230. A. Meyer-Lindenberg, From maps to mechanisms through neuroimaging of schizophrenia. *Nature* **468**, 194-202 (2010).
231. A. F. Arnsten, M. J. Wang, C. D. Paspalas, Neuromodulation of thought: flexibilities and vulnerabilities in prefrontal cortical network synapses. *Neuron* **76**, 223-239 (2012).
232. J. Lisman, Excitation, inhibition, local oscillations, or large-scale loops: what causes the symptoms of schizophrenia? *Curr Opin Neurobiol* **22**, 537-544 (2012).
233. X. Wang, M. Carlen, Optogenetic dissection of cortical information processing-shining light on schizophrenia. *Brain Res* **1476**, 31-37 (2012).
234. C. Tourino, A. Eban-Rothschild, L. de Lecea, Optogenetics in psychiatric diseases. *Curr Opin Neurobiol* **23**, 430-435 (2013).
235. R. Brisch *et al.*, The role of dopamine in schizophrenia from a neurobiological and evolutionary perspective: old fashioned, but still in vogue. *Frontiers in psychiatry* **5**, 47 (2014).
236. J. M. Beaulieu, R. R. Gainetdinov, The physiology, signaling, and pharmacology of dopamine receptors. *Pharmacol Rev* **63**, 182-217 (2011).
237. J. K. Seamans, C. R. Yang, The principal features and mechanisms of dopamine modulation in the prefrontal cortex. *Prog Neurobiol* **74**, 1-58 (2004).
238. D. Durstewitz, J. K. Seamans, The dual-state theory of prefrontal cortex dopamine function with relevance to catechol-o-methyltransferase genotypes and schizophrenia. *Biol Psychiatry* **64**, 739-749 (2008).
239. R. J. Ralph *et al.*, The dopamine D2, but not D3 or D4, receptor subtype is essential for the disruption of prepulse inhibition produced by amphetamine in mice. *J Neurosci* **19**, 4627-4633 (1999).
240. S. Gee *et al.*, Synaptic activity unmasks dopamine D2 receptor modulation of a specific class of layer V pyramidal neurons in prefrontal cortex. *J Neurosci* **32**, 4959-4971 (2012).
241. P. Seeman, S. Kapur, Schizophrenia: more dopamine, more D2 receptors. *Proc Natl Acad Sci U S A* **97**, 7673-7675 (2000).
242. O. Yizhar *et al.*, Neocortical excitation/inhibition balance in information processing and social dysfunction. *Nature* **477**, 171-178 (2011).
243. K. M. Tye, K. Deisseroth, Optogenetic investigation of neural circuits underlying brain disease in animal models. *Nat Rev Neurosci* **13**, 251-266 (2012).
244. P. J. Uhlhaas, C. Haenschel, D. Nikolic, W. Singer, The role of oscillations and synchrony in cortical networks and their putative relevance for the pathophysiology of schizophrenia. *Schizophrenia bulletin* **34**, 927-943 (2008).
245. P. J. Uhlhaas, W. Singer, Abnormal neural oscillations and synchrony in schizophrenia. *Nat Rev Neurosci* **11**, 100-113 (2010).
246. J. A. Cardin *et al.*, Driving fast-spiking cells induces gamma rhythm and controls sensory responses. *Nature* **459**, 663-667 (2009).
247. M. Carlen *et al.*, A critical role for NMDA receptors in parvalbumin interneurons for gamma rhythm induction and behavior. *Mol Psychiatry* **17**, 537-548 (2012).
248. P. J. Uhlhaas, W. Singer, Neural synchrony in brain disorders: relevance for cognitive dysfunctions and pathophysiology. *Neuron* **52**, 155-168 (2006).

249. S. E. Hyman, Addiction: a disease of learning and memory. *Am J Psychiatry* **162**, 1414-1422 (2005).
250. T. E. Robinson, K. C. Berridge, The neural basis of drug craving: an incentive-sensitization theory of addiction. *Brain Res Brain Res Rev* **18**, 247-291 (1993).
251. P. W. Kalivas, N. D. Volkow, The neural basis of addiction: a pathology of motivation and choice. *Am J Psychiatry* **162**, 1403-1413 (2005).
252. P. W. Kalivas, C. O'Brien, Drug addiction as a pathology of staged neuroplasticity. *Neuropsychopharmacology* **33**, 166-180 (2008).
253. S. E. Hyman, R. C. Malenka, E. J. Nestler, Neural mechanisms of addiction: the role of reward-related learning and memory. *Annu Rev Neurosci* **29**, 565-598 (2006).
254. P. W. Kalivas, The glutamate homeostasis hypothesis of addiction. *Nat Rev Neurosci* **10**, 561-572 (2009).
255. J. Peters, T. Pattij, T. J. De Vries, Targeting cocaine versus heroin memories: divergent roles within ventromedial prefrontal cortex. *Trends Pharmacol Sci* **34**, 689-695 (2013).
256. L. Hogarth, B. W. Balleine, L. H. Corbit, S. Killcross, Associative learning mechanisms underpinning the transition from recreational drug use to addiction. *Ann N Y Acad Sci* **1282**, 12-24 (2013).
257. R. Z. Goldstein, N. D. Volkow, Dysfunction of the prefrontal cortex in addiction: neuroimaging findings and clinical implications. *Nat Rev Neurosci* **12**, 652-669 (2011).
258. B. T. Chen *et al.*, Rescuing cocaine-induced prefrontal cortex hypoactivity prevents compulsive cocaine seeking. *Nature* **496**, 359-362 (2013).
259. J. L. Rogers, S. Ghee, R. E. See, The neural circuitry underlying reinstatement of heroin-seeking behavior in an animal model of relapse. *Neuroscience* **151**, 579-588 (2008).
260. E. Koya *et al.*, Role of ventral medial prefrontal cortex in incubation of cocaine craving. *Neuropharmacology* **56 Suppl 1**, 177-185 (2009).
261. J. McLaughlin, R. E. See, Selective inactivation of the dorsomedial prefrontal cortex and the basolateral amygdala attenuates conditioned-cued reinstatement of extinguished cocaine-seeking behavior in rats. *Psychopharmacology (Berl)* **168**, 57-65 (2003).
262. A. L. Willcocks, G. P. McNally, The role of medial prefrontal cortex in extinction and reinstatement of alcohol-seeking in rats. *Eur J Neurosci* **37**, 259-268 (2013).
263. B. R. Lubbers *et al.*, Prefrontal Gamma-Aminobutyric Acid Type A Receptor Insertion Controls Cue-Induced Relapse to Nicotine Seeking. *Biol Psychiatry*, (2014).
264. M. T. Stefanik *et al.*, Optogenetic inhibition of cocaine seeking in rats. *Addict Biol* **18**, 50-53 (2013).
265. M. T. Stefanik, P. W. Kalivas, Optogenetic dissection of basolateral amygdala projections during cue-induced reinstatement of cocaine seeking. *Frontiers in behavioral neuroscience* **7**, 213 (2013).
266. D. J. Calu *et al.*, Optogenetic inhibition of dorsal medial prefrontal cortex attenuates stress-induced reinstatement of palatable food seeking in female rats. *J Neurosci* **33**, 214-226 (2013).
267. E. Martin-Garcia *et al.*, Frequency of cocaine self-administration influences drug seeking in the rat: optogenetic evidence for a role of the prelimbic cortex. *Neuropsychopharmacology* **39**, 2317-2330 (2014).
268. P. W. Kalivas, N. Volkow, J. Seamans, Unmanageable motivation in addiction: a pathology in prefrontal-accumbens glutamate transmission. *Neuron* **45**, 647-650 (2005).

269. P. Voorn, L. J. Vanderschuren, H. J. Groenewegen, T. W. Robbins, C. M. Pennartz, Putting a spin on the dorsal-ventral divide of the striatum. *Trends Neurosci* **27**, 468-474 (2004).
270. K. McFarland, C. C. Lapish, P. W. Kalivas, Prefrontal glutamate release into the core of the nucleus accumbens mediates cocaine-induced reinstatement of drug-seeking behavior. *J Neurosci* **23**, 3531-3537 (2003).
271. J. M. Bossert *et al.*, Role of projections from ventral medial prefrontal cortex to nucleus accumbens shell in context-induced reinstatement of heroin seeking. *J Neurosci* **32**, 4982-4991 (2012).
272. R. T. LaLumiere, P. W. Kalivas, Glutamate release in the nucleus accumbens core is necessary for heroin seeking. *J Neurosci* **28**, 3170-3177 (2008).
273. Y. Y. Ma *et al.*, Bidirectional Modulation of Incubation of Cocaine Craving by Silent Synapse-Based Remodeling of Prefrontal Cortex to Accumbens Projections. *Neuron*, (2014).
274. J. T. Isaac, M. Ashby, C. J. McBain, The role of the GluR2 subunit in AMPA receptor function and synaptic plasticity. *Neuron* **54**, 859-871 (2007).
275. M. K. Lobo, S. L. Karsten, M. Gray, D. H. Geschwind, X. W. Yang, FACS-array profiling of striatal projection neuron subtypes in juvenile and adult mouse brains. *Nat Neurosci* **9**, 443-452 (2006).
276. M. K. Lobo *et al.*, Cell type-specific loss of BDNF signaling mimics optogenetic control of cocaine reward. *Science* **330**, 385-390 (2010).
277. M. K. Lobo *et al.*, DeltaFosB induction in striatal medium spiny neuron subtypes in response to chronic pharmacological, emotional, and optogenetic stimuli. *J Neurosci* **33**, 18381-18395 (2013).
278. V. Pascoli, M. Turiault, C. Luscher, Reversal of cocaine-evoked synaptic potentiation resets drug-induced adaptive behaviour. *Nature* **481**, 71-75 (2012).
279. V. Pascoli *et al.*, Contrasting forms of cocaine-evoked plasticity control components of relapse. *Nature* **509**, 459-464 (2014).
280. C. Luscher, K. M. Huber, Group 1 mGluR-dependent synaptic long-term depression: mechanisms and implications for circuitry and disease. *Neuron* **65**, 445-459 (2010).
281. T. Seif *et al.*, Cortical activation of accumbens hyperpolarization-active NMDARs mediates aversion-resistant alcohol intake. *Nat Neurosci* **16**, 1094-1100 (2013).
282. S. T. Tiffany, C. A. Conklin, A cognitive processing model of alcohol craving and compulsive alcohol use. *Addiction* **95 Suppl 2**, S145-153 (2000).
283. G. D. Stuber *et al.*, Excitatory transmission from the amygdala to nucleus accumbens facilitates reward seeking. *Nature* **475**, 377-380 (2011).
284. V. S. Sohal, Insights into cortical oscillations arising from optogenetic studies. *Biol Psychiatry* **71**, 1039-1045 (2012).
285. F. C. Cruz *et al.*, New technologies for examining the role of neuronal ensembles in drug addiction and fear. *Nature Reviews Neuroscience* **14**, 743-754 (2013).
286. X. Liu *et al.*, Optogenetic stimulation of a hippocampal engram activates fear memory recall. *Nature* **484**, 381-385 (2012).
287. H. M. Lee, P. M. Giguere, B. L. Roth, DREADDs: novel tools for drug discovery and development. *Drug discovery today* **19**, 469-473 (2014).
288. R. D. Airan, K. R. Thompson, L. E. Fenno, H. Bernstein, K. Deisseroth, Temporally precise in vivo control of intracellular signalling. *Nature* **458**, 1025-1029 (2009).

289. R. Lujan, E. Marron Fernandez de Velasco, C. Aguado, K. Wickman, New insights into the therapeutic potential of Girk channels. *Trends Neurosci* **37**, 20-29 (2014).
290. M. C. Hearing, A. N. Zink, K. Wickman, Cocaine-induced adaptations in metabotropic inhibitory signaling in the mesocorticolimbic system. *Rev Neurosci* **23**, 325-351 (2012).
291. S. M. Sternson, B. L. Roth, Chemogenetic tools to interrogate brain functions. *Annu Rev Neurosci* **37**, 387-407 (2014).
292. X. Han *et al.*, A high-light sensitivity optical neural silencer: development and application to optogenetic control of non-human primate cortex. *Frontiers in systems neuroscience* **5**, 18 (2011).
293. X. Han *et al.*, Millisecond-timescale optical control of neural dynamics in the nonhuman primate brain. *Neuron* **62**, 191-198 (2009).
294. A. Gerits *et al.*, Optogenetically induced behavioral and functional network changes in primates. *Curr Biol* **22**, 1722-1726 (2012).
295. M. Jazayeri, Z. Lindbloom-Brown, G. D. Horwitz, Saccadic eye movements evoked by optogenetic activation of primate V1. *Nat Neurosci* **15**, 1368-1370 (2012).
296. J. Cavanaugh *et al.*, Optogenetic inactivation modifies monkey visuomotor behavior. *Neuron* **76**, 901-907 (2012).
297. I. Diester *et al.*, An optogenetic toolbox designed for primates. *Nat Neurosci* **14**, 387-397 (2011).
298. A. J. Cole, D. W. Saffen, J. M. Baraban, P. F. Worley, Rapid increase of an immediate early gene messenger RNA in hippocampal neurons by synaptic NMDA receptor activation. *Nature* **340**, 474-476 (1989).
299. J. F. Guzowski, B. L. McNaughton, C. A. Barnes, P. F. Worley, Environment-specific expression of the immediate-early gene Arc in hippocampal neuronal ensembles. *Nat Neurosci* **2**, 1120-1124 (1999).
300. J. F. Guzowski *et al.*, Mapping behaviorally relevant neural circuits with immediate-early gene expression. *Curr Opin Neurobiol* **15**, 599-606 (2005).
301. L. G. Reijmers, B. L. Perkins, N. Matsuo, M. Mayford, Localization of a stable neural correlate of associative memory. *Science* **317**, 1230-1233 (2007).
302. T. Herdegen, J. D. Leah, Inducible and constitutive transcription factors in the mammalian nervous system: control of gene expression by Jun, Fos and Krox, and CREB/ATF proteins. *Brain Res Brain Res Rev* **28**, 370-490 (1998).
303. S. R. Pagliusi, M. Tessari, S. DeVevey, C. Chiamulera, E. M. Pich, The reinforcing properties of nicotine are associated with a specific patterning of c-fos expression in the rat brain. *Eur J Neurosci* **8**, 2247-2256 (1996).
304. M. A. Pezzone, W. S. Lee, G. E. Hoffman, B. S. Rabin, Induction of c-Fos immunoreactivity in the rat forebrain by conditioned and unconditioned aversive stimuli. *Brain Res* **597**, 41-50 (1992).
305. G. E. Schafe, I. L. Bernstein, Forebrain contribution to the induction of a brainstem correlate of conditioned taste aversion: I. The amygdala. *Brain Res* **741**, 109-116 (1996).
306. E. Knapska, S. Maren, Reciprocal patterns of c-Fos expression in the medial prefrontal cortex and amygdala after extinction and renewal of conditioned fear. *Learn Mem* **16**, 486-493 (2009).
307. F. C. Cruz, F. Javier Rubio, B. T. Hope, Using c-fos to study neuronal ensembles in corticostriatal circuitry of addiction. *Brain Res*, (2014).

308. L. M. Robertson *et al.*, Regulation of c-fos expression in transgenic mice requires multiple interdependent transcription control elements. *Neuron* **14**, 241-252 (1995).
309. A. L. Barth, R. C. Gerkin, K. L. Dean, Alteration of neuronal firing properties after in vivo experience in a FosGFP transgenic mouse. *J Neurosci* **24**, 6466-6475 (2004).
310. C. J. Guenthner, K. Miyamichi, H. H. Yang, H. C. Heller, L. Luo, Permanent genetic access to transiently active neurons via TRAP: targeted recombination in active populations. *Neuron* **78**, 773-784 (2013).
311. E. Koya *et al.*, Targeted disruption of cocaine-activated nucleus accumbens neurons prevents context-specific sensitization. *Nat Neurosci* **12**, 1069-1073 (2009).
312. A. R. Garner *et al.*, Generation of a synthetic memory trace. *Science* **335**, 1513-1516 (2012).
313. L. A. Gouty-Colomer *et al.*, Arc expression identifies the lateral amygdala fear memory trace. *Mol Psychiatry* **21**, 364-375 (2016).
314. L. A. DeNardo *et al.*, Temporal evolution of cortical ensembles promoting remote memory retrieval. *Nat Neurosci* **22**, 460-469 (2019).
315. C. A. Denny *et al.*, Hippocampal memory traces are differentially modulated by experience, time, and adult neurogenesis. *Neuron* **83**, 189-201 (2014).
316. A. Sahay *et al.*, Increasing adult hippocampal neurogenesis is sufficient to improve pattern separation. *Nature* **472**, 466-470 (2011).
317. I. Imayoshi *et al.*, Roles of continuous neurogenesis in the structural and functional integrity of the adult forebrain. *Nat Neurosci* **11**, 1153-1161 (2008).
318. G. I. Tasaka *et al.*, Genetic tagging of active neurons in auditory cortex reveals maternal plasticity of coding ultrasonic vocalizations. *Nat Commun* **9**, 871 (2018).
319. A. E. Girasole *et al.*, A Subpopulation of Striatal Neurons Mediates Levodopa-Induced Dyskinesia. *Neuron* **97**, 787-795.e786 (2018).
320. J. Y. Jeong *et al.*, One-step sequence- and ligation-independent cloning as a rapid and versatile cloning method for functional genomics studies. *Appl Environ Microbiol* **78**, 5440-5443 (2012).
321. M. J. Ruitenberg, R. Eggers, G. J. Boer, J. Verhaagen, Adeno-associated viral vectors as agents for gene delivery: application in disorders and trauma of the central nervous system. *Methods* **28**, 182-194 (2002).
322. S. Zolotukhin, M. Potter, W. W. Hauswirth, J. Guy, N. Muzyczka, A "humanized" green fluorescent protein cDNA adapted for high-level expression in mammalian cells. *J Virol* **70**, 4646-4654 (1996).
323. M. J. Krashes *et al.*, Rapid, reversible activation of AgRP neurons drives feeding behavior in mice. *J Clin Invest* **121**, 1424-1428 (2011).
324. A. Y. Higashi *et al.*, Direct hematological toxicity and illegitimate chromosomal recombination caused by the systemic activation of CreERT2. *Journal of immunology* **182**, 5633-5640 (2009).
325. B. Esmaeili, Z. Basseda, S. Gholizadeh, M. Javadi Paydar, A. R. Dehpour, Tamoxifen disrupts consolidation and retrieval of morphine-associated contextual memory in male mice: interaction with estradiol. *Psychopharmacology (Berl)* **204**, 191-201 (2009).
326. B. R. Lubbers *et al.*, The Extracellular Matrix Protein Brevican Limits Time-Dependent Enhancement of Cocaine Conditioned

Place Preference. *Neuropsychopharmacology* **41**, 1907-1916 (2016).
327. P. Rao-Ruiz *et al.*, Retrieval-specific endocytosis of GluA2-AMPARs underlies adaptive reconsolidation of contextual fear. *Nat Neurosci* **14**, 1302-1308 (2011).
328. S. Tonegawa, X. Liu, S. Ramirez, R. Redondo, Memory Engram Cells Have Come of Age. *Neuron* **87**, 918-931 (2015).
329. K. Z. Tanaka *et al.*, Cortical representations are reinstated by the hippocampus during memory retrieval. *Neuron* **84**, 347-354 (2014).
330. D. Marr, Simple memory: a theory for archicortex. *Philos Trans R Soc Lond B Biol Sci* **262**, 23-81 (1971).
331. T. Kitamura *et al.*, Engrams and circuits crucial for systems consolidation of a memory. *Science* **356**, 73-78 (2017).
332. P. Goelet, V. F. Castellucci, S. Schacher, E. R. Kandel, The long and the short of long-term memory--a molecular framework. *Nature* **322**, 419-422 (1986).
333. T. J. Ryan, D. S. Roy, M. Pignatelli, A. Arons, S. Tonegawa, Memory. Engram cells retain memory under retrograde amnesia. *Science* **348**, 1007-1013 (2015).
334. P. K. Dash, B. Hochner, E. R. Kandel, Injection of the cAMP-responsive element into the nucleus of Aplysia sensory neurons blocks long-term facilitation. *Nature* **345**, 718-721 (1990).
335. R. Bourtchuladze *et al.*, Deficient long-term memory in mice with a targeted mutation of the cAMP-responsive element-binding protein. *Cell* **79**, 59-68 (1994).
336. B. Kathirvelu, B. S. East, A. R. Hill, C. A. Smith, P. J. Colombo, Lentivirus-mediated chronic expression of dominant-negative CREB in the dorsal hippocampus impairs memory for place learning and contextual fear conditioning. *Neurobiol Learn Mem* **99**, 10-16 (2013).
337. S. Kida *et al.*, CREB required for the stability of new and reactivated fear memories. *Nat Neurosci* **5**, 348-355 (2002).
338. J. H. Han *et al.*, Neuronal competition and selection during memory formation. *Science* **316**, 457-460 (2007).
339. Y. Zhou *et al.*, CREB regulates excitability and the allocation of memory to subsets of neurons in the amygdala. *Nat Neurosci* **12**, 1438-1443 (2009).
340. A. J. Silva, Y. Zhou, T. Rogerson, J. Shobe, J. Balaji, Molecular and cellular approaches to memory allocation in neural circuits. *Science* **326**, 391-395 (2009).
341. B. L. Roth, DREADDs for Neuroscientists. *Neuron* **89**, 683-694 (2016).
342. F. C. Cruz, F. Javier Rubio, B. T. Hope, Using c-fos to study neuronal ensembles in corticostriatal circuitry of addiction. *Brain Res* **1628**, 157-173 (2015).
343. S. M. Ferguson *et al.*, Transient neuronal inhibition reveals opposing roles of indirect and direct pathways in sensitization. *Nat Neurosci* **14**, 22-24 (2011).
344. G. Vetere *et al.*, Chemogenetic Interrogation of a Brain-wide Fear Memory Network in Mice. *Neuron* **94**, 363-374 e364 (2017).
345. B. A. Silva, A. M. Burns, J. Graff, A cFos activation map of remote fear memory attenuation. *Psychopharmacology (Berl)* **236**, 369-381 (2019).
346. G. M. Alexander *et al.*, Remote control of neuronal activity in transgenic mice expressing evolved G protein-coupled receptors. *Neuron* **63**, 27-39 (2009).
347. W. A. Carlezon, Jr. *et al.*, Regulation of cocaine reward by CREB. *Science* **282**, 2272-2275 (1998).
348. M. Sheng, G. McFadden, M. E. Greenberg, Membrane depolarization and calcium induce c-fos transcription via

phosphorylation of transcription factor CREB. *Neuron* **4**, 571-582 (1990).
349. S. K. Barot, A. Chung, J. J. Kim, I. L. Bernstein, Functional imaging of stimulus convergence in amygdalar neurons during Pavlovian fear conditioning. *PLoS One* **4**, e6156 (2009).
350. A. L. Wheeler *et al.*, Identification of a functional connectome for long-term fear memory in mice. *PLoS computational biology* **9**, e1002853 (2013).
351. R. Marek, Y. Sun, P. Sah, Neural circuits for a top-down control of fear and extinction. *Psychopharmacology (Berl)* **236**, 313-320 (2019).
352. J. M. Moscarello, S. Maren, Flexibility in the face of fear: Hippocampal-prefrontal regulation of fear and avoidance. *Curr Opin Behav Sci* **19**, 44-49 (2018).
353. E. Lesburgueres *et al.*, Early tagging of cortical networks is required for the formation of enduring associative memory. *Science* **331**, 924-928 (2011).
354. K. K. Tayler, K. Z. Tanaka, L. G. Reijmers, B. J. Wiltgen, Reactivation of neural ensembles during the retrieval of recent and remote memory. *Curr Biol* **23**, 99-106 (2013).
355. S. A. Josselyn, S. Kohler, P. W. Frankland, Finding the engram. *Nat Rev Neurosci* **16**, 521-534 (2015).
356. Y. Dong *et al.*, CREB modulates excitability of nucleus accumbens neurons. *Nat Neurosci* **9**, 475-477 (2006).
357. S. Middei *et al.*, CREB selectively controls learning-induced structural remodeling of neurons. *Learn Mem* **19**, 330-336 (2012).
358. J. Viosca, M. Lopez de Armentia, D. Jancic, A. Barco, Enhanced CREB-dependent gene expression increases the excitability of neurons in the basal amygdala and primes the consolidation of contextual and cued fear memory. *Learn Mem* **16**, 193-197 (2009).
359. C. A. McClung, E. J. Nestler, Regulation of gene expression and cocaine reward by CREB and DeltaFosB. *Nat Neurosci* **6**, 1208-1215 (2003).
360. Y. Zhang, U. Werling, W. Edelmann, SLiCE: a novel bacterial cell extract-based DNA cloning method. *Nucleic Acids Research* **40**, e55-e55 (2012).
361. A. Wikler, Dynamics of drug dependence. Implications of a conditioning theory for research and treatment. *Arch Gen Psychiatry* **28**, 611-616 (1973).
362. M. T, L. SD, Ed. (TOADDJ, 2010), vol. 3, pp. 92-101.
363. Y. Y. Ma *et al.*, Bidirectional modulation of incubation of cocaine craving by silent synapse-based remodeling of prefrontal cortex to accumbens projections. *Neuron* **83**, 1453-1467 (2014).
364. M. T. Stefanik, Y. M. Kupchik, P. W. Kalivas, Optogenetic inhibition of cortical afferents in the nucleus accumbens simultaneously prevents cue-induced transient synaptic potentiation and cocaine-seeking behavior. *Brain Struct Funct* **221**, 1681-1689 (2016).
365. B. L. Warren *et al.*, Separate vmPFC Ensembles Control Cocaine Self-Administration Versus Extinction in Rats. *J Neurosci* **39**, 7394-7407 (2019).
366. I. F. Augur, A. R. Wyckoff, G. Aston-Jones, P. W. Kalivas, J. Peters, Chemogenetic Activation of an Extinction Neural Circuit Reduces Cue-Induced Reinstatement of Cocaine Seeking. *J Neurosci* **36**, 10174-10180 (2016).
367. D. R. Sparta *et al.*, Activation of prefrontal cortical parvalbumin interneurons facilitates extinction of reward-seeking behavior. *J Neurosci* **34**, 3699-3705 (2014).

368. D. G. Tervo *et al.*, A Designer AAV Variant Permits Efficient Retrograde Access to Projection Neurons. *Neuron* **92**, 372-382 (2016).
369. K. I. van Aerde, D. Feldmeyer, Morphological and physiological characterization of pyramidal neuron subtypes in rat medial prefrontal cortex. *Cereb Cortex* **25**, 788-805 (2015).
370. S. A. Josselyn, S. Köhler, P. W. Frankland, Finding the engram. *Nat Rev Neurosci* **16**, 521-534 (2015).
371. Y. Nakagami, A. Watakabe, T. Yamamori, Monocular inhibition reveals temporal and spatial changes in gene expression in the primary visual cortex of marmoset. *Front Neural Circuits* **7**, 43 (2013).
372. C. L. Thompson *et al.*, Molecular and anatomical signatures of sleep deprivation in the mouse brain. *Front Neurosci* **4**, 165 (2010).
373. T. Kawashima *et al.*, Functional labeling of neurons and their projections using the synthetic activity-dependent promoter E-SARE. *Nat Methods* **10**, 889-895 (2013).
374. A. Marco *et al.*, Mapping the epigenomic and transcriptomic interplay during memory formation and recall in the hippocampal engram ensemble. *Nat Neurosci*, (2020).
375. D. J. Morrison *et al.*, Parvalbumin interneurons constrain the size of the lateral amygdala engram. *Neurobiol Learn Mem* **135**, 91-99 (2016).
376. T. Stefanelli, C. Bertollini, C. Luscher, D. Muller, P. Mendez, Hippocampal Somatostatin Interneurons Control the Size of Neuronal Memory Ensembles. *Neuron* **89**, 1074-1085 (2016).
377. K. A. Cummings, R. L. Clem, Prefrontal somatostatin interneurons encode fear memory. *Nat Neurosci* **23**, 61-74 (2020).
378. L. S. Brebner *et al.*, Extinction of cue-evoked food-seeking recruits a GABAergic interneuron ensemble in the dorsal medial prefrontal cortex of mice. *Eur J Neurosci*, (2020).
379. L. E. Fenno *et al.*, Targeting cells with single vectors using multiple-feature Boolean logic. *Nat Methods* **11**, 763-772 (2014).
380. E. Visser *et al.*, A persistent alcohol cue memory trace drives relapse to alcohol seeking after prolonged abstinence. *Sci Adv* **6**, eaax7060 (2020).
381. L. Restivo, G. Vetere, B. Bontempi, M. Ammassari-Teule, The formation of recent and remote memory is associated with time-dependent formation of dendritic spines in the hippocampus and anterior cingulate cortex. *J Neurosci* **29**, 8206-8214 (2009).
382. L. Nadel, M. Moscovitch, Memory consolidation, retrograde amnesia and the hippocampal complex. *Curr Opin Neurobiol* **7**, 217-227 (1997).
383. M. Moscovitch, L. Nadel, G. Winocur, A. Gilboa, R. S. Rosenbaum, The cognitive neuroscience of remote episodic, semantic and spatial memory. *Curr Opin Neurobiol* **16**, 179-190 (2006).
384. M. J. Sekeres, G. Winocur, M. Moscovitch, The hippocampus and related neocortical structures in memory transformation. *Neurosci Lett* **680**, 39-53 (2018).
385. E. Teng, L. R. Squire, Memory for places learned long ago is intact after hippocampal damage. *Nature* **400**, 675-677 (1999).
386. A. P. Yonelinas, C. Ranganath, A. D. Ekstrom, B. J. Wiltgen, A contextual binding theory of episodic memory: systems consolidation reconsidered. *Nat Rev Neurosci* **20**, 364-375 (2019).
387. G. R. Sutherland, B. McNaughton, Memory trace reactivation in hippocampal and neocortical neuronal ensembles. *Curr Opin Neurobiol* **10**, 180-186 (2000).

388. T. Nakashiba, D. L. Buhl, T. J. McHugh, S. Tonegawa, Hippocampal CA3 output is crucial for ripple-associated reactivation and consolidation of memory. *Neuron* **62**, 781-787 (2009).
389. H. Eichenbaum, Hippocampus: mapping or memory? *Curr Biol* **10**, R785-787 (2000).
390. C. Lever, T. Wills, F. Cacucci, N. Burgess, J. O'Keefe, Long-term plasticity in hippocampal place-cell representation of environmental geometry. *Nature* **416**, 90-94 (2002).
391. L. S. Brebner *et al.*, The Emergence of a Stable Neuronal Ensemble from a Wider Pool of Activated Neurons in the Dorsal Medial Prefrontal Cortex during Appetitive Learning in Mice. *J Neurosci* **40**, 395-410 (2020).
392. R. Marek, P. Sah, Neural Circuits Mediating Fear Learning and Extinction. *Adv Neurobiol* **21**, 35-48 (2018).
393. P. Sah, E. S. Faber, M. Lopez De Armentia, J. Power, The amygdaloid complex: anatomy and physiology. *Physiol Rev* **83**, 803-834 (2003).
394. E. Lanuza, J. Moncho-Bogani, J. E. Ledoux, Unconditioned stimulus pathways to the amygdala: effects of lesions of the posterior intralaminar thalamus on foot-shock-induced c-Fos expression in the subdivisions of the lateral amygdala. *Neuroscience* **155**, 959-968 (2008).
395. F. Condé, E. Maire-Lepoivre, E. Audinat, F. Crépel, Afferent connections of the medial frontal cortex of the rat. II. Cortical and subcortical afferents. *J Comp Neurol* **352**, 567-593 (1995).
396. A. J. McDonald, Cortical pathways to the mammalian amygdala. *Prog Neurobiol* **55**, 257-332 (1998).
397. C. Herry *et al.*, Switching on and off fear by distinct neuronal circuits. *Nature* **454**, 600-606 (2008).
398. S. Maren, Neurobiology of Pavlovian fear conditioning. *Annu Rev Neurosci* **24**, 897-931 (2001).
399. E. Knapska *et al.*, Functional anatomy of neural circuits regulating fear and extinction. *Proc Natl Acad Sci U S A* **109**, 17093-17098 (2012).
400. F. Sotres-Bayon, D. Sierra-Mercado, E. Pardilla-Delgado, G. J. Quirk, Gating of fear in prelimbic cortex by hippocampal and amygdala inputs. *Neuron* **76**, 804-812 (2012).
401. H. Sun *et al.*, Development of a CRISPR-SaCas9 system for projection- and function-specific gene editing in the rat brain. *Sci Adv* **6**, eaay6687 (2020).
402. R. Marek *et al.*, Author Correction: Hippocampus-driven feed-forward inhibition of the prefrontal cortex mediates relapse of extinguished fear. *Nat Neurosci* **21**, 1291 (2018).
403. J. N. Krueger *et al.*, Recently formed context fear memories can be retrieved without the hippocampus. *bioRxiv*, 843342 (2019).
404. G. Vetere *et al.*, Chemogenetic Interrogation of a Brain-wide Fear Memory Network in Mice. *Neuron* **94**, 363-374.e364 (2017).
405. N. Scheel, P. Wulff, J. G. de Mooij-van Malsen, Afferent connections of the thalamic nucleus reuniens in the mouse. *J Comp Neurol* **528**, 1189-1202 (2020).
406. R. P. Vertes, W. B. Hoover, K. Szigeti-Buck, C. Leranth, Nucleus reuniens of the midline thalamus: link between the medial prefrontal cortex and the hippocampus. *Brain Res Bull* **71**, 601-609 (2007).
407. K. R. Ramanathan, R. L. Ressler, J. Jin, S. Maren, Nucleus Reuniens Is Required for Encoding and Retrieving Precise, Hippocampal-Dependent Contextual Fear Memories in Rats. *J Neurosci* **38**, 9925-9933 (2018).
408. K. R. Ramanathan, S. Maren, Nucleus reuniens mediates the extinction of contextual fear conditioning. *Behav Brain Res* **374**, 112114 (2019).

409. B. E. Hauer, S. Pagliardini, C. T. Dickson, The Reuniens Nucleus of the Thalamus Has an Essential Role in Coordinating Slow-Wave Activity between Neocortex and Hippocampus. *eNeuro* **6**, (2019).
410. J. R. Taylor, P. Olausson, J. J. Quinn, M. M. Torregrossa, Targeting extinction and reconsolidation mechanisms to combat the impact of drug cues on addiction. *Neuropharmacology* **56 Suppl 1**, 186-195 (2009).
411. M. E. Bouton, Context and behavioral processes in extinction. *Learn Mem* **11**, 485-494 (2004).
412. B. N. Bender, M. M. Torregrossa, Molecular and circuit mechanisms regulating cocaine memory. *Cell Mol Life Sci* **77**, 3745-3768 (2020).
413. D. E. Moorman, M. H. James, E. M. McGlinchey, G. Aston-Jones, Differential roles of medial prefrontal subregions in the regulation of drug seeking. *Brain Res* **1628**, 130-146 (2015).
414. S. Riaz *et al.*, Prelimbic and infralimbic cortical inactivations attenuate contextually driven discriminative responding for reward. *Sci Rep* **9**, 3982 (2019).
415. S. Jonkman, A. C. Mar, A. Dickinson, T. W. Robbins, B. J. Everitt, The rat prelimbic cortex mediates inhibitory response control but not the consolidation of instrumental learning. *Behav Neurosci* **123**, 875-885 (2009).
416. R. Saffari *et al.*, NPY+-, but not PV+- GABAergic neurons mediated long-range inhibition from infra- to prelimbic cortex. *Transl Psychiatry* **6**, e736 (2016).
417. B. Rudy, G. Fishell, S. Lee, J. Hjerling-Leffler, Three groups of interneurons account for nearly 100% of neocortical GABAergic neurons. *Dev Neurobiol* **71**, 45-61 (2011).
418. X. Wang, P. Liu, L. Ma, F. Wang, Opioid signal transduction regulates the dendritic morphology of somatostatin and parvalbumin interneurons in the medial prefrontal cortex. *Neuroreport* **30**, 592-599 (2019).
419. C. Jiang *et al.*, Morphine coordinates SST and PV interneurons in the prelimbic cortex to disinhibit pyramidal neurons and enhance reward. *Mol Psychiatry*, (2019).
420. J. M. Otis *et al.*, Prefrontal cortex output circuits guide reward seeking through divergent cue encoding. *Nature* **543**, 103-107 (2017).
421. J. A. Parkinson, R. N. Cardinal, B. J. Everitt, Limbic cortical-ventral striatal systems underlying appetitive conditioning. *Prog Brain Res* **126**, 263-285 (2000).
422. H. W. Berendse, Y. Galis-de Graaf, H. J. Groenewegen, Topographical organization and relationship with ventral striatal compartments of prefrontal corticostriatal projections in the rat. *J Comp Neurol* **316**, 314-347 (1992).
423. T. D. Goode, S. Maren, Common neurocircuitry mediating drug and fear relapse in preclinical models. *Psychopharmacology (Berl)* **236**, 415-437 (2019).
424. E. J. Kim, N. Kim, H. T. Kim, J. S. Choi, The prelimbic cortex is critical for context-dependent fear expression. *Front Behav Neurosci* **7**, 73 (2013).
425. G. J. Quirk, D. Mueller, Neural mechanisms of extinction learning and retrieval. *Neuropsychopharmacology* **33**, 56-72 (2008).
426. N. Suto *et al.*, Distinct memory engrams in the infralimbic cortex of rats control opposing environmental actions on a learned behavior. *eLife* **5**, (2016).
427. S. Pfarr *et al.*, Choice for Drug or Natural Reward Engages Largely Overlapping Neuronal Ensembles in the Infralimbic Prefrontal Cortex. *J Neurosci* **38**, 3507-3519 (2018).

428. A. F. Lacagnina *et al.*, Distinct hippocampal engrams control extinction and relapse of fear memory. *Nat Neurosci* **22**, 753-761 (2019).
429. X. Sun *et al.*, Functionally Distinct Neuronal Ensembles within the Memory Engram. *Cell* **181**, 410-423.e417 (2020).
430. L. R. Whitaker *et al.*, Bidirectional Modulation of Intrinsic Excitability in Rat Prelimbic Cortex Neuronal Ensembles and Non-Ensembles after Operant Learning. *J Neurosci* **37**, 8845-8856 (2017).
431. G. Neves, S. F. Cooke, T. V. Bliss, Synaptic plasticity, memory and the hippocampus: a neural network approach to causality. *Nat Rev Neurosci* **9**, 65-75 (2008).
432. P. Rao-Ruiz, E. Visser, M. Mitrić, A. B. Smit, M. C. van den Oever, A Synaptic Framework for the Persistence of Memory Engrams. *Front Synaptic Neurosci* **13**, 661476 (2021).
433. J. H. Choi *et al.*, Interregional synaptic maps among engram cells underlie memory formation. *Science* **360**, 430-435 (2018).
434. H. P. Davis, L. R. Squire, Protein synthesis and memory: a review. *Psychol Bull* **96**, 518-559 (1984).
435. H. Matthies, In search of cellular mechanisms of memory. *Prog Neurobiol* **32**, 277-349 (1989).
436. P. Rao-Ruiz *et al.*, Engram-specific transcriptome profiling of contextual memory consolidation. *Nat Commun* **10**, 2232 (2019).
437. A. R. Nectow *et al.*, Rapid Molecular Profiling of Defined Cell Types Using Viral TRAP. *Cell Rep* **19**, 655-667 (2017).
438. M. B. Chen, X. Jiang, S. R. Quake, T. C. Südhof, Persistent transcriptional programmes are associated with remote memory. *Nature* **587**, 437-442 (2020).
439. B. C. Dillingham *et al.*, Fear Learning Induces Long-Lasting Changes in Gene Expression and Pathway Specific Presynaptic Growth. *bioRxiv*, 571331 (2019).

English Summary

From the moment that humans became aware that our collection of memories defines who we are, many efforts have been made to better understand how memories are acquired, stored and retrieved. This may be with the goal to precisely describe how new memories are formed and retained or with the goal to change/erase memories that have already been formed. Both perspectives might prove crucial for a proper understanding of aberrant behavior, as is the case with substance abuse disorder or Post Traumatic Stress Disorder. The medial prefrontal cortex (mPFC) is considered an important hub for normal and aberrant memory processing and therefore I aimed in this thesis to identify memory-encoding neurons in the mPFC and to disentangle intrinsic mPFC circuits that support memory expression and extinction.

In **Chapter 2**, I have described the mPFC circuitry in light of findings obtained using optogenetics technology. Temporal and spatial precise manipulation of the activity of mPFC neurons using light resolved sometimes contradicting results obtained with lesion, pharmacological and electrophysiological methods. At the same time, optogenetics, and now also chemogenetics, provide new insights into the role of specific mPFC neurons and circuits in diverse cognitive behaviors and disease states. Optogenetics technology enabled the direct manipulation of neuronal projections within and between brain regions. With respect to the mPFC circuitry, this has led to a better understanding of intra-mPFC connectivity and the role of afferent and efferent mPFC projections in cognitive processes and mental disorders. Additionally, the use of opto- and chemogenetics together with transgenic targeting of specific cell-types facilitates the manipulation of behaviorally-relevant neuronal ensembles.

In **Chapter 3,** I designed and tested viral-TRAP, a new method that enables the expression of a permanent molecular tag in activated neurons in wild-type animals. I provide evidence that with viral-TRAP, a Cre-dependent molecular tag is expressed in a 4-hydroxytamoxifen (4TM) controlled manner in neurons that express Fos. This was achieved both *in vitro* and *in vivo*. By testing different viral titers *in vivo*, I managed to control the leakiness (i.e., non-specific tagging) of viral-TRAP, which was assessed by a reduced population of tagged neurons in the mPFC of animals that remained in their home-cage (less neuronal activation) in the absence and presence of 4TM treatment. Comparison of these mice with littermates that underwent contextual

fear conditioning (CFC) and received 4TM 2 h thereafter showed that conditioning significantly enhanced the size of the tagged mPFC ensemble. More specifically, the *in vivo* use of of AAV-Fos::CreER^{T2} at final titer of 2.4 X 10^{10} gc/mL combined with AAV5-hSyn::DIO-hM3Dq-mCherry at a titer of 5 X 10^{12} gc/mL, allowed us to tag CFC-activated neurons with limited leakiness and thereby to permanently express a molecular tag that facilitates further neuronal visualization and/or manipulation.

Viral-TRAP allowed the study described in **Chapter 4**, in which we aimed to unravel the role of mPFC neuronal ensembles in the consolidation of an aversive memory. Using viral-TRAP we demonstrate that memory allocation to mPFC neurons occurs after CFC using a mild training protocol (single 0.7 mA foot-shock). The activity of the tagged ensemble is necessary for the expression of a one-month-old CFC memory. We did not observe this when animals retrieved a 4-day-old fear memory. Interestingly, chemogenetic stimulation of the tagged mPFC ensemble in a neutral context induced freezing behavior at a recent and remote timepoint after learning, suggesting that these specific neurons are already encoding the fear memory at an early stage, but that they are not involved in recent memory expression. Surprisingly, an mPFC ensemble that was tagged after strong CFC (using 3 foot-shocks) was not required for remote memory expression. This differential involvement of mPFC in memory expression was further elucidate when we observed that CFC-activated mPFC neurons were preferentially reactivated during remote, but not recent memory retrieval, following 1US and not 3US conditioning. In line with these findings, manipulation of recent retrieval (1US) mPFC tagged neurons was not sufficient to enhance freezing behavior in a neutral context, whereas a smaller neuronal subset tagged during remote retrieval was sufficient to at least partially recover memory expression. Furthermore, we described how memory consolidation in mPFC tagged neuronal population is dependent on CREB expression since disruption of CREB function in mPFC neurons activated during CFC induced a time-dependent impairment in conditioned freezing. The findings of Chapter 4 allowed us to conclude that upon a mild fearful experience the fear memory is allocated to cortical neurons already during learning and is thus not gradually transferred from the hippocampus to the neocortex after the experience. Together, our data provide crucial insight into the spatiotemporal principles of memory consolidation in cortical networks and reveal that the strength of an aversive learning experience determines whether neuronal ensembles

in the mPFC will function as an important network hub in expression of remote memory following a time- and CREB-dependent maturation process.

In **Chapter 5** we focused on mPFC local neuronal circuits that regulate extinction of an appetitive memory. We first identified projections from the ventral area of the mPFC (vmPFC) that target the dorsal subregion of the mPFC (dmPFC). We then studied the role of this projection in extinction of cocaine conditioned place preference (CPP) memory. The vmPFC-to-dmPFC projecting neurons are activated when animals are re-exposed to a cocaine-associated context without drug reinforcement, which promotes extinction learning. Furthermore, chemogenetic suppression of the activity of these vmPFC-to-dmPFC projecting neurons prevented extinction of a cocaine CPP memory. Next, we described that vmPFC projecting neurons influence local network activity of the dmPFC via excitation of Parvalbumin (PV)-expressing interneurons that in turn inhibit dmPFC pyramidal neurons. This is typical for feed-forward inhibition in cortical networks. In line with this, chemogenetic suppression of dmPFC PV interneurons impaired the extinction of context-evoked cocaine memory. We conclude that extinction learning related to cocaine-associated cues requires recruitment of GABAergic inhibition in the dmPFC by vmPFC projections. Activity of vmPFC pyramidal neurons and dmPFC PV interneurons has previously been implicated in extinction of conditioned responses triggered by other rewards and aversive stimuli. Hence, together with my data, this suggests that intrinsic vmPFC-dmPFC connectivity has a critical role in behavioral inhibition and regulation of adaptive behavior in general.

With this research, I provide novel insights into the role of mPFC neurons and circuitry in memory processing. While these findings improve and detail our understanding of memory consolidation and extinction learning, they also open new avenues of research. Firstly, my data stresses the relevance of how conditioning strength shapes neuronal ensembles and the brain-wide neuronal circuit that supports remote memory expression. Secondly, I revealed a novel internal mPFC circuit that controls extinction learning through interaction between the ventral and dorsal mPFC (vmPFC and dmPFC). These results challenge the assignment of a simple stop and go function to the vmPFC and dmPFC, respectively. Furthermore, I also implicate the role of a specific GABAergic interneuron population in memory extinction and how it mediates the interplay between the dorsal and

ventral areas of the mPFC. Taken together, my thesis reinforces the necessity of combining the local and interregional identification of behaviorally-specific neuronal ensembles and neuronal circuitry supporting memory encoding, consolidation, retrieval and extinction, with the ultimate goal to develop better treatment options for debilitating memory disorders.

Acknowledgments

I arrive at the last part of my thesis, but without a doubt a very important one. Actually, most books start with a thank you note but in this case, saved the best for last. It also means I can finally give freedom to my novel writing vein!

To begin with, I must thank my supervisor, Michel. I remember vividly our first meeting, when I traveled to the Netherlands. You had the amazing thought that I was the perfect candidate, thank you for that. The production of this work and ultimately this thesis has a special taste for me as much as it has for you. As your first PhD student I believe this was a learning experience for the both of us. Looking back to the Me leaving Portugal and a few years later, the Me leaving the Netherlands, I can only say there is an ocean between (actually its a huge stretch of land but let's stick with the metaphor for now). We did a lot in 5 years (almost), much more than I could one day have imagined and you provided me with such an incredible experience in the MCN lab. I do not intend to beautify the struggle that we (also) had to endure but you never left me feel stuck even though you are more sceptical than me. This may sound tacky but I once dreamed of using light to control neuronal activity after watching Gero Miesenböck TED talk, still in my scientist infancy days. You helped me to make that dream come true and some many more I didn't know I wanted to achieve. Ultimately thank you for showing me what it means to be a great scientist and to set the bar to what one should aim to reach.

Guus, thank you for making everyone in the MCN department feel welcomed and valued. Its incredible how everyone's personality fit together and I do think this is a good and continuous work from your side. You are more than our boss; I see you as someone that knows how to lead without wearing the cloak and this is not an easy task to take. I enjoyed our regular meetings and discussions, that always gave me new perspectives and helped set priorities. Moreover, I will always hold dear in my heart the moment when you supported me outside my science career.

To the **committee that accepted to read my thesis**, thank you so much for saying yes to my invitation and taking the time to assess my work. I can't wait to hear your ideas and discuss science with you. This

day will stay with me forever and in this way, so will all of you. Thank you once more!

To every MCNener, thank you for a great time together and for going on this journey with me, both in and outside the lab.

Sabine, thank you for your good energy every time we would meet and for feeling my victories and losses. A thank you note for believing in the CognitionNet project and for opening the MCN doors to so many different people while caring for each and every one of them.

Ronald, the very first person from the MCN I talked with. Thank you for directing me to Michel's office and for the warm welcome on my first visit.

Mark, it was always such a good moment to see your smile whenever I would appear at your office door looking for Michel, and there were a lot of times. Thank you for your contagious good mood and laugh.

KaWan, even if my PhD did not involve proteomics, you continuously showed interest in my results. Thank you for your input during the PhD meetings.

Priyanka, thank you immensely for the fruitful discussions and for being so passionate about science. That made a difference to me and my daily lab life!

Yvonne, the lab commander! I have to confess that at first, I was very intrigued by your personality and pose. Quickly I realized that I could count on you for everything and sooner than later we were sharing hugs and jokes. Thank you for your help with my projects, more so when I was not in the lab and for teaching me different techniques. A plus thank you note for all the effort you had to create and organize amazing lab outings and such good atmosphere.

Rolinka, my sweet and super RoRo!! You are the very best! It is jaw dropping how much you can do in one day of work and I am still to meet someone with your energy. Thank you for all your help in and out the mouse house and for always being there for me and my furry buddies. Can't wait to hug and celebrate this with you.

Brigitte you are the MCN laugh. We usually can't hold it back when someone is laughing but with you there was always a twist. Probably because your constant good disposition and laughter made me feel that everything was going to be alright. Thank you for all the warm hugs,

love and conversations. You are so special to me and can't wait to see you again and also welcome you any day you want, in Portugal.

Marion, Titia and Roel, thank you for all the help in the lab and for always being available. Titia, I don't think you know how your scripts made my life so much easier.

Iryna, thank you for being so easy going! It was such a pleasure to meet you in the lab and to pause and chit-chat a bit. I miss your sweet smile.

Remco, thank you for the funny moments when we were working at the same time in the DNA lab. It is incredible how focused and organized you are in the lab doing complex and time-consuming tasks while being able to talk about everything and make jokes.

To the previous legacy, Céline, Leanne, Anne-Lieke, Nikhil, Loek, Esther, Sigrid, Mariette, Bart and Danai, thank you for the warm welcome and such nice environment at the MCN.

Part of this work would not be achieved if it wasn't for the help from the INF department. Huib, thank you for giving us room and time to pursuit our ideas.

Joshua, Bastiaan, Sybren, Huub, Tim, Antonio and Laurens, thank you for all the discussion and venting about the optogenetics struggle. It was nice to meet you all. Ayoub, our conversations in the mouse house during those long surgery hours made the day pass by in a blink. You're such a sweet and great person and I am so happy I got to meet you.

Thank you to every FGA person on the floor above, that were like an extended MCN family. Robbie thank you for helping me build the tools I used for this work. You were there anytime I needed and always happy to help. Thank you for the fun moments we shared watching football games and the endless conversations. Joost, thank you for constantly greeting me when we saw each other on the FGA or MCN corridors and for the constant cheer up words. Joke, your presence made most days either at the mouse house or the em room way easier to go by.

To my students, Han, Lineke, Lizz and Floor, thank you for accepting to be my master students and for so many good moments over the 5 years. All of you taught me different things about science and myself and I am very grateful for each one of you.

To my CognitionNet friends, I can not thank you enough for all the good times and all the moments we shared!

Demiroooooo, my habibi! Words are fleeting and can not convey how much you mean to me! You are like another brother, always supportive and always available to listen to me. We laughed so much and created a strong bond that I will forever cherish. Thank you for being you, funny, warm and pure.

Elena, bella ragazza della mia vita. Thank you for stopping by our office and make our day instantly cheerful. You were smiling all the time and making everyone feel happy and hopeful. I had lots of fun with you and loved when we shared my room for 2 days in a row, my quietest guest ever :). Will never forget my Omazita.

Martina/ Mefy/ Martuna, my office partner for so long! You are such a surprise box. There is so much more to you than what you allow others to see! Thank you for letting me see the different Martina's ;) Thank you for also being such a calm and chill travel buddy. I promise to visit you whenever I revisit Italy.

Miguelito, you are such a good guy! I visited your office many times and interrupted you a lot, hahahahhaha, but in each and every single time you were there, you were always up for a good talk. Thank you for being a good friend and listener. Ah, and thank you for laughing at my jokes even when I was not funny at all! Gracias por todo hermano.

Sophie, if I had to describe you in one word it would be, light. You did not walk those corridors, to me you always seemed to float. Thank you for your serene presence and for putting up with so many loud office visitors ;)

To the scientists that soon followed, Youngmei, Christina, Mandy, Miao, Leonidas, Andrea, Suzanne and Azra, thank you for coming to the MCN and adding to the lab diversity.

Ioannis, thank you for everything you did and for believing in our data. I enjoyed working with you and will be forever grateful that you accepted to take a chance on some crazy ideas. In the office I got to know you better and the moments we spent talking about everything helped make the lab a nicer place. You'll be glad to know that the dogs are big, sweet and will welcome you anytime.

Mio, I know that I did not welcome you properly but I am pretty sure I left the desk clean and more than ready for you! Thank you for continuing the work and for contributing so much into this thesis. I wish you all the best and a bright future in science.

Esther, I am sorry but I need to treat you like, my Visser! The one and only. Where shall I begin!!! I am the luckiest girl in this world because I get to have you as my friend. The kind of friendship that only grows stronger. Thank you for being one of the most amazing people I know. You were my very first (there were a lot of first during these 5 years I realized now) master student, and I know you think you learned with me but you got it wrong girl. It was me that learned a lot with you and still do. It is unmatched the way you care about your friends, how much you put of yourself in everything you do and how genuine you are. You are an inspiration to me and a safe haven. Thank you can not even begin to describe it. I will thank you till the very last day. I dedicate this thesis to you (and my Mum). This work has your love, sweat and input and it is as mine as it is yours. Last, let me thank you for being my paranymph. You can't imagine what it means to me to have you by my side.

Maria, you were such a good friend. Nice to come home to, have dinner with, watch football games, party and so much more. I really enjoyed the days that you, me and Aina shared a flat. Thank you for your patience and for welcoming my family. Hope I get to see you next time I visit Barcelona.

Koskinen, Aina and Sarah, oh oh! My fantastic trio. My family away from home. What I feel when I am with you is like a warm hug and I feel at peace. I don't think I ever told you this, but we share such bond that whenever I am alone with one of you it is like the four of us are together.

Koskinen, you have such a gentle soul. So many days when I was tired and felt there was not enough time, I would think of you and imagined how you managed to do it all, scientist, mother, independent woman, free spirit, and always with a smile. You are a nature force that inspires me deeply. You have my uttermost respect. Just wish Finland was closer, but I carry you in my heart everyday.

Aina, my happiest person! Thank you, a thousand times, for agreeing to share a flat with me. It was one of my brightest ideas. We had sunny, foodie, laughing, sleepy, cozy, moments and I would not change a thing. You taught me a lot, how to be more present, more extrovert and funnier. Remembering our nights together doing whatever, still cracks me up. The best days were with you! Et vull tant.

Sarah, with or without the h, I will always be with you. Since the day I met you, me as a fresh PhD student and you fresh off a Master degree, I have this sense that we were supposed to get to know each other. You

made me a better person. I am more aware, kinder and understanding because of you. I intensely wish the world had more people like you, showing others how beautiful this world could be. We had it all; living together, living in different spots but still doing pretty much everything together, travelling the world, parties, happy and sad moments. Its 8 years now but it feels like a lifetime. Nothing better than to have you by my (other) side. My Habibi and paranymph! Tu me manques!

Some people, I got the chance to get to know better outside the lab. Priyanka and Danai, there were never dull moments with you. You brought more happiness to my life and for that I thank you. Pri, if I could I would hug you everyday. You have such a big embrace and I could feel your love in that short moment, always. Thank you for liking hugs. You taught me a lot and every time I would have new results, I immediately wanted to share them with you. Thank you for the sweet ways you showed me you care, for your wicked humour and for welcoming me into your family. Martin, so glad that I got to know you and celebrate many good days with you. You're indeed one of the good guys. Danai, you're the dest! I think of you and immediately the song "Don't stop me now" comes to mind. You would come every day burning through the MCN and from the moment you opened the office door there was never, but i mean never a sad or depressive day. Thank you for making me happy, and for being so friendly and funny, you sexy lady. Also, thank you for trusting me with your cat's wellbeing ;). Soon we will party again.

Tatiana, obrigada pelas longas conversas em Português e por nunca me teres deixado sentir sozinha quando me queixava das saudades. És a minha lisboeta preferida!

Emmy, que bom que foi encontrar uma holandesa tuga. Cheguei de armas e bagagens aos Países Baixos sem ter onde morar e quis o destino que me cruzasse com uma rapariga de Coruche. Temos umas quantas histórias para contar e muitas etapas vividas juntas. Obrigada por teres andado a saltar de casa em casa comigo e nunca te teres fartado da minha companhia e de quem me visitava. Obrigada Age, pelos momentos divertidos e por nos teres ajudado a criar um "ninho" acolhedor.

Aos meus amigos desde o 7º (mais ou menos), Aníbal, Ana, Gerovsky, Danilo e Tina, já lá vão 23 anos. Quando penso nisto até fico sem voz. Já vivemos juntos tantas coisas e eu não quereria que fosse de outra maneira. Obrigada pelo vosso apoio e por sempre me mostrarem a

importância da amizade. Sei que por mais que andemos embrenhados nas nossas vidas, perto ou longe, podemos sempre contar uns com os outros. Vocês são fonte de inspiração e forças. Obrigada por tudo. Aníbal aqui está o resultado depois de tantos anos a "assombrar" (não posso dizer o que realmente me acusavas de) os ratinhos :).

A todos que me acompanham desde a licenciatura ou primeiros estágios em início carreira, muito obrigada por serem tao excelentes companheiros de viagem. Obrigada também por sempre mostrarem interesse no que andava a tramar nos Países Baixos. Isabelita, tenho muito orgulho na cientista que és e quero que saibas que aprendi imenso contigo. Foi ótimo ter-te tão próxima estes anos todos e saber que podia e posso contar contigo para tudo. Divertida dentro e fora do lab, adoro ser tua amiga. Mizinha, meu docinho! Obrigada pelo teu olhar carinhoso, pelas longas mensagens carregadas de amor e preocupação e por seres uma presença tão constante na minha vida. Didi, pequerrucha, ainda me lembro do dia que nos conhecemos no antigo laboratório. Era uma moca partilhar aquele espaço contigo. Tinhas sempre histórias engraçadas para partilhar, os nossos dias apesar de intensos eram sempre cheios de risadas e confidências. Incrível tudo o que conseguiste até hoje e a dedicação que tens. Obrigada pelo exemplo. Di, não há tristeza que perdure ao teu lado. És a alma da festa, sempre bola para a frente que atrás vem gente e ninguém te consegue ficar indiferente. Obrigada pelas risadas (e que não foram poucas, bastantes até) e pela alegria contagiante. És um portento! Maggie, és muita areia para o meu camião. Adoro a tua ironia e forma de estar na vida. Por favor continua assim e a esbanjar estilo e pinta por esse mundo fora. Espero que sejas a minha médica de família ;). Ana, ninguém te pára. Obrigada por mostrares que é possível seguirmos os nossos sonhos muito calmamente e respeitando toda a gente. Raquelita, continuarás a ser a nossa pequenita e a encher-nos de orgulho. O pessoal que saia da frente porque aí vai gente. Obrigada pela amizade e boa disposição. Zé Pedro, obrigada por seres tão fora da caixa, um divertido, fácil de falar com e constante lembrança do que é dedicação à ciência.

Ao Carlos, Sandra, Vasco, Clara, Hélder e Prof Deolinda, obrigada por acreditarem que eu conseguia fazer isto e por nunca me deixarem desanimar. Carlos, eternamente grata pelos seus ensinamentos e por sempre me empurrar para a frente.

Ao meu chefe e colegas maksensianos, Pedro, Rafael, César, Fernando, Rui, Carina, Walter, Miguel, Diogo e André, obrigada por me receberem tão bem e por serem impecáveis. Follow the light!

À minha família, as palavras nunca vão chegar para descrever o quanto vos devo e a sorte que tive por nascer no vosso seio.

Às mulheres da minha vida, minha Mãe Ana e Avó Laura. Não dá para desenlaçar uma da outra e nem dizer onde começa uma e a outra acaba, saídas da mesma forja e feitas das mesmas raízes. Mãe, obrigada por me ensinares a amar e a cuidar dos outros. A tua resiliência e persistência sem dúvida que correm nas minhas veias. Obrigada por seres um exemplo em todas as facetas da minha vida. Dedico-te este livro porque acredito gostares um pouco mais de ciência do que e eu. Obrigada por teres cortado o cordão umbilical e por teres aguentado a distância. Também por isso este livro é em tua honra. És o meu verdadeiro Amor e só lamento não ter encontrado antídoto para o lento desvanecer dos dias.

Avó Laura, mulher de luta e fibra. Apesar de não viveres este dia connosco sei que também o devo a ti, porque nos moldaste a todos com a tua garra. Apesar de nunca teres entendido muito bem porque raio alguém deixaria o seu país e família nunca me disseste para desistir e voltar, até porque desistir não fazia parte do teu vocabulário. Obrigada pelos teus beijinhos sempre no regresso e na ida e por teres sido a minha Avó.

Ao meu Pai, que eu sei gostaria de estar neste momento comigo e festejar, obrigada pelos passos que deste ao meu lado e por teres aceite sempre com graça o meu feitio. Festejo contigo em mente.

Ao meu irmão, Rafael, ambos sabemos o que somos um para o outro e nada vai mudar isso. Obrigada por sempre me apoiares e olhares pelos meus interesses. Sei que não há nada que não faças por mim e que darás o corpo ao manifesto sempre que necessário. Estou para conhecer alguém com a tua ética de trabalho e o suor e lágrimas que investes sempre que te dedicas a algo. Resta também saber o que não consegues fazer. Wish you could believe in yourself like I believe in you. Thank you for getting the brains while I got the looks ;). Mon tickyticouer.

Às minhas sobrinhas Beatriz e Leonor, obrigada por todos os abraços, beijinhos e amor. Sou uma sortuda por os vossos pais vos terem feito tao perfeitas e irresistíveis. Obrigada pela vossa forte personalidade e por me darem uns cabelos brancos.

À minha cunhada Cláudia, obrigada por cuidares desta malta enquanto eu não pude e por sempre me ajudares quando era preciso arranjar maneira rápida de viajar. Obrigada também pelos momentos em família, mesmo quando era de deixar os cabelos em pé.

Aos meus tios e tias, obrigada pelo carinho imenso que chegava sempre até mim a 2000km de distância. Nunca houve altura em que não me sentisse protegida por todos vocês. Tio Paulo, obrigada por te teres chegado à frente e decidido ser o meu pai extra. Obrigada também por tudo o que fazes pelos meus.

A todos os meus primaços do Bernardo, obrigada pelas visitas, pelas gargalhadas e por serem tão fixes. Fazem-me sentir uma sortuda. Certamente em termos de família ganhei a lotaria.

Finalmente ao André, o meu rochedo quer faça tormenta quer faça sol. Obrigada pelo abraço que não cansa e pelo carinho que não esmorece. O teu ombro e colo foram feitos na perfeição para eu poder ter abrigo e descansar. Obrigada por me fazeres rir e por me achares engraçada (não sei como, mas ainda bem). Obrigada por sempre me mostrares que não há nada que não se ultrapasse ou problema que não se resolva. Quero contar as décadas contigo.